(1)

Department of the Navy
Office of Naval Research

Electrochemistry in Colloids and Dispersions

Volume I

ELECTROANALYTICAL METHODS AND APPLICATIONS

ELECTROSYNTHESIS AND ELECTROCATALYSIS

POLYMERS AND LATEXES

A final report to the Department of the Navy, compiled by the

Division of Colloid and Surface Chemistry

of the American Chemical Society

4 February 1992

GRANT NO. N00014-91-J-1616
MODIFICATION NO. P00001

ABSTRACT

This report summarizes the current status of experimental and theoretical studies which address fundamental and applied aspects of electrochemistry in colloids and dispersions. The range of such microheterogeneous fluids examined includes micellar solutions, microemulsions, emulsions, latexes, and dispersions of solids in liquids. Several broad subtopics are described. These topics include electroanalytical methods and applications, solute distribution, diffusion, and transport, electrosynthesis and electrocatalysis, polymers and latexes, and colloidal metals and semiconductors.

This report is presented in three volumes, I, II, and III.

CONTENTS

CONTENTS

CONTENTS

(1) VOLTAMMETRY OF QUINONES IN ANIONIC MICELLES

E.Fisicaro[a], C.Minero[#] and E.Pelizzetti[#]

[a] Istituto di Chimica Fisica Applicata, Università di Parma, 43100 Parma, Italy.

[#] Dip. di Chimica Analitica, Università di Torino, 10125 Torino, Italy.

ABSTRACT

A voltammetric study of a series of differently substituted benzendiols has been carried out in aqueous anionic micellar solutions. The partitioning of the probes between the bulk aqueous and the micellar pseudophase affects both the observed currents and the half-wave potentials. The results are discussed in terms of probe-aggregate interactions and compared with kinetics of electron transfer reactions involving benzenediol/quinone couples.

INTRODUCTION

Benzenediols/quinones redox equilibria play a prominent function in living systems through their ability to undergo electron transfer processes (1). This role is fundamental in energy-transforming processes, e.g. photosynthesis (2), as well as in the function of vitamins like vitamin A, E, D and K. In other fields it can be highlighted that many organic dyes contain quinonoid structures and that benzenediols are a commercially important case of classical organic developing agents in the photographic process (3).

Since many of these electron transfer reactions occur at the membrane interfaces or in dispersed systems like emulsions, the investigation of the influence on the electrochemical reactions of molecular structured assemblies originating from self aggregation of amphiphiles molecules (micelles, microemulsions) (4) can give insight to the mechanisms operating in these systems.

EXPERIMENTAL SECTION

Materials.

The investigated benzenediols are reported in Chart 1. All compounds but Q6 were obtained from Aldrich and recrystallized before use. Q6 was a gift from 3M-Italia. Sodium Dodecylsulphate (SDS, Fluka) was also doubly recrystallized from ethanol.

Apparatus and Procedure.

Voltammetric measurements were performed with Amel mod 472 polarograph, using glassy carbon (GCE), saturated calomel (SCE) and platinum electrodes as working, reference and auxiliary electrode, respectively. Experiments were performed in the range of SDS = 0.015-0.2 M, NaCl 0-0.10 M or K_2SO_4 0.10 M, with probe concentration of $1.5\text{-}3.0\times10^{-4}$ M at rotation rate of GCE= 3000 rpm. A 10% precision was easily attainable.

Methods and Results.

In the reported experimental conditions all the voltammograms show only one wave for the oxidation process of the quinols. In the rotating disk electrode voltammetry, the limiting current i_d is given by the equation (5):

$$i_d = 0.62\ n\ F\ A\ D^{2/3}\ \nu^{-1/6}\ \Omega^{1/2}\ C \qquad (1)$$

where n is the number of electrons exchanged in the electrode reaction, F is the Faraday, A is the electrode surface area, D is the diffusion coefficient of the electroactive particle, ν is the kinematic viscosity, Ω is the angular velocity and, finally, C is the concentration of the probe in the bulk of the solution.

The applicability of eq.(1) to benzenediols reported in Chart 1 in the presence of micellar systems was checked by following the dependence of i_d on $\Omega^{1/2}$ and C. The results are reported in Fig.1a and 1b for the compound Q3. Analogous plots were obtained for the other investigated diols. The proportionality of the limiting current to $\Omega^{1/2}$ shows that diffusion control of the electrode reaction takes place in the micellar system under study.

I-2

DISCUSSION

The half wave potential for the reversible two-electron oxidation of QH_2 to Q are located at about 200-500 mV higher with respect to SCE potential in aqueous solution (see Table I) (6). In micellar solutions limiting currents are also proportional to the diol concentration as shown in Fig.1b. The dependence of i_d on the surfactant concentration is shown in Fig.2.

The presence of micellar aggregates creates a microdomain with which an organic probe interact on the basis of electrostatic and hydrophobic forces (4). The probes depicted in Chart 1 are expected to have different interactions with ionic micelles. These can be grouped as follows: (i) non-associating probes, e.g. Q1; (ii) probes partitioned between aqueous and micellar pseudophase; (iii) completely associated probes, e.g. Q5. The electrochemical properties of the different groups are then expected to be influenced by unionic micelles in remarkably different ways (7-13).

When the probe is completely solubilized in the micelle (i.e. Q5), the diffusion coefficient D in eq.(1) would correspond to the micelle diffusion coefficient. When the probe does not interact, virtually no effect due to the presence of aggregates is observed (i.e. Q1). In the case that the probe is partitioned between aqueous and micellar pseudophases, the diffusion current is the sum of two contributions, namely:

$$D_{app}^{2/3} = f_w D_w^{2/3} + f_m D_m^{2/3} \qquad (2)$$

where D_{app} is the measured diffusion coefficient, D_w and D_m are the diffusion coefficient of the free probe and of the micelle, respectively, and f is the fraction of probe in the aqueous (w) and micellar (m) pseudophases. Recently, the effect of various parameters and the applicability of eq.(2) to the measurement of diffusion coefficients of the aggregates have been extensively discussed (14-20). SDS based micelles and microemulsions have been deeply investigated and the diffusion coefficients thus evaluated have been compared with those determined through different techniques (16,17,19,21).

Since f depends on the total surfactant concentration, a dependence of the diffusion current on SDS concentration is expected. Measurements for probes Q2-Q5 are reported in Fig.2 and show the behavior predicted by eq.(2). Interestingly, for a strongly interacting compound such as Q5 in anionic micelles, the diffusion current

is quite small, underlining that the probe is barely available to the electron transfer. Similar results have been obtained for the reaction of hydrated electrons with the strongly associated vitamin K in SDS micelles (22).

The voltammetric measurements also allow the estimation of the half-wave potential $E_{1/2}$ of the electroactive species (5). The interaction of the probe with the aggregate is expected to change the availability to the electron transfer process. The main factors influencing the measured $E_{1/2}$ are the surface potential of the micelle and medium effects (polarity, viscosity) due to the microenvironment in which the probe is located. All these factors can be accounted for in the partition coefficient of the oxidized and reduced probe between the two pseudophases. By using the Nerst equation at the electrode, in the case of a solute partitioned between water and micelles, from eq.(1) and (2), the half-wave potential $E_{1/2,app}$ is given by:

$$E_{1/2,app} = E^{\circ\prime}_{w} + \frac{RT}{nF} \ln \frac{(D_{rid}^{2/3}+D_{m}^{2/3}K_{rid}C_d)}{(D_{ox}^{2/3}+D_{m}^{2/3}K_{ox}C_d)} \qquad (3)$$

where K_{ox} and K_{rid} are the partition coefficient for the oxidized and reduced probe, respectively, D_{ox} and D_{rid} are their diffusion coefficients in water, $E^{\circ\prime}_{w}$ is the formal standard potential in the medium conditions used (salt and pH) and C_d is the concentration of micellized surfactant. From eq.(3) it can be easily seen that in the limit of $C_d \to 0$, $E_{1/2,app} \to E_{1/2,w}$, or alternatively, that when $K_{ox}, K_{rid} \to \infty$, $E_{1/2,app} \to E_{1/2,m}$ By combining these two asintotic formulas, eq.(4) is obtained:

$$E_{1/2,m} = E_{1/2,w} + \frac{RT}{nF} \ln \frac{(D_{rid}^{\cdot 2/3}K_{rid})}{(D_{ox}^{\cdot 2/3}K_{ox})} \qquad (4)$$

Equations (3-4) assume a fast exchange of the probe between aqueous and micellar pseudophases, thus ensuring that a single wave is observed as in the present case.

The effect of micelles on electron transfer involving single electron transfer, such as $MV^{2+}/MV^{+\cdot}$ (MV=methylviologen) (25), Fc^{+}/Fc (Fc=ferrocene)(26), $Q/Q^{-\cdot}$ (Q=quinone)(22,24), $MPTZ^{+\cdot}/MPTZ$ (MPTZ=N-methylphenothiazine)(27) has been extensively reported and discussed in term of association to aggregates and medium influence.

An equation similar to eq.(4) has been derived and applied to systems in which both forms interact with the aggregates, such as $MV^{2+/+}$ in anionic micelles. The shift toward more anodic potentials has been assigned to a higher value for the binding constant of $MV^{\cdot+}$ with respect to MV^{2+}, in spite of the higher electrostatic interaction of the latter. The more hydrophobic character of $MV^{\cdot+}$ has been taken as responsible of this behavior (25). Similar effects of the charge on hydrophobicity has been also observed in the $MPTZ^{\cdot+}$/MPTZ system in SDS micelles (27).

In the present case, the redox equilibrium involves two electrons and two protons, according to:

$$Q + 2\,H^+ + 2\,e^- \;\langle\!=\!\rangle\; QH_2 \qquad (5)$$

Fig.3 shows the behavior of $E_{\frac{1}{2},app}$ as a function of the surfactant concentration for the investigated compounds. As for i_d, no effect of SDS concentration on $E_{\frac{1}{2},app}$ is observed for non-interacting or completely bound probes (f_w=1 or f_m=1, respectively). For the intermediate situation the behavior could be tentatively rationalized in the light of eq.(3). For most of the presently investigated systems, the values of the transfer constant from water to micelles for QH_2 are available (23), but few data are reported for the corresponding quinone structures (24). Comparison between the binding constants for the tetramethylquinol ($K_{rid} \approx 30\ M^{-1}$) (23) and the corresponding tetramethylquinone ($K_{ox} \approx 9\times10^3\ M^{-1}$) (24) suggests that the ratio between the binding constants of the couple Q/QH_2 is of the order of 3×10^2 in SDS. Table 1 lists the binding constants indipendently evaluated (23) for the presently investigated QH_2 compounds.

Then, simply taking into account the above considerations on the binding constants of benzenediols and quinones, a different trend on $E_{\frac{1}{2},app}$ as a function of surfactant concentration should be expected. It must however be considered that eq.(5) represents the overall process that involves different electron and proton transfer, i.e. in the present pH range

$$QH_2^{\cdot+} + e^- \;\langle\!=\!\rangle\; QH_2 \qquad (6)$$

$$QH_2^{\cdot+} \;\langle\!=\!\rangle\; Q^{\cdot-} + 2\,H^+ \qquad (pK_2 \approx 4\text{-}5) \qquad (7)$$

$$Q + e^- \;\langle\!=\!\rangle\; Q^{\cdot-} \qquad (8)$$

Proton concentration and apparent dissociation constants are strongly influenced by the micellar microdomains (32). The values of $E_{\frac{1}{2},m}$ listed in Table 1 are thus obtained by simple extrapolation to high surfactant concentration, when the couple can be assumed to be largely partitioned in the micelle.
The value of $E_{\frac{1}{2}}$ for the equilibrium (5) appears to be higher of ca. 0.08-0.12 V in the micellar medium with respect to the aqueous phase.

For the present systems, comparing the $E_{\frac{1}{2},m}$ values with those obtained when the equilibrium (5) is measured in 95:5 v/v ethanol:water (28,29), the increase of E° (formal redox potential) in the presence of micelles is considerable.

It is also interesting to compare the kinetic behavior of these compounds when they are involved in electron transfer reactions in aggregates. In fact, the ratio of the specific rate constants for the electron transfer between inorganic complexes, such as FeL_3^{3+} (L=phenanthroline or bipyridil-like ligands) and benzenediols in water with respect to anionic micelles, k_w/k_m, is only slightly higher than 1 (30). The rate determining step was shown to be the extraction of the first electron (with formation of $QH_2^{\cdot+}$, see eq.(6)) and to be related to the variation of the free energy involved (31). This means that the specific rate constant is related to the difference between $E^\circ_{FeL3}{}^{3+/2+}$ and $E^\circ_{QH2^{\cdot+}}/E^\circ_{QH2}$, which is in turn directly related to the difference with E°_Q/E°_{QH2} (31). Since $E^\circ_{FeL3}{}^{3+/2+}$ in SDS micelles was found higher of ca. 0.11-0.12 V in comparison with water (13), the present increase of E° for Q/QH_2 from water to SDS micelles gives a reasonable explanation on the basis of the free energy only, for the similar values of k_w and k_m. It is worth noting that in a medium of low polarity, such as the micellar interface, the reaction rate is lowered (23), thus justifying that the ratio k_w/k_m is slightly higher than 1.

CONCLUSIONS

In naturally occurring systems or in industrial processes, electron transfer reactions mostly occur in and around membranes or in dispersed systems. In these conditions, physical properties such as dielectric constant and electrical field strength change in very short distances. Voltammetric studies of probes bearing different hydrophobic substituents in the presence of microaggregates (micelles, microemulsions) allow to obtain some useful information on the effect of the microscopic medium on the electron transfer properties of an important class of organic compounds, such as quinones.

TABLES

Table I: Electrochemical data and binding constants for benzenediols.

probe	binding constant K for QH_2, M^{-1}	$E_{\frac{1}{2},w}$, mV	$E_{\frac{1}{2},m}$, mV
Q1	---	550	---
Q2	3.5	300	380*
Q3	65	290	365*
Q4	110	190	345
Q5	$> 10^3$	---	240
Q6	110	320	455

* estimated.

CAPTION TO FIGURES

Figure 1. Plots of the diffusion current against the square root of the angular velocity (a) and against the concentration of the probes (b) in SDS micelles. Conditions are reported in the Experimental Section.

Figure 2. Plots of diffusion current as a function of SDS concentration for the investigated benzenediols shown in Chart 1.

Figure 3. Effect of the SDS concentration on the half-wave potential of investigated benzenediols.

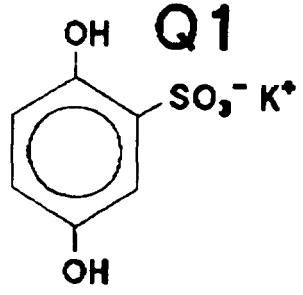

K–2,5–dihydroxybenzene sulphonate

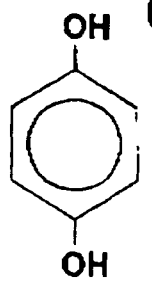

Benzene–1,4–diol

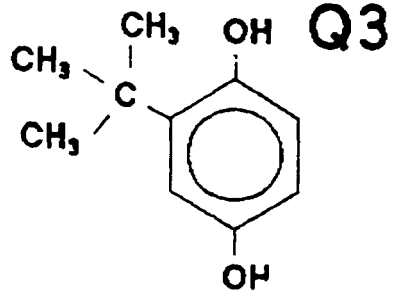

2–tert–butylbenzene–1,4–diol

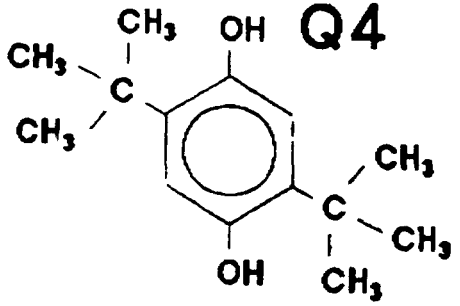

2,5–di–tert–butylbenzene–1,4–diol

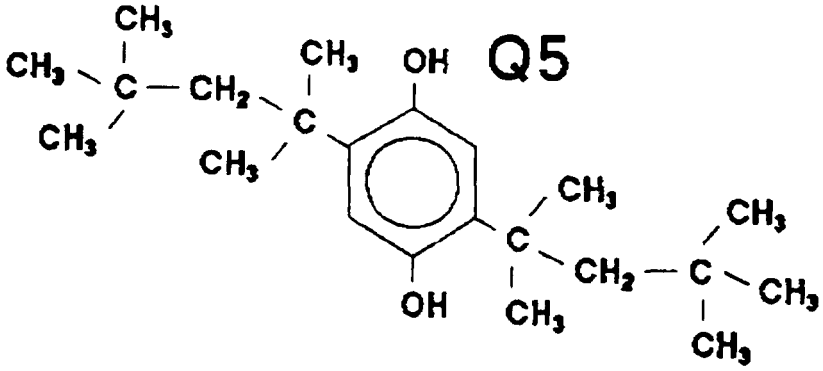

2,5–di–[(1,1,3,3–tetramethyl)–butyl]benzene–1,4–diol

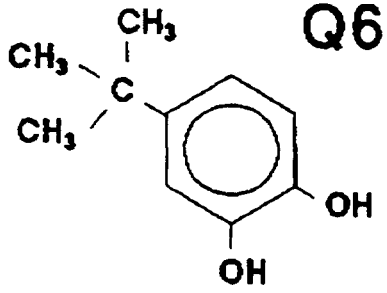

4–tert–butylbenzene–1,2–diol

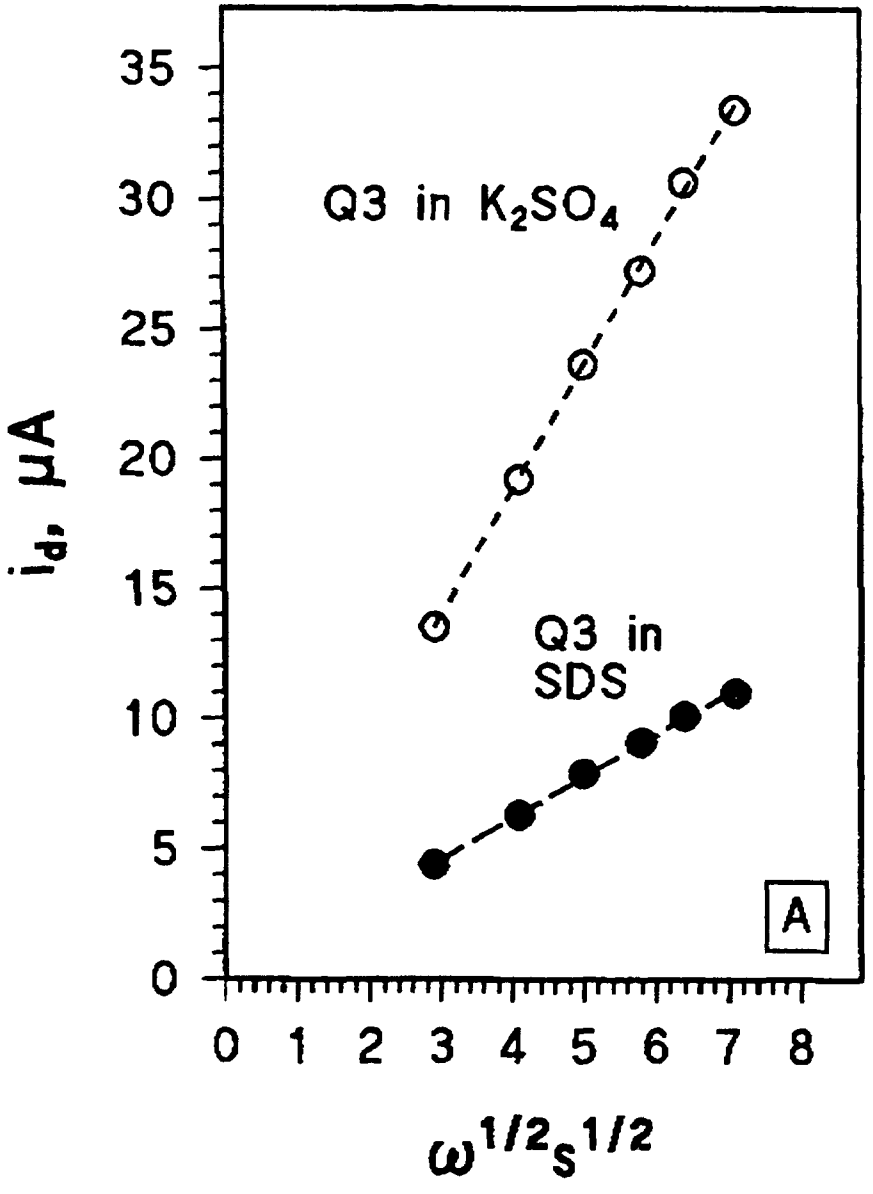
Q3 in K_2SO_4
Q3 in SDS
A
i_d, μA
$\omega^{1/2}s^{1/2}$
0
5
10
15
20
25
30
35
0 1 2 3 4 5 6 7 8

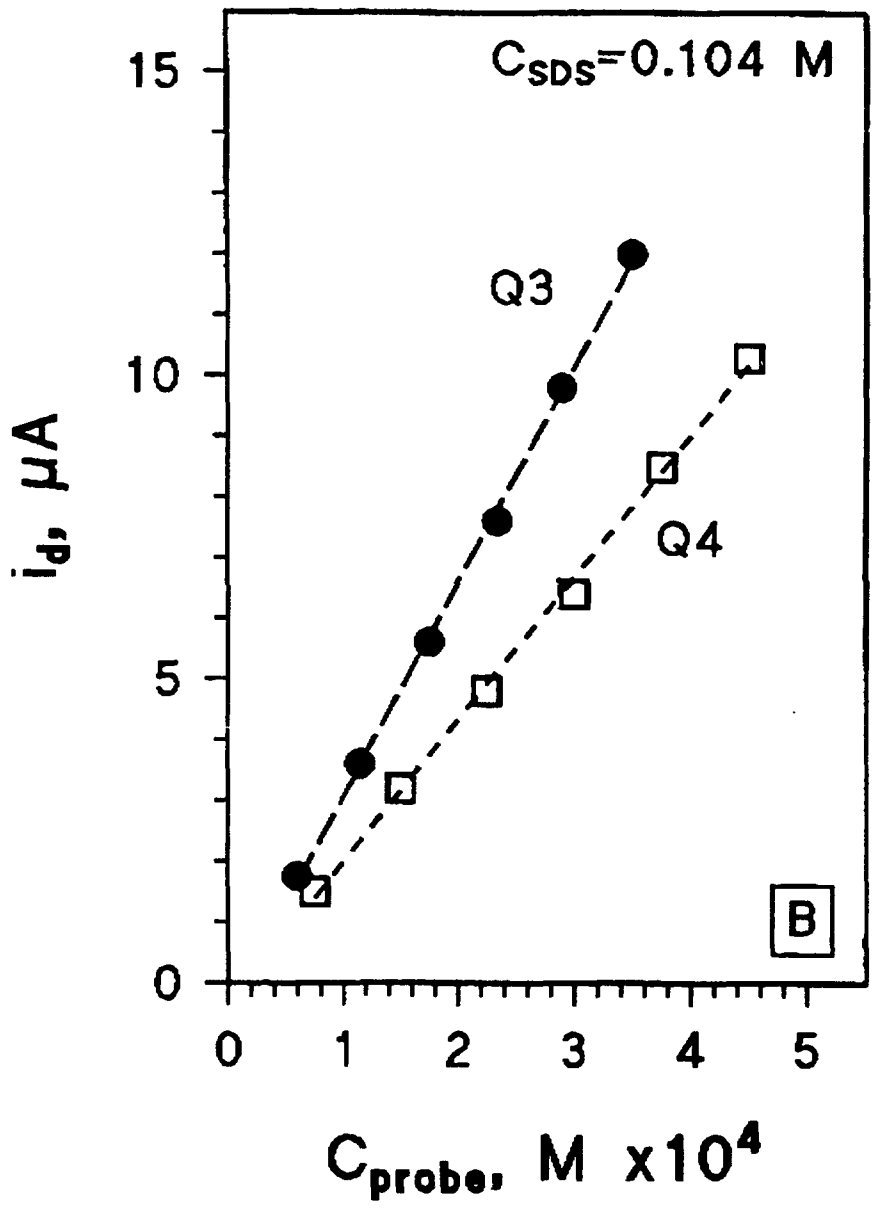
C_{SDS}=0.104 M
Q3
Q4
B
i_d, μA
C_{probe}, M x10^4
0
5
10
15
0 1 2 3 4 5

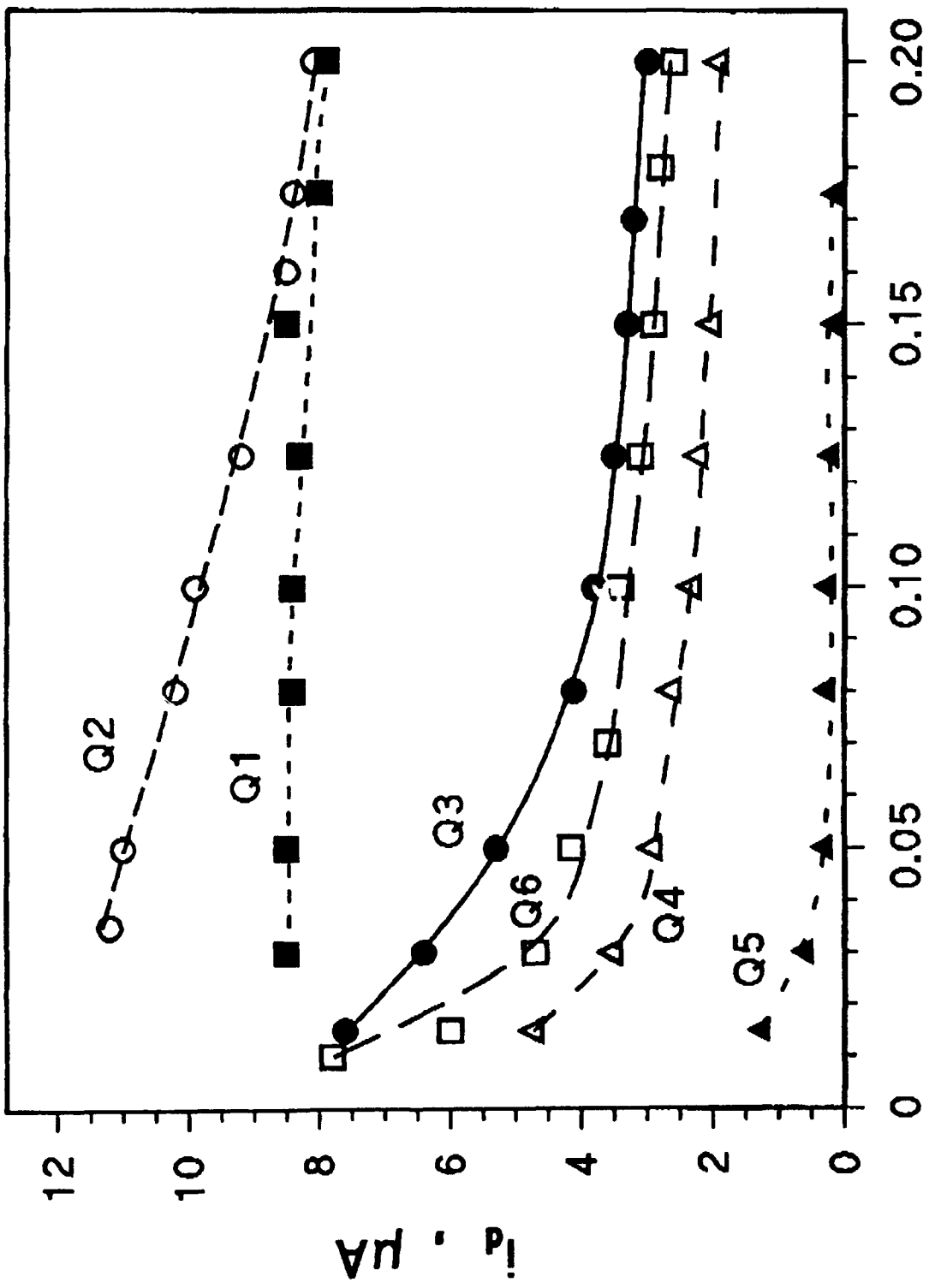
Q2
Q1
Q3
Q6
Q4
Q5
12
10
8
6
4
2
0
0
0.05
0.10
0.15
0.20
[SDS], M
i_d , μA

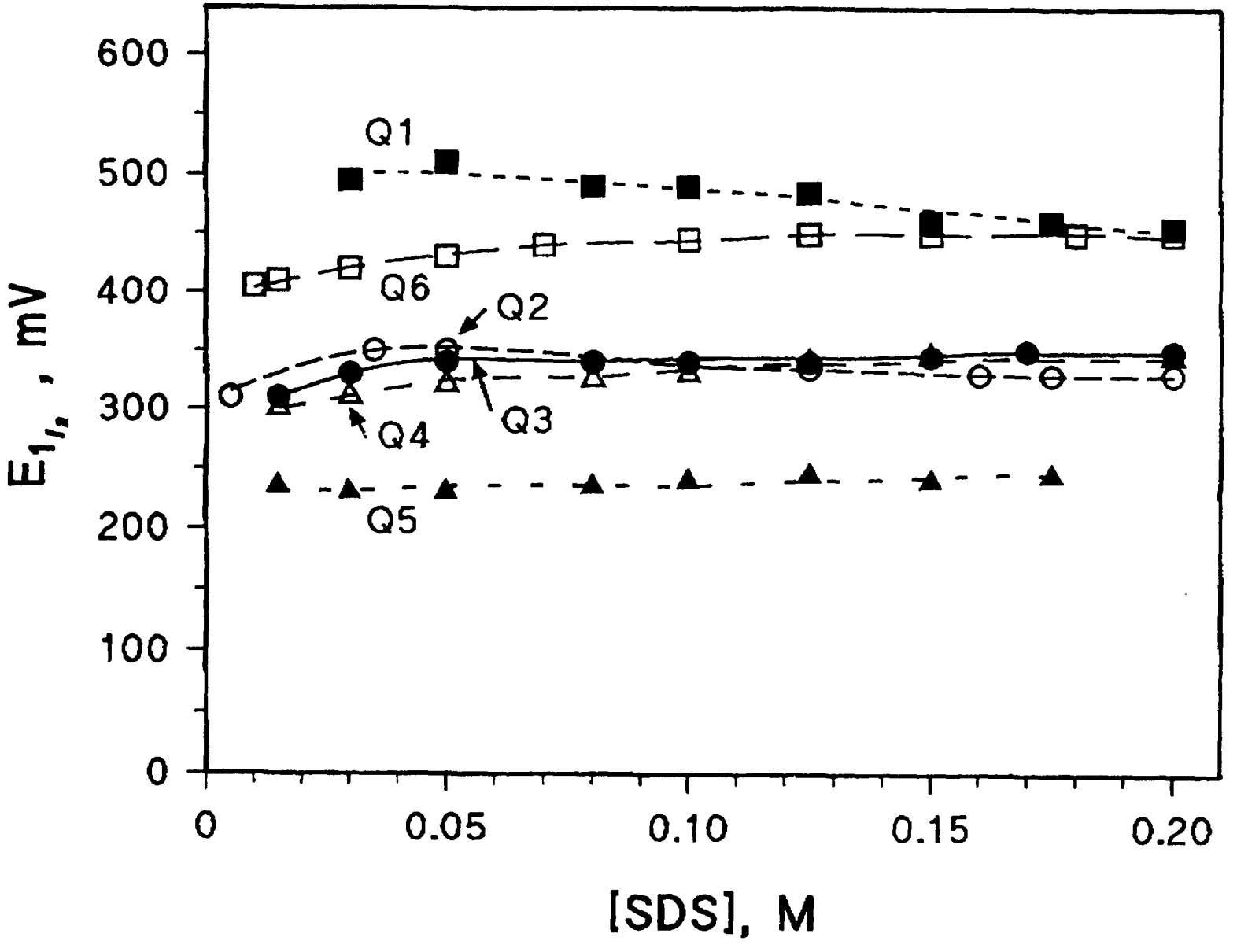
600
500
400
300
200
100
0
0
0.05
0.10
0.15
0.20
$E_{1/2}$, mV
[SDS], M
Q1
Q2
Q3
Q4
Q5
Q6

REFERENCES

1. "*The Chemistry of the Quinonoid Compounds*", S.Patai ed., Wiley, London, 1974, Part I and II.
2. B.L.Trumpower, ed., "*Function of Quinones in Energy Conserving Systems*", Academic Press, New York, 1982.
3. "*The Theory of the Photographic Process*", T.H.James ed., MacMillan, N.Y., 1977.
4. J.H.Fendler, "*Membrane Mimetic Systems*", Wiley, New York, 1982.
5. A.M.Bond ed., "*Modern Polarographic Methods in Analytical Chemistry*", Dekker, N.Y., 1980.
6. J.Q.Chambers, in ref.1, vol.2, ch.14 .
7. R.A.Mackay, *Adv.Colloid Interface Sci.*, **1981**, 15, 131.
8. R.A.Mackay, N.S.Dixit, R.Agarwal and R.P.Seiders, *J.Dispersion Sci.*, **1983**, 4, 397.
9. E.Pelizzetti, E.Pramauro and C.Minero, *Ann.Chim.(Rome)*, **1987**, 77, 127.
10. E.Pelizzetti and E.Pramauro, *Anal.Chim.Acta*, **1985**, 169, 1
11. T.C.Franklin and M.Iwunze, *Anal.Chem.*, **1980**, 52, 973.
12. G.L.McIntire, D.M.Chiappardi, R.L.Casselberry and H.N.Blount, *J.Phys.Chem.*, **1982**, 86, 2632.
13. Y.Oshawa, Y.Shimazaki and S.Aoyagui, *J.Electroanal.Chem.*, **1980**, 114, 235.
14. R.Zana and R.A.Mackay, *Langmuir*, **1986**, 2, 109.
15. T.Matsubara and J.Texter, *J.Colloid Interface Sci.*, **1986**, 112, 1121.
16. J.F.Rusling, C.N.Shi and T.F.Kumosinski, *Anal.Chem.*, **1988**, 60, 1260.
17. R.E.Verralle, S.Milioto, A.Giraudeau and R.Zana, *Langmuir*, **1989**, 5, 124
18. R.A.Mackay, S.A.Myers, L.Bodalbhai and A.Brajter-Toth, *Anal.Chem.*, **1990**, 62, 1084.
19. E.Dayalan, S.Qutubuddin and A.Hussam, *Langmuir*, **1990**, 6, 715.
20. J.F.Rusling, Z.Wang and A.Owlia, *Coll.Surfaces*, **1990**, 48, 173.
21. J.P.Kratohvil and T.M.Aminabhavi, *J.Phys.Chem.*, **1982**, 86, 1254.
22. S.M.Hubig, B.C.Dionne and M.A.J.Rodgers, *J.Phys.Chem.*, **1986**, 90, 5873.
23. E.Pelizzetti and E.Pramauro, *J.Phys.Chem.*, **1984**, 88, 990.
24. M.Almgren, F.Grieser and J.K.Thomas, *J.Phys.Chem.*,**1979**, 83, 3232.
25. A.E.Kaifer and A.J.Bard, *J.Phys.Chem.*, **1985**, 89, 4876.

26. J.J.Donohue and D.A.Barthry, *Langmuir*, **1989**, 5, 671.

27. C.Minero, E.Pramauro, E.Pelizzetti and D.Meisel, *J.Phys.Chem.*, **1983**, 87, 399.

28. W.M.Clark, "*Oxidation-Reduction Potentials of Organic Systems*", Williams & Wilkins, Baltimore, 1960.

29. C.Minero, E.Pramauro, E.Pelizzetti, N.J.Blandamer, J.Burgess and S.Radulovic, *Inorg.Chim.Acta*, **1990**, 173, 43.

30. E.Pelizzetti, E.Pramauro and D.Croce, *Ber.Bunsenges.Phys.Chem.*, **1980**, 84, 265.

31. E.Pelizzetti, E.Mentasti and C.Baiocchi, *J.Phys.Chem.*, **1976**, 80, 2979.

32. C.Minero and E.Pelizzetti, *Adv.Colloid Interface Sci.*, in press.

I-14

(2) # The Use of Cationic Surfactants in Anodic Voltammetric and Coulometric Analysis of Insoluble, Difficultly Oxidizable Compounds in Aqueous Systems.

Thomas C. Franklin, Remi Nnodimele and Robert C. Duty
Baylor University, Department of Chemistry, P.O. Box 97348
Waco, Tx. 76798-7348

Two major problem areas in conventional electroanalytical chemistry are the analysis of difficultly soluble and difficultly oxidizable or reducible substances.

(1) Difficultly soluble substances. There are many compounds such as minerals that are difficult to analyze by electroanalytical methods because they are not soluble in either aqueous or nonaqueous system. However, more common are compounds that are not soluble in one of these types of solvents. The largest group of compounds in this class are organic compounds in aqueous solutions. Most organic compounds are insoluble in aqueous systems and thus electrochemistry of organic compounds has been primarily limited to nonaqueous solvent systems.

(2) Difficultly oxidizable or reducible substances. In all solvent systems there is a voltage window that is available for use. Beyond this voltage window one gets destruction of the solvent or the supporting electrolyte. In aqueous systems on the anodic side one usually gets the formation of oxygen and on the cathodic side one gets the evolution of hydrogen. These windows limit the number of compounds that can be analyzed electrochemically in aqueous solutions.

Surfactants have been shown, in a number of cases (1-6), to be capable of overcoming both of these problems. There have been several reviews of the use of surfactants in electroanalytical chemistry (7-13). Surfactants are known to aid in the suspending of insoluble substances in the form of micelles and emulsions and this has been a common use in analytical chemistry. In addition, acting as hydrotropic salts, they have been used to increase the solubility of organic compounds not only for analysis but also for

synthesis reactions, such as the commercial dehydrodimerization of acrylonitrile to adiponitrile (14-16). However, the property that has been of most interest in our laboratory has been the ability of surfactants to film an electrode and to convert it from a hydrophilic surface on which the water can be easily electrolyzed to a hydrophobic surface which inhibits water from getting to the electrode. In essence on an electrode coated with a hydrophobic film one is able to do a nonaqueous electrolysis in an aqueous solution. Thus, one can increase the potential needed to oxidize water and, by increasing the voltage window, one can increase the number of compounds that can efficiently be oxidized in aqueous systems.

The effect of film formation on voltammetric curves.

Addition of anionic or neutral surfactants to aqueous solutions causes only slight changes in the oxidation potential for formation of oxygen (1-3). However, cationic surfactants increase the oxidation potential markedly. It was concluded that the increase is caused by the presence of a hydrophobic film formed by ion pairing of the surfactant ions with the strongly adsorbed anions on the anode surface. In the first voltammetric curve the surfactant undergoes oxidation, as shown by an oxidation peak, but, after several oxidation voltage sweeps, this large oxidation peak decreases to a small steady state indicating the formation of a film. This hydrophobic film blocks water from the electrode and increases the water oxidation potential. In the case of Hyamine 2389 (predominantly methyldodecyltrimethyl ammonium choride) the increase is 0.9v. If one stabilizes the Hyamine 2389 film by codepositing it with polystyrene, so that it can not desorb readily, one observes a very low residual current and the decomposition potential of water is increased by another 0.7 v (3). These films, however, are only held to the electrode by the layer of adsorbed anions, and if one sweeps the potential in the cathodic direction one observes a desorption peak at about - 0.6v, and one has to start all over again reoxidizing to make the stable film. It is interesting to note that these useful films have only been made

using cationic surfactants in the study of anodic reactions. It has not been possible, as yet, to develop corresponding surfactant films to increase the reduction window for cathodic reactions.

This increase in the anodic voltage window allows one to do voltammetric studies in a potential region that has not been available before in aqueous solutions. Fig 1 shows the effect of Hyamine 2389 films on the voltammetric curve obtained for the oxidation of benzilic acid on a platinum anode in 2M sodium hydroxide. The acid is soluble in this solution so that the observed effects are attributable only to the filming of the electrode. It can be seen that without any surfactant present one observes no oxidation wave. In the presence of Hyamine 2389 alone one sees two distinct waves because the oxidation potential for water has been increased. In fact, since the normal oxidation potential for water in the sodium hydroxide-Hyamine system is about 1.6v, it is evident that the product formed in the second oxidation wave also forms an insoluble film increasing the oxidation potential of water further to about 2 volts. In the Hyamine polystyrene system the oxidation potential of water is shifted to about 2.5v. One can now observe 3 distinct waves. The fact that styrene acts as a free radical trap however shifts the potential of the waves. The surfactant films alone and with the stabilizing polystyrene greatly increase the number of compounds that one can study by voltammetric techniques (2,3).

<u>The effect of the surfactant on characteristic oxidation potentials.</u>

One of the major problems that has existed in anodic voltammetry of organic compounds is the lack of an electrode system that will yield anodic half wave potentials that are characteristic of the oxidation potential of the organic compound. It has been shown that for platinum electrodes (17) the oxidation of most compounds proceeds through electrochemical oxidation of the platinum followed by chemical oxidation of the organic compound. As a result the oxidation potentials are clustered around the two potentials for formation of platinum oxides. When the electrode is filmed with surfactant one sees a

clustering around the potential of oxidation for the surfactant (3), indicating that the oxidation of a number of compounds occurs by electrooxidation of the Hyamine 2389 followed by a chemical reaction with the organic compound. However, it was also found (3) that in the surfactant systems there are a number of the waves that are characteristic of the compound indicating that this type of system can increase the number of compounds that can qualitatively be identified by voltammetry.

Direct voltammetric analysis of solids.

Another area that is difficult to handle by conventional electrochemistry is the direct analysis of insoluble solids such as minerals. Conductive solids can in some cases be fashioned into electrodes (18-20) and some studies have been made by incorporating the solid in wax impregnated graphite electrode (21,22) but, in the main, electrochemical analysis and studies of solids start with the destruction of the solid. The surfactant suspensions furnish a method of studying the direct electrooxidation of solids. Again, the introduction of the surfactant has two effects, the solubilization of the solid and the inhibition of the destruction of water. In order to separate these two effects two type of cells were used (4-6). One cell was the standard three electrode bulk cell. The other cell was a two electrode sandwich cell in which the working electrode was a platinum foil electrode on which was placed a paste made from the insoluble solid and the supporting electrolyte (1M NaCl or 2M NaOH). On top of this was placed a filter paper moistened with the supporting electrolyte which separated the cathode from the paste. This was topped with a silver/silver chloride foil electrode. The effect of the surfactant in the bulk cell is a result of both solubilization and film formation, while in the sandwich cell there is no solubilization effect.

Fig 2 shows a typical comparison of the type of results obtained with the two cells. It can be seen that in the oxidation of molybdenum diselenide ($MoSe_2$) in 2N sodium hydroxide in the sandwich cell one sees only a small wave on the side of the oxygen

evolution wave without a surfactant (curve A), but with the surfactant present one sees three distinct waves (curve C) (These waves have been shown, in order of occurence, to be caused by oxidation to (1) MoO_2 + Se; (2) MoO_3 + SeO_3^{-2}; and (3) MoO_3 + SeO_4^{-2}). However, in the bulk solution cell, even though the surfactant extends the voltage range, one sees only one oxidation peak. Apparently in the oxidation of the $MoSe_2$ a product is produced in this one peak that is solubilized in the surfactant suspension, and, thus, it does not remain at the electrode interface for further oxidation.. On the other hand, in the oxidation of galena (PbS) (5) one observes four waves for the production of S, $PbSO_3$, $PbSO_4$ and PbO_2, both in the bulk and sandwich cells. All of these are insoluble and remain on the electrode so that one observes the same number of waves in both sandwich and bulk solution cells.

Qualitative voltammetric analysis of solid systems such as minerals has one severe drawback. When trying to identify one ore out of a series, as for example would be necessary in identifying a specific sulfide ore, one must compare a series of sulfides to determine what the interferences are. However, the first oxidation wave destroys the crystal structure and from that point on one observes (Table 1) essentially the same potentials for the waves for the oxidation of the sulfur species in the sulfide compounds. The only types of sulfides in which one can observe major differences are cases in which the metal component undergoes an oxidation (6).

Table I. Half Wave Potentials for the Oxidation of Several Sulfides in the Sandwich Cell. Supporting Electrolyte-2N NaOH, Pt Working Electrode, Ag/Ag Cl Counterand Reference Electrodes.

	Half-wave Potential (V)		
Insoluble Sulfide	$S^{-2} \rightarrow S^{o}$	$S^{o} \rightarrow SO_3^{-2}$	$SO_3^{-2} \rightarrow SO_4^{-2}$
MnS	0.40	0.79	1.86
NiS	0.63	0.82	1.83
PbS	0.52	0.83	1.13 *

*The product in this case is the insoluble $PbSO_4$, not the soluble SO_4^{-2} therefore the oxidation potential is different.

Voltammetry of different types of inorganic compounds.

Obviously in pure ionic binary solids such as the previously described oxides, sulfides, selenides and tellurides (5, 6), where the bonding is primarily electrovalent and the electrons have been transferred from one element to the other, one expects to be able to observe waves for the oxidation of the reduced anion back to the free element. In many cases, because the potential range available is so large, one can oxidize both the cation and anion to higher oxidation states. Thus in the $MoSe_2$ case (Fig 2) one can observe waves for the oxidation to higher oxidation states of molybdenum and selenium. In some cases these states are higher than are normally expected to exist in aqueous solutions. Thus one can form nickel (III), copper (III), manganese (III), barium superoxide, bismuth (V) and antimony (V). Some of these are quite unstable in aqueous solutions, but the formation of insoluble compounds and the presence of the surfactant inhibits the reaction of the higher oxidation states with water, stabilizing them long enough so that they can be utilized in reactions with other compounds in the solution. Thus in Fig 3 one observes, in the oxidation of manganese (II) oxide, two oxidation waves. Coulometric measurements

shows that the number of faradays per mole (n) corresponds to the formation of manganese (III) in the first wave and manganese (IV) oxide in the second wave. Table II shows coulometric values obtained for the formation of several higher oxidation states.

Table II Coulometric Values of the Number of Faradays Per Mole (n) of Compounds Oxidized to form Higher Metal Oxidation States in the Sandwich Cell.

Reactant	Major products	Theoretical n	Experimental n	Avg. Dev From Mean
PbSe	$PbO_2 + SO_4^{-2}$	10	9.65	0.12
NiS	$NiO\text{-}OH + SO_4^{-2}$	9	8.96	0.13
MnS	$MnO_2 + SO_4^{-2}$	10	9.97	0.06
MoS_2	$MoO_3 + SO_3^{-2}$	14	13.99	0.12
CuO	Cu (III) oxide	1	1.03	0.03
MnO	Mn (III) oxide	1	1.2	0.1
MnO	MnO_2	2	2.1	0.3
BaO_2	BaO_2^+	1	0.91	0.01

With nonionic compounds that are insulators, where the electrons can not readily flow from one atom to the other, one would expect to observe separate oxidation waves for each element with their potentials shifted from the position for the element. This is what is observed with silicon carbide (Fig 4). In cases where the products are soluble or conductive one can do coulometry and charactize the reaction. In cases where the products are insoluble insulators one does not obtain complete oxidation and thus the coulometric experiments are meaningless. This is true with silicon carbide, however one can compare half wave potentials and get an idea of which component is oxidized in each voltage region.

Quantitative Analysis

Once one has obtained a voltammetric curve for a compound one should be able to use the height of the voltammetric peak or wave as a quantitative measure of the concentration of the substance in the system (2,23). Fig 5 shows typical calibration curves, indicating that this is possible.

In the quantitative analysis of solid systems, however, a complication arises. In studies of the oxidation of galena and iron pyrite when the surfactant concentration was above the critical micelle concentration (CMC) (4,5) plots of the height of the major voltammetric peak against the weight of solid added were not linear. Instead they were composed of several regions. The curve at higher concentrations of the solid is what would normally be expected from a situation in which the reactive species is a complex between the micelle and the solid. There is a regular rise eventually reaching a level region. The results can be explained with a simple Langmuir adsorption isotherm. However, at lower concentrations of the solid there is a periodic rise and fall in the curve. This was attributed to the formation of surfactant multilayers, either on the electrode or on the solid. The rate of oxidation varies as the electrode shifts back and forth between a hydrophilic and a hydrophobic surface. This periodic behavior has been observed in several heterogeneous processes (24-27).

One can develop a quantitative method of analysis for the solid or for components in the solid either by using the latter part of the curve or by dropping the concentration of the surfactant below the CMC (28). It has been shown that the technique of using surfactant concentrations below the CMC can be used for the analysis of lead in dried paint. Below the CMC the plot of the height of the peak vs the concentration of lead in the solid paint was linear. The results obtained by this method agreed reasonably well with results obtained on the solid paint sample using X-ray fluorescence. At present, insoluble samples, especially solids, often must undergo an extensive pretreatment process in order to put them in solution for analysis. The use of the surfactant suspension would be a

convenient method for analysis of solids in that all that is necessary is to grind the material to a powder, suspend it, equilibrate it, and then run the voltammetric curve,

Coulometric analysis.

Once one obtains voltammetric curves one can then select potentials and make controlled potential coulometric studies. The sandwich cell has shown itself to be particularly useful for these studies (4-6). Since the size of the sample in the sandwich cell is quite small the time to make a coulometric study is much less than the time needed in a bulk solution cell. Table II shows coulometric results for a series of solids measured in the sandwich cell. It can be seen that the method gives consistent results that can be used in the study of the oxidation of the solids.

Another question that arises in coulometric analysis is whether one can separate different reactions that occur with the same compound. Table III shows results obtained with molybdenum diselenide. One can see, that controlled potential coulometric studies give results that agree very well with the expected results from the reaction showing that one can readily separate the reactions in this system.

Table III. Coulometrically Determined "n" Values and Reactions Associated with each Wave in the Oxidation of Molybdenum (IV) Selenide on a Hyamine 2389 Electrode.

Wave #	Average n	Reactions	Oxidation Potential (V)
1	4.00±0.12	$MoSe_2+4OH^- \rightarrow MoO_2+2Se^0+2H_2O+4e^-$	0.83
2	13.97±0.24	$MoSe_2+18OH^- \rightarrow MoO_3+2SeO_3^{2-}+9H_2O+14e$	1.80
3	17.89±0.26	$MoSe_2+22OH \rightarrow MoO_3+2SeO_4^{2+}11H_2O+18e-$	2.17

Summary

Because of the ability of cationic surfactants to solubilize difficultly soluble materials in aqueous systems and to increase the oxidation potential of water by the formation of a film on the anode it has been possible to perform anodic voltammetric and coulometric analyses of insoluble, difficultly oxidizable compounds.

Acknowledgment

Appreciation is expressed to the Robert A. Welch Foundation of Houston and Mitsui Toatsu Chemicals, Inc., for the financial assistance given to this research.

REFERENCES

(1) Franklin, T.C.; Sidarous, L. J. Electrochem. Soc., 1976, 124, 65-69.

(2) Franklin, T.C.; Iwunze M. Anal Chem, 1980, 52, 973-976.

(3) Franklin, T.C.; Ohta, M. Surface Technology, 1982, 18, 63-76 .

(4) Franklin, T.C.; Nnodimele, R.; Adeniyi, W.K. J. Electrochem. Soc., 1987, 134, 2150-2154 .

(5) Franklin T.C.; Nnodimele, R.; Adeniyi W.K.; Hunt, D. J. Electrochem. Soc., 1988, 135, 1944-1947 .

(6) Franklin, T.C.; Adeniyi, W.K.; Nnodimele, R. J. Electrochem. Soc., 1989, 137, 480-484 .

(7) Hinze, W.L. In Solution Chemistry of Surfactants; Mittal, K.L., Ed.; Plenum Press, New York, 1979,Vol. 1, pp.79.

(8) Shinozuka, N.; Hayano, S. In Solution Chemistry of Surfactants; Mittal, K.L., Ed.; Plenum Press, New York, 1979,Vol. 2, pp. 599-623.

(9) Love, L.J.C.; Habarta, J.G.; Dorsey, J.G. Anal. Chem.,1984, 56, 1133A-1134A, 1136A, 1138A, 1140A, 1142A, 1144A, 1146A, 1148A.

(10) Pelizzetti, E.; Pramauro, E. Anal. Chim. Acta, 1985, 169, 1-29.

(11) McIntire, G.L. Amer. Lab., 1986, 173-4, 176-8, 180.

(12) Malik., W.U.; Chand, P; Saleem, S.M. Talanta, 1968, 15, 133.

(13) Franklin, T.C.; Mathew, S. In Surfactants in Solution; Mittal, K.L., Ed.; Plenum Press, New York, 1989, Vol 10, pp. 267-286.

(14) Baizer, M.M. J. Electrochem. Soc., 1964, 111, 215-226.

(15) Childs, W.V.; Walters, A.C. AICHE Symp. Ser., 1979, 75, 19-25.

(16) Lund, H. In Organic Electrochemistry, Baizer, M.M., Lund, H., Ed.; Second Edition, Marcel Dekker, Inc. New York, N.Y., 1983, Pg. 195.

(17) Franklin T.C.; Liang, C. Electrochim. Acta, 1964, 9, 517-530.

(18) Gardner, J.R.; Woods, R.J. J. Electroanal. Chem. 1979, 100, 447-459.

(19) Paul, R.L.; Nichol, M.J.; Diggle, J.W.; Saunders, A.P. Electrochim. Acta, 1978, 23, 625-633.

(20) Hamilton, I.C.; Woods, R. In Electrochemistry in Mineral and Metal Processing; Richardson, P.E.; Srinivasan S.; Woods, R., Eds. The Electrochem. Soc. Pennington, N.J., 1984, pp. 259-285.

(21) Anh, J.H.; Wadsworth, M.E. In Electrochemistry in Minerals and Mineral Processing II; Richardson, P.E.; Woods, R., Eds.; The Electrochem. Soc., Pennington, N.J., 1988, pp.280-302.

(22) Ahlberg, E.; Broo, A.E. In Electrochemistry in Mineral and Mineral Processing II; Richardson, P.E.; Woods, R., Eds.; The Electrochem. Soc., Pennington, N.J. 1988 pp. 36-48.

(23) Franklin, T.C.; Iwunze, M. J. Electroanal. Chem., 1980, 108, 97-106.

(24) Franklin, T.C.; Iwunze, M. J. Amer. Chem. Soc., 1981, 103, 5937.

(25) Franklin, T.C.; Ball, D.; Rodriquez, R.; Iwunze, M. Surface Technology, 19084, 21, 223-231.

(26) Franklin, T.C.; Adeniyi, W.K. Analytical Chimica Acta, 1988, 207, 311-317.

(27) Franklin, T.C.; Aktan, A. J. Electrochem Soc, 1988, 135, 1635-1638.

(28) Franklin, T.C.; Nnodimele, R. Anal. Chim. Acta, 1990, 229, 291-294.

LIST OF FIGURES

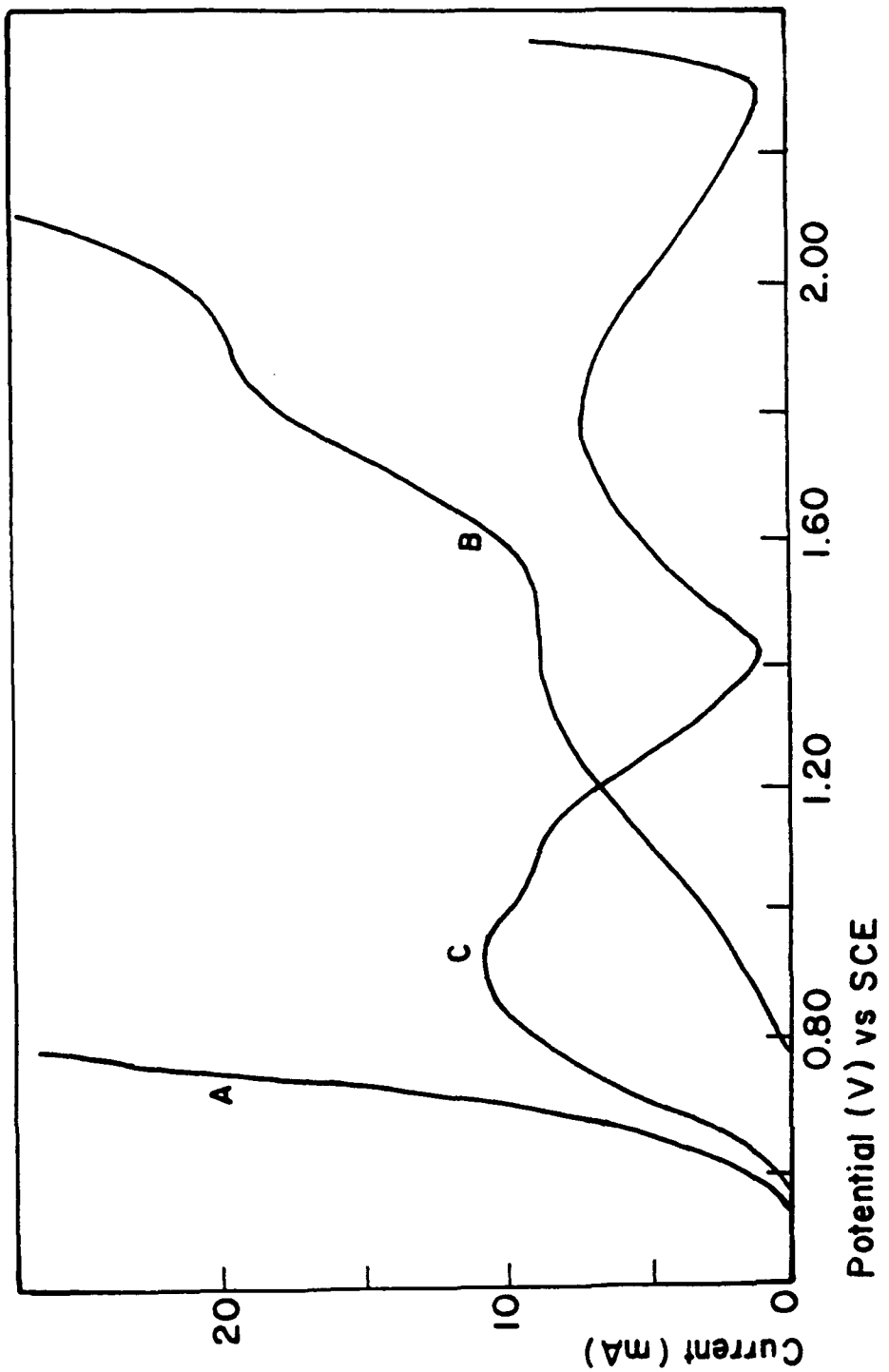
Current (mA)
20
10
0
0.80
1.20
1.60
2.00
Potential (V) vs SCE
A
B
C

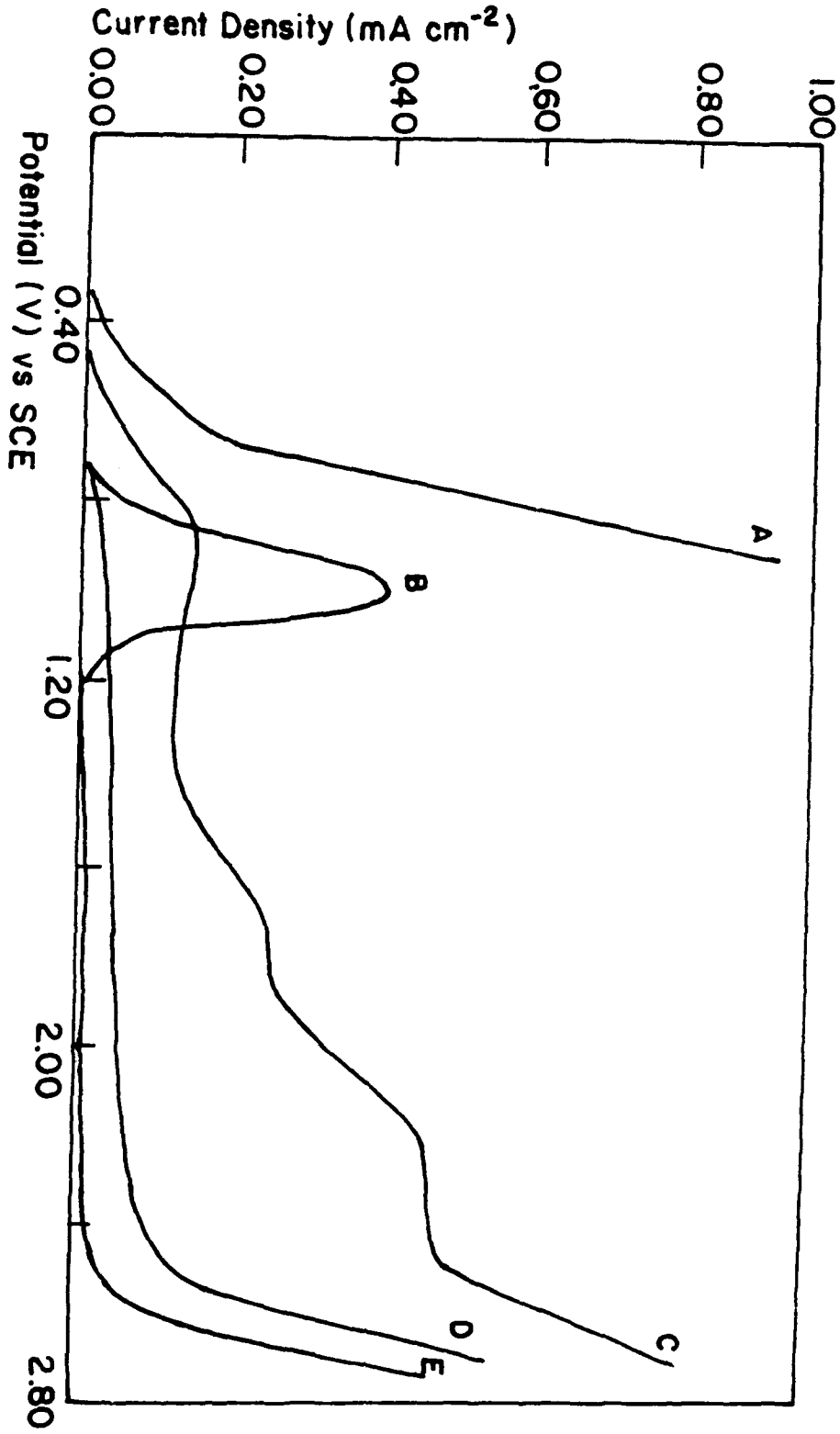
Current Density (mA cm^{-2})
0.00
0.20
0.40
0.60
0.80
1.00
Potential (V) vs SCE
0.40
1.20
2.00
2.80
A
B
C
D
E

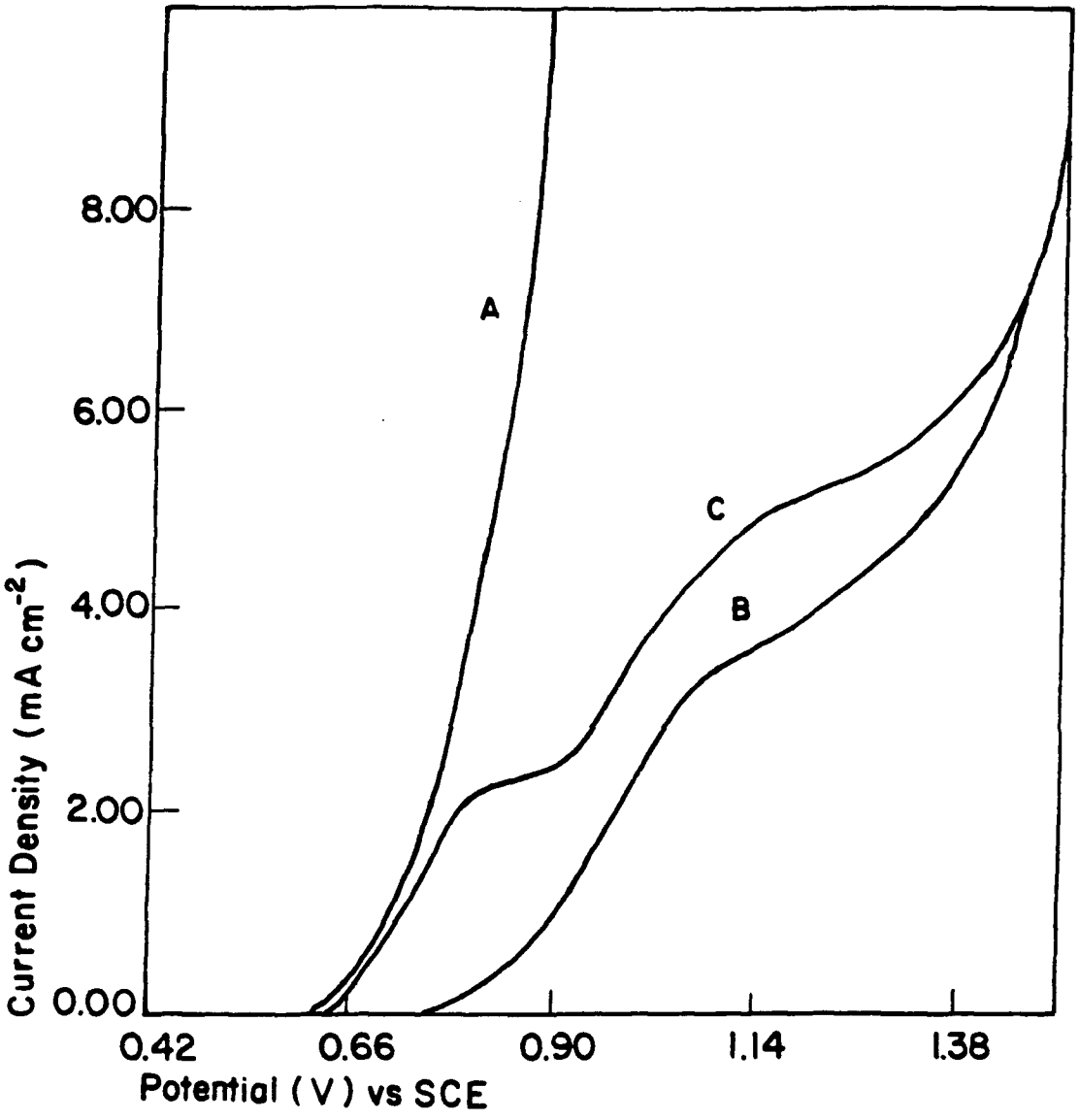
8.00
6.00
4.00
2.00
0.00
Current Density (mA cm^{-2})
A
B
C
0.42
0.66
0.90
1.14
1.38
Potential (V) vs SCE

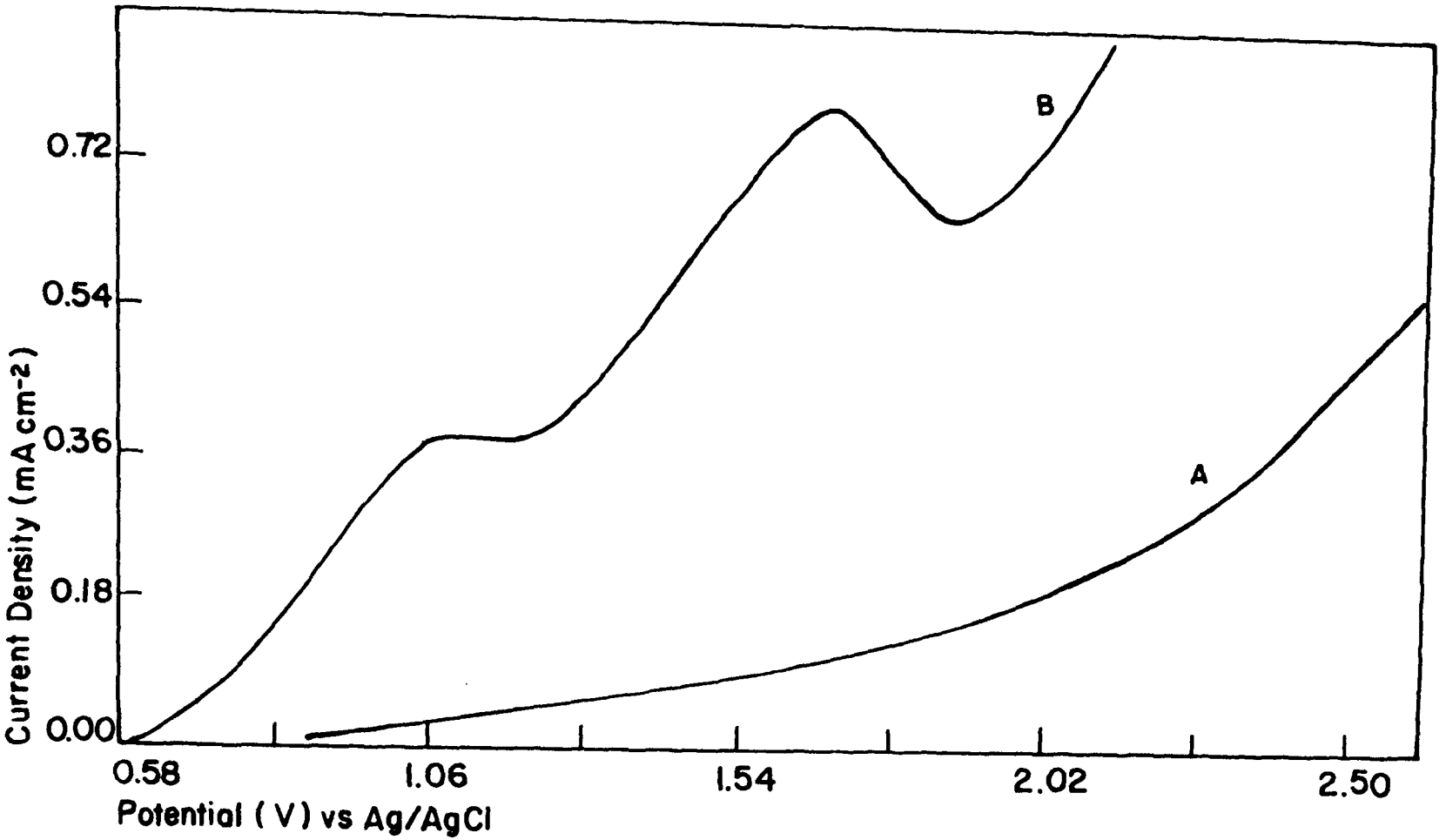
B
A
0.72
0.54
0.36
0.18
0.00
Current Density (mA cm-2)
0.58
1.06
1.54
2.02
2.50
Potential (V) vs Ag/AgCl

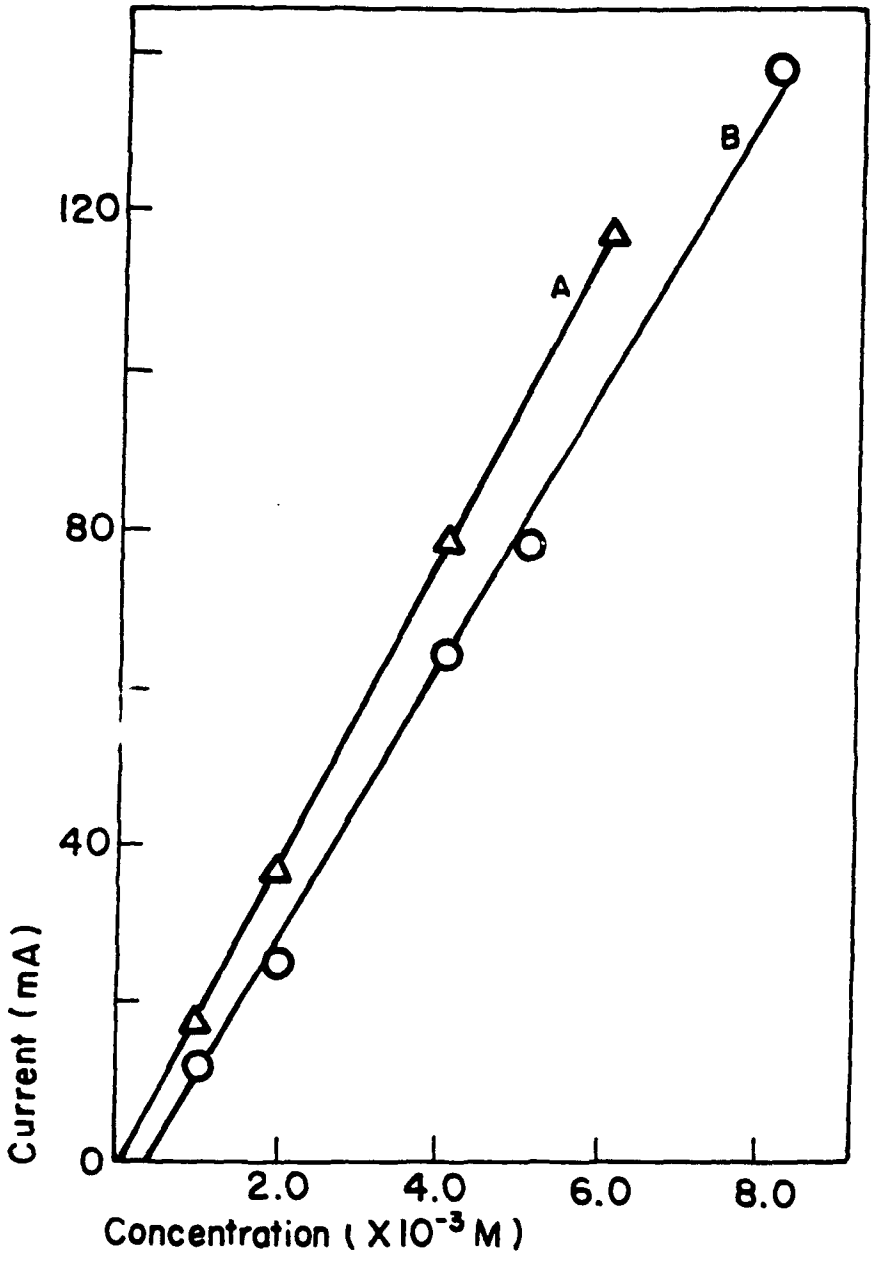
120
80
40
0
Current (mA)
A
B
2.0
4.0
6.0
8.0
Concentration (X 10⁻³ M)

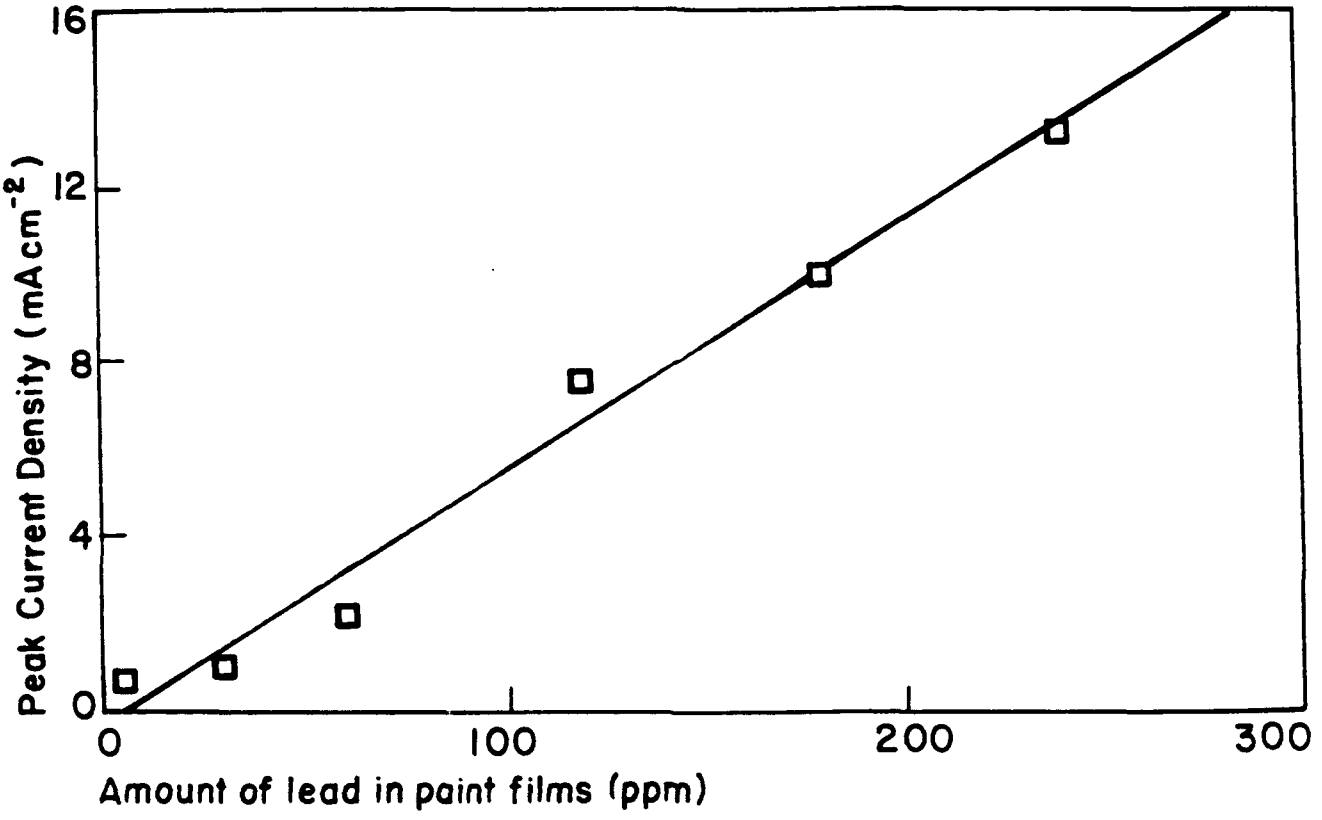
16
12
8
4
0
Peak Current Density (mAcm^{-2})
0
100
200
300
Amount of lead in paint films (ppm)

(3) # Electrochemical and Spectroelectrochemical Measurements in Sodium Dodecyl Sulfate Micellar Solution as a Function of Electrolyte Concentration

by

Jon R. Kirchhoff*, John D. Skelton, Jr., and Kregg T. Brooks

Department of Chemistry, University of Toledo, Toledo, Ohio 43606

INTRODUCTION

Micellar solutions have shown promise and utility for a wide variety of applications. The unique amphiphilic structure of surfactants and their aggregation properties in aqueous solution provide a multifunctional environment for the solubilization and partitioning of aqueous soluble and insoluble solute molecules. As a result, micellar solutions have been used in many areas of chemistry for analysis (1-5), the control of reactivity (6), and as models for biological membranes or systems (7). Further advantages of micellar media can also be envisioned in terms of their cost, toxicity, and disposal relative to an organic based medium.

Electroanalytical measurements have also benefitted from the use of surfactant solutions. Initial applications have used surfactants to enhance the selectivity and sensitivity of quantitative determinations of inorganic complexes (8,9), and for the suppression of current maxima in polarographic measurements (10). More recently, micellar solutions have been effectively used in electrocatalysis (11-14) and thin film formation (15-18).

Our research has focused on obtaining electrochemical data in aqueous solutions for aqueous insoluble inorganic complexes, and in particular understanding the factors that influence the electron-transfer process that occurs between a micelle solubilized metal complex and an electrode (19-20). Initial results have indicated that the voltammetric behavior was very dependent on the (i) surfactant, (ii) lipophillicity of the coordinated ligand environment, (iii) charge of the complex, and (iv) nature of the supporting electrolyte (19 The influence of added electrolyte on voltammetric measurements has prompted this more detailed study on the effect of added electrolyte

on electrochemical and spectroelectrochemical measurements of $[Re(dmpe)_2Cl_2]^+$ in dodecyl sulfate micelles.

EXPERIMENTAL

Materials. $[Re(dmpe)_2Cl_2]^+$, where dmpe is 1,2-bis(dimethylphosphino)ethane, was prepared as the PF_6^- or $CF_3SO_3^-$ salt by a literature procedure (21). Sodium dodecyl sulfate (SDS) from Boehringer Manheim or BDH Laboratories was used as received with identical results. Polarographic grade tetramethylammonium perchlorate (TMA^+), tetraethylammonium perchlorate (TEA^+), tetra-*n*-butylammonium perchlorate (TBA^+), and tetra-*n*-hexylammonium perchlorate (THA^+) were obtained from G. F. Smith Chemicals. The electrolytes were dried over P_2O_5 in a vacuum oven for approximately 4 h at 80 °C. Orange OT, Solvent orange 2[1-(*o*-tolylazo)-2-napthol, was obtained from Aldrich and used as received. Solutions were prepared with distilled deionized water purified by a Barnstead Organicpure filtration system. All other chemicals were of reagent grade quality.

Instrumentation. Voltammetric measurements were made with a Bioanalytical Systems Inc. BAS-100A electrochemical analyzer. Voltammograms were recorded on a Houston Instruments DMP-40 plotter. The potentiostat for the spectroelectrochemical measurements was a BAS CV-1B. The potentials were monitored in the spectroelectrochemical experiments by a Keithley 178 digital multimeter. The working electrode for voltammetry was a glassy carbon electrode (GCE (BAS)), while the spectroelectrochemical measurements used a optically transparent thin-layer electrode (OTTLE). The OTTLE cells were constructed with 100 wires/in Au minigrid by the method of DeAngelis and Heineman (22) An aqueous Ag/AgCl (3 M NaCl) electrode (BAS) and

a platinum wire were used as the reference and auxiliary electrodes, respectively. All potentials are reported versus the Ag/AgCl (3 M NaCl) electrode. Absorption spectra were obtained with a Hewlett-Packard 8452A UV-vis diode array spectrophotometer, which was modified for incorporation of the spectroelectrochemical cell and an inert gas inlet.

Methods. Critical micelle concentrations (cmc) as a function of electrolyte were determined at 25 °C by the solubilization of Solvent Orange OT. At each electrolyte concentration a series of SDS solutions were prepared to bracket the cmc. To the surfactant and electrolyte solution, an excess of Orange OT was added and the solutions were allowed to agitate in a thermostated shaker bath. After at least 36 h, the solutions were filtered with 0.45 μm pore syringless filters (Whatman) and the absorbance at 496 nm was measured. The values of cmc were determined from a plot of the absorbance versus the surfactant concentration. Electrolyte concentrations were as follows: TMA^+: 0.005, 0.010; TEA^+: 0.0, 0.005, 0.010, 0.025, 0.050, 0.100, 0.150; TBA^+: 0.005, 0.010; THA^+: 0.005, 0.010.

Spectroelectrochemistry measurements were conducted by established procedures (23). Each spectrum in the spectropotentiostatic experiments was recorded 10 mins after potential application to ensure equilibrium values of [O]/[R] in the thin-layer cell. The GCE working electrode was polished with alumina between electrochemical measurements to ensure a reproducible surface. Deoxygenation was accomplished by an argon purge in the voltammetric measurements at the GCE or by reduction of O_2 to H_2O in the thin layer cell. 0.1 M SDS solutions with the appropriate electrolyte concentration were prepared for voltammetry and spectroelectrochemistry by dilution of standard stock solutions. The

micelle concentration (24) is estimated to be approximately 1.5 mM. The ratio of $[Re(dmpe)_2Cl_2]^+$ to micelle was maintained at approximately 1 for all solutions.

RESULTS

Voltammetric Measurements in SDS. Typical Osteryoung square wave voltammograms and the corresponding cyclic voltammograms (0.1 M SDS, 0.1 M TEA^+ and Na^+) are shown in Figure 1. The peak potentials from square wave voltammetry are used for comparison purposes due to the poorly defined cathodic wave observed for the Re(III) to Re(II) reduction in several cyclic voltammograms. These results are summarized in Table I. Cyclic voltammograms of 1.5 mM $[Re(dmpe)_2Cl_2]^+$ in 0.1 M SDS as a function of added TEA^+ are shown in Figure 2. The peak current from square wave voltammetry is observed to increase as the concentration of TEA^+ increases.

Spectroelectrochemical measurements were also performed as a function of electrolyte in 0.1 M SDS. The results are also summarized in Table I. The spectropotentiostatic reduction of a 1.5 mM solution of $[Re(dmpe)_2Cl_2]^+$ in 0.1 M SDS/0.100 M TEA^+ is shown in Figure 3, and is considered representative of the series. Absorption maxima for the Re(III) complex occur at 408 and 436 nm. The Re(II) maxima are shifted to higher energy and are observed at 390 and 342 nm. The two redox states interconvert about an isosbestic point at 399 nm, which indicates the chemical stability of both redox states in the medium. A Nernst plot (22) E_{app} vs. log([O]/[R]), for the data at 436 nm in Figure 3 is linear and yields $E^{o'}$ = -0.598 V and n = 1.03. The absorption

maxima and isosbestic point are relatively constant (±1 nm) for each TEA^+ concentration.

DISCUSSION

Electrochemistry Characteristics of the $[Re(dmpe)_2Cl_2]^+$ Redox Probe. The electrochemistry of $[Re(dmpe)_2Cl_2]^+$ in nonaqueous solvents has been characterized by two reversible one-electron reductions as indicated by Eqns. 1 and 2 (25). In aqueous solution $[Re(dmpe)_2Cl_2]^+$ is only slightly

$$[Re(dmpe)_2Cl_2]^+ + e^- \rightleftharpoons [Re(dmpe)_2Cl_2]^o \quad (1)$$

$$[Re(dmpe)_2Cl_2]^o + e^- \rightleftharpoons [Re(dmpe)_2Cl_2]^- \quad (2)$$

soluble, and when reduced, $[Re(dmpe)_2Cl_2]^o$ precipitates on the electrode surface and irreversible electrochemistry is observed. However in 0.1 M TEA^+ not only is the solubility of the cationic form enhanced, but the electrogenerated neutral complex is stabilized by the presence of micelles, and thus solubilized. This results in diffusion controlled reversible cyclic voltammograms (19). For this reason and the fact the $[Re(dmpe)_2Cl_2]^{+/o}$ complexes exhibit ligand-to-metal charge-transfer bands (LMCT) in the visible with molar absorptivities of approximately 3000 M^{-1} cm^{-1}, $[Re(dmpe)_2Cl_2]^+$ is an excellent choice as an electrochemical and spectroelectrochemical probe of micellar solutions.

Electrolyte Effects. Heterogeneous electron-transfer of redox active solution species is a multi-step process. Each step can be influenced by the addition of a surfactant and the formation of micelles with the cumulative effect being the result of an interplay among several competing thermodynamic and kinetic factors. Addition of supporting electrolyte to micellar solutions further complicates the interpretation of

electrochemical data. In general, electrolytes do not directly participate in electrochemical processes. However in micellar solution,it is well documented that the addition of electrolyte can significantly alter the micellar structure and properties (6, 26). A change in the micellar structure can influence how solute molecules are solubilized by the micelle and in turn alter the electron-transfer properties. The peak potential for the Re(III/II) couple of $[Re(dmpe)_2Cl_2]^+$ shifts to more negative potentials in 0.1 M SDS (-0.659 V) as compared to 0.5 M KNO_3 (-0.516 V) (19). The fact that the complex is harder to reduce in SDS has been attributed to the net stabilization of the cationic complex in the anionic micelle (19). When the concentration of TEA^+ is increased, the data in Table I indicates a clear shift in the E_p from square wave voltammetry or $E^{o'}$ values from spectroelectrochemistry to more positive potentials occurs.In addition, the cyclic voltammograms of Figure 2 show (i) the appearance of the reduction wave out of the background , (ii) a gradual increase in the peak currents, and (iii) i_{pc}/i_{pa} values which approach unity at 0.1 M TEA^+. Scan rate studies in 0.1 M TEA^+ and 0.1 M SDS indicate the electrochemistry of $[Re(dmpe)_2Cl_2]^+$ is diffusion-controlled and reversible based on the standard criteria for reversibility (27). As TEA^+ is added, an ion-exchange occurs at the surface of the dodecyl sulfate micelles. Almagren and Swarup (28) have studied this exchange by fluorescence quenching and concluded that the exchange of TEA^+ for Na^+ results in a more closely packed micellar environment since the larger TEA^+ cation can act as a spacer and prevent repulsions between the negatively charged surfactant head groups. Berr and coworkers (29) have reached similar conclusions from neutron scattering experiments with TMA^+ with SDS. The electrochemical results in Table I and Figure 2 are consistent with this interpretation. A change in the micellar environment from

the more open structure of SDS to the mo... ..osely packed structure of TEADS is consistent with the observation that the potential shifts more positive toward the value observed in 0.5 M KNO_3/H_2O. At low TEA^+ concentrations, $[Re(dmpe)_2Cl_2]^+$ may have significant interactions with the hydrophobic micelle core, but as the micelle structure becomes more compact the solubilization may be primarily on the aqueous periphery of the micelle. Consistent with this is the fact that the current increase at higher TEA^+ concentrations signifying a enhance rate of electron transfer.

An advantage of the spectroelectrochemistry measurements is that simultaneous electrochemical and spectroscopic information can be obtained. Absorption spectroscopy can be very sensitive to the changes in the solubilization environment of optical probes. In the case of $[Re(dmpe)_2Cl_2]^+$, the absorption bands are insensitive to the changes in the solubilization environment. The orbitals responsible for the LMCT band originate on the Cl^- ligand rather than the more lipophilic phosphine. It is reasonable to assume that solubilization in the hydrophobic region occurs through interactions the phosphine ligand and thus has limited effect on the energy of the absorption bands.

REFERENCES

1) McIntire, G.L.; *Critical Rev. Anal. Chem.* **1990**, *24*, 257.

2) Pramauro, E.; Pelizzetti, E. *Trends Anal. Chem.* **1989**, *7*, 260.

3) *Ordered Media in Chemical Separations*; Hinze, W.; Armstrong, D.W., Eds.; ACS Symposium Series 342; American Chemical Society, Washington, DC, **1987**.

4) Pelizzetti, E.; Pramauro, E. *Anal. Chim. Acta* **1985**, *169*, 1.

5) Cline-Love, L.J.; Harbarta, J.G.; Dorsey, J.G. *Anal. Chem.* **1984**, *56*, 1132A.

6) Fendler, J.H.; Fendler, E.J. *Catalysis in Micellar and Macromolecular Systems*; Academic, New York, **1975**.

7) Fendler, J.H. *Membrane Mimetic Chemistry*; Wiley-Interscience: New York, **1982**.

8) Jacobsen, E.; Kalland, G. *Anal. Chim. Acta.* **1963**, *29*, 215.

9) Gundersen, N.; Jacobsen, E. J. *J. Electroanal. Chem.* **1969**, *20*, 13.

10) Meites, L. *Polarographic Techniques*, 2nd Ed.; Wiley Interscience: New York, **1965**.

11) Rusling, J.F. *Acc. Chem. Res.* **1991**, *24*, 75.

12) Kamau, G.N.; Rusling, J.F. *J. Electroanal. Chem.* **1988**, *240*, 217.

13) Rusling, J.F.; Shi, C.-N.; Gosser, D.K.; Shukla, S.S. *J. Electronal. Chem.* **1988**, *240*, 201.

14) Rusling, J.F.; Kamau, G.N. *J. Electroanal. Chem.* **1985**, *187*, 355.

15) Hosino, K.; Saji, T. *J. Am. Chem. Soc.* **1987**, *109*, 5881.

16) Saji, T.; Hoshino, K.; Aoyayui, S. *J. Am. Chem. Soc.* **1985**, *107*, 6865.

17) Saji, T.; Hoshino, K.; Aoyagui, S. *J. Am. Soc., Chem. Commun.* **1985**, 865.

18) Saji, T.; Ishii, Y. *J. Electrochem. Soc.* **1989**, *136*, 2953.

19) Kirchhoff, J.R.; Heineman, W.R. Deutsch, E. *Inorg. Chem.* **1988**, *27*, 3608.

20) Kirchhoff, J.R.; Heineman, W.R.; Deutsch, E. *Anal. Lett.* **1989**, *22*, 1323.

21) Vanderheyden, J.-L.; Heeg, M. J.; Deutsch, E. *Inorg. Chem.* **1985**, *24*, 1666.

22) DeAngelis, T.P.; Heineman, W.R. *J. Chem. Educ.* **1976**, *53*, 594.

23) Rohrbach, D.F.; Heineman, W.R.; Deutsch, E. *Characterization of Solutes in Nonaqueous Solvents*; Mamantov, G., Ed.; Plenium: New York, **1978**, 177.

24) [M] = ([S] - cmc)/A, where [M] = micelle concentration, [S] = total surfactant concentration, cmc = critical micelle concentration, and A = aggregation number[6].

25) Kirchhoff, J. R.; Heineman, W. R.; Deutsch, E. *Inorg. Chem.* **1987**, *26*, 3108.

26) Mukerjee, P.; Mysels, K. J. *Critical Micelle Concentrations of Aqueous Surfactant Systems*; National Bureau of Standards Report No. NSRDS-NBS 36; U.S. Government Printing Office: Washington, DC, **1971**.

27) Kissinger, P. T.; Preddy, C. R.; Shoup, R. E.; Heineman, W. R. In *Laboratory Techniques in Electroanalytical Chemistry*; Kissinger, P. T., Heineman, W. R., Eds.; Dekker: New York, **1984**; Chapter 2.

28) Almgren, M.; Swarup, S. *J. Phys. Chem.* **1983**, *87*, 876.

29)

FIGURE CAPTIONS

Figure 1. Comparative cylic voltammograms and square wave voltammograms of 1.5 mM $[Re(dmpe)_2Cl_2]^+$ in (A) and (B) 0.1 M Na^+/0.1 M SDS, and (C) and (D) 0.1 M TEA^+/0.1 M SDS.

Figure 2. Cyclic voltammetry of 1.5 mM $[Re(dmpe)_2Cl_2]^+$ in 0.1 M SDS as a function of TEA^+ concentration: (A) 0.000, (B) 0.005, (C) 0.010, (D) 0.025, (E) 0.050, (F) 0.100.

Figure 3. Spectropotentiostatic reduction of 1.5 mM $[Re(dmpe)_2Cl_2]^+$ in 0.1 M TEA^+/0.1 M SDS.

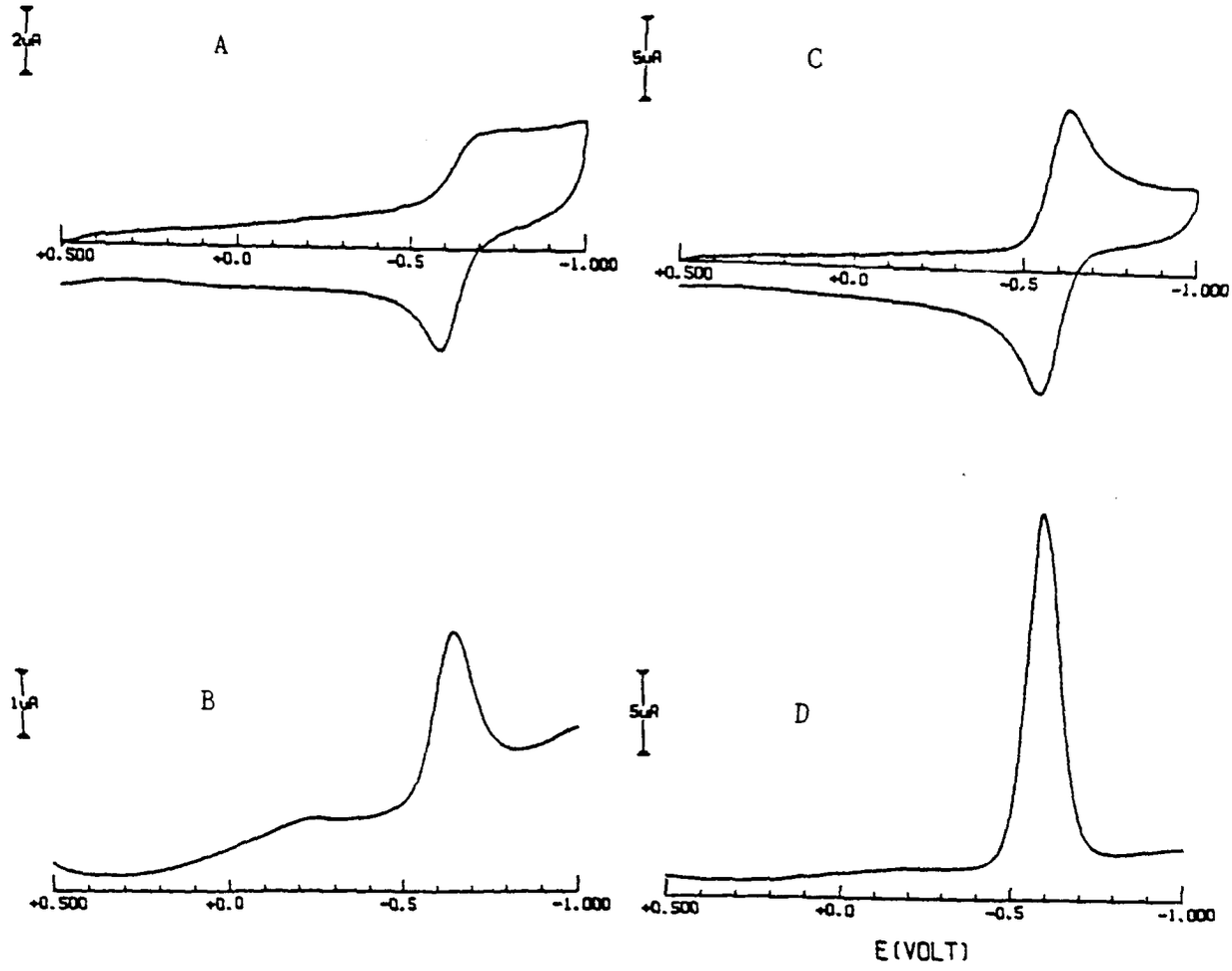
2μA
A
+0.500
+0.0
-0.5
-1.000
5μA
C
+0.500
+0.0
-0.5
-1.000
1μA
B
+0.500
+0.0
-0.5
-1.000
5μA
D
+0.500
+0.0
-0.5
-1.000
E(VOLT)

Figure 1.

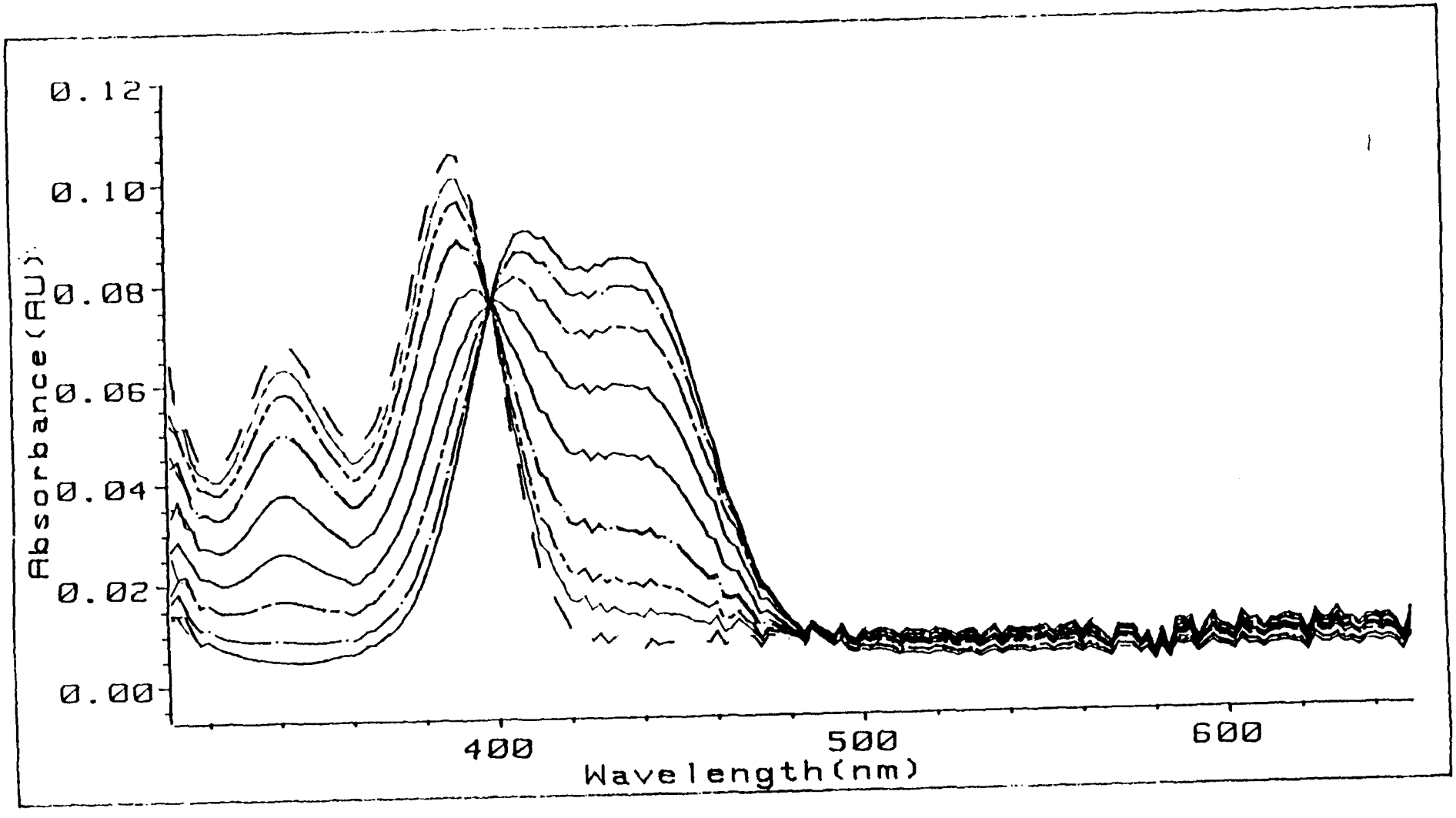
0.12
0.10
0.08
0.06
0.04
0.02
0.00
Absorbance(AU)
400
500
600
Wavelength(nm)

Figure 3.

96-I

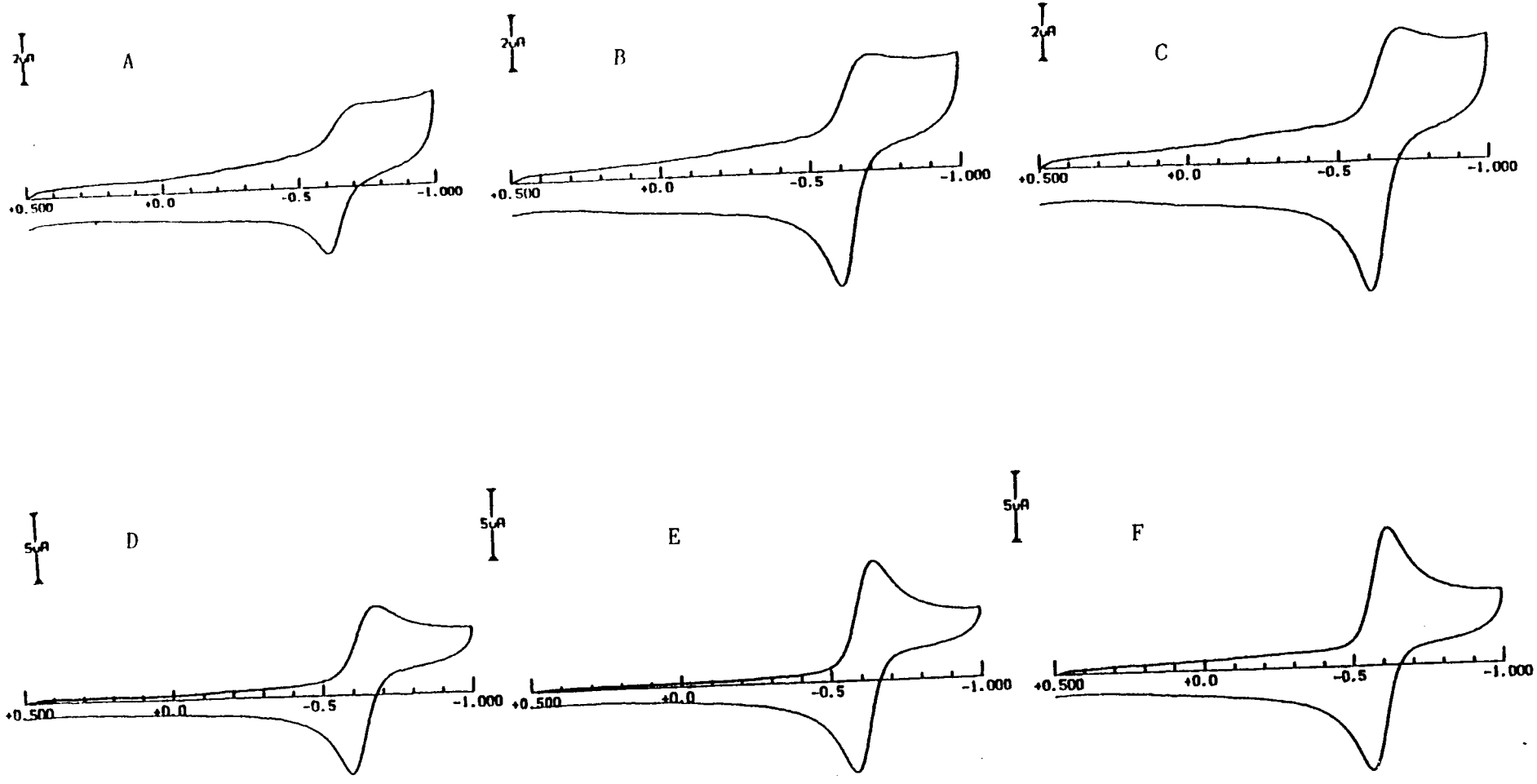

Figure 2.

TABLE I. Critical Micelle Concentrations and Electrochemical Data as a Function of TEA^+ Concenntration.[a]

$[TEA^+]$, M	cmc, mM	E_p[b]	$E^{o'}$[c]	n[c]
0.000	8.11	-0.659	-0.699	0.91
0.005	2.68	-0.637	-0.665	1.01
0.010	1.81	-0.632	-0.672	0.88
0.025	1.04	-0.624	-0.645	1.03
0.050	0.76	-0.608	-0.614	0.98
0.100	0.44	-0.588	-0.598	1.03
0.150	0.47	-0.580	-0.588	1.10

[a] 25 °C

[b] 0.1M SDS, Peak potential for $[Re(dmpe)_2Cl_2]^+$ from Osteryoung square wave voltammetry.

[c] 0.1M SDS, $E^{o'}$ and n determined by spectropotentiostatic reduction of $[Re(dmpe)_2Cl_2]^+$.

④ Electrified Immiscible Liquid Boundaries: Conventional and Microscopic Interfaces

Petr Vanýsek

Northern Illinois University, Department of Chemistry

DeKalb, IL 60115 (U.S.A.)

ABSTRACT

Transport studies on interfaces between immiscible phases bridges the field of heterogeneous electrode electrochemistry and that of homogeneous solution chemistry. Early work on liquid/liquid boundary was concerned with large area (square centimeter) interfaces. Recent work investigates phenomena on interfaces rendered in pores, capillaries and small holes. The behavior of such interfaces interfaces in the presence of dodecyl sulfate, forming micelles, is investigated. Voltammetry and amperometry on these small interfaces reveals that the accompanying voltammetric characteristics are similar to that of metal ultramicroelectrodes.

INTRODUCTION TO ELECTRIFIED LIQUID/LIQUID INTERFACES

Interfaces between two immiscible solutions containing ionic species are of interest to a broad spectrum of scientific disciplines, ranging from theoretical physical electrochemistry, to analytical application in sensor design, to the use in interpretation of processes occurring on the biological membrane level and in biological systems.

The interface between two immiscible electrolyte solutions (ITIES) was studied for the first time at least 100 years ago, when Nernst performed the first experiments that provide the theoretical basis for today's potentiometric and voltammetric studies of interfaces (1). In 1963 Blank and Feig (2) suggested that an interface between two immiscible liquids could be used in an approximation as a model for one–half of a biological membrane. Later Koryta et al. (3) noted, that ITIES should behave similarly to an interface between an electronic conductor (i.e., an electrode) and a bathing ionic solution. Experiments that followed revealed that this predicted similarity is indeed real and the field of experimental electrochemistry on ITIES became open.

The similarities between ITIES and electrode electrochemistry make available a pool of electrochemical techniques that have been previously well tested in more common electroanalytical chemistry. To understand the similarities in the behavior, it is more useful to look at the differences first. The Faradaic current that flows through an electrochemical cell is associated with redox processes occurring on the electrode surface. The analog of an electrode surface in ITIES is the interface itself. In that case, however, the net current observed when the interface is polarized from an outside electric source is not a result of a redox process at the interface. It is, rather an effect, that is caused by transport of ions

from one phase into the other through the interface. The overall macroscopic observable, current flow between two connecting electrodes, is the same in both cases. Once again, in L/L electrochemistry, it is the interface itself that is responsible for the manifested voltammetric behavior; there is no metal electrode and a redox pair in the ITIES system that give a rise to voltammetric behavior. This becomes more clear when when the typical voltammetric cell is considered (Fig. 1). The cell has provisions for connecting two reference electrodes, one on each side of the interface. This 2–reference electrode connection, that translates, in potentiostatic regime, to utilization of a 4–electrode potentiostat, is yet another difference between ITIES and electrode processes.

Total analysis of the closed circuit will of course reveal that redox processes occur in the system. But they take place on the two current supplying counter (or auxiliary) electrodes. As long as the potentiostat functions properly, polarization of these electrodes is inconsequential. Of course, care has to be taken to avoid any electrolysis products to enter the vicinity of the interface.

Common boundary between ITIES experiments and the studies of microdomains is in the experimentation with so called microinterfaces. The first liquid/liquid (L/L) microinterface was introduced by Taylor and Girault (4). In this experiment the L/L interface was supported on a capillary tip. The philosophy behind this approach is that diffusion to and from the small interface is governed by hemispheric, rather then linear symmetry. The same is observed with metallic ultramicrointerfaces, electrode discs with diameters below 10 μm. The advantage of the hemispheric diffusion is lower contribution of the *IR* drop and higher current densities at steady state in comparison with that of a large surface interface. The capillary support lacks the ideal geometry that would allow unhindered hemispheric diffusion on both sides of the interface. Inside the capillary the

diffusion is cylindrical. To remedy this problem more work has been done on interfaces supported on flat partitionings (5–8). The work on microinterfaces supported on a tip of a capillary continues to provide important kinetic results (9).

Study of microdomain systems benefits from another research field related closely to the work on microinterfaces. It is the area of microelectrodes, recently referred to as ultramicroelectrodes. This field is some 10 years old (10) and already enjoys a degree of maturity and recognition. The aim of manufacturing ever smaller electrodes, already relevant to the microheterogeneous dimensions resulted in constructing of a "nanoelectrode," (11) a metal electrode with almost atomic dimensions. Remarkable success in fabrication of minute size electrodes has been achieved by Martin (12) by growing miniature metal rods inside insulating tubules and by Potje–Kamloth et al. (13) by successful electrical insulation of a single carbon fiber by reliable electrical insulation via electropolymerization.

Because of the negligible contribution of *IR* drop on the small surfaces, these electrodes are suitable for kinetic measurements of fast rate processes requiring high voltammetric scan rates (14). Wightman (15) demonstrated practicality of scan rates up to 10^5 V.s^{-1}. Baranski (16) gave theoretical foundation for optimization of AC voltammetric measurements on microelectrodes. Taylor et al. (17) presented results obtained for digital simulation of charge transfer on microelectrodes.

Micelles in liquid/liquid interface systems

To make the ITIES electrochemical experiment work, both the aqueous and the nonaqueous solutions must contain dissolved salts. To dissolve a salt in a

nonaqueous phase, the molecule has to be relatively large (hydrophobic). Similarly, ions that produce signals on liquid/liquid interfaces are semihydrophobic species of intermediate Gibbs energy of transfer. Consequently, a number of molecules that are of interest to L/L work will have the properties of a surfactant.

Surfactant (surface active agent) molecules are molecules that possess both hydrophilic and hydrophobic moieties. They may aggregate under favorable conditions in water and form microscopic domains called micelles. The original description of these aggregates dates back to Hartley (18). The interest in this field has grown tremendously in the last several years. For example, in the period from 1980 to 1990 350 reviews (not primary articles) have been published on this subject (19). All fields of chemistry were touched by research of micelles. The most relevant to the studies done by us in liquid/liquid electrochemistry are the works on micelles in physical chemistry, analytical chemistry (20, 21) and, in particular, in electrochemistry. Recent review on analytical applications of micelles was given by McIntire (19) in 1990. The same author also presented a review on electrochemistry in micelles in 1986 (22). A monograph on the physical chemistry of micelles and microemulsions appeared recently (23). Electrochemistry remains an important tool of studying micellar systems. Polarography was used to measure micellar diffusion coefficients (24). Conductivity is used conveniently in studies of micelle formations (25), as well as, is voltammetry (26).

Micellar chemistry is important to the studies on L/L interfaces even in cases when micelles are not actively formed or pursued. The ITIES systems under study contain, by the necessity of dissolving lipophilic salts in organic solvent, amphiphilic species. Salts soluble in nonaqueous solvent, such as nitrobenzene, will be usually large (tetrabutylammonium, tetraphenylborate, cetyltrimethylammonium, dodecylsulfate). The lipophilic moiety responsible for solubility in

organic solvent can be well separated from the charged functionality responsible for salt dissociation, solution conductivity and electrochemical activity (cetyltrimethylammonium), or the charge can be localized inside bulky, symmetrical lipophilic structure (tetraphenylborate, tetraphenylarsonium, tetrabutylammonium). The first class of compounds will have the inherent tendency to form self–assembled aggregates or layers on the surface of interfaces with different hydrophilicities, whereas the second group, with higher symmetry, will be less prone to aggregation and surface adsorption. In the prevailing work on ITIES, it is not desirable to introduce a detergent (amphiphilic molecule) into the system. The typical experiment is based on charge transport studies across interface between two liquids. It is desirable to have this interface well defined. With a detergent present, there is always the danger that the interface will be perturbed and smeared out. However, in careful experiments where mechanical perturbation of the interface is absent, this rarely causes serious problem.

At low concentration of the surfactant in water, its molecules are simply dissolved and uniformly distributed throughout the solution. As the concentration is increased, the solution conductivity increases and the surface tension decreases. Upon reaching certain concentration of the surfactant, its molecules start to aggregate with the nonpolar tails of the molecule being packed together in the interior and the hydrophilic heads pointing outwards, forming roughly spherical objects. This aggregation occurs at a critical concentration, specific and different for each system and it is known as the critical micelle concentration (CMC). At concentrations above the CMC the concentration of unassociated surfactant remains virtually constant. Further addition of monomer causes increase in number of micelles. Thus surface tension remains virtually unchanged after the CMC. Similarly, the increase in conductance suddenly almost stops. It never levels

off though, because the micelles, whose concentration keeps increasing, also contribute to the overall conductivity. Due to their large size (low mobility), the contribution of the micelles to overall conductivity of the solution is quite small. The size of the micelles depends on the nature of the surfactant, for example an SDS micelle aggregate has a weight of 17,000, which corresponds to 59 monomers in the unit (27). The typical size for most micelles is between 60 and 100 monomers, typical size 3 to 6 nm. Therefore, the macroscopic solution behaves as homogeneous, filtration does not separate micelles, and the solution does not exhibit light scattering. The micelle itself is not a static entity; there is a dynamic exchange between the micelle and the solvated monomer. Replacement of the whole micelle takes place in the course of a millisecond to seconds.

Most often, micelles are formed within aqueous solutions, thus the hydrophilic moiety of the surfactant points outward. These micelles are called normal. In a mirror image situation, surfactants can also aggregate in nonpolar media, forming reverse or inverse micelles (28, 29) (Fig. 2). The hydrophobic moiety extends to the bulk of the nonpolar solution, while the polar ends of the surfactant molecules are drawn together to form the hydrophilic core of the inverted micelle. Very often any water present in the system will tend to be included inside the reverse micelle aggregates. In liquid/liquid electrochemical experiments on a free standing interface there is a possibility of micelle formation in the presence of a surfactant in both the aqueous and the nonaqueous (less polar) phase. In many cases formation of micelles in studies of well behaved systems is undesirable.

Low concentrations of surfactants (below the CMC) have long been used in polarography to suppress maxima. Concentrations above the CMC have been used only sparingly. The possibility of the use of micelles in electrochemistry can be

divided into several categories, that include electrochemical masking, electrocatalysis and the provision of a low–cost and nontoxic alternative to nonaqueous solvents (19, 22). In the studies in L/L electrochemistry, micelles become a species of interest due to the fact that they are carriers of a charge in the solution.

Electrochemists tend to discount nonelectrochemically active substances as unimportant (21). In L/L electrochemistry the concept of "electroactive species" is different from the one in electrode studies. In L/L the species have to have a charge and be able to be transported across the interface to be noted on voltammetric curve. Electron transfer is not taking place. Thus, one can detect fairly nonreactive species such as the tetramethylammonium cation.

Even if the substance is not transportable across the L/L interface, its adsorptive behavior can be of great importance. Vanýsek and Sun (30) studied transport of probe ion (Cs^+) in the presence of bovine serum albumin, and the capacitive behavior of the interface in response to protein concentration, pH and temperature.

Equilibrium thermodynamics of liquid/liquid interfaces is based on several simple principles. Hung (31) first presented an implicit equation that is based on the equality of the electrochemical potentials of each participating species between the two solvents in contact and on the general requirement of electroneutrality.

$$\sum_{i=1}^{j} z_i c_i^o \Big/ \left\{ 1 + \frac{\gamma_i^a}{\gamma_i^\beta} \exp\left[\frac{z_i F}{RT} (\Delta\varphi - \Delta\varphi_i^o) \right] \right\} = 0 \qquad (1)$$

$\Delta\varphi$ is the interfacial equilibrium potential, $\Delta\varphi_i^o$ is the standard potential of transfer for ion i, z_i is the ion charge, c_i is the total analytical concentration of i in both

phases and γ is the activity coefficient in phase α and β.

Although the principle is simple, the implications are not immediately obvious. Buck and Vanýsek (32, 33) used the concept of equilibria and the Gibbs energy of transfer for calculating a series of equations for various interfacial systems, including L/L equilibria. In many instances, micellar systems can be regarded as related to L/L systems. Caselli and Maestro (34) used the concept of Gibbs energy change between water and lipophile to calculate equilibrium micellar radius of reverse micelles as a function of saline solution concentration in aqueous phase. This concept is quite far–reaching, e.g., it has been applied to interaction of oil dispersion in photographic developer systems (35).

Water/nitrobenzene experiments

Typical studies of ion transport between two immiscible electrolytes involve the interface between water and nitrobenzene (8). Nitrobenzene is used since it is essentially immiscible with water. Because of its relatively large relative permittivity (ϵ - 35) salts soluble in nitrobenzene dissociate, thus rendering a conductive, nonaqueous, water immiscible medium.

For an ion transfer experiment between water and nitrobenzene, two suitable supporting electrolytes are chosen such that one of these salts in not soluble in each phase. Typically, the salt used in water is very hydrophilic, LiCl, whereas the salt suitable for the nonaqueous phase can be a lipophilic tetrabutylammonium tetraphenylborate (TBATPB). In such a configuration, the supporting electrolytes are preferentially contained in their original solvent phases and application of a potential on the interface from an external source will cause

only a small degree of salt transport into the opposite phase. Thus, one obtains an interface on which an arbitrary potential within a certain range can be applied, without causing significant current flow. Such an interface is called an ideally polarizable interface in parallel with electrode electrochemistry terminology.

Addition of a semihydrophobic ion into either phase provides the L/L system with a charged species that can be driven across the interface from one phase into another, as a function of the applied potential on the polarizable interface. The transport of the charged species is manifested in the external electric circuit as current. Experimental voltamperometric characteristics of the L/L system exhibits a current–voltage dependence similar to that of a voltammogram of a reversibly reducible species. Figure 3 illustrates an example of the transfer of the semihydrophobic cation, tetramethylammonium, between water and nitrobenzene. Unlike in electrode electrochemistry, where the peaks correspond to reduction and subsequent oxidation of a species, here the peaks correspond to the transport of $TMeA^+$ from water to nitrobenzene (top, right) and the peak on the reverse sweep is caused by transport of $TMeA^+$ from nitrobenzene to water. Since the transport of the cation across the interface in the presence of high concentration of supporting electrolytes is governed by the same principles of diffusion, the L/L voltammetric curves are very similar to those obtained for redox processes on metal electrodes.

The ionic species (both cations and anions) that can be followed voltammetrically on the described interface, must be less hydrophilic that the supporting electrolyte in water and at the same time they must be less lipophilic than the supporting electrolyte in the nonaqueous phase. Since the potential window of the ideally polarizable interface is fairly narrow (approximately 500 mV for the described system), only a few ions can be directly observed. They include

quaternary ammonium cations shorter than butyl, choline, acetylcholine, picrate, perchlorate, thiocyanate, Rb^+, Cs^+ and several others. From our interest, it is important that laurylsulfate, which forms micelles at certain concentrations, also can be transported within this potential window.

Water and nonaqueous solvent is not the only immiscible solution system, that can be used for ITIES studies. There are a number of aqueous two phase systems that show, at least, a promise in ITIES electrochemistry applications. A two phase aqueous system can arise when two polymers (e.g., polyethylene glycol and dextran) are dissolved in water, with one polymer predominating in each phase (36, 37). Such systems are being used for physical separation of a wide range of biomolecules (38). The advantages quoted for these separations are primarily biocompatibility (contents of water is 75–90%). For the most part, the work that involved two phase aqueous systems was mostly centered on extraction and separation techniques, although potentiometric work has been also reported (39).

In our work we are reporting potentiometric results on several systems including dodecyl sulfate. Voltammetric studies on these interfaces were also performed. Because the Gibbs energy of transport of ionic species between the two phases is quite low, we were not able to establish a system with appropriate supporting electrolytes that would provide a potential window sufficiently wide for any kind of meaningful measurement.

MATERIALS AND METHODS

Voltammetric studies of laurylsufate (sodium salt of dodecylsulfate, SDS) on a water/nitrobenzene interface were done on a microinterface (6). The cell used in this work is shown in Fig. 4. It was made from two pieces of a No. 9 O–ring Pyrex glass joint. An opening in one of the arms was filled with thinly blown glass in which a small hole was introduced by Tesla coil discharge. An alternative reliable way of realization of small interface is in Fig. 5. The probe device was made from a 7–mm teflon rod, drilled out with a 5–mm flat bottom drill so that only about 0.3 mm thick teflon bottom remained. An opening of 0.1 mm was drilled in the bottom. Due to the nature of teflon, the hole closed somewhat after smoothing on the lathe. The typical opening in both the glass and the teflon wall were - 50 μm. Although this diameter does not accomplish entirely the prerequisite for hemispheric diffusion, the contribution of *IR* drop is negligible and a 2–electrode system for polarization can be used. More suitable techniques for manufacturing small partitioning were described by Girault (40, 41).

The electrical circuit requires only a 2–electrode connection, but care has to be exercised in sufficient amplification of the small currents and in shielding electrical noise. Keithley 470 current amplifier was used for the current to voltage conversion at a typical setting 10^7 V/A. The circuit diagram used for the low current voltammetric experiments is shown in Fig. 6.

For the aqueous/aqueous interface the experiment was potentiometric. Figure 7 shows the schematics of the apparatus used to measure the potential difference between the two aqueous phases. The reference electrodes were Ag/AgCl wires immersed in 0.1 mol.l^{-1} KCl in a salt bridge separated from the polymer gel solutions by a vycor glass frit. The potential difference between the two reference

electrodes was measured with a pH meter set on the mV scale.

A constant potential reference electrode for nonaqueous solution requires additional water/organic interface with a common ion. The shorthand notation of the water/organic voltammetric cell is in the following scheme:

$$\begin{array}{c|c|c||c|c|c|c} \underset{(s)}{Ag} & \underset{(s)}{AgCl} & LiCl\ (+\ SDS) & TBATPB & TBACl & \underset{(s)}{AgCl} & \underset{(s)}{Ag} \\ & & (aqueous) & (nitrobenzene) & (aqueous) & & \end{array} \quad (2)$$

The interface on which the transfer of interest takes place is marked by the two vertical lines. The potential on this interface and its variation produced the analytical signal. All other interfaces have known and constant potential. The function of the tetrabutylammonium chloride (TBACl) bathing the right hand reference Ag/AgCl electrode is to establish constant potential on the water/nitrobenzene interface by virtue of sharing common TBA^+ ion. As long as the activity of the TBA^+ in both phases remains constant, the interfacial potential will be also constant and its value will be given by the Nernst–Donnan equation:

$$\Delta\varphi = \Delta\varphi_i^\circ + \frac{RT}{nF} \ln \frac{a_i(\alpha)}{a_i(\beta)}, \quad (3)$$

where $\Delta\varphi_i^\circ$ is the standard potential of transfer of a common ion i from phase α to phase β. For equal concentrations of the tetrabutylammonium cation for water/nitrobenzene this potential difference is -248 mV. The sign denotes the polarity of the aqueous phase.

The polymers used for the two phase aqueous system experiments were polyethylene glycol (PEG), average m.w. 3 350 (Sigma, No. P–3640) and dextran, average m.w. 67 900 (Sigma, No. D–1390). Sodium dodecyl sulfate was supplied by Aldrich. Water doubly distilled from glass was used throughout. All experiments were done at 25 ^{o}C.

RESULTS

Figure 8 shows the voltammetric response of an interface between two liquids created in a thin glass window. The diameter of the opening was ~ 130 μm. Voltammetric curve *C* shows the response of the system containing only the base electrolytes, 0.02 mol.l^{-1} LiCl in water and 0.02 mol.l^{-1} TBATPB in nitrobenzene. Only negligible current flows in the central potential range known as the potential window. Subsequent curves 1 – 4 show voltammograms obtained with the base electrolyte system upon addition of 0.4 mmol.l^{-1} dodecyl sulfate (sodium salt) into the aqueous phase. The response at several scan rates is shown. At lower scan rates the voltammogram does not display a peak; a current plateau is formed instead. As mentioned earlier, this small interface is expected to display similar behavior as do ultramicroelectrodes. At slower scan rates the diffusion towards the interface has hemispheric symmetry. The ions are approaching the interface from the volume of a hemisphere. Thus, a constant, steady state current is observed. At higher scan rates the symmetry becomes semilinear with the ions approaching the interface from one direction only. The voltammetric curves reach a maximum after which diffusion continues to deplete the amount of ions available for interfacial transport.

Because the L/L interface can be formally treated in the same way as an electrode/electrolyte interface, the equation describing the limiting current under conditions of hemispheric diffusion can be written for an ion i in the following form (4):

$$I = 4\,FD_i c_i r, \tag{4}$$

where F is the Faraday constant, D_i and c_i are the diffusion coefficient and the bulk concentration of ion i and r is the radius of the interface (6). Similarly, an approximate equation can be derived from the spherical term of the voltammetric curve derived by Nicholson and Shain (42) in the limit of the radius of the electrode tending to zero:

$$I_{r\to 0}^{(approx)} = 2\,\pi nFDcr. \tag{5}$$

We have published this equation in (6) and (7), but with the factor 2 inadvertently omitted.

At higher scan rates, when the mass transport is controlled by linear diffusion, the voltammetric curves display peaks on both the positive and negative scans. Since the transport of SDS is reversible (i.e., transport can proceed unhindered across the interface in both directions), the separation of peaks for this univalent ion is about 58 mV on repetitive cycling. In agreement with diffusion theory, the peak current is directly proportional to the square root of the scan rate (Fig. 9).

It has also been shown that in accordance with expected behavior, the peak current at a given scan rate is proportional to the concentration of the transported

ion. Figure 10 gives the dependence for picrate, tetramethylammonium, and choline. The results for dodecyl sulfate, which was also investigated (43), were erratic at higher concentrations in comparison with the other ions. The probable cause was twofold. SDS acts as a detergent, which can solubilize nitrobenzene in water or vice versa. This problem was apparent especially in mechanically perturbed systems such as those where ITIES is realized in the form of a dropping electrode. The critical micellar concentration for SDS is 8 $mmol.l^{-1}$ (27). Above that concentration, the concentration of solubilized SDS remains essentially constant. That is not to say, that the transport of SDS must level off at the CMC. Instead, the micelles contribute to the total amount of SDS available for interfacial transport. But the contribution is further complicated by the rate of aggregation/disaggregation and also by the fact that the concentration of the analyte is nearing that of the supporting electrolytes (20 $mmol.l^{-1}$) and the transport description is further complicated by migration component.

Unusual phenomena on L/L interface were observed in the presence of colloids, such as denaturated proteins (insuline, ovalbumine) and even dispersed particles of polystyrene (44). It was observed that current across the interface increases and the potential window of the supporting electrolytes narrows. This phenomenon has been explained in a qualitative way by availability of charged colloidal particles for interfacial transport.

Potentiometric experiments on nitrobenzene/water interface were performed in a similar setup as is the one for potentiometric measurements on the two–phase aqueous systems. Heavier nitrobenzene was placed on the bottom of the cell, nonaqueous reference electrode was immersed next and the nitrobenzene phase was topped with the aqueous phase. Then the second reference electrode was placed in the aqueous phase. The aqueous phase reference electrode was an

Ag/AgCl wire immersed in 0.01 mol/l LiCl. The reference electrode used in nitrobenzene was an Ag/AgCl wire immersed in aqueous 0.01 mol/l tetrabutylammonium chloride. Since the nitrobenzene layer contains 0.1 mol/l tetrabutylammonium tetraphenylborate, the TBA^+ ion common to both phases establishes the constant reference potential.

In ITIES voltammetric experiments it is usual practice to allow about 10 minutes to equilibrate the system after setting it up. We have followed the protocol, but as we were able to monitor the interfacial potential from the very beginning of setting up the cell, lot of variation between systems was observed. Fig. 11 shows that with the SDS experiments, the steady state values were reached almost immediately.

Figure 12 shows the interfacial potential dependence as the function of sodium dodecylsulfate concentration in the aqueous phase. The dependence shows sharp decrease in the potential of the aqueous phase (relative to the nitrobenzene solution) in the concentration range from 0.1 to 1 mmol/l. This behavior is in sharp contrast to the potentiometric curves obtained for example for picrate, where the dependence is essentially linear through several orders of concentrations. Above 10 mmol/l SDS the potential is no more dependent on the analytical concentration of SDS. This agrees with the micellar concept; the concentration of free SDS above CMC remains virtually constant.

The two–phase aqueous system was prepared by preparing separately 30% dextran and polyethylene glycol solutions in water or appropriate supporting electrolyte (0.1 mol/l LiCl). For the experiment, a layer of the heavier phase (dextran) was placed on the bottom first, then the lower phase reference electrode was immersed, after which the top layer of polyethylene glycol solution was injected carefully with a syringe. Finally, the second reference electrode was placed

in the top layer.

The established interface was allowed to equilibrate. The time necessary for the equilibration was determined from diminishing drift of the potential difference. The required waiting varied widely with used systems. For the SDS experiments, the steady potential value was reached almost immediately.

Figure 13 is a concentration dependence of the two–phase aqueous interfacial potential as a function of concentration of dodecyl sulfate. In contrast with the results obtained at the water/nitrobenzene interface, the PEG/dextran system does not display any leveling off at higher concentrations. The CMC is a constant only for given environment. It varies greatly with ionic strength and solvent medium. The steady change of interfacial potential with increasing SDS concentration is indicative of lack of micellar formation in the aqueous polymers system.

Experimentation on electrified immiscible interfaces has been applied in this chapter to problems that relate to the studies in microheterogeneous systems. Although the aim of ITIES electrochemistry is mostly towards aspects of large size heterogeneous systems (interfaces), microheterogeneity is occasionally investigated as well. Miniaturization of the liquid/liquid interfaces is one such case. With proper techniques the interfaces can be rendered sufficiently small to alter the diffusion to the interface from linear to hemispheric symmetry. Second aspect of microheterogeneity discussed here was formation of micelles in L/L systems. Case of dodecyl sulfate micelle formation in water/nitrobenzene has been documented. So far rarely studied interface between two aqueous polymer solutions was also presented. In this environment, different from bulk water, micelle formation of sodium dodecylsulfate below concentration 0.1 mol/l was not observed.

DRAFT

This work and the author's research work described herein were supported in part by the Office of Naval Research. Experimental contribution to the potentiometric studies by Jennifer Kefer is acknowledged.

Literature cited

1. Nernst, W. *Z. Phys. Chem.* **1888**, *2*, 613–637.
2. Blank, M.; Feig, S. *Science* **1963**, *95*, 561–572.
3. Koryta, J.; Vanýsek, P.; Březina, M. *J. Electroanal. Chem.*, **1976**, *67*, 263–266.
4. Taylor, G.; Girault, H. H. J. *J. Electroanal. Chem.*, **1986**, *208*, 179–183.
5. Vanýsek, P.; Hernandez, I. C. *Anal. Lett.* **1990**, *23*, 771–785.
6. Vanýsek, P.; Hernandez, I. C.; Xu, J. *Microchem. J.* **1990**, *41*, 327–329.
7. Vanýsek, P.; Hernandez, I. C. *J. Electrochem. Soc.* **1990**, *137*, 2763–2768.
8. Vanýsek, P. *Anal. Chem.* **1990**, *62*, 827A–835A.
9. Stewart, A. A.; Taylor, G.; Girault, H. H.; McAleer, J. *J. Electroanal. Chem.* **1990**, *296*, 491–515.
10. Wightman, R. M.; Wipf, D. O. In *Electroanalytical Chemistry*; Bard, A. J., Ed.; Vol. 15; Marcel Dekker; New York, **1989**; pp 267–353.

11. Penner, R. M.; Heben, M. J.; Longin, T. L.; Lewis, N. S. *Science* **1990**, *250*, 1118–1121.

12. Penner, R. M.; Martin, C. R. *Anal. Chem.* **1987**, *59*, 2625–2630.

13. Potje–Kamloth, K.; Janata, J.; Josowicz, M. *Ber. Bunsenges. Phys. Chem.* **1989**, *93*, 1480–1485.

14. Andrieux, C. P.; Garreau, D.; Hapiot, R.; Pinson, J.; Saveant, J. M. *J. Electroanal. Chem.* **1988**, *243*, 321–335.

15. Howell, J. O.; Wightman, R. M. *Anal. Chem.* **1984**, *56*, 524–529.

16. Baranski, A. S. *J. Electroanal. Chem.* **1991**, *300*, 309–324.

17. Taylor, G.; Girault, H. H.; McAleer, J. *J. Electroanal. Chem.* **1990**, *293*, 19–44.

18. Hartley, G. S. *Trans. Faraday. Soc.* **1935**, *31*, 31–50.

19. McIntire, G. L. *Crit. Rev. Anal. Chem.* **1990**, *21*, 257–278.

20. Cline Love, L. J.; Habarta, J. G.; Dorsey, J. G. *Anal. Chem.* **1984**, *56*, 1132A–1148A.

21. Pelizzetti, E.; Pramauro, E. *Anal. Chim. Acta* **1985**, *169*, 1–29.

22. McIntire, G. L. *Am. Lab.* **1986**, *18*, 173–180.

23. Chen, S. H.; Rajagopalan, R. (Eds.). *Micellar solutions and microemulsions: Structure, dynamics and statistical thermodynamics*; Springer: New York, **1990**.

24. Zana, R., Mackay, R. A. *Langmuir* **1986**, *2*, 109–113.

25. Georges, J.; Desmettre, S. *J. Colloid Interface Sci.* **1987**, *118*, 192–200.

26. Texter, J.; Horch, F. R.; Qutubuddin, S.; Dayalan, E. *J. Colloid Interface Sci.* **1990**, *135*, 263–271.

27. Zubay, G. *Biochemistry*; Addison–Wesley: Reading, **1983**, p. 590.

28. Fendler, J. H.; Fendler, E. J. *Catalysis in Micellar and Macromolecular Systems*; Academic Press: New York, 1975.

29. Pileni, M. P. (Ed.) *Structure and reactivity in reverse micelles.* In: *Studies in physical and theoretical chemistry.* Vol 65. Elsevier: Amsterdam, 1989.

30. Vanýsek, P.; Sun, Z. *Bioelectrochem. Bioenerget.* 1990, *23*, 177–194.

31. Hung, L. Q. *J. Electroanal. Chem.* 1980, *115*, 159–174.

32. Vanýsek, P.; Buck, R. P. *J. Electroanal. Chem.* 1991, *297*, 19–35

33. Buck, R. P.; Vanýsek, P. *J. Electroanal. Chem.* 1990, *292*, 73–91.

34. Caselli, M.; Maestro, M. *J. Electroanal. Chem.* 1990, *283*, 67–75.

35. Texter, J; Ross, D. S; Matsuboru, T. *J. Imaging Sci.* 1990, *34*(*4*) 123–131.

36. Walter, H.; Brooks, D. E.; Fisher, D. (Eds.) (1985): *Partitioning in aqueous two–phase systems.* Academic Press, London.

37. King, R. S.; Blanch, H. W.; Prausnitz, J. M. *AIChE J.* 1988, 34, 1585–1594.

38. Albertsson, P.–A. (1986): *Partition of cell particles and macromolecules.* 3rd ed. Wiley–Interscience, New York.

39. Brooks, D. E.; Sharp, K. A.; Bamberger, S.; Tamblyn, C. H.; Seaman, G. V. F.; Walter, H. *J. Colloid Interface Sci.* 1984, *102*, 1–13.

40. Campbell, J. A.; Stewart, A. A.; Girault, H. H. J. *J. Chem. Soc., Faraday Trans. I*, 1989, *85*, 843–853.

41. Campbell, J. A.; Girault, H. H. *J. Electroanal. Chem.* 1989, *266*, 465–469.

42. Nicholson, R. S.; Shain, I. *Anal. Chem.* 1964, *36*, 706–723.

43. Hernandez, I. C. Thesis: Investigation of transport behavior of semihydrophobic ions across a microscopic interface between nitrobenzene and water. Northern Illinois University. DeKalb 1989.

44. Vanýsek, P. Ph.D. Thesis, Czechoslovak Academy of Sciences, J. Heyrovský Institute of Physical Chemistry and Electrochemistry, Prague, 1982.

Legend for figures

Fig. 1 Voltammetric cell for 4–electrode ITIES work.

Fig. 2 Schematic representation of organized structures in of surfactants in different media.

Fig. 3 Transport of $TMeA^+$ across water/nitrobenzene interface

Fig. 4 Electrochemical cell used for μITIES studies on glass partitioning.

Fig. 5 Compartment for μITIES work realized in a teflon tube.

Fig. 6. Diagram for measurement of low current signals.

Fig. 7 Schematic of the apparatus for L/L potentiometric measurements.

Fig. 8 Cyclic voltammograms of SDS–transfer (0.4 mmol/l) for several scan rates in mV s^{-1}: (1) 10, (2) 50, (3), 200, (4) 1000. Curve (0) is base electrolyte only at 25 mV s^{-1}. Base electrolytes, 0.02 mol l^{-1} LiCl in H_2O and 0.02 mol l^{-1} TBATPB in nitrobenzene.

Fig. 9 Peak currents (for forward scan) as a function of the square root of scan rate. Concentration of the studied ions 0.4 mmol l^{-1}. Base electrolytes, 0.02 mol l^{-1} LiCl in H_2O and 0.02 mol l^{-1} TBATPB in nitrobenzene. (□) $TMeA^+$, (△) picrate, (⟨⟩) choline and (○) dodecyl sulfate.

Fig. 10 Plot of peak current (forward scan) versus concentration (□) choline, (△) picrate and (○) $TMeA^+$. Scan rate 25 mV s^{-1}. Base electrolytes, 0.02 mol l^{-1} LiCl in H_2O and 0.02 mol l^{-1} TBATPB in nitrobenzene.

Fig. 11 Time dependence of potential on a water/nitrobenzene interface.

Fig. 12 Potentiometry of SDS in water/nitrobenzene system.

Fig. 13 Potentiometry of SDS in aqueous polyethylene glycol/dextran system.

(5) EFFECTS OF DISPERSED PHASES IN NATURALLY OCCURRING SAMPLES ON THE ELECTROREDUCTION OF $Ru(NH_3)_6Cl_3$

S. Daniele, P.Ugo, G.A. Mazzocchin and D. Rudello

Department of Physical Chemistry, The University of Venice, Calle Larga S. Marta, 2137, 30123 Venice, Italy.

ABSTRACT

Many naturally occurring fluids, such as milk and cream, contain dispersed phases characteristic of complex liquids. These fluids contain organized molecular assemblies such as micelles and emulsions. We demonstrate that models of organized structures can be applied to these naturally occurring systems and that quantitative information relevant to redox probes can be obtained in such fluids. The dispersed phases do not adversely affect analytical determination utilizing these probes. $Ru(NH_3)_6Cl_3$ is used as an electrochemical probe, and added to milk and cream without pretreatment and addition of the supporting electrolyte. Conventional and microelectrodes of platinum have been used. Use of the microelectrode obviates problems associated with low electrochemical conductivity in, for example, cream samples.

INTRODUCTION

In recent years, we have been concerning with the aspect to consider real or naturally occurring liquid samples, as media for direct electrochemical studies and analyses [1-6]. For homogeneous fluid-matrices, this aim can be achieved easily because few preparation steps, often restricted to the addition of the supporting electrolyte and the acidification of the sample, are only required. For very complex matrices and for physically heterogeneous fluids, this is a more difficult task, as indicated from the scarce reports found in the literature on this subject.

In this paper we show an application of electrochemical measurements in dairy products such as milk and cream.

Milk is a complex fluid containing many components in several states of dispersion. Water is more abundant than other constituent and contains dissolved inorganic salts and organic species as a continuos and homogeneous phase. Fat globules, mainly made up of triglycerides, float in a turbid liquid-plasma which contains proteinaceous particles and casein micelles. Most amphiphilic molecules are not very soluble in water and they tend to associate into micelles as well. A milk derivative is cream, which is that part of milk rich in fat and obtained by skimming. Although the proportion of fat present in cream varies greatly, the relative proportions of the other components remain the same as in the milk from which the cream has been derived. Notwithstanding the complexity of the matrices, both milk and cream have a relatively simple and well-studied structure [7].

These media are really naturally occurring organized molecular assemblies such as micellar and emulsified systems [8]. At variance with

the synthetic systems, milk and cream are not optically transparent. It follows that some experimental techniques like, for instance, UV-VIS spectroscopy, are not suitable for direct measurements. Conversely, electrochemical methods have the advantage to be employed even under these unfavourable optical conditions.

The aim of this paper is to show that models of organized structures can be applied to these naturally occurring systems and that quantitative information relevant to redox probes can be obtained in such fluids.

In a previous paper [4] we have examined the effects of the dispersed phases of milk and cream in dissolving, in their hydrophobic core, molecule scarcely soluble in the aqueous phase. Ferrocene has been employed as the probe molecule.

We are now concerned with the effects of the dispersed phases of milk and cream on the voltammetric behaviour of species very soluble in the aqueous phase. $Ru(NH_3)_6Cl_3$ has been used as an electrochemical probe and added to milk and cream employed as withdrawn from their conteiner without pretreatment or addition of the supporting electrolyte, this to avoid the existing chemical equilibria to be alterated.

Conventional and microelectrodes of platinum have been employed as working electrodes. Use of microelectrode obviates problems associated with low conductivity, in particular, in cream samples.

EXPERIMENTAL

Reagents

Hexammineruthenium(III) trichloride from Mattey Bishop was purified as reported [9]. All inorganic salts employed and casein were of analytical-reagent grade. Bovine milk and cream samples 35% fat were those commercially available. Cream samples of 11% and 20% fat were prepared by mixing skim milk and cream 35 % fat in the proper amounts. These samples were than checked for fat content by the Gerber method. Doubly distilled water was used throughout to prepare aqueous solutions. Nitrogen (99.99%) from SIAD was used when necessary for deoxygenation.

Electrodes and instrumentation

A conventional platinum electrode of 1.5mm radius was employed as working electrode. Platinum wires of 2.5, 5.0, 10.0 and 12.5 μm radius were sealed in glass as reported previously [10]. The effective radius of the electrodes employed were estimated by employing eqns. (4) and (5) (see later) and the peak and the steady-state currents, respectively of the cyclic voltammetry for the oxidation of ferrocene in acetonitrile whose diffusion coefficient is 2.4×10^{-5} $cm^2 s^{-1}$ [11]. Prior to each measurement the electrodes were polished with graded alumina powder (down to 0.05 μm) on polishing micro-cloth. The reference electrode employed was always a saturated calomel electrode (SCE).

For experiments with microelectrodes, a two electrode cell configuration was used for cyclic voltammetry (CV) which was generated by a PAR 175 function generator; a Keithley 485 picoammeterserved as current-measuring device and data were plotted with an X-Y recorder Helwett-Packard 7045 B. For cyclic, differential pulse (DPV) and square

wave voltammetry(SWV) with conventional electrodes as well as for DPV and SWV with microelectrodes a potentiostat PAR 273 controlled with an Olivetti M 380 personal computer via a EG&EG PAR 270 software was employd. In these last conditions a three-electrode cell was used. The cell for experiments with microelectrodes was maintained in a Faraday cage made of sheets of aluminium.

Bulk viscosity were measured with a Ostwald viscosimeter calibrated with pure water. All the measurement were carried out at $20^{0}C \pm 0.1$.

Procedure

Unless otherwise stated, about 25 ml of milk and cream samples as wothdrawn from their commercial package and with no deliberate addition of the supporting electrolyte, were transferred into the electrochemical cell under nitrogen atmosphere for measurements. When prolonged experiments or addition of the reagents in the media were necessary and for aqueous solutions, the samples were deareated before each measurement by bubbling nitrogen for at least 10 min.

RESULTS and DISCUSSION

Cyclic voltammetric behaviour of $Ru(NH_3)_6^{3+}$ in milk and cream

Typical cyclic voltammograms obtained at both conventional and microelectrodes for milk and cream samples, not containing added solutes, are reported in Fig. 1. For milk the processes involved either in the cathodic and the anodic regions have been discussed in detail elsewere [3]. Cream shows a similar region in which external added solutes can emerge from background or separated from the processes due to species naturally present in the sample. No further investigations have been carried out to get more insights on these media. However, from a qualitative comparison between the voltammetric behaviour observed in milk and cream, it can be said that the processes of cream samples up to 35% fat, studied by us, probably parallel those of milk. That is, the cathodic and anodic limits, in which the background is flat, are dictated from water discharge, while the main cathodic peak at about -0.850 V at microelectrode and -0.650 V at the conventional electrode, respectively, should belong to acids either dissolved in the water phase or bound to casein micelles[3]. With respect to milk, the lower current signals relevant to these last processes, are consistent with a lower acidity of cream [12].

A higher background current is generally observed in cream samples with the conventional electrode and it depends also on the sweep rate employed. This is expected by considering that both the higher amount of hydrophobic phases dispersed and the higher viscosity of the media may contribute to capacitive current and ohmic drop enhancements. The backgrownd current is lower at the microelectrodes in agreement with the general observation that the faradaic to capacitive current ratio is

higher and the ohmic drop negligible to the smaller electrodes [13].

Fig. 2 shows typical cyclic voltammograms obtained in some of the samples examined with added $Ru(NH_3)_6Cl_3$. Peak current or diffusion limiting current at conventio al and microelectrodes, respectively, were linearly dependent on concentration of solute in the range studied with this technique, i.e., $2x10^{-4}$-$2x10^{-3}$M in milk and over a slight lower range for cream, i.e. $3x10^{-4}$ -10^{-3} M . In milk at a given concentration of solute, with the conventional electrode the cathodic peak current, i_p, of $Ru(NH_3)_6^{3+}$ resulted linear vs the square root of the scan rate $v^{1/2}$ over the range 0.01-0.2 V. The anodic to cathodic peak separation (Δ E) depended on the sweep rates employed; it resulted only slightly higher than 59/n mV, theoretical value expected for a reversible one electron process within 10-30 mVs^{-1}, while it was even far higher than 60 mV for higher scan rates (see Table I). The backward to forward peak current ratio, (i_{pb}/i_{pc}), is close to one at any scan rate employed, thus indicating diffusive character of the process involved with no kinetic complications. Increases in ΔE could be attributed to uncompensated ohmic drop rather than to a slow heterogeneous electron transfer. However, attempts to compensate ohmic drop by a positive feedback almost failed for sweep rates higher than 50 mVs^{-1} probably because capacitive currents may lead to distortion of the waves. This view is also supported by the fact that the half-wave potential (see Table I), determined as midpoint between the cathodic and anodic peak potentials of the same cyclic voltammograms, were independent on the sweep rates.

The voltammetric pictures obtained with the conventional electrodes in cream samples, did not differ much from those obtained in milk apart that Δ E was quite far from the 59 mV/n (n =1) value at any scan rate employed (see TableI). However the half-wave potentials, which are

located at a value very close to that obtained in milk, did not vary by changing the scan rate (see Table I). The plot of cathodic peak current vs $v^{1/2}$ was linear over a smaller range of scan rates, whereas the i_{pb}/i_{pc} was almost one in any medium. Also in this case attempts to compensate the ohmic drop failed. The results so far reported indicate that the reduction of $Ru(NH_3)_6^{3+}$ undergoes an almost reversible electron transfer in all the media investigated.

With the microelectrodes better defined voltammograms were recorded even in cream samples (see Fig. 2 for the 12.5 μm radius electrode). The parameters which characterize the voltammetric curves, e.g., , slope of the plot of log (id-i)/i vs E (i_d is limiting current), $E_{1/4}-E_{3/4}$ [14] and $E_{1/2}$ were evaluated and reported in Table II for the microelectrode of 25 μm radius. The semilogarithmic plots were linear and their slopes, are consistent with a reversible one electron transfer process. It is so also for the differences $E_{1/4}-E_{3/4}$ equal to RT/nFln(9) [14] (0.0554 for n=1, F= 96488 C and at 20^0C) for a reversible one-electron transfer process.

Since $Ru(NH_3)_6^{3+}$ is a water soluble molecule, blank measurements were also carried out in aqueous solutions. This system has already been studied in aqueous solutions, but some dicrepances exist on the electrochemical parameters found, often due to the different experimental conditions employed. A series of mesuremnts was carried out to confirm data reported in the literature (see for instance Reff. [15-19]).

The voltammograms were obtained in two cases with two different suppoting electrolytes: 0.1 M $NaClO_4$ and 0.1 M phosphate buffer at pH=7. This last supporting electrolyte should mimic well both pH (= 6.7) and milk-salt composition. In fact hydrogen phosphates are present in

large amount in these media and the pH of fresh whole milk is very close to that of phosphate buffer. The data obtained both at conventional and microelectrodes, collected in Tables I and II, indicate that the redox species undergoes a reversible process. In fact at the largest electrode cathodic peak currents vs $v^{1/2}$ were linear and Δ E was 60 ±2 mV regardless both of the sweep rate and supporting electrolytes employed. At the microelectrode the semilogarithmic plot was invariantly linear with a slope of 59 ±2 mV and the $E_{1/4}-E_{3/4}$ equal to the theoretical value within the experimental errors. It must be noted moreover, that if the currents responses obtained at both conventional and microelectrodes in aqueous solution are compared with those obtained in the dairy products, for the same apparent concentration of solute, the former resulted 4-5 times higher.

Determination of heterogeneous rate constants and diffusion coefficients

Other electrochemical parameters characterizing the process under investigation such as standard heterogeneous rate constant (k^0) and diffusion coefficient are useful to get insights on the differences in the behaviour occurring among the media investigated. The dispersed phases, in fact, can affect the mass transport or the rate of the electron transfer and also the stability of the intermediate of the electrode process [8].

By judjing from the Δ E reported in Table I one would say that at the macroelectrodes the process is a quasireversible one. Thus (k^0) could be estimated from anodic-cathodic peak potential differences of the CVs over a range of scan rates in which this difference is higher than 60 mV [21]. As mentioned above, however, the data obtained with this transient technique are probably affected, even strongly, from interferences due

to ohmic drop and charging currents. Alternatively, steady-state experiments made at the microelectrodes are almost completely unaffected from charging-current problems uncompensated ohmic drop. Thus, from measurements with microelectrodes the rate of the heterogeneous electron transfer were studied in detail.

From an experimental point of view the meaning reversible is related to the upper limit on measurable rate constant which depends on the technique employed. Thanks to the enhanced mass transport associated to the microelectrodes, it has been shown that reliable k^0 values of the order of 10^{-2} ms^{-1} can be determined by steady state voltammetric experiment with inlaid disc working microelectrodes [22]. The method requires that several voltammograms be recorded, using microdiscs covering a range of radii. The equation allowing to calculate k^0 is the following:

$$E_{1/2} - E_h = -2RTD_O/(nFk^0r) \qquad 1)$$

in which

$$E_h = E^0 + RT/nF \ln(D_R/D_O) \qquad 2)$$

$E_{1/2}$ is the half-wave potential for a nearly reversible steady-state voltammogram, which differs little from the reversible value E_h. E^0 is the standard potential; D_R and D_O are the diffusion coefficients of the reduced and oxidized forms, respectively; r is the radius of the microelectrode and other symbols have their usual meanings. Equation (1) shows that a plot of $E_{1/2}$ versus 1/r will give a straight line whose slope, A, is

$$A = -2RTD_O/(nFk^0) \qquad 3)$$

from which k^0 is easily calculable with an error of about 22% [22].

The half-wave potentials for the reduction of $Ru(NH3)_6^{3+}$ in the media investigated were determined for electrode radii within 2.5 and

12.5 μm. Notwithstanding precise potential measurements were made, accurate to 1mV, the $E_{1/2}$ values did not change by changing the electrode radius with respect to those reported in Table II for the 12.5 μm radius. From this result only a lower limit of k^0 can be given by assuming that the variation of $E_{1/2}$, over the electrode radii employed, is equal to the accuracy (i.e. 1mV). By this procedure and assuming as D_O the bulk diffusion coefficients determined with the microelectrodes (see later), the k^0 reported in Table III were obtained. The lower limits found in water are in line with the k^0 reported in the literature and obtained in different ways. Values ranging from 0.92 and 1.8x10-2 m^2s^{-1} have been in fact reported [15,18]. The estimated values of k^0 support a posteriori the hypothesis made before that the large ΔE recorded with the conventional electrodes is due to both charging currents and ohmic drop. In fact with the conventional electrodes a ΔE higher than 60 mV should have been observed only at very high scan rates, say for instance > 100V/s, to compete to some extent with the heterogeneous electron transfer rate.

Diffusion coefficients were obatined, in the range of linear dependence of current responses on the concentration, by using either the conventional and microelectrodes. With the macroelectrode the apparent diffusion coefficients were determined from the cyclic voltammetric peak currents by using the Randles-Sevcik equation :

$$i_p = kn^{3/2}FAD^{1/2}v^{1/2}C^* \qquad 4)$$

The slopes of the plots i_p vs $v^{1/2}$, evaluated by the least-square method, were actually employed instead of a single current response recorded at a given v. With the microelectrodes the diffusion coefficients were evaluated from the equation (5) holding for measurement under steady-state conditions [13]:

$$id = 4nFDC^{*}r \qquad 5)$$

C^{*} is the bulk concentration. In this case either direct insertion of the bulk concentration in the eqn. (5) and the id vs r plot were employed. The results obtained are reported in Table IV. It must be emphasized that the electrochemical parameters obtained for milk and cream are apparent values, since given the heterogenousity of the media, they may depend on the amount of dispersed phases.

For any medium at least five measurements on different samples either coming from the same or different lots were made and each datum is mediated over at least three replicates. Although milk and dairy products are, in a qualitative sense, fairly constant in composition and properties, there are considerable variations. Chemical composition, size and stability of structural elements, and physical properties may all differ among lots of milk and cream, due also to processing treatments (homogeneization, heat treatment, etc.).It follows that diffusion coefficients may change from one sample to another. Table V reports some typical values obtained in different samples of milk and cream from which those reported in Table IV were mediated. From this table the expected differences from one lot to another are evident.

In order to take into account a possible concentration effect due to preferential solubilization of $Ru(NH3)_6^{3+}$ in the aqueous phase, the concentration oi the probe molecule was also corrected as follows: $C' = C^{*} / (1-\Phi)$, where Φ is the volume fraction of the disperse phase. In milk and cream Φ has been evaluated on the basis of three main contributions [23]: protein particles (Φ_p), lactose molecules (Φ_l) and milk fat (Φ_f). All these species have hydrodynamic radius ≥0.5 nm. For proteins (including casein micelles) and lactose an overall value of 0.16 has been shown to fit theoretical curves, assuming Newtonian

behaviour [23]. Thus, Φ can be determined by the following relationship: $\Phi = 0.16+\Phi_f$ which hold up to $\Phi = 0.7$. The D' values reported in table IV were obtained by using the C' in equations (4) and (5). From table IV appears that the D and D' values differ also as much as five times in 35% fat cream sample with the conventional electrodes, whereas there is less difference among those obtained with the microelectrodes. This fact depends on the particular forms of the equations relating diffusion coefficient and concentration with the two types of working electrodes, as shown from eqns. (4) and (5). Therefore, it is evident that uncertainty on concentration cause a less accurate evaluation of D to be done with the conventional electrodes.

Interpretation of the mass transport

The results so far obtained pose puzzling features on the role played by dispersed phases in milk and cream. From the data of heterogeneous electron transfer constant, it would seem that no influences arise from these phases on the one-electron reduction of $Ru(NH_3)_6^{3+}$. The voltammograms obtained with the microelectrodes, where both charging currents and ohmic drop are negligible, maintain characteristics of high reversibility in all the media investigated. Moreover, for a given medium, no shift of the half-wave potential was observed by changing the electrode radius and the estimated k^0 values in water and in the heterogeneous samples compare quite well. These facts mean that the electron uptake, from the electroue to the probe molecule, probably takes place in the aqueous phase. Likewise no negative effect seems to arise from the organic matter dissolved in the aqueous phase. Their adsorbtion onto the electrode surface might have hindered to some extent the electron transfer.

Different conclusions should be drawn out by considering the

dependence of half wave potentials and the diffusion coefficients of the probe molecule on the composition of the different media. The negative shift in the half-wave potential at both types of electrodes along with the lower diffusion coefficients obtained when going from water to milk and cream would rather suggest the occurrence of some interaction between the probe molecule and the dispersed phases. It has been usually found, in fact, that molecule probes in synthetic water-micellar [24-27] or water-emulsion [28,29] systems can display two types of behaviour just depending on whether they interact or not with the micelles or the emulsion droplets. In the former case a peak current depression (because a decrease of the diffusion coefficient) and a half-wave potential shift towards more negative values have been found, for reduction (vice versa, for oxidation). The potential shift has been taken in many cases as experimental evidences suggestive of microenvironmental changes [30]. On the contrary, in the latter case no changes were observed either in the current responses and in the half-wave potentials.

The micelles or the emulsions in milk and cream may actually bind the probe molecule either in its reduced or oxidized forms. Under the hypothesis that the electron transfer occurs in the aqueous phase, a chemical reaction (exit of the molecule from the micelle or emulsion) needs to precede the electron transfer itself. Under these conditions only an infinitely fast exit-entry reaction, and of only one form (bound or free) electroactive, would have no effects on the apparent reversibility of the process, as it corresponds to the case of a single diffusing species [31-33]. However, in this case the half-wave potentials would also depend on the equilibrium constant relevant to the partition of the probe molecule between the continuos and the dispersed

phases.

In other cases, as for instane in micellar solutions of 0.1M hexadecyltrimethyl ammonium bromide (CTAB), the water soluble ferrocyanide displayed a shift of the half-wave potential which has been accounted for as a possible interaction of ferrocyanide (-4) charged anion with the positively head groups of the surfactants [20]. A similar interaction of negatively charged species of milk and cream with $Ru(NH_3)_6^{3+}$ may be invoked to explain the about 40 or 20 mV half-wave potential shift at conventional and microelectrodes, respectively, from water to milk and cream. It is not unlike that some of the numerous species present in milk may interact elettrostatically with the probe molecule, even if it is very difficult to get some evidence of this fact under our experimental conditions. Another possibility is that $Ru(NH_3)_6^{3+}$ undergoes a ligand exchange reaction in the primary coordination sphere with some of the species present (dissolved in the water phase) in milk and cream and this reaction is in equilibrium.

No sensible half-wave potential shift or high decrease of the diffusion coefficient was instead observed going from skim milk to cream. If we take milk-fat as the surfactant for our media, this result do not parallel the voltammetric behaviour observed for specie which are bound or dissolved in the micelles or microemulsions upon changing the surfactants to water ratios [31,34]. On the other hand if we take casein (or the other proteins) as surfactants a shift was observed by going from water solutions to water solutions added of about 2.5 g/l of casein, as indicated from data reported in Table II. Thus it can be concluded that if interaction exists between probe molecule and other species, this primarily involves proteins either water soluble or in micelles.

The role played by the bulk viscosity of the medium was also examined. In Table VI are reported the bulk viscosities and the relevant diffusion coefficients obtained with the microelectrode of 12.5 μm radius. From this table it is evident that no correlation exists between bulk viscosities and diffusion coefficients. It is more likely, as shown in other cases, that the diffusion coefficient of the bulk phase probe is strictly related to the microviscosity of the medium [28,35]. This would explain for the relatively high diffusion coefficient determined in 35 % cream sample fat, in spite of its very high bulk viscosity. This observation too suggests preferential solubilization of $Ru(NH_3)_6^{3+}$ in the aqueous phase.

As reported by Mackay, the diffusion coefficient of a water soluble species in microemulsions (D) can be predicted from the relevant value in the water phase (D_0) by the following equation:

$$D = D_0(1-\Phi comp)^{n+1} \qquad 6)$$

where Φcomp is the phase volume as determined by composition and the exponent n is 1.5 at low oil content and decreases towards the value 0.5 for a coarse emulsion. For our types of emulsions, it is not easy to give exact values to both Φ and n. However, estimate values can be tentatively drawn by considering the average composition of the media investigated. In particular the weight-fraction water has been determined by subtracting from the overall weight, fat and solid-not fat [38] and specific gravity of the microemulsion was assumed to be that of milk fat (equal to 0.916 Kgm^{-3} at 20^0C). As the n value is concerned we used 1.5 which has been reported in Ref. [36] to fit for the case of Cd^{2+} reduction of in microemulsions. Finally we assumed D_0 to be equal to that of $Ru(NH_3)_6^{3+}$ in phosphate buffer-water solution. Table VII collects the values so calculated. From comparison of the values of this

table with those of Table IV appears that the average diffusion coefficients determined im cream sample at high fat content are somehow predictable by eqn. (6), whereas for the other samples the values calculated are overestimated. This can be due to a wrong assumption made for D_0 since it does not correspond to the water solution which might be drawn from milk or cream if all colloidal forms were separated. In addition further investigation must probably be done to better account for both Φ and n values.

CONCLUSIONS

We have shown that electrochemical measurements relevant to a water soluble redox species, with both conventional and microelectrodes, can be performed in milk and cream. No strong effects arise from the dispersed phases on the reduction process of $Ru(NH_3)_6^{3+}$ for the electrode material employed in this work. The measurements are almost completely free from errors due to background currents at the microelectrode, so they should be recommended for studies to be performed in these systems.

In order to verify whether detection of low concentration levels can be made in these media, preliminary measurements have been carried out by using more sensitive electroanalytical techniques like differential pulse and square wave voltammetry other than cyclic voltammetry.

Detection limits taken as three times of the current backgrownd were 8x10-5 and 6x10-5 M for conventional and microelectrode, respectively from $Ru(NH_3)_6^{3+}$ CVs. The lower detection limits were of $7x10^{-6}$ and $8x10^{-6}$ for DPV and $9x10^{-6}$ and $1x10^{-5}$ for SWV at the micro and conventional electrodes, respectively.

LITERATURE CITED

1) Daniele, S.; Baldo, M.A.; Ugo, P.; Mazzocchin, G.A., Anal. Chim. Acta, 1989, 219, 9-18.

2) Daniele, S.; Baldo, M.A.; Ugo, P.; Mazzocchin, G.A., Anal. Chim. Acta, 1989, 219, 19-25.

3) Daniele, S.; Baldo, M.A.; Ugo, P.; Mazzocchin, G.A., Anal. Chim. Acta, 1990, 238, 357-366.

4) Daniele, S.; Baldo, M.A.; Ugo, P.; Mazzocchin, G.A., J. Electroanal Chem. 1990, 295, 95-111.

5) Gennaro, M.C.; Bertolo, P.L.; Baldo, M.A.; Daniele, S.; Mazzocchin, G.A., J. Liq. Chromatogr. 1991, 14, 115-138.

6) Baldo, M.A.; Daniele, S.; Mazzocchin, G.A.; Donati, M., Analyst, in press.

7) Walstra, P.; Jenness, R.; Dairy Chemistry and Physics, Wiley, New York, 1984.

8) Pellizzetti, E; Pramauro, E., Anal. Chim. Acta 1985, 169, 1-29.

9) Pladziewicz, R.; Meyer, T.; Broomhead, .A.; Taube, H., Inorg. Chem. 1973, 12, 639-643.

10) Fleischmann, M.; Lsserre, F.; Robinson, J.; Swan, D., J. Electroanal. Chem. 1984, 177, 97-114.

11) Kuwana, T.; Bublitz, D.T.; Hog, G., J.Am. Chem. Soc. 1960, 82, 5811-5817.

12) Walstra, P.; Jenness, R.; Dairy Chemistry and Physics, Wiley, New York, 1984, pp. 192-197.

13) Wightman, R.M.; Wipf, D.O., in Electroanalytical Chemistry, Bard Ed., 1989, vol.15, pp.267-353.

14) Bond ,A.M.; Oldham, K.B.; Zoski, C.G., Anal. Chim. Acta, 1989, 216, 177-330.

15) Endicott,J.F.; Schroeder, R.R.; Chidester, D.H.; Ferrier, D.R., J. Phys. Chem. 1973, 77, 2579-2583.

16) Wehmeyer, K.R.; Whightman, R.M., Anal. Chem. 1985, 57, 1989-1993.

17) Shea, T.V.; Bard, A.J., Anal. Chem., 1987, 59, 2101 2111.

18) Sabatani, E.; Rubinstein, I., J. Phys. Chem. 1987, 91, 6663-6669.

19) Rusling, J.F.; Zhang, H.; Willis, W.S., Anal. Chim. Acta, 1990, 235, 307-315.

20) Iwunze, M.O.; Sucheta, A.; Rusling, J.F., Anal. Chem. 1990,62, 644-649.

21) Nicholson, R.S., Anal. Chem. 1965, 37, 1351-1355.

22) Oldham, K.B.;Zoski, C.G.; Bond, A.M., J. Electroanal. Chem. 1987, 248, 467-473.

23) Van Vliet, T.; Walstra, P., J. Texture Studies, 1980, 11, 65-68.

24) Berthod, A.; Georges, J., Anal. Chim. Acta, 1983, 147, 41-51.

25) Ohsawa, Y.; Aoyagui, S., J. Electroanal. Chem. 1983, 145, 109-116.

26) Kaifer, A.E., Bard, A.J., J. Phys. Chem. 1985, 89, 4876.

27) Rusling, J. F., Shi, G.N.; Kumosiuski, T.F., Anal. Chem. 1988, 60, 1260-1267.

28) Georges,J.; Berthod, A., Electrochim. Acta 1983, 28, 735.

29) Chen, J.W.; Georges, J., J. Electroanal. Chem. 1986, 210, 205-211.

30) Ohsawa, Y.; Shimazaski, Y.; Aoyagui, S., J. Electroanal. Chem. 1980, 114, 235-246.

31) Eddowes, M.J.; Gratzel, M., J. Electroanal. Chem., 1984, 163, 31-62.

32) Evans, D.H., J. Electroanal Chem. 1989, 258, 451-456.

33) Texter, J., J. Electroanal. Chem., 1991, 304, 257-262.

34) Ohsawa, Y.; Aoyagui, S., . Electroanal. Chem. 1982, 136, 353-360.

35) Owlia, A.; Wang, Z.; Rusling, J.F., J. Am. Chem. Soc. 1989, 111, 5091-5098.

36) Mackay, R.A., J. Colloid. Int. Sci, 1978, 65, 225-231.

37) Mackay, R.A., Adv. Colloid. Int. Sci, 1981, 15, 131-156.

38) Egan, H.; Kirsk, R.S.; Sawyer, R., Chemical Analysis of Foods, Pearson' S Ed., 1981, p.p 433-472.

Table I

Results of cyclic voltammetry at a platinum electrode 1.5 mm radius for 1mM $Ru(NH_3)_6$ 3+ in the media indicated at 20^0C.

Medium	Scan rate/ mVs^{-1}	Δ E*/ ±2 mV	$-E_{1/2}$*/ ±0.002 V	i_{pb}/i_{pc}*
Water + 0.1M	10	60	0.170	1.10
$NaClO_4$	20	60	0.170	1.05
	50	61	0.171	1.01
	100	59	0.169	1.02
	200	61	0.172	0.99
Water + 0.1M	10	60	0.170	1.05
Phosphate buffer	20	59	0.171	1.02
	50	60	0.171	1.03
	100	61	0.170	0.99
	200	62	0.172	0.98
Skim milk	10	70	0.215	0.90
	20	80	0.216	0.98
	50	105	0.217	1.02
	100	110	0.218	1.04
	200	110	0.217	0.98
Whole milk	10	70	0.214	0.95
	20	70	0.210	0.98
	50	90	0.210	1.01
	100	100	0.217	1.04
	200	100	0.213	0.97
Cream (11%)	10	90	0.214	0.92
	20	90	0.213	0.94
	50	105	0.210	0.98
	100	110	0.213	0.95
	200	100	0.214	0.97
Cream (20%)	10	83	0.216	0 98
	20	100	0.213	0.95
	50	119	0.216	0.94
	100	112	0.219	0.97
	200	112	0.219	1.01
Cream (35%)	10	120	0.214	0.99
	20	140	0.212	0.95
	50	145	0.216	0.93
	100	145	0.214	0.91
	200	145	0.214	0.89

*Average values from at least three replicates.
Parenthesis, fat percentage.

Table II

Results of Cyclic voltammetry at a platinum electrode 12.5 μm radius for 1mM $Ru(NH_3)_6$ 3+ in the media indicated at 20°C.

Medium	slope* of log(id-i)/i vs E/ ±2mV	$E_{1/4}-E_{3/4}$*/ ±2mV	$-E_{1/2}$*/ ±0.002 V
Water + 01M $NaClO_4$	59 [0.999]	55	0.170
Water + 01M phosphate buffer	62 [0.999]	56	0.175
Water + 01M phosphate buffer + 2.5 gl^{-1} casein	60 [0.999]	54	0.190
Skim milk	62 [0.999]	60	0.190
Whole milk	60 [0.998]	55	0.195
Cream (11%)	59 [0.999]	59	0.200
Cream (20%)	59 [0.999]	59	0.195
Cream (35%)	58 [0.997]	58	0.200

*Average values from at least three replicates.

( ), fat percentage.

[] correlation coefficients of the relevant straight lines

Table III

Lower limits estimated for the heterogeneous electron transfer rate for the reduction of $Ru(NH_3)_6^{3+}$ in the media investigated at 20^0C

Medium	k^0 10^{-2} ms^{-1}
Water + 01M $NaClO_4$	0.32
Water + 0.1M phosphate buffer	0.30
Water + 0.1M phosphate buffer + 2.5 g/l Casein	0.14
Skim milk (0.3%)	0.11
Whole milk (4%)	0.10
Cream (11%)	0.10
Cream (20%)	0.10
Cream (35%)	0.10

Parenthesis, fat percentage.

Table IV

Diffusion coefficients obtained from measurements with conventional and microelectrodes in the media indicated at 20^0C.

r / Medium	$10^6 D^*/cm^2 s^{-1}$		$10^6 D'^*/cm^2 s^{-1}$	
	0.15	12.5×10^{-4}	0.15	12.5×10^{-4}
Water + 01M $NaClO_4$	6.08	6.30		
Water + 0.1M phosphate buffer	5.85	5.98		
Water + 0.1M phosphate buffer + 2.5 g/l Casein	2.87	2.41		
Skim milk (0.3%)	1.54	2.07	1.08	1.73
Whole milk (4%)	1.50	2.04	0.96	1.63
Cream (11%)	1.32	1.85	0.73	1.34
Cream (20%)	1.14	1.30	0.47	1.04
Cream (35%)	1.10	1.52	0.26	0.78

*Average values from at least five data obtained from samples of different lots.

% fat percentage.

r= electrode radius/ cm.

Table V

Typical bulk diffusion coefficients obtained with conventional and microelectrodes on same of the samples investigated at 20^0C.

Medium		r	$10^6 D^*/cm^2 s^{-1}$ 0.15	$10^6 D^*/cm^2 s^{-1}$ 12.5×10^{-4}
Whole milk 4%				
sample N^0	1		1.01(±0.09)	1.82(±0.09)
	2		1.27(±0.11)	2.35(±0.21)
	3		1.10(±0.15)	1.70(±0.12)
	4		1.40(±0.23)	2.01(±0.20)
	5		2.81(±0.32)	2.32(±0.12)
Cream 35%				
sample N^0	1		1.20(±0.23)	1.90(±0.15)
	2		1.11(±0.16)	1.50(±0.18)
	3		1.03(±0.19)	1.20(±0.16)
	4		1.21(±0.32)	1.34(±0.11)
	5		1.01(±0.21)	1.54(±0.15)

% fat

*Average value from at least four replicates

( ) standard deviation.

r= electrode radius/ cm.

Table VI

Diffusion coefficients of $Ru(NH_3)_6^{3+}$ obtained at platinum electrode 12.5 μm radius and viscosities of the media at 20^0C.

Medium	$10^6 D^*/cm^2 s^{-1}$	$10^{-2}*/Kgm^{-1}s^{-1}$
Water +0.1M phosphate buffer	6.25(±0.31)	1.031(±0.006)
Skim milk 0.3%	2.05(±0.12)	1.68(±0.03)
whole milk 4%	2.01(±0.15)	1.82(±0.04)
Cream 35%	1.70(±0.21)	6.90(±0.68)

* Average from three replicates

% fat

( ) standard deviation

Table VII

Determination of diffusion coefficients by means of eqn. (6) at the given Φ_{comp}.

Medium	Φ_{comp}	$10^6 D/cm^2 s^{-1}$
Skim milk(0.3%)	0.14	4.32
Whole milk(4%)	0.17	3.95
Cream (11%)	0.25	3.07
Cream (20%)	0.31	2.49
Cream (35%)	0.44	1.48

Parenthesis, fat %

FIGURE CAPTIONS

Fig.1- Cyclic voltammograms recorded on a whole milk sample at a) platinum 12.5×10^{-4} cm radius and b) platinum 0.15 cm radius, and a cream 35%-fat sample at c) platinum 12.5×10^{-4} cm radius and d) platinum 0.15 cm radius. Scan rate 10 mVs^{-1} for a) and c) and 100mVs^{-1} for b) and d).

Fig.2- Cyclic voltammograms recorded on a whole milk sample with added 1mM $Ru(NH_3)_6Cl_3$ at a) platinum 12.5×10^{-4} cm radius and b) platinum 0.15 cm radius, and a cream 35%-fat sample with added 0.8mM $Ru(NH_3)_6Cl_3$ at c) platinum 12.5×10^{-4} cm radius and d) platinum 0.15 cm radius. Scan rate 10 mVs^{-1} for a) and c) and 50mVs^{-1} for b) and d).

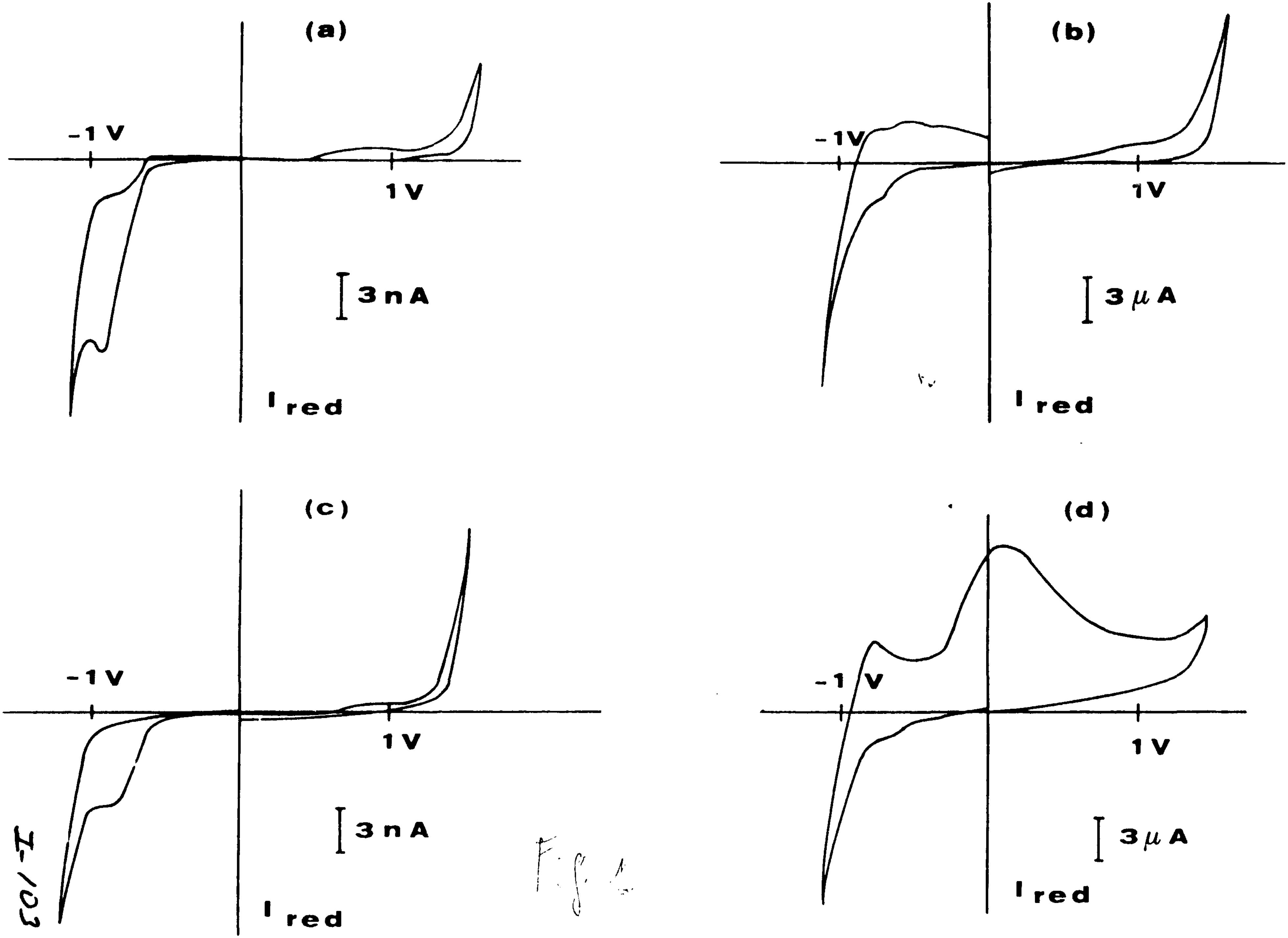

Fig. 6

I-103

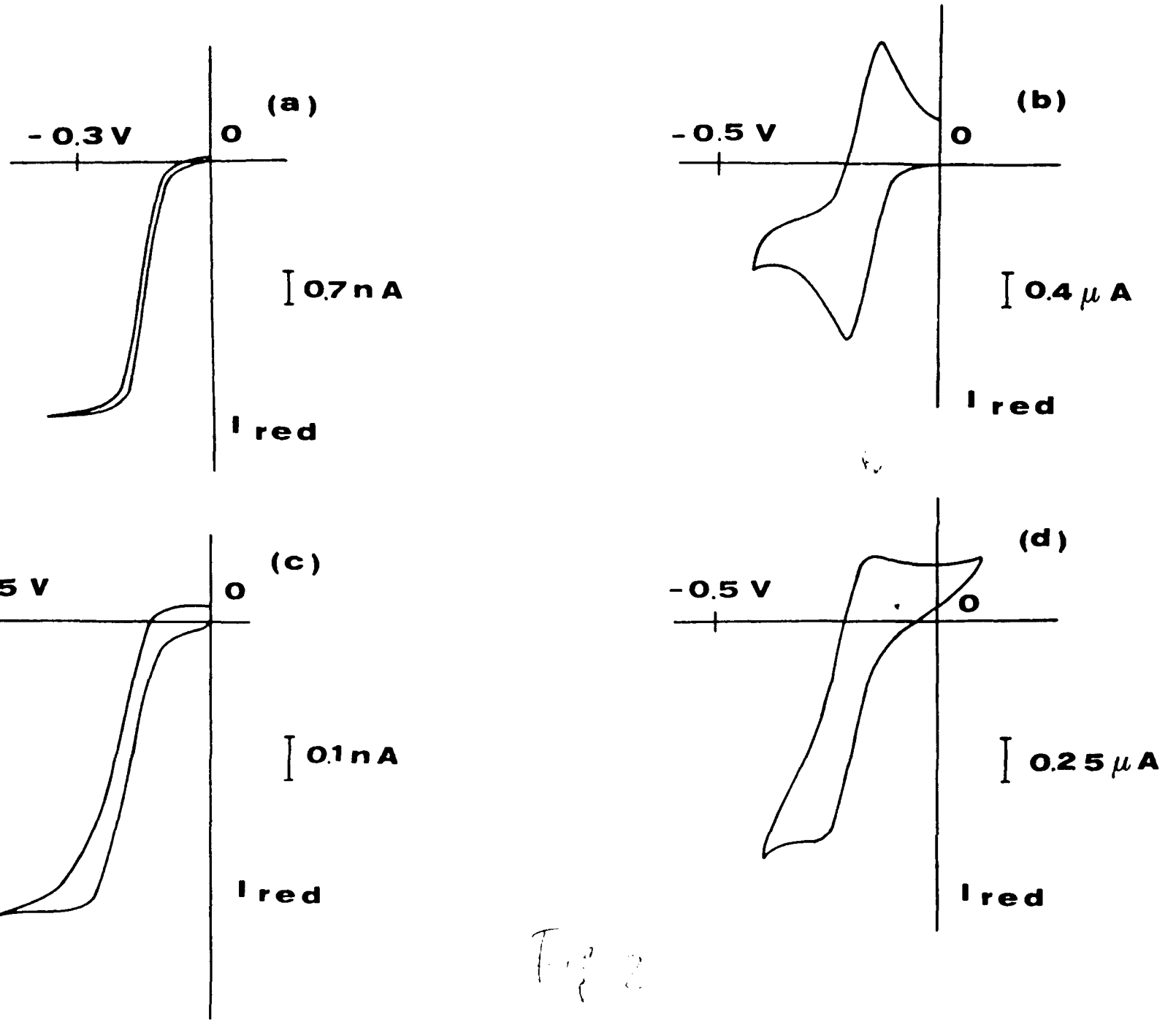
(a)
-0.3 V
0
0.7 nA
I red
(b)
-0.5 V
0
0.4 μA
I red
(c)
-0.5 V
0
0.1 nA
I red
(d)
-0.5 V
0
0.25 μA
I red

Fig 2

(6) ELECTROCHEMICAL CATALYSIS IN SURFACTANT MEDIA

James F. Rusling*, Naifei Hu[1], Heping Zhang,

David Howe, Chang-ling Miaw, and Eric Couture

Department of Chemistry (U-60),

University of Connecticut, Storrs, CT 06269-3060.

ABSTRACT

Rate enhancement can be achieved in electrochemical catalysis by using surfactants to preconcentrate reactants at electrodes. Control of reactivity can also be attained. The use of micelles and w/o microemulsions for these purposes is reviewed briefly.

Recent work is reviewed in which insoluble cationic surfactant films on electrodes are used to incorporate catalysts such as metal phthalocyanine tetrasulfonates ($MPcTS^{4-}$) and Co(III) corrinhexacarboxylates by ion exchange. Remarkable stabilization of didodecyldimethylammonium bromide (DDAB) films is achieved when $MPcTS^{4-}$s are incorporated, but not with Co(III) corrin hexacarboxylate. Composite DDAB-clay films are not ion exchangers. Unsubstituted metal phthalocyanines were incorporated into these composites by casting from a common chloroform solution.

Both DDAB and DDAB-clay films have been used for catalytic dechlorination of trichloroacetic acid. Kinetics of electron transfer between reduced catalyst and trichloroacetic acid in these films will be compared. Films adsorbed from DDAB dispersions onto electrodes were used for bulk catalytic reduction of polychlorinated biphenyls (PCBs).

---

[1]On leave from Beijing Normal University, Beijing, China.

Introduction

Extensive studies of thermal and photochemical reactions over the past several decades showed that surfactant media can enhance rates and help control reactivity in bimolecular reactions.[1-3] Rates of chemical reactions (R_{obs}) in micellar solutions are usually considered to be the sum of rates in the continuous aqueous phase (R_w) and the micellar "pseudophase" (R_m):

$$R_{obs} = R_w + R_m \qquad (1)$$

For a bimolecular reaction between A and B in aqueous micelles, for example, the simplest case is where both reactants are bound completely to micelles. Then the rate of the reaction in the water phase is negligible and

$$R_{obs} = [A][B]k_{obs} = [A]_m[B]_m k_m \qquad (2)$$

where observed rate constant k_{obs} reflects the moles of A and B in the total volume of the system, V_t. Actual concentrations of reactants at micellar reaction sites are approximately $[A]_m = [A]/\phi_m$ and $[B]_m = [B]/\phi_m$, where ϕ_m is the volume fraction of the micellar core. Substitution of these concentration terms into eq 2 gives:

$$k_{obs} = k_m/\phi_m^2 \qquad (3)$$

Eq 3 shows that the observed rate is enhanced by compartmentalization of reactants into the reaction volume $V\phi_m$, producing an apparent catalysis. Rate enhancement is mainly a consequence of high reactant concentrations in the micellar volume, which contains all the reactants. This rate enhancement is of considerable practical importance. Although much more sophisticated treatments of kinetics in micelles are available,[1-3] the simple concepts described above are useful for a qualitative understanding of chemical reactions coupled to electron transfer at electrodes in micellar solutions.

The principles of rate control and enhancement by surfactant aggregates can

also be applied to electrochemical catalysis.[4] In this method, a catalyst (mediator) shuttles electrons between electrodes and substrates that are otherwise difficult to reduce or oxidize. The main advantage is that the catalyzed reaction needs less energy (i. e., smaller overpotential) and is faster than direct electron exchange between substrate and electrode. The rate determining steps in these reactions are often bimolecular electron transfers, and are amenable to micellar alteration of kinetics (cf. eqs 1-3).

In this paper, we will refer to model reactions involving two-electron reductive cleavage of carbon-halogen bonds. Reactions include dechlorinations of aryl halides, alkyl vicinal dihalides, and haloacetic acids, yielding as products aromatic hydrocarbons, alkenes, and acetic acid, respectively. Such reactions can be catalyzed by organic catalysts such as anthracene derivatives and macrocyclic complexes including metal corrins and phthalocyanines. A typical reaction pathway, where R = $-CH_2COOH$ or a phenyl ring, is as follows:[5-8]

Scheme I

$$P + e \rightleftharpoons Q \qquad E^o \qquad \text{(at electrode)} \qquad (4)$$

$$RX + Q \underset{k_2}{\overset{k_1}{\rightleftharpoons}} RX^{\cdot -} + P \qquad (5)$$

$$RX^{\cdot -} \xrightarrow{k} R^{\cdot} + X^- \qquad (6)$$

$$R^{\cdot} + Q \rightarrow P + R^- \qquad \text{(fast)} \qquad (7)$$

$$R^- + (H+) \rightarrow RH \qquad \text{(fast)} \qquad (8)$$

Catalyst P is dissolved in the surfactant medium or immobilized on the electrode. At potentials near E^o, P is reduced to its activated form Q at the electrode (eq 4). Q transfers electrons to acceptor RX (eq 5).

Eq 5 is the rate-determining step (rds) in many aryl halide and haloacetic acid reductions,[5-8] but cleavage of radical $RX^{\cdot -}$ in eq 6 may become important for aryl halides in micellar media when rates of eq 5 are greatly

enhanced.[7] For aliphatic halides, eqs 5 and 6 are probably concerted.[9a] In both cases, a second ET and protonation (eqs 7 and 8) yield RH.[9b] The resulting advantage is that RX is reduced to RH at the formal potential (E^o) of the catalyst, rather than the more negative potential for direct reduction of RX at the electrode. P is regenerated in the catalytic cycle, and gets reduced again at the electrode. The electrochemically measured peak current for reduction of P (eq 1) is larger when RX is present. This is called the "catalytic" current and can be used to evaluate kinetic constants.[6] It is also proportional to the concentration of RX. Many of the organohalide reactants discussed here are toxic environmental pollutants.[4] Thus, electrochemical catalytic reductions in surfactant media can be the basis for detection and decomposition of environmental pollutants.

In this paper, we briefly review recent history of electrochemical catalysis in micelles and microemulsions by way of examples from our own laboratory. We then discuss recent results on the use of stable liquid crystal surfactant films on electrodes for these reactions. Finally, we present applications involving bulk dechlorination of polychlorinated biphenyls in surfactant dispersions which form similar films on electrodes.

Catalysis in Micelles and Microemulsions.

Enhancement of Rates. Thus far, the best rate enhancements for catalytic dehalogenations in micellar systems were found with nonpolar catalysts and substrates and cationic surfactants. At potentials negative of -2 V vs. SCE, the nonpolar reactants were bound almost entirely to surfactant aggregates. One system investigated in detail employed 9-phenylanthracene (9-PA) as catalyst and 4-bromobiphenyl (4-BB) as substrate. The surfactant was cetyltrimethylammonium bromide (CTAB) and the cathode was Hg. In this system debromination of 4-BB occurs at an applied potential of about -2.1 V vs SCE.

The observed value of k_1 for reaction of 9-PA anion radical with 4-BB was about 10^7 $M^{-1}s^{-1}$ in 0.1 M CTAB compared to 300 $M^{-1}s^{-1}$ in dimethylformamide.[7] The reason for the better than 1000-fold rate enhancement is embodied in eq 3. This reaction occurs with the nonpolar reactants and surfactant coadsorbed in a thick film of surfactant on the Hg electrode (Fig. 1), making local reactant concentrations quite large. Nonionic and anionic surfactants gave poor protection against side reactions for the active 9-PA anion radical formed at the electrode (eq 4).

Similar reactions in aqueous CTAB with catalysts having E^o's more positive than -2 V vs SCE also gave rate enhancements, but not greater than 25-fold in any case. At these potentials, preconcentration of reactants by CTAB films on the electrode was not effective; these reactions occurred mainly in diffusing micelles.[10] In such cases, reactants are statistically distributed[4] among micelles, decreasing their concentration product at micellar reaction sites compared to situations where both reactants are concentrated in a thick film on the electrode.

Control of Reactivity. We also studied the kinetics of catalytic reduction of several alkyl vicinal dibromides by vitamin B_{12}, a water soluble cobalt corrin complex, in w/o microemulsions. The reaction pathway is similar to scheme I, but the rds is an *inner sphere* electron transfer between $B_{12}Co(I)$ and the alkyl dibromide (eq 10).[11,12] This can occur by a radical mechanism as in eqs 10,11, or by a concerted E2 elimination. These two pathways are kinetically indistinguishable and both give alkene as the product.

Scheme II

$$Co(II) + e = Co(I) \quad \text{(at electrode)} \qquad (9)$$

$$Co(I) + RX_2 \xrightarrow{k_1} RX^{\cdot} + X^- + Co(II) \quad \text{(rds)} \qquad (10)$$

$$RX^{\cdot} + Co(I) \longrightarrow \text{alkene} + X^- + Co(II) \qquad (11)$$

In w/o microemulsions of Aerosol OT (AOT, bis(2-ethylhexyl)sulfosuccinate)/water/isooctane, the highly water soluble vitamin B_{12a} resides entirely in water pools. Substrates ethylene dibromide (EDB), 1,2-dibromobutane (DBB), and trans-1,2-dibromocylohexane (t-DBC) are present mainly in the continuous isooctane phase.[12] Thus, catalyst and substrate are spatially separated in the two phases of the microemulsion (Fig. 2).

Because of the high resistance of w/o microemulsions, microelectrode voltammetry was required to observe k_1. The reaction occurred at diffusing water microdroplets, rather than on the electrode surface. Observed apparent k_1's were three orders of magnitude smaller in the w/o microemulsion than in acetonitrile/water. Attenuation of rates occurs because of the spatial segregation of the reactants.

Relative observed k_1-values for DBB:EDB:t-DBC were 1:2:4 in water/MeCN and 1:4:20 in the microemulsion.[12] Thus, the microemulsion alters the relative reactivities of the alkyl dibromides. The increase in relative reactivity of t-DBC in the microemulsion may be caused by selective interaction of this cyclic substrate with the AOT hydrocarbon tails at the outer surface of the water pools.

Electrochemical Catalysis in Cast Surfactant Films.

Enhancements in rates of mediated bimolecular reductions under conditions where co-adsorption of thick cationic surfactant films and reactants occurred on the surface of electrodes encouraged us to prepare films usable for

catalysts with a broad range of E^os. As discussed, very negative electrode potentials were required to spontaneously adsorb cationic surfactant coatings useful for reactant preconcentration. We sought more general surfactant coatings usable over a wide potential window. We also hoped that the films could preconcentrate reactants and lead to practical rate enhancements.

To achieve these goals, we recently began to investigate films of insoluble cationic surfactants and surfactant-clay composites cast onto pyrolytic graphite electrodes. Such films were studied previously in free-standing forms as semipermeable membranes.[13-15] Permeabilities of these films to water soluble neutral organic probes respond to phase changes. In the solid-like gel phase, hydrocarbon chains of the surfactant are in an ordered all-trans orientation and the films are nearly impermeable to the probes. Above phase transition temperature T_c, kinks in the hydrocarbon chains develop and cause the onset of a fluid liquid crystal phase.[16] Soluble probes readily pass through the films in the liquid crystal phase.

Structures for these films (Fig. 3) were proposed[13-15] on the basis of phase transition, permeability, X-ray diffraction, and spectroscopic data. As we shall see, these structures are qualitatively consistent with our electrochemical results.[17,18]

I. Dialkyldimethylammonium Films on Pyrolytic Graphite Electrodes.

Preparation of films. We have studied electrochemical and catalytic properties of films of water-insoluble double chain surfactants didodecyl- and dioctadecyldimethylammonium bromide (DDAB and DODAB) on pyrolytic graphite (PG, HPG type, Union Carbide) disk electrodes. The films were prepared by making solutions 0.01 to 0.2 M of surfactant in chloroform, and placing a measured amount of this solution with a syringe onto a PG disk. In our present preparation method, the chloroform is allowed to evaporate overnight after

placing a small bottle over the electrode to serve as a closed evaporation chamber. The coated electrode is subsequently cured in air overnight. This method gave more uniform and reproducible films than an earlier technique of evaporation in air,[17] although results with both methods of preparation are similar. The films are from 1-40 μm thick corresponding to about 500 to 10,000 monolayers of surfactant. Surfactant coatings are generally stable for at least five days when used in aqueous KBr solutions.

Electrochemical properties. The films take up large amounts of electroactive multivalent anions such as ferrocyanide (ca. 3.5×10^{-8} mol cm^{-2} for 20 μm thick DDAB films at 25 ^{o}C and 35 ^{o}C)[17] or multianionic metal macrocyclic complexes from aqueous solution at temperatures above their gel-to-liquid crystal phase transitions. They reject hydrophilic electroactive cations and are permeable to hydrophobic cations. Electrochemistry of incorporated anions can be turned off by bringing the films to the gel phase, and turned on again by returning to the liquid crystal phase.

Uptake of multivalent anions is illustrated (Fig. 4) by increasing currents in repetitive scan cyclic voltammograms of a DDAB coated PG electrode in a solution of vitamin B_{12} hexacarboxylate at pH 5.7 (Fig. 5). This macrocyclic complex has a pK_a of 4.8; it is fully ionized an pH 6.3. Its concentration builds up in the film by ion exchange, causing the successively increased currents on repeated scans. When no more of the vitamin B_{12} hexacarboxylate can enter the film, the peak currents remain constant. This is called the steady state condition under which most characterization experiments were done.

In addition to vitamin B_{12} hexacarboxylate and ferrocyanide, we studied uptake and retention of copper phthalocyanine tetrasulfonate ($CuPcTS^{4-}$), and nickel phthalocyanine tetrasulfonate ($NiPcTS^{4-}$) (Fig. 5) in DDAB and DODAB films. All of these ions showed a rapid uptake similar to that in Fig. 3. An

approximately 30% increase in peak current was found when 0.2 M butanol was present in the electrolyte solutions. This suggests an increase in fluidity of the film caused by incorporation of butanol.[17]

When DDAB-PG electrodes prepared as described above and loaded with ferrocyanide or vitamin B_{12} hexacarboxylate were placed in solutions of aqueous electrolyte not containing electroactive anions, successive CVs revealed that 75% of the ions in the film leached out in an hour or two. In contrast, DDAB-PG electrodes loaded to the steady state condition with $NiPcTS^{4-}$ or $CuPcTS^{4-}$ showed remarkable stability when placed in an electrolyte solution free of electroactive anions. For example, a DDAB-PG electrode loaded with $NiPcTS^{4-}$ (3.4×10^{-8} mol/cm^2) and placed in $NiPcTS^{4-}$-free 0.1 M KBr decreased from the initial cathodic CV peak current by only about 10% over 11 days of immersion!

What is the reason for this remarkable stability when $NiPcTS^{4-}$ are present? This point is still under active study in our laboratory. Preliminary results show that CVs of the $MPcTS^{4-}$ ions are much more reversible when the ions are in the film (Fig. 6) compared to dissolved in aqueous electrolyte. Also, CVs change continuously during uptake of the $MPcTS^{4-}$ and maximum stability is not reached until full loading and steady state conditions are achieved (Fig. 7). The poor electrochemical behavior of $MPcTS^{4-}$'s in solution is likely related to aggregation of the ions in solution, leading to very small diffusion coefficients,[19] and also aggregation on the surface which may render some $MPcTS^{4-}$ electrochemically inactive.[19,20]

Aggregation of these species can be followed via their electronic absorption spectra.[19] Preliminary spectroscopic studies suggest that the $MPcTS^{4-}$ in DDAB films may be much less aggregated than at equivalent concentrations in water. Furthermore, the amount of aggregation increases as

concentration of $MPcTS^{4-}$ in the film increases. Our present working hypothesis is that aggregation and film stability may be related in some way. This is further supported by the observation that films only partly loaded with $MPcTS^{4-}$s lost these ions quickly in blank electrolyte solutions.

Phase Transitions. The transition between the solid-like gel and liquid crystal phases, as driven by increasing temperature, turns on the electrochemistry in the film.[17] CVs were recorded at different temperatures for DDAB and DODAB films loaded to a steady state with $Fe(CN)_6^{4-}$ in 0.1 M KBr. For DODAB films in 0.1 M KBr, peak oxidation current was very small at temperatures less than 50 °C, but increased dramatically at T>50 °C. Loaded DODAB films in 0.1 M KBr/0.2 M butanol showed a break at 42 °C. Similar temperature effects were found for electrodes coated with DDAB. The break point in peak current vs. T (i-T) plots was 9(±1)°C in 1 mM ferrocyanide/0.1 M KBr. The break point for DDAB films was 2(±1) °C when 0.2 M butanol was present in solution (Table I ***include all T_c values*****).

Gel-to-liquid crystal phase transitions have also been observed for cast films of insoluble tetraalkylammonium surfactants by differential scanning calorimetry and optical techniques.[13,14] The i_p vs. T behavior of the DDAB and DODAB films can be interpreted in terms of this phase transition. The i-T break for DDAB is at about 9 °C, very close to the T_c value found for DDAB vesicles suspended in water.[15] The break for DODAB in 0.1 M KBr/0.2 M butanol was at 42 °C, slightly lower than that for DODAB vesicles in water (44 °C).[21] In accord with the effect of short chain alcohols on T_c values of phosphatidylcholine bilayers,[22] the i-T break point for DDAB was lowered from 9 to 2 °C in the presence of 0.2 M butanol.

Thus, electrochemistry of ions can be turned off by lowering temperature below T_c, and turned on again by raising temperature above T_c. In films

previously loaded with ferrocyanide, much of the ferrocyanide remained upon transfer of the electrodes from solutions at a temperatures below T_c to a ferrocyanide-free solution above T_c.[17] Thus, shutting off the electrochemistry appears to involve the increased rigidity of the gel state, slowing charge transport dramatically, rather than expulsion of ferrocyanide ions from the films.

The observation of phase transitions suggests at least partially ordered multibilayer structures for the films. Water and incorporated anions are presumably associated with surfactant head groups. However, preliminary experiments on DDAB films loaded with $NiPcTS^{4-}$ have not revealed a clear T_c point above 0 °C. However, DODAB films loaded with $NiPcTS^{4-}$ showed a sharp phase transition in CV data at about 42 °C, about the same as when loaded with ferrocyanide. Further phase transition studies by electrochemistry and scanning calorimetry are underway.

Catalytic Reduction of Tricloroacetic Acid. All catalytic reactions were studied under conditions where films were liquid crystalline. Preliminary studies showed that DDAB films loaded with vitamin B_{12} hexacarboxylate, $CuPcTS^{4-}$, and $NiPcTS^{4-}$ were all active for catalytic reductive dechlorination[8] of trichloroacetic acid dissolved in solution. Quantitative comparisons of catalytic efficiency will be reported.

II. Composite Films of Dialkyldimethylammonium Surfactants and Clay.

Natural clays are cation exchangers. Colloidal forms of the clays with sodium as the only exchangeable cation are easily prepared.[23,24] These sodium ions are readily replaced by cationic surfactants.[23] Electrodes coated with colloidal clay and used in aqueous micellar solutions of CTAB were shown to coadsorb surfactant and reactants in dehalogenation reactions, leading to mild rate enhancements.[4,24]

Films of water-insoluble tetraalkylammonium surfactants intercalated between colloidal clay layers were recently prepared by Okahata and Shimizu[15] as membranes with controlled permeability. X-ray diffraction and gel to liquid crystal phase transition data suggested that surfactant molecules in tail-to-tail bilayer orientations separated the clay layers (cf. Fig. 3b). In the liquid crystal phase, surfactant-clay films were permeable to water-soluble organic compounds. Permeability was turned off by bringing the films to the solid-like gel phase. These films are apparently held together by coulombic attraction between the clay and surfactant head groups combined with hydrophobic interactions between surfactant tails. Stability of surfactant-clay composites to extremes of ionic strength, temperature and pH was excellent.[15]

We studied electrochemical properties and catalysis using films made from clay colloids and DDAB or DODAB. Metal phthalocyanine mediators incorporated in these films before casting were extremely stable during catalytic reduction of trichloroacetic acid. Unlike films made entirely from surfactants, the surfactant-clay composites are not ion exchangers.

Preparation. A dispersion of 0.5 g colloidal sodium bentonite clay[24] in 25 mL water was mixed with an aqueous dispersion of 1.2 mmol DDAB or DODAB in 10 mL water and stirred at 70°C for one hour.[15] The white surfactant-clay

precipitate was filtered, washed with water, and resuspended in 15 mL chloroform. Methanol was added until the suspension became cloudy. This mixture was aged at 35 ^{o}C for 30 min., allowed to cool to room temperature, and filtered under vacuum until the solvent was removed.

Films were made by depositing 60 uL of a dispersion of the surfactant-clay composite (2 mg mL^{-1}) in chloroform onto a freshly polished PG disk. Chloroform was evaporated overnight in air.

Films containing iron(II) or cobalt(II) phthalocyanine (FePc or CoPc) were made by mixing 1 mL of the above surfactant-clay dispersion with 1 mL of a 10 mM solution of the FePc or CoPc in chloroform. This mixture was sonicated for 0.5 hr and a measured amount (usually 120 uL) was deposited onto a PG disk.

Electrochemical Properties. These composite films acted as charge transfer barriers toward both positive and negative multivalent electroactive ions in solution such as ferrocyanide(4-) and rutheniumhexammine (3+). Thus, the films are not ion exchangers.[18] They took up ions with hydrophobic ligands, e.g. tris(2,2'-bipyridyl)cobalt(II). The films were permeable to the water soluble neutral p-quinone.

Catalytic Reduction of Trichloroacetic Acid. Metallophthalocyanines (MPc) without ring substituents are very insoluble in water and have a wide range of catalytic activities for redox reactions [12]. FePc and CoPc were dissolved in DDAB-clay dispersions before casting on PG (see above). The resulting films contained 0.6 μmol MPc and 0.12 mg of composite. CV gave very small peaks for MPc-DDAB-clay electrodes in electrolyte solutions. Thus, we studied these films with square-wave voltammetry (SWV) to get the required sensitivity.

FePc films gave two sets of reversible SWV forward and reverse peaks (Fig. 8), attributed to reductions of Fe(II)Pc and $Fe(I)Pc^{-}$, respectively.[19] The CoPc film gave forward and reverse peaks at -0.45$\pm$0.02 V vs. SCE consistent

with a reversible Co(II)Pc/Co(I)Pc$^-$ redox couple. In general, at frequencies (f) below about 100 Hz, thin layer electrochemistry was found. Diffusion-like behavior was indicated at f$\geq$400 Hz.[18]

In solutions of trichloroacetic acid, CoPc-DDAB-clay electrodes gave increases in SWV current (Fig. 9) were found at about -0.5 V. This peak was about 0.5 V positive of that for unmediated direct reduction of trichloroacetic acid on an electrode coated with DDAB-clay, but not CoPc. Catalytic efficiency expressed as the ratio of catalytic SWV forward current (i_c) to the forward current for the CoPc film in solutions not containing trichloroacetic acid (i_d) decreased with increasing f, as expected for an electrochemical catalytic reduction.[26] At fixed f, catalytic current increased with concentration of trichloroacetic acid.

FePc-DDAB-clay electrodes also gave peaks of increased height in solutions of trichloroacetic acid. In solutions containing this substrate, amplification of cathodic CV and forward and difference SWV currents occurred at potentials of the second reduction peak of FePc, -1.30 V. This is only about 50 mV positive of the direct reduction peak of trichloroacetic acid on DDAB-clay electrodes. Catalytic efficiency decreased with increasing f. SWV peak current increased with concentration of trichloroacetic acid.

MPc-DDAB-clay electrodes gave stable catalytic currents for over 10 days. In fact, a 10% increase in current was observed over this time. CoPc-DDAB-clay electrodes were also removed from solution, washed, and dried in air. Upon returning to 10 mM trichloroacetic acid in 0.1 M KBr the next day, nearly the same catalytic current was obtained.

Results for composite MPc electrodes in trichloroacetic acid solutions are consistent with catalytic dechlorination[8] of the acid by Co(I)Pc and Fe(I)Pc^{2-} in the films. This reaction is similar to that catalyzed by vitamin

B_{12}hexacarboxylate, and the $MPcTS^{4-}$ mediators in DDAB films as discussed above. The following two-electron pathway, similar to Scheme II, describes the kinetics:

Scheme III

$$Co(II)Pc + e = Co(I)Pc^- \quad (12)$$

$$Co(I)Pc^- + RCl \xrightarrow{k_2} Cl^- + Co(II)Pc + R\cdot \quad (13)$$

$$Co(I)Pc^- + R\cdot \longrightarrow Co(II)Pc + R^- \text{ (fast)} \quad (14)$$

The rate determining step is assumed to be reaction of Co(I)Pc with substrate RCl (eq 13), as in other reactions of this type.[4] Eq 14 is a source of the second electron. As in scheme II, a kinetically equivalent alternative is a concerted E2 elimination to give R^- directly. R^- presumably undergoes rapid protonation to give product RH.

Using SWV theory[26] for one-electron catalysis, we computed a theoretical working curve of i_c/i_d vs. log k/f for our experimental conditions. This was used to estimate apparent pseudo-first-order rate constants ($k = k_2[RCl]$) for the two catalytic electrodes from the catalytic efficiency ratios measured under diffusion-like conditions, where i_d is proportional to $f^{1/2}$. We compared $i_c/2i_d$ to the working curve to account for the two electrons needed to reduce the C-Cl bond. Good agreement of experimental and theoretical catalytic efficiencies were found in the diffusion-controlled frequency range (Fig. 10). Average values of k were $5.7\pm0.6\times10^3$ s^{-1} for CoPc and $0.16\pm0.04\times10^3$ s^{-1} for FePc.

Since exact concentrations of reactants at the reaction site are unknown, k-values in Table I are apparent rate parameters only. Nevertheless, they can be used for comparisons. The apparent k for the CoPc film is 35-fold larger than that of the FePc film. Also, the CoPc film lowers the overpotential for

reduction of trichloroacetic acid by about 0.5 V.

Thus, mediation of reduction of trichloroacetic acid by the CoPc film is faster than that of FePc films. In the latter, catalysis occurs at potentials of the second peak, where $Fe(I)Pc^{2-}$ is formed in the film. $Fe(I)Pc^{-}$ is unreactive. Overpotential for reduction of trichloroacetic acid is decreased by less than 0.1 V by FePc films.

Phase Transitions. Catalytic reductions with MPc films were examined at a series of temperatures (T). Plots of forward SWV peak current vs. T for MPc-DDAB-clay films in solutions of trichloroacetic acid showed discontinuities at 5 ^{o}C, below which catalytic current remained nearly constant. Temperature dependence of the catalytic current was also followed in a film made from clay and dioctadecyldimethylammonium bromide (DODAB), which has a higher gel-to-liquid crystal phase transition temperature[15] than DDAB-clay. Peak current measured by CV and SWV vs. T for FePc-DODAB-clay in solutions of trichloroacetic acid showed a discontinuity at 54 ^{o}C.

As with the pure surfactant films, structural and charge transport properties of surfactant-clay composites are governed by temperature. Previously measured values[15] of T_c by differential scanning calorimetry and permeability were 15 ^{o}C for DDAB-clay and 54 ^{o}C for DODAB-clay. (These values were 5-10 ^{o}C higher than for aqueous bilayer dispersions of the surfactants [8]). T_c values for the composites are similar to temperatures of breaks in catalytic current vs. T curves found for DDAB-clay (5 ^{o}C) and DODAB-clay (54 ^{o}C). Results of these experiments indicate that charge transport through the films is considerably faster in the liquid crystal phase than in the gel phase.

III. Bulk Catalytic Dehalogenation of Polychlorinated Biphenyls.

An ongoing application in our work has been bulk dehalogenation of polychlorinated biphenyls (PCBs) PCBs and their commercial mixtures (Aroclors). PCBs and the related chlorodioxins are aryl halides. They are often found in aquatic sediments.[27] These nonpolar compounds bind strongly to surfactant aggregates, and thus are excellent substrates for attempting rate enhancements. Electrochemical catalysis in surfactant media does not require excess chemical reagents. Surfactant media facilitate stepwise catalytic dechlorination (Scheme I) in the presence of water and particulates which are found with PCBs in the environment. Toxic, expensive organic solvents can be avoided.

As working electrodes for these bulk electrolytic reactions, we use carbon felt or mercury cathodes of geometric areas 10-35 cm^2. Zinc phthalocyanine (ZnPc) has thus far been the most active catalyst tested.[4,7,10,18,24] These catalytic reductions are very selective for stepwise dehalogenation. No products other than biphenyl, its reduced products, and lower PCB congeners have been detected by HPLC or by GC-MS.

Our most successful dehalogenations of PCBs employed ZnPc in aqueous acidified dispersions of didodecyldimethylammonium bromide (DDAB), present in water as lamellar liquid crystal aggregates.[28] Carbon felt cathodes were used at -2.3 V vs SCE with intermittent ultrasound to enhance mass transport. Aroclor 1016 (42% Cl, 12 mg in 25 mL of DDAB dispersion) was completely dehalogenated in 25 hr. Less than 10% dehalogenation was found for analogous reaction conditions in aqueous CTAB.

DDAB facilitates strong coadsorption of ZnPc and PCBs onto the negative cathode. In DDAB dispersions, the reaction takes place in a DDAB film on the electrode surface. These findings illustrate once again that reaction rates are enhanced by coadsorbing reactants with surfactant coatings on electrodes. The

negative cathode provides a favorable surface for adsorption of dispersed cationic DDAB aggregates. Coadsorption of nonpolar reactants with DDAB on the electrode improves rates of dehalogenation compared to micellar CTAB,[28] which is less completely adsorbed on the electrode.

Very recent work in our laboratory has shown that the use of DDAB dispersions containing acetate buffer and using intense ultrasound gave better bulk dechlorination rates for 4,4'-dichlorobiphenyl to the acidified DDAB dispersions. Controls using ultrasound alone showed that dechlorinations were purely electrolytic, but that ultrasound improved yields presumably by improving mass transport. These experiments gave significant yields of reduced biphenyl derivatives as well as biphenyl. Preliminary work with Hg and Pb electrodes indicate that they give better yields than carbon felt electrodes (Table II). This may be because reduction of hydrogen ions is a less efficient competitor for catalytic dehalogenation on the metal electrode surfaces. Further studies on these reactions are in progress.

IV. Summary and Conclusions.**********

Acknowledgment. Financial support for this work was provided by U.S. PHS Grant ES03154 awarded by the National Institute of Environmental Health Sciences, from the donors of the Petroleum Research Fund administered by the American Chemical Society, from the Department of Higher Education of the State of Connecticut, and from the Research Foundation and Environmental Research Institute, University of Connecticut.

References and Notes

(1) Bunton, C. A. Cat. Rev. Sci. Eng. 1979, 20, 1-56.

(2) Fendler, J. H. "Membrane Mimetic Chemistry", Wiley: New York, 1982

(3) Gratzel, M. "Heterogeneous Photochemical Electron Transfer"; CRC Press, Boca Raton, FL, 1989.

(4) Rusling, J. F. Accts. Chem. Res., 1991, 24, 75-81.

(5) Andrieux, C. P.; Blocman, C.; Dumas-Bouchiat, J.-M.; Saveant, J. M. J. Am. Chem. Soc. 1979, 101, 3431-3441.

(6) (a) Connors, T. F.; Rusling, J. F.; Owlia, A. Anal. Chem. 1985, 57, 170-174; (b) Arena, J. V.; Rusling, J. F. J. Phys. Chem. 1987, 91, 3368-3373.

(7) Rusling, J. F.; Shi, C.-N.; Gosser, D. K.; Shukla, S. S. J. Electroanal. Chem. 1988, 240, 201-216.

(8) Rusling, J. F.; Miaw, C. L.; Couture, E. C. Inorganic Chem. 1990, 29, 2025-2027.

(9) (a) Andrieux, C. P.; Saveant, J. M.; Su, K. B. J. Phys. Chem. 1986, 90, 3815-3823. (b) Other reactions following eq 6, e. g. H-atom abstraction from solvent or electrolyte by R·, can also be involved in reductions of aryl halides. For a discussion, see Andrieux, C. P.; Saveant, J. M.; Zann, D. Nouv. J. Chim. 1984, 8, 107-116.

(10) Rusling, J. F.; Shi, C.-N.; Couture, E. C.; Kumosinski, T. F. in Dryhurst G.; Niki, K. (Eds.) "Redox Chemistry and Interfacial Behavior of Biological Molecules" Plenum, N. Y., 1988, pp. 565-581.

(11) Connors, T. F.; Arena, J. V.; Rusling, J. F. J. Phys. Chem. 1988, 92, 2810-2816.

(12) Owlia, A.; Wang, Z.; Rusling, J. F. J. Am. Chem. Soc. 1989, 111, 5901-5908.

(13) Nakashima, N.; Ando, R.; Kunitake, T. Chem. Lett. 1983, 1577-1580.

(14) Kunitake, T.; Shimomura, M.; Kajiyama, T.; Harada, A.; Okuyama, K.; Takayanagi, M. Thin Solid Films, 1984, 121, L89-91.

(15) Okahata, Y.; Shimizu, A. Langmuir, 1989, 5, 954-959.

(16) (a) Lee, A. G. Biochim. Biophys. Acta 1977, 472, 237-281. (b) Nagle, J. F. Ann. Rev. Phys. Chem. 1980, 31, 157-195.

(17) Rusling, J. F.; Zhang, H. Langmuir, 1991, in press.

(18) Hu, N.; Rusling, J. F. Anal. Chem., submitted.

(19) Owlia, A.; Rusling, J. F. J. Electroanal. Chem., 1987, 234, 297-314.

(20) Zecevic, S.; Simic-Glavaski, B.; Yeager, E.; Lever, A. P. B.; Minor, P. C. J. Electroanal. Chem. 1985, 196, 339 and references therein.

(21) Shimomura, M.; Kunitake, T. Polymer J. 1984, 16, 187-190.

(22) (a) Rowe, E. S. Biochemistry, 1983, 22, 3299-3305. (b) Simon, S. A.; McIntosh, T. J. Biochim. Biophys. Acta 1984, 773, 169-172.

(23) (a) Nakamura, T.; Thomas, J. K. Langmuir, 1987, 3, 234-239. (b) Viaene, K.; Caigui, J.; Schoonheydt, R. A.; DeSchryver, F. C. Langmuir, 1987, 3, 107-111.

(24) (a) Rusling, J. F.; Shi, C.; Suib, S. L. J. Electroanal. Chem. 1988, 245, 331-337. (b) Shi, C.; Rusling, J. F.; Wang, Z.; Willis, W. S.; Winiecki, Ann M.; Suib, S. L. Langmuir, 1989, 5, 650-660.

(25) (a) Moser, F. H.; Thomas, A. L. "The Phthalocyanines", Vol. I, CRC Press: Boca Raton, FL.; 1983. (b) Scheffold, R. in Scheffold, R. (Ed.) "Modern Synthetic Methods", V. 3, Wiley, New York: 1983; pp. 355-439.

(26) Zeng, J.; Osteryoung, R. Anal. Chem. 1986, 58, 2766-2771.

(27) D'Itri, F. M.; Kamrin, M. A. (Eds.) "PCB's: Human Environmental Hazards" Butterworths: Woburn, MA, 1983.

(28) Iwunze, M. O.; Rusling, J. F. J. Electroanal. Chem. 1989, 266, 197-201.

Figure Captions

Fig. 1. Conceptual representation of catalytic reduction of organohalides [R = aromatic ring, R'XCH-CH_2-, or -CH_2COOH] using mediator P in a surfactant film on an electrode.

Fig. 2. Conceptual representation of Co(I) form of vitamin B_{12} in water pool of w/o microemulsions with vicinal dihalide reactant in the oil phase.

Fig. 3. Idealized drawings of two types of surfactant films that can be cast on electrodes from organic solvent: (a) multibilayer film such as obtained with DDAB; (b) DDAB-clay composite film. In practice, such films are hundreds to thousands of bilayers thick.

Fig. 4. Repetitive cyclic voltammograms at 0.10 V s^{-1} of DDAB-PG electrode placed in solution of 1 mM $B_{12}(COO^-)_6$, 7 mM HCN, 0.2 M phosphate buffer pH 5.7. Successive scans give increasing peak currents.

Fig. 5. Structures of two types of metal macrocyclic catalysts: (1a) Co(III)corrinhexacarboxylate; (1b) metal phthalocyaninetetrasulfonate.

Fig. 6. Cyclic voltammograms on pyrolytic graphite electrodes at 0.10 V s^{-1} in solutions of 0.2 mM $NiPcTS^{4-}$/0.1 M KBr: (a) bare PG; (b) PG coated with ca. 1 μm DDAB, steady state after multiple scans.

Fig. 7. Cyclic voltammograms at 0.10 V s^{-1} in solutions of 0.2 mM $NiPcTS^{4-}$ in 0.1 M KBr with PG electrode coated with ca. 1 μm DDAB: (a) after 3 min repetitive scanning; (b) steady state after 144 min. repetitive scanning.

Fig. 8. Forward and reverse SWV in 0.1 M KBr for FePc-DDAB-clay electrode at f = 1500 Hz, amplitude 25 mV, step height 2 mV.

Fig. 9. SWV forward currents at 500 Hz, 25 mV amplitude in 0.1 M KBr (a) CoPc-DDAB-clay, no trichloroacetic acid; (b) DDAB-clay without CoPc in 10 mM trichloroacetic acid; (c) CoPc-DDAB-clay, 10 mM trichloroacetic acid.

Fig. 10. Theoretical (solid line) and experimental (Δ) catalytic efficiencies as i_c/i_d for step height 2 mV, SW pulse height 25 mV, k = 5.7 x 10^3 s^{-1}. Theoretical line computed by method in ref. 26.

Table I. Phase transition temperatures from CV and DSC. to be added.

Table II. Results of 3 hr electrolyses of 8.5 mg 4,4'-dichlorobiphenyl in DDAB dispersions[a] using ZnPc as catalyst

Electrode	HPLC analysis, mol %			
	biphenyl	reduced[b] biphenyls	monochloro	dichloro
mercury	30	62	2	6
carbon felt	25	29	6	40

[a]Electrolyte solution contained 0.08 M DDAB, 0.1 M acetate buffer pH 3.5, 0.1 M tetraethylammonium bromide, 1 mM suspended ZnPc. Applied E = -2.3 V vs SCE in undivided cell with carbon rod counter electrode and ultrasound for mass transport. [b]Fully dechlorinated.

I-128

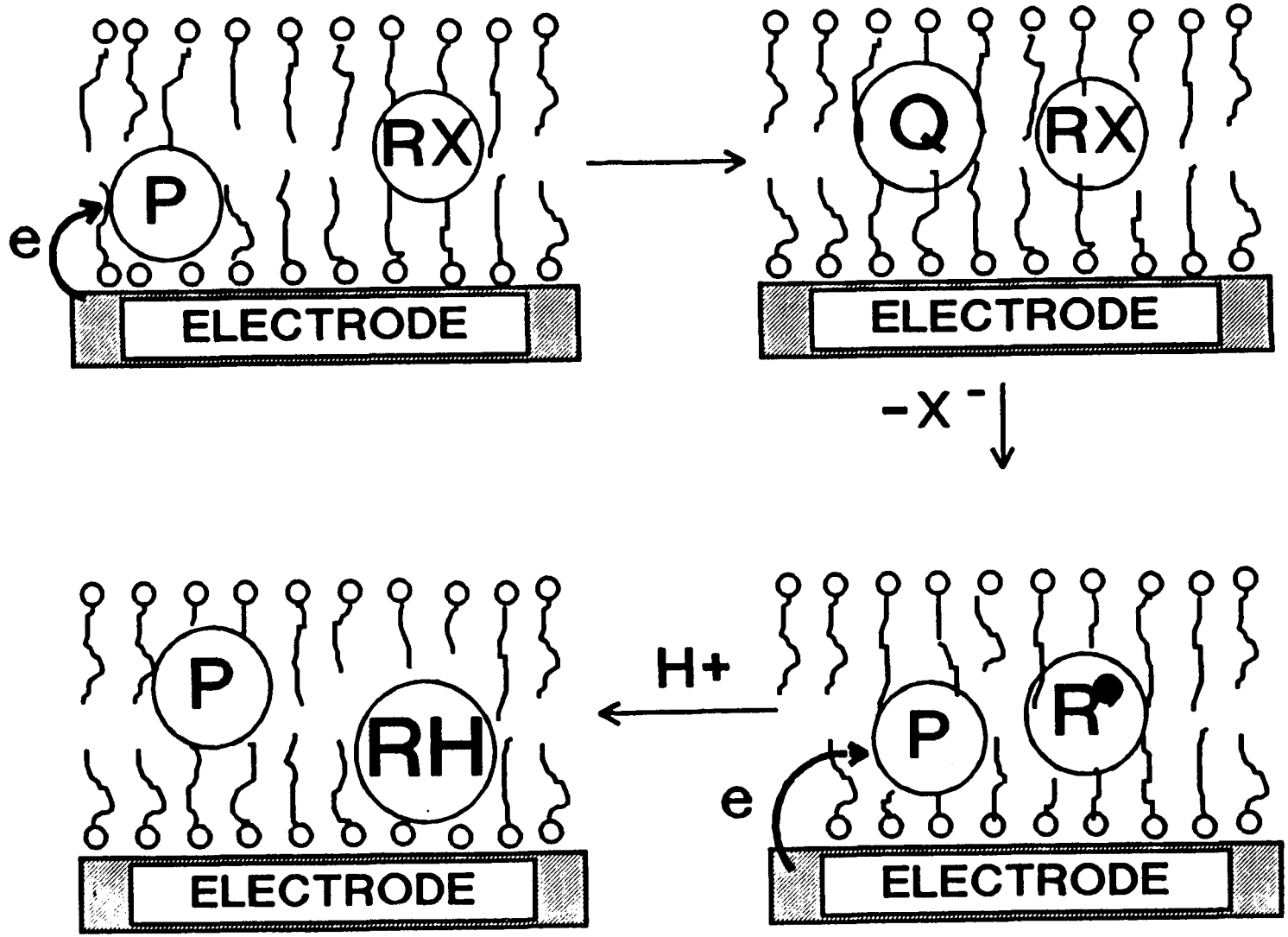
RX
P
e
ELECTRODE
Q
RX
ELECTRODE
-X⁻
P
RH
ELECTRODE
H+
P
R
e
ELECTRODE

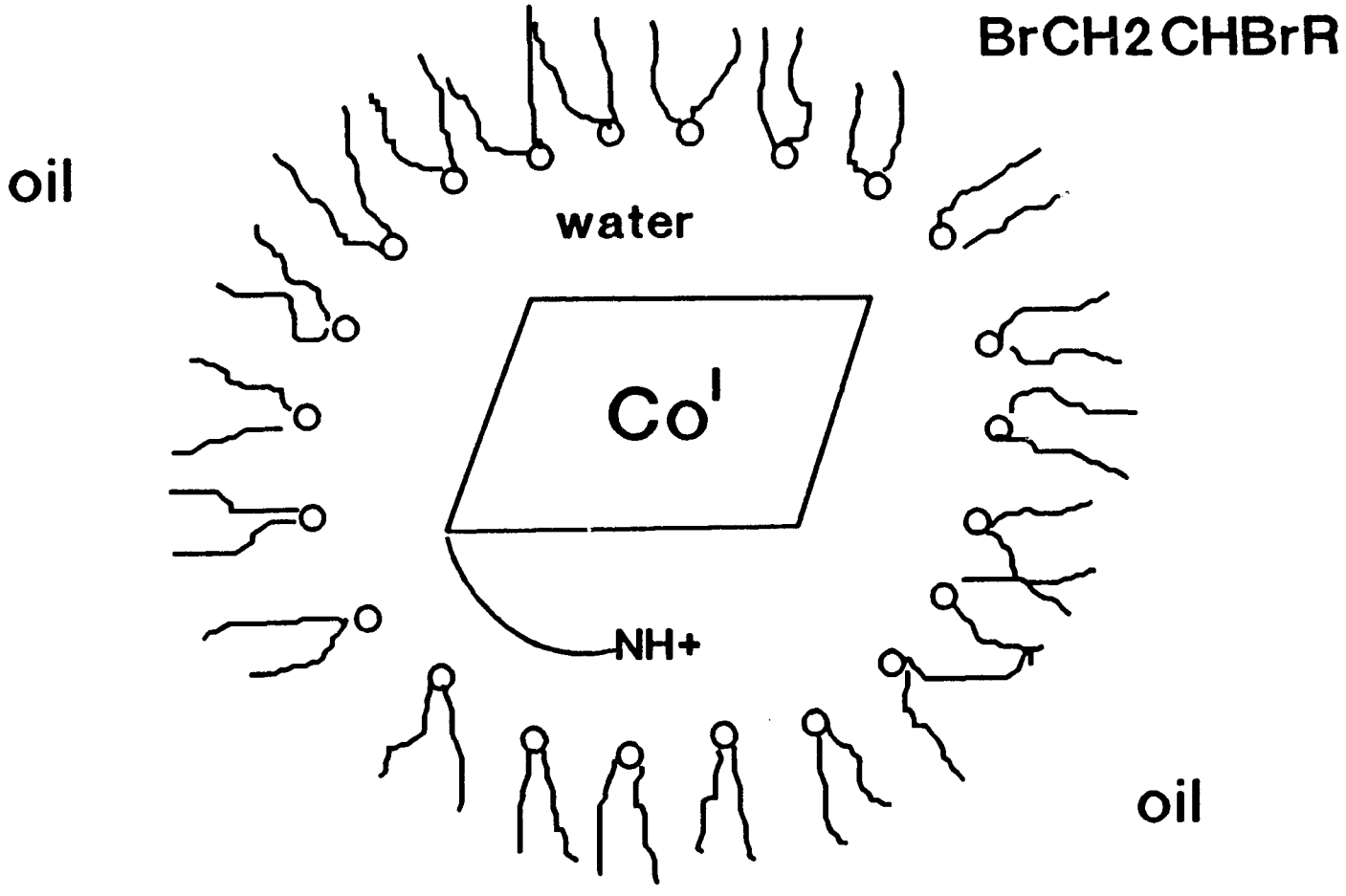
BrCH2CHBrR
oil
water
Co'
NH+
oil

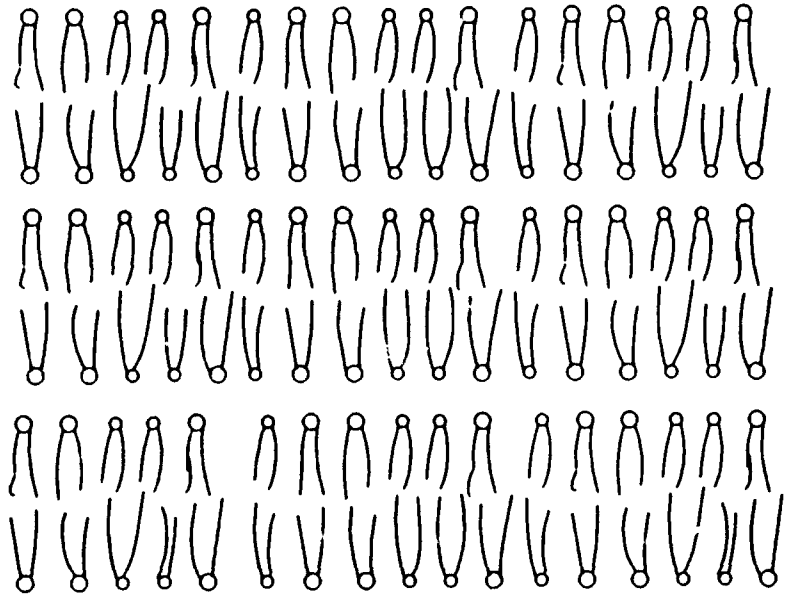

a

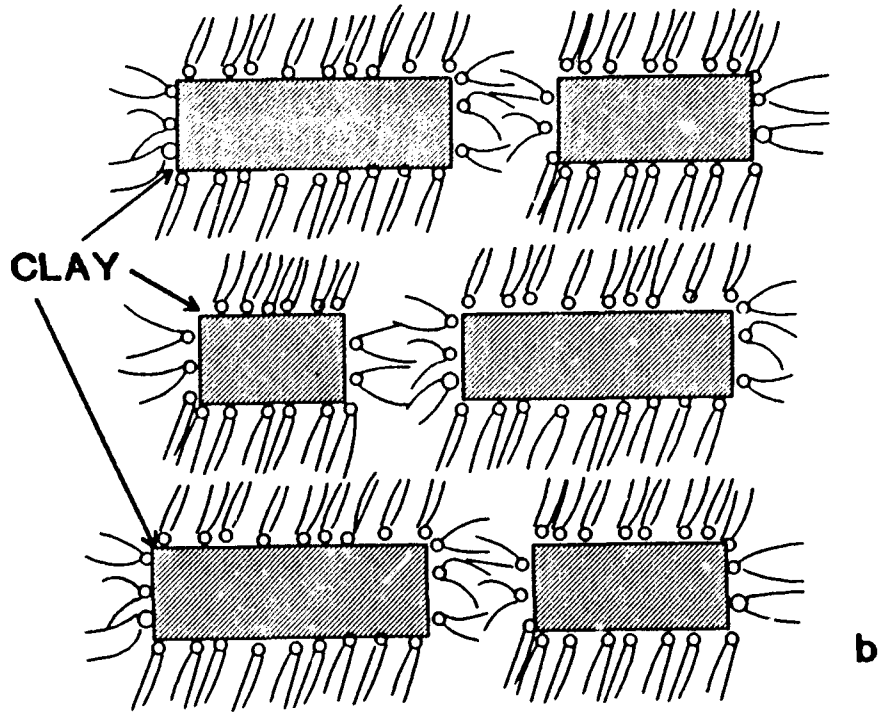

b

Fig. 3

pH 5.7 (0.2M) phosphate buffer
7 mM HCN
1 mM $B_{12}(COOH)_6$

Total Scans 20 cycles
Scan Rate: 100 mV/sec
WKE PG + DDAB f.lm
(0.1M, 20 uL coating)

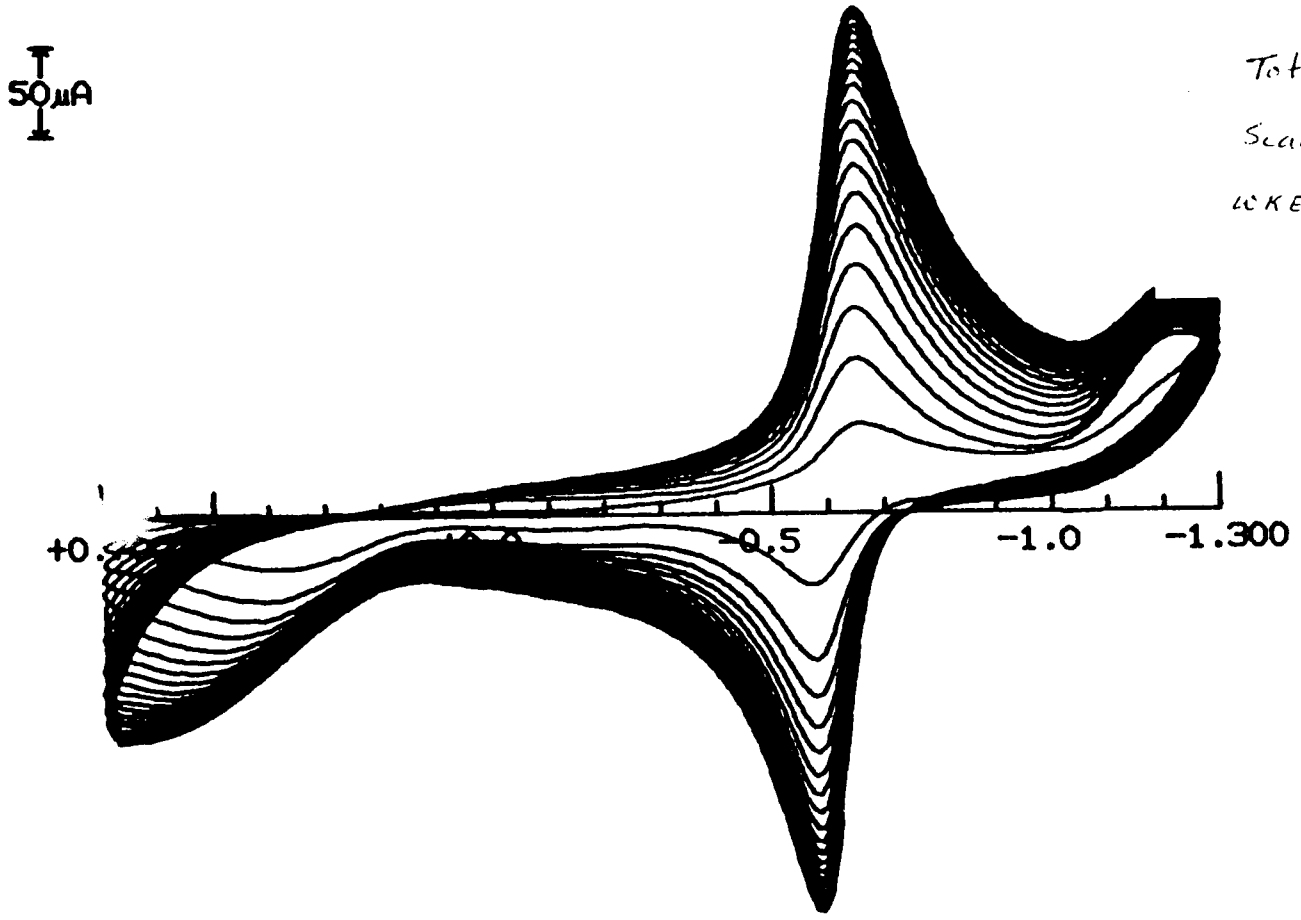

Fig. 4

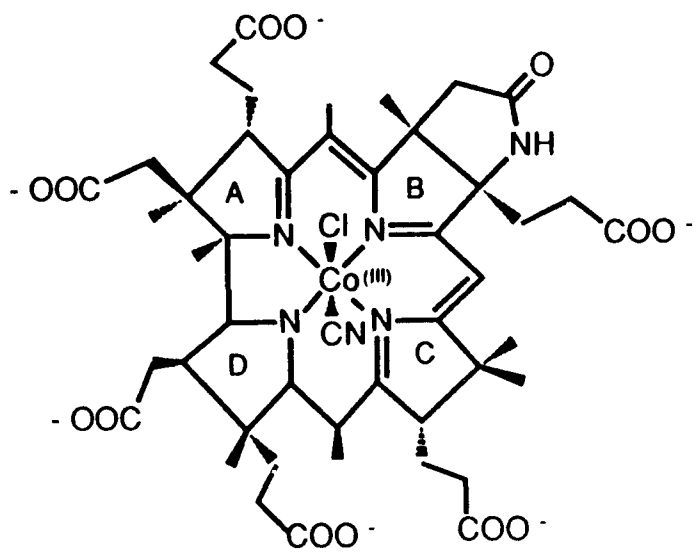

1a

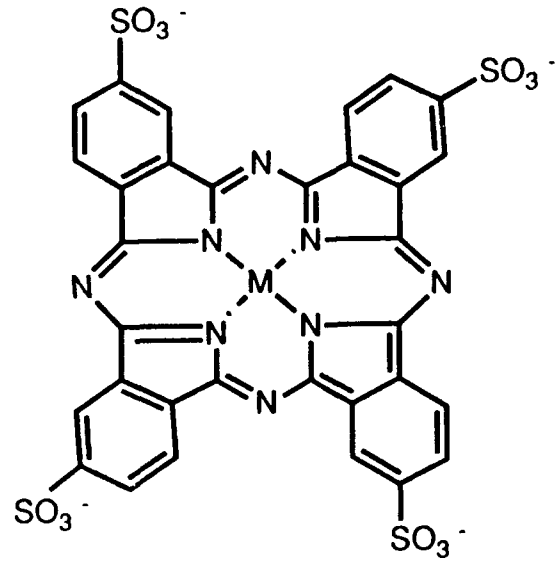

1b

Fig. 5

EP1-1

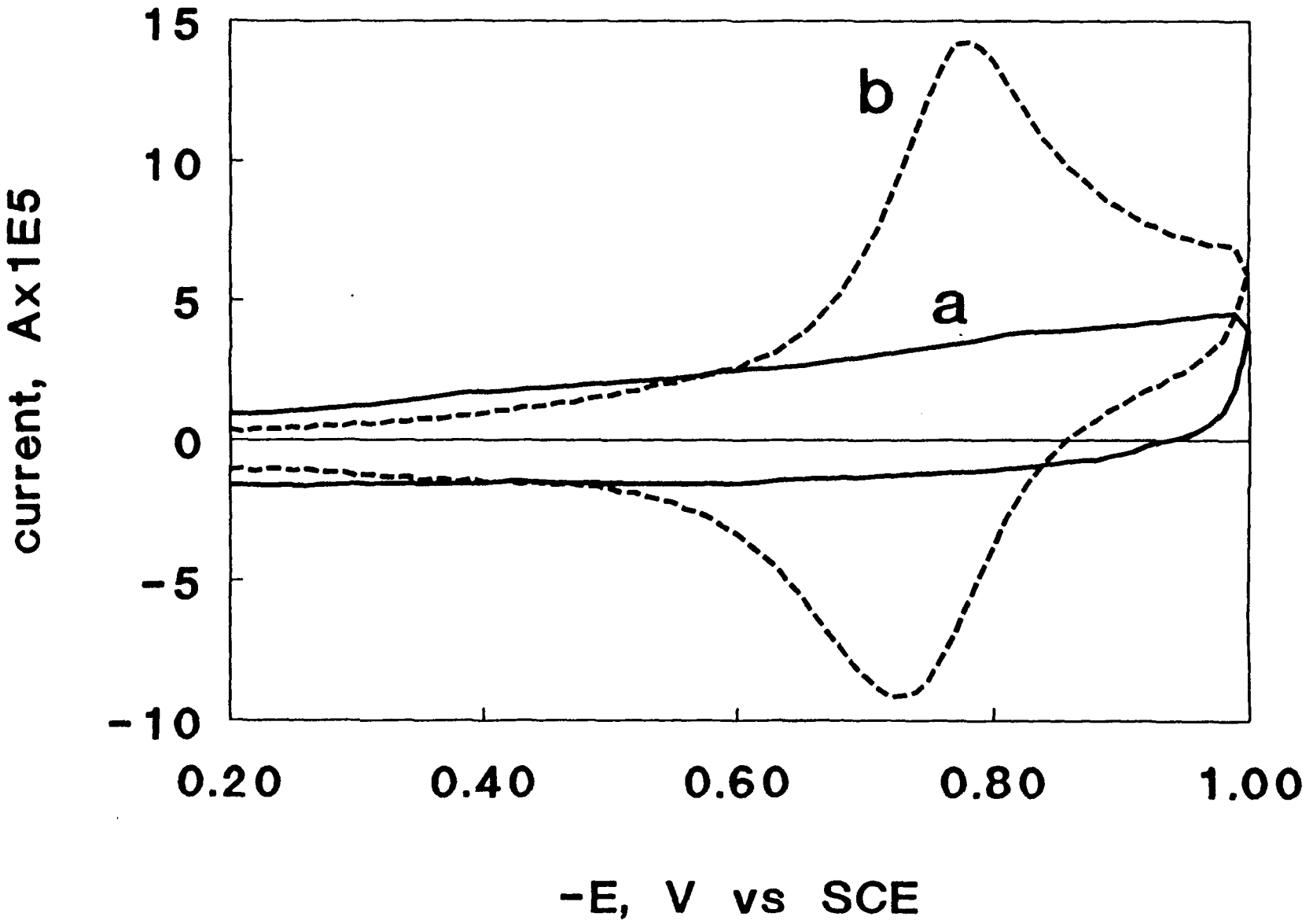
15
10
5
0
-5
-10
current, Ax1E5
b
a
0.20
0.40
0.60
0.80
1.00
-E, V vs SCE

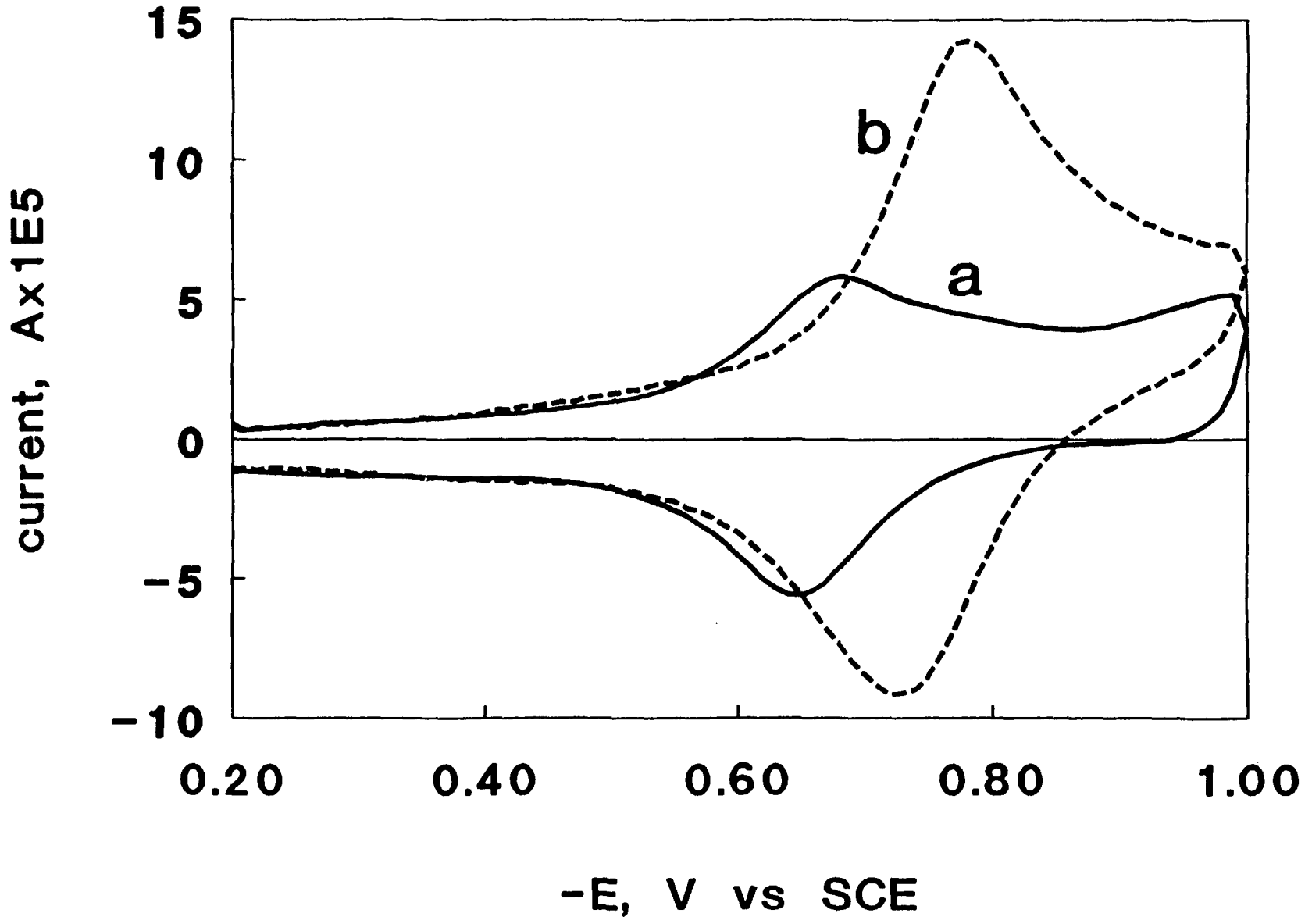

Fig. 7

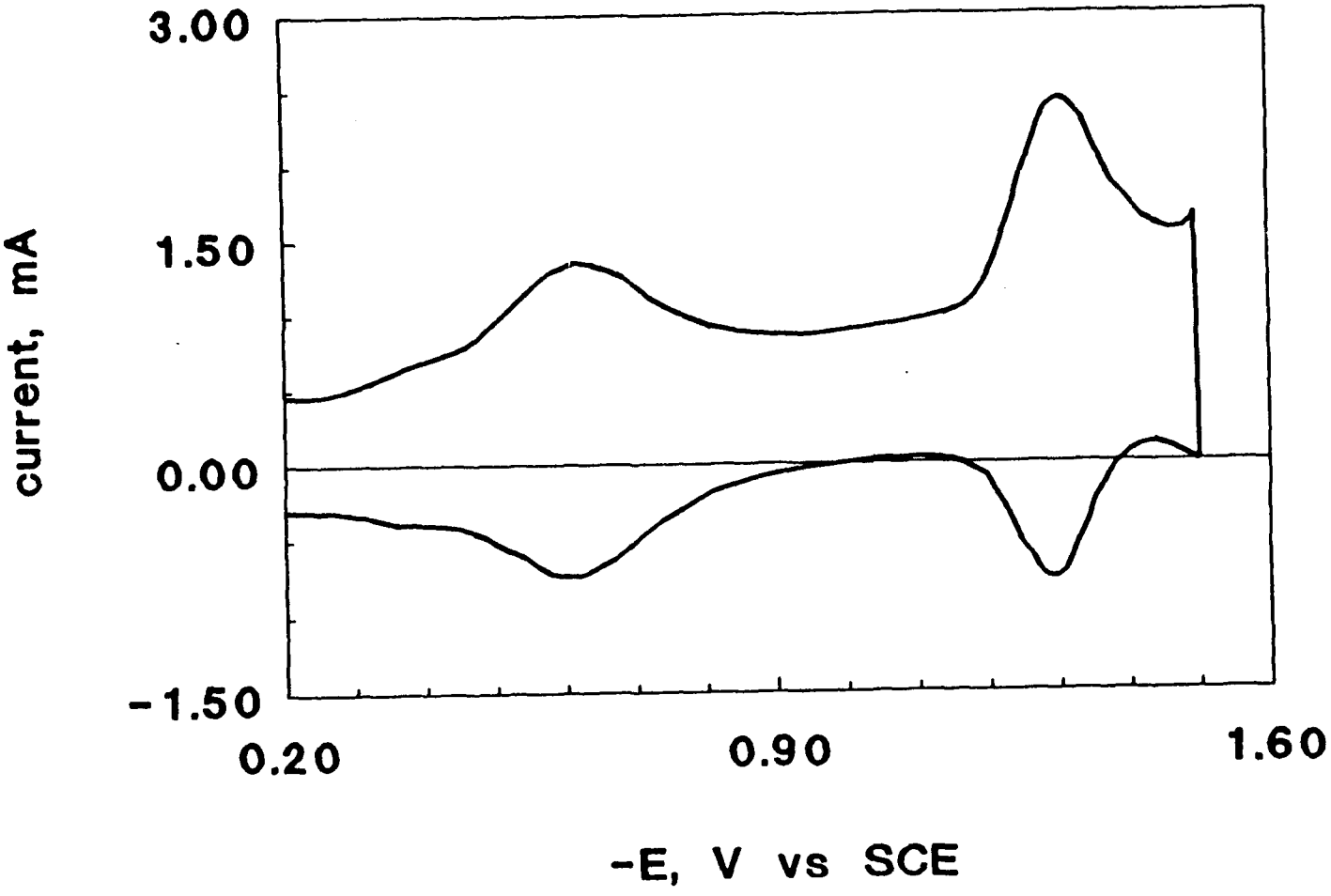

Fig. 8

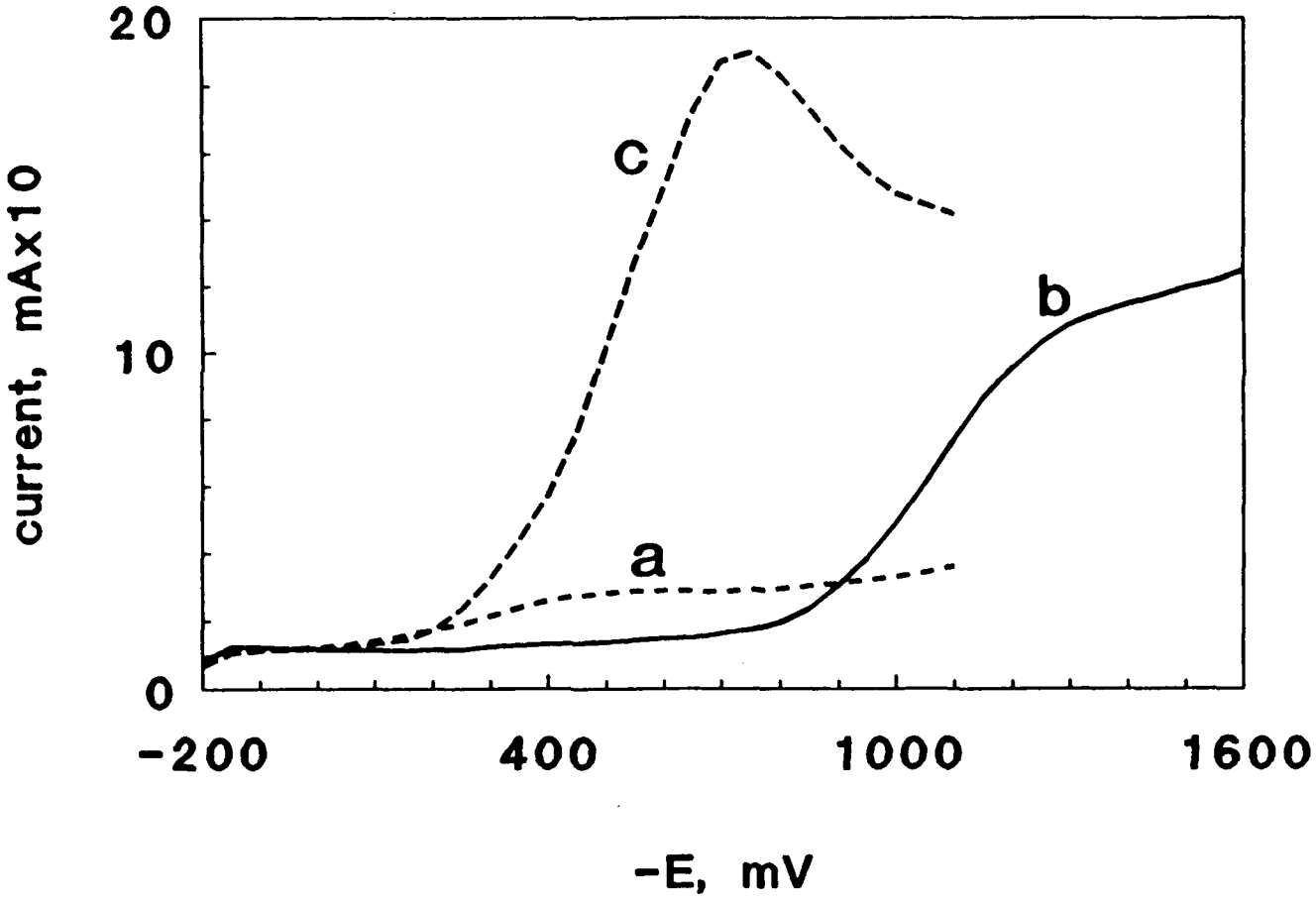
20
10
0
current, mAx10
c
b
a
-200
400
1000
1600
-E, mV

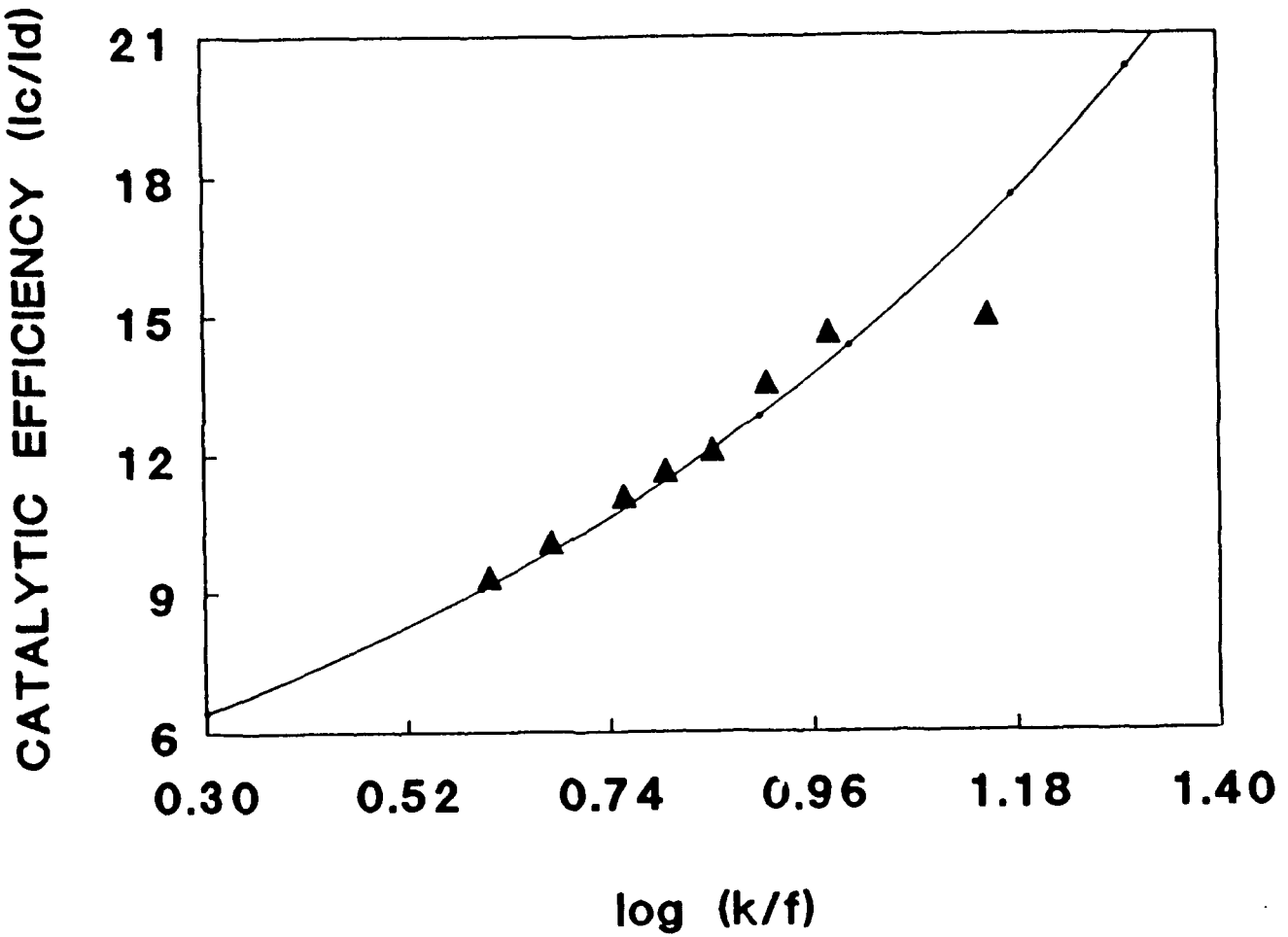
CATALYTIC EFFICIENCY (Ic/Id)
21
18
15
12
9
6
0.30
0.52
0.74
0.96
1.18
1.40
log (k/f)

Fig. 10

(7) The Development of Heterogeneous Catalysts for Use in Anodic Electrosyntheses and Electrodestruction of Organic Compounds in Aqueous Surfactant Systems.

Thomas C. Franklin, Jerald Darlington, Remi Nnodimele and Robert C. Duty
Baylor University, Department of Chemistry
Waco, Tx. 76798

Practical electro-oxidation of organic compounds at inert electrodes such as platinum encounters a number of difficulties (1). Among these are:

1. Most organic compounds are insoluble in the most desirable solvent for electrolysis, water. There are several basic difficulties with doing practical electrosynthesis and destruction in nonaqueous systems. The high resistance of most nonaqueous solvents causes large power losses and the increasing regulation of the use of the common nonaqueous solvents has made them less and less desirable.
2. The available potential range in aqueous systems is limited by the relatively low potential of oxidation of water.
3. Oxidations at inert electrodes do not appear to have characteristic potentials of oxidation. The mechanism for most oxidation reactions of organic compounds involves the electrochemical oxidation of the metal to oxides or hydroxides followed by chemical oxidation of the organic chemicals.
4. The cost of electricity is relatively high.

Surfactants have been used to get around the first problem by solubilizing organic compounds in the aqueous systems in micelles and emulsions. It has been found, in addition, that cationic surfactants, different from anionic and neutral surfactants, solve the second problem by forming hydrophobic films on the electrode, which increase the potential of oxidation of water by up to 1.7V (2-7). In addition the change of the electrode

Revised 1-17-91 JD

surface from the inert metal to the hydrophobic film also helps in the solution of problem 3 in that it increases the number of compounds that can be oxidized at characteristic potentials (3,4). This combination of the solubilization of the organic compounds and the increase in the available useful oxidation potentials, has made it possible to perform a number of electrosynthetic reactions that proceed only slightly in the absence of the surfactant. Cationic surfactants have been shown to cause marked increases in the yields, when compared with anionic and neutral surfactants (2,8-11). This increase is primarily because the hydrophobic film strongly inhibits the oxidation of water. However, in emulsion systems, other workers have concluded that the cause of the increase was the fact that the cationic surfactant acts as a phase transfer catalyst (12-15). Although immobilizing the cationic surfactants on the electrode with polystyrene (4) has extended the potential window for practical use of water as a solvent by about 1.7V, there are still compounds whose oxidation potentials occur even beyond this water oxidation potential . Therefore, recent work has focused on the development of heterogenous catalysts that will allow these extremely difficult oxidations to be performed in the aqueous systems (16-18).

Experimental

Two types of cells were used , a regular three electrode bulk solution cell and a two electrode sandwich cell. The sandwich cell was a two electrode cell which consisted of a small platinum foil anode and a large silver/silver chloride cathode separated by a piece of a filter paper (5,6). The sandwich cell allowed one to study the effect of the filming action of the surfactant without having the results affected by the solubilization characteristics. The sample was ground to a powder and seived with a 279 mesh seive. The powder was mixed with the supporting electrolyte to form a paste. This paste was placed on the anode which was covered with a layer of the cationic surfactant and the supporting electrolyte.

This system was then covered with moistened filter paper, which was then covered with a large Ag/Ag Cl cathode.

Voltammetric curves were obtained in the sandwich cell using a variety of different insoluble oxides to determine whether the added oxide formed a higher oxide. Once an oxidation peak was obtained indicating the formation of a higher oxide, controlled potential coulometric oxidation studies were made to determine the valence state of the metal in the product. Where possible, X-ray diffraction measurements are made to identify solid products.

The general procedure has been to use voltammetric measurements in a sandwich cell to determine if one can, within the potential range allowed by the cationic surfactants, oxidize various insoluble inorganic compounds to form unusual oxidation states. Voltammetric curves were then obtained in systems containing the inorganic compounds in the presence and absence of organic compounds in the bulk solution cell. An increase in height often occurred upon addition of the organic compound indicating oxidation of the organic compound by the higher oxidation state. The formation of the unusual oxidation state as an insoluble salt, along with the presence of the protective hydrophobic surfactant, stabilized the unusual state against reaction with water. This allowed time for it to react with the organic compound. This voltammetric study was followed by electrolysis in the bulk solution cell to determine whether the inorganic compound was a catalyst for the reaction with the organic compound.

Experimental Results

The results of voltammetric studies of barium peroxide have been previously described (16). Figure 1 shows the current voltage curve for the oxidation of copper (I). It can be seen that this oxidation goes through two separate reactions. Controlled potential coulometric oxidation studies of compounds were performed in the potential region of the observed peaks, and Table I shows the results. It can also be seen in Table I that the

Table I.
Coulometric Studies of the Oxidation
of Several Oxides

Compound	Product	Oxidation Potential (V)	# of Faradays per mole	Avg. Dev. from means
BaO_2	BaO_2^+ (16)	0.9	0.92	0.02
Cu_2O	CuO	0.80	1.80	0.20
CuO	CuO^+	1.70	1.03	0.03
MnO	MnO^+	0.78	1.2	0.1
MnO	MnO_2	1.16	2.1	0.1

oxidation of barium peroxide produced an active intermediate which was concluded to be barium superoxide (BaO_2^+). The first oxidation wave of copper (I) oxide was attributed to the formation of copper (II) oxide (CuO), while the second one was caused by formation of copper (III). The first oxidation wave of manganese (II) oxide forms manganese (III) oxide (MnO^+) while the second oxidation produced manganese dioxide. The superoxide and copper (III) and manganese (III) oxides are normally unstable in aqueous systems without some type of stabilization. These reactive intermediates will react with a variety of organic compounds. Fig 2 shows the effect of 2 chloroethyl ethyl sulfide on the oxidation wave for formation of copper (III) oxide. The marked increase in current in the potential region for formation of the higher oxide shows the ability of the oxide to react with the compound.

Most of the work to date has concentrated on the barium superoxide (16-18). The superoxide is known to be a strong nucleophile and its reactions in nonaqueous solvents have been the subject of a number of studies. Sawyer and his coworkers (19,20) have shown that the superoxide ion, prepared by electrolytic reduction of oxygen in nonaqueous

solvents, is capable of destroying halogenated hydrocarbons. With this background, a series of reactions was performed to determine if halogenated hydrocarbons could be destroyed by this aqueous system. Voltammetric curves (16-18) indicate no oxidation of these organic compounds in the absence of barium peroxide. However in the presence of barium peroxide one observes, superimposed on the barium peroxide oxidation wave, a series of waves indicating that the intermediate is being electrolytically oxidized. Table II

Table II
The Effect of Electro-Oxidizing Barium Peroxide on the Oxidation of $6x10^{-2}$M Hexafluorobenzene (HFB) in 50 mls 0.1 M NaCl; 2 mls DTAC; 25°C; 1 hrs; 6 cm 2 Graphite Anode; 0.5g BaO_2 Initial pH, 5.

Experimental Conditions	%HFB Destroyed
1. No electrolysis, With Barium Peroxide	0
2. Electrolysis, No Barium Peroxide	0
3. Controlled Potential Electrolysis (0.9V vs SCE) With Barium Peroxide	70±5
4. Controlled Current Electrolysis (16.6m mA/cm2), With Barium Peroxide	74±4

shows typical results obtained in electrodestruction experiments using barium peroxide as an electrochemical catalyst. It can be seen that in the blanks, either without barium peroxide or without electrolysis, very little of the compound was lost, but in the presence of both electrolysis and the barium peroxide there was an appreciable percentage lost. In fact, the amount lost was concluded to be caused primarily by losses in the extraction procedure rather than by destruction (16-18).

The current efficiencies for all of the oxidations with barium peroxide are much higher than 100% indicating that appreciable amounts of the intermediate are being chemically oxidized by the barium peroxide.The barium peroxide can be regenerated by reduction of oxygen at the cathode in the presence of barium ions. However, no attempts have been made to adjust the pH to a point that would allow recycling of the barium peroxide. Analysis of the products in several experiments showed the presence of barium carbonate and soluble halide. Quantitative analysis of products obtained with several halogenated hydrocarbons gave results indicating that the amount of halide was close to the expected theoretical amount. For example, in the destruction of 1,2 dibromoethane the analyzed amount of bromide obtained was 1.91± 0.13 moles of bromide per mole of compound. It can be seen that the majority of the halide is converted to the soluble form. However, in each case analyzed a small amount of the halide was not recovered. In practically all cases no product was observed by gas chromatographic means.

The Stability of Barium Superoxide

It has been concluded (16-18) that the mechanism of action of the barium peroxide involved the electrolytic formation of an active intermediate which was hypothesized to be barium superoxide. This intermediate reacted with the organic compounds to produce a compound which was oxidizable both electrolytically and by barium peroxide. The superoxide ion is normally unstable in aqueous systems and, given time, it will decompose to hydrogen peroxide (16). However, the presence of barium ions (21,22) and cationic surfactants (21-24) are known to stabilize the superoxide ion. A cyclic voltammetric study was made to obtain some idea of the half life of the intermediate in this system. Fig 3 shows a typical set of cyclic voltammograms. It can be seen that in the first voltage scan which initially went in the cathodic direction the curve indicates a transport limited reduction of the barium peroxide on both the forward and reverse scans. As one moves into the anodic potential region one observes a wave for the oxidation of hte barium

peroxide which has been previously interpreted to be caused by the formation of barium superoxide (16). On scan 2 into the cathodic region one observes a peak in the reduction wave indicating that the oxidation of the barium peroxide has placed on the electrode a film of a reducible species. Scan 3, was held at +0.003v (approximately zero current) for 1 minute before the voltage was scanned into the cathodic region. The fact that scans 2 and 3 are essentially the same indicates that this film on the electrode surface is reasonably stable. If a halogenated hydrocarbon is placed in the suspension there is a slow decrease in the height of the reduction peak, but apparently the film on the electrode is reacting slowly. If the potential is held in a region where reduction occurs or in the region of oxygen evolution one observes destruction of this reduction peak. The fact that the organic compound reacts slowly with the layer on the electrode indicates that the destructive reaction probably occurs in the more mobile layers beyond the first layer.

Similar results can be obtained with hydrogen peroxide in basic solutions (Fig. 4). However, if one does the experiments in 1M sodium chloride without any added base one does not observe the formation of this reduction peak with hydrogen peroxide. This is consistent with the observation that in aqueous sodium chloride one does not get destruction of the halogenated hydrocarbon when hydrogen peroxide is substituted for barium peroxide.

In some of the work the potential was pulsed with square wave pulses between 0.300, a potential where the barium peroxide was oxidized and 0.000 V., a potential at which oxidation did not occur, in order to determine whether some of the barium carbonate formed on the electrode could be desorbed from the electrode so that the current would not drop off as rapidly as was normally observed. In no case was any significant change observed in the results. It is apparent from these cyclic voltammetric studies that pulsing between these two potentials would have no effect on the strongly bonded layer at the surface.

The Effect of Orientation of the Reacting Organic Compounds.

It has been shown (30) that the micelle system is capable, because of charge or orientation, of selecting one reaction over another. A study was made to determine which way the organic compound needed to be oriented in the micelle in order to obtain the most reaction. In Table III one can see the results obtained for the oxidation of bromobenzene,

Table III.
The Effect of Compound Structure on the Percent Destruction Obtained by Electrooxidation in the Presence of Barium Peroxide. Experimental Conditions: Pt working and counter electrodes, Ag/AgCl reference Electrode; 75 ml 1.07M $NaNO_3$, 7.5 ml t-butylammonium hydroxide (TBAOH), 250 mg BaO_2. Potential pulsed cyclically between 0.300V (2 min) and 0.000V (45 sec).

Compound	Amt (mg)	Total Time of Electrolysis (hrs)	% Compound Unreacted
Bromobenzene	110.0	18	0
p-bromotoluene	110.3	17	0
p-bromoaniline	134.6	15.3	100
p-bromobenzoic acid	101.2	16.3	99
o-bromobenzoic acid	110	15	93

and a series of its derivatives. It is reasonable to believe that the most hydrophilic end in the bromobenzene and p-bromotoluene and p-methoxybenzene experiments, and therefore the end oriented into the water, was the one containing the bromine. On the other hand one would expect that for p-bromobenzoic acid and p-bromoniline, the carboxyl group would be the most hydrophilic and would be oriented into the water, and as a result the bromine end would be oriented into the micelle interior. It can be seen that the compounds in which the bromine is oriented into the aqueous solutions reacted completely while in those in which the bromine is in the hydrophobic region of the micelle the reaction is essentially zero. (25,26). These results show clearly that reaction with the polar end occurs at the aqueous interface. It can also be seen in Table III that o-bromobenzoic acid is not destroyed. This shows that this selection by orientation is very selective.

Reactions Using Copper (III) and Manganese (III) Oxides as Electrochemically Generated Intermediates.

Electrochemically generated soluble complexes of manganese (III) and copper (III) formed as a film on copper electrodes (27-29) have been used as reagents in performing organic reactions. Electrochemically generated insoluble oxides of these species also serve as active reagents. This can be seen from voltammetric studies (Fig 3) or synthesis studies. Table IV shows a comparison of the results for the oxidation of 2-chloroethyl ethyl sulfide. These results are complicated by the normal hydrolysis of this compound. However, it can be seen that under these conditions copper (III), manganese (III) and manganese (IV) cause loss of this compound. It can also be seen that in the presence of copper (III) oxide the sulfoxide if formed as a product. This reaction of the copper (III) oxide to produce the sulfoxide can be seen more clearly in the oxidation of diethylsulfide (Table V). In this case hydrolysis is not problem.

Table IV. Comparison of the Effects of Electrolytically Produced Copper (III) Oxide, Manganese (III) Oxide and Manganese (IV) Oxide on the Anodic Oxidation of 2-Chloroethyl Ethyl Sulfide in 2 N NaOH-DTAC in 3 hrs.

Oxidant	Percent lost (sulfide)	Percent product (sulfoxide)	Percent * destroyed (sulfide)
Copper (III) oxide pot.1.14V	68 ± 7	19 ± 2	49
Manganese (III) oxide pot.0.78V	60 ± 0	0	60
Manganese (IV) oxide pot.1.16V	84 ± 1.5	0	84
No oxidant (Hydrolysis)	18 ± 7.5	0	18

* This column was calculated by substracting the % product and the % hydrolyzed from the % lost.

Table V. The Effect of Electrochemical Oxidation of Copper (II) Oxide on the Anodic Oxidation of Diethyl Sulfide in 2N NaOH-DTAC in the Bulk Solution Cell for 3 hrs.

Experimental conditions	Percent extracted (sulfide)	Percent lost (sulfide)	Percent product (sulfoxide)
Stirred with CuO (3 hrs, no electrolysis)	98 ± 2	2 ± 2	0
Electrolysis (3 hrs, no CuO)	98 ± 0.2	2 ± 0.2	0
Electrolysis (with CuO, 3 hrs)	21 ± 0.2	79 ± 0.2	45 ± 0.2

Reductive Destruction of the Organic Compounds.

There are two obvious objections to the commercial use of the barium peroxide in electrooxidation processes, either for destruction or synthesis. The first of these is the fact that the barium peroxide is destroyed and must be replaced. The second common objection to the use of electrochemical techniques in organic chemistry is the cost of electricity. The first attack on these two problems was to determine if barium peroxide could be generated at the cathode. This should be possible since it is known that oxygen can be reduced to peroxide. Electrolysis was done in 1M sodium chloride solution saturated with oxygen containing barium chloride. A white precipitate was formed, and chemical tests showed it to be barium peroxide. The yield on the basis on the amount of barium added was 15% after 4 hrs.

It is also known that in nonaqueous solvents the reduction of oxygen produces the superoxide ion. It thus should be possible to produce the superoxide ion in the surfactant system by reduction of oxygen and observe a corresponding destruction of halogenated hydrocarbons. Table VI shows the results of these experiments. It can be seen that the

Table VI. The Effect of Reducing Oxygen in the Presence of Barium Ions on the Destruction of 1, 3, 5-Trichlorobenzene for 1 hr., Controlled Current Density, 16.6 mA/cm^2, Graphite Anode and Platinum Cathode.

Experimental conditions	Percent extracted	Percent lost
No electro., with barium chloride, and oxygen.	97 ± 3	3 + 3
Controlled current electro., with oxygen, no barium chloride	86 ± 0	14 ± 0
Controlled current electro., with barium chlordie and oxygen	81 ± 1	19 ± 1
Controlled current electro., with barium chloride, no oxygen.	96 ± 5	4 ± 5

reduction of oxygen produces destruction of TCB in the neighborhood of the cathode. It can also be seen that there is an increase in the percent of destruction in the presence of barium ions. This is logical since the barium ion stabilizes the superoxide ion against reaction with water (21-22). Under similar conditions with barium peroxide in the system 63% of the TCB was destroyed (18). Although one gets much more rapid destruction in the presence of the barium peroxide it can be seen that even its absence the reduction of oxygen causes some destruction of the TCB.

Fuel Cells for the Destruction of Organic Compounds.

Any large volume electrochemical process starts with one major strike against it, the cost of electricity. Whether one is concerned with electrodestruction or electrosynthesis it is best to develop methods that use less electricity. Since many of these reactions have negative free energies (ΔG) it would be best to design a fuel cell that could, while doing the destruction or synthesis, generate electricity rather than utilize it.

Table VII shows typical results obtained with chloroform and 1,3,5 trichlorobenzene (TCB) using graphite and platinum electrodes and the same bulk electrolysis cells previously used. However in these experiments the electrodes were connected directly to a meter or through a resistive load to the meter rather than being connected to a potentiostat or galvanostat.

It can be seen that it is not necessary to apply electricity. Instead one can use this fuel cell to generate electricity while, at the same time, destroying the halogenated hydrocarbon. In the absence of the connected electrodes one obtained a negligible amount of destruction.

Table VII. The Destruction of 1, 3, 5-Trichlorobenzene and Chloroform in a Battery. Experimental Conditions: TCB- 1.2×10^{-3} moles, Chloroform $CHCl_3$ (Amounts given in table), 50 mL 1N NaCl, BaO_2-1g, DTAC (2mL of a 50% solution), Electrode system A- Graphite anode, Pt cathode, Areas unknown, Electrode system, B- Graphite anode ($12cm^2$), Pt cathode ($1.3cm^2$); Electrode system C- Graphite anode ($10.3cm^2$), Pt cathode ($5.2cm^2$).

Experimental Conditions	Time (min)	Current mA	Exterior Load (ohms)	% Destruction
$CHCl_3$-48µL	00	0.50	0	25
O_2 saturated	06	0.87		
Undivided cell	25	1.03		
Electrode A	60	0.97		
CHCl-06µL	00	0.95		
O_2 satd.	05	1.06	0	43
Undivided cell	80	2.5		
Electrode A				
$CHCl_3$144µL	00	4.2		
O_2 satd.				
Undivided cell	30	3.0	0	89
Electrode A				
$CHCl_3$96µL	00	2.17	9	55
O_2 satd.	10	2.38		
Undivided cell	30	1.84		
Electrode B	65	1.63		
	145	0.65		
TCB-	0	5.5		
In air	5	2.3		
Undivided cell	15	2.8	0	56
Electrode - C	30	1.6		
	45	1.3		
	60	1.1		

Conclusion

Studies have shown that in aqueous cationic suspensions several insoluble oxides can be electrolytically oxidized to produce species that normally are unstable in water systems. The reactions studied were the oxidation of barium peroxide to the superoxide, copper (II) oxide to copper (III) oxide, and manganese (II) oxide to manganese (III) oxide. These active intermediates apparently are stabilized by the presence of the precipitating ion and the surfactant against reaction with water. The products last long enough to react with several organic compounds. Primarily these reactions result in destruction of the organic compound.

It was shown in the barium peroxide studies that the layer of intermediate adjacent to the electrode was quite stable and did not react either with the organic compounds or water. It was concluded that the reaction with the organic compounds occurred in the outer layers of the surfactant film as the superoxide was dispersed by the surfactant into solution. It was also demonstrated that one could make a fuel cell based on the oxidation of halogenated hydrocarbons by oxygen using barium peroxide as a catalyst.

Acknowledgment

Appreciation is expressed to the Robert A. Welch Foundation of Houston and Mitsui Toatsu Chemicals, Inc., for the financial assistance given to this research.

REFERENCES

(1) Lund, H., In Organic Electrochemistry; Baizer, M.M.; Lund, H., Eds.; 2nd Ed. Marcel Dekker, Inc. New York, N.Y. 1983, Chapter 5.

(2) Franklin, T.C.; Sidarous, L. J. Electrochem. Soc., 1976, 124, 65-69.

(3) Franklin, T.C.; Iwunze, M. Anal Chem, 1980. 52, 973-976.

(4) Franklin, T.C.; Ohta, M. Surface Technology, 1982, 18, 63-76.

(5) Franklin, T.C.; Nnodimele, R.; Adeniyi, W.K. J. Electrochem. Soc.,1987, 134, 2150-2154.

(6) Franklin, T.C.; Nnodimele, R.; Adeniyi, W.K.; Hunt, D. J. Electrochem. Soc., 1988, 135, 1944-1947.

(7) Franklin, T.C.; Adeniyi, W.K.; Nnodimele, R.A. J. Electrochem. Soc., 1989, 137, (2) 480-484.

(8) Franklin, T.C.; Honda, T. Electrochimica Acta, 1978, 23, 439-444.

(9) Franklin, T.C.; Iwunze, M. J. of Electroanal. Chem., 1980, 108, 97-106

(10) Franklin, T.C.; Jimbo, T. J. Electrochem. Soc., 1987, 134, 2169-2172.

(11) Franklin, T.C. Surface Technology, 1982, 15, 345-355 .

(12) Eberson, L.; Helgee, B. Acta Chem. Scand, 1977, **B31**, 813-817.

(13) Ellis, S.R.; Pletcher, D.; Gough, P.; Korn, S.R. J. Appl. Electrochem., 1982, **12**, 687-691.

(14) Eberson, L.; Helgee, B. Acta Chem. Scand., 1978, **B32**, 157-161.

(15) Ellis, S.R.; Pletcher, D.; Bamlen, P.H; Healy, K.P. J. Appl. Electrochem., 1982, **12**, 693-699.

(16) Franklin, T.C.; Darlington, J.; Adeniyi, W.K. J.Electrochem.Soc., 1990, **137** 2124-2126.

(17) Franklin, T.C.; Darlington, J.; Solouki, T. J. Electrochem. Soc., 1991, **138**, 747-750.

(18) Franklin, T.C.; Darlington, J.; Solouki, T.; Tran, N. J.Electrochem.Soc., (In Press)

(19) Sawyer, D.T.; Valentine, J.S. Acc. Chem. Res. 1981, **14**, 393-400.

(20) Sugimoto, H.; Matsumoto, S.; Sawyer, D.T.; Kanofsky, J.R.; Chowdbury, A.K.; Wilkens, C.L. J. Am. Chem Soc. 1988, **110**, 5193.

(21) Bray, R.C.; Mauler, G.; Fielden, E.M.; Carle, C.I. In Superoxide Dismutases; Michelson, A.M.; McCord, J.M.; Fridovich, I., Eds.; 1977, **p 61**, Academic Press, New York.

(22) Argese, E.; Orsega, E.F.; Enzo, S.; Ugo, P.; Rigo, A. J. Electroanal. Chem. Interfacial Electrochem., 1988, **246**, 155-163.

(23) Chevalet, J.; Roulle, F.; Gierst, L.; Lambert, J.P. J. Electroanal. Chem., 1972, **39**, 201-216.

(24) Kastening, B.; Kazemilford, G. Ber. Bunsenges. Phys. Chem., 1970, **74**, 551-556.

(25) Ramaswamy, R.; Venkatachalapathy, M.S.; Udupa, H.V.K. J. Electrochem. Soc. 1963, 110, 202-204.

(26) DeJonge, C.R.H.I. In Organic Synthesis by Oxidation with Metal Compounds; Mijs, W.J.; DeJonge, C.R.H.I., Eds.; Plenum Pubs., New York, 1986, 262.

(27) Vassilijsev, Y.B.; Khazova, O.A.; Kolaeva, N.N.N. J. Electroanal. Chem. 1985, 196, 127-144.

(28) Prabhu, S.V.; Baldwin, R.P. Anal. Chem., 1989, 61, 2258-2263.

(29) Prabhu, S.V. Baldwin, R.P., Anal. Chem., 1989, 61, 852-856.

(30) Reim, R.E., Van Effen, R.M., Anal. Chem., 1986, 58, 3203-3207.

(31) Link, C.M., Jansen, D.K., Sukenik, C.N., J. Am. Chem. Soc., 1980, 102, 7798-7799.

LIST OF FIGURES

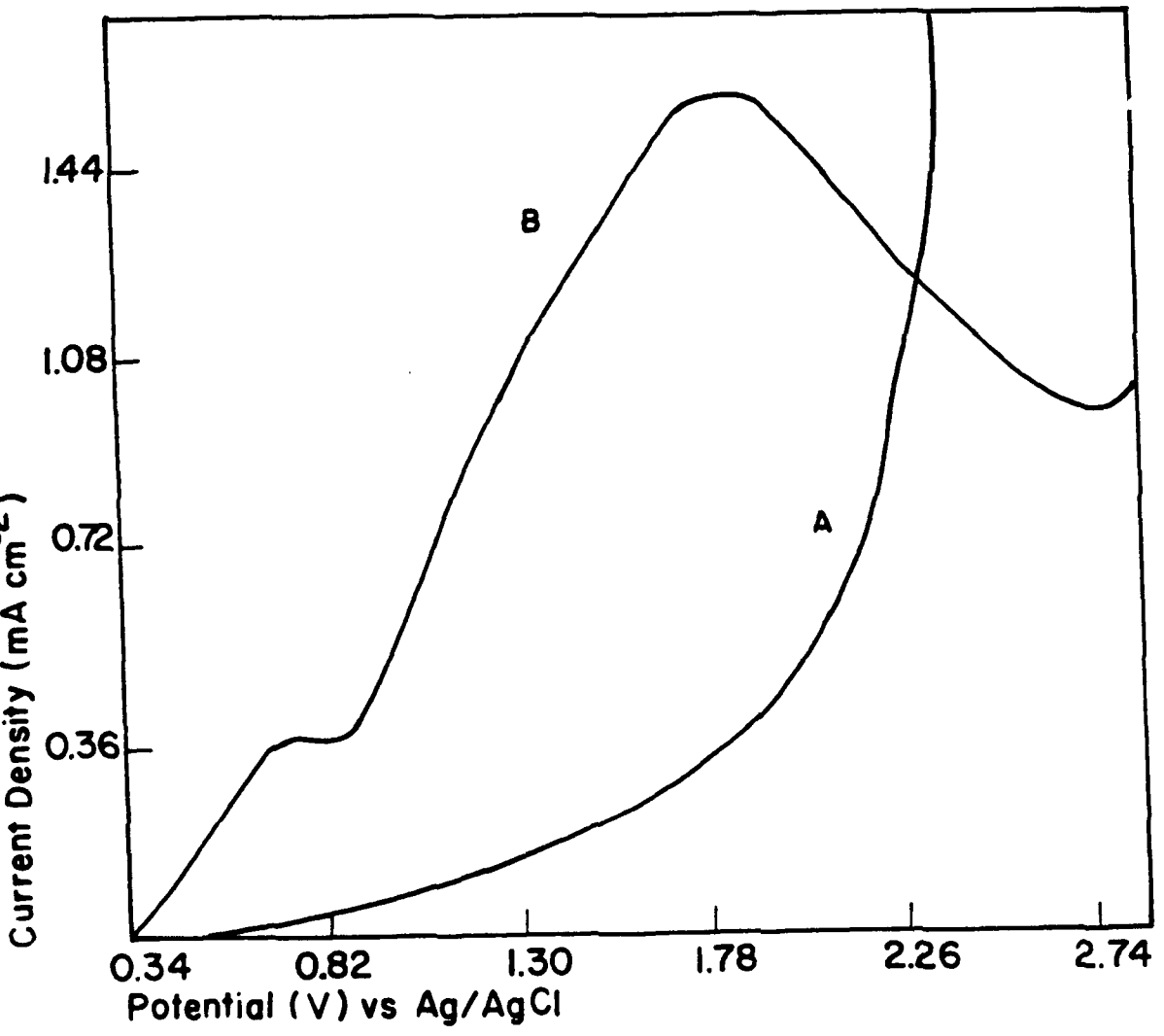
1.44
1.08
0.72
0.36
Current Density (mA cm^{-2})
B
A
0.34
0.82
1.30
1.78
2.26
2.74
Potential (V) vs Ag/AgCl

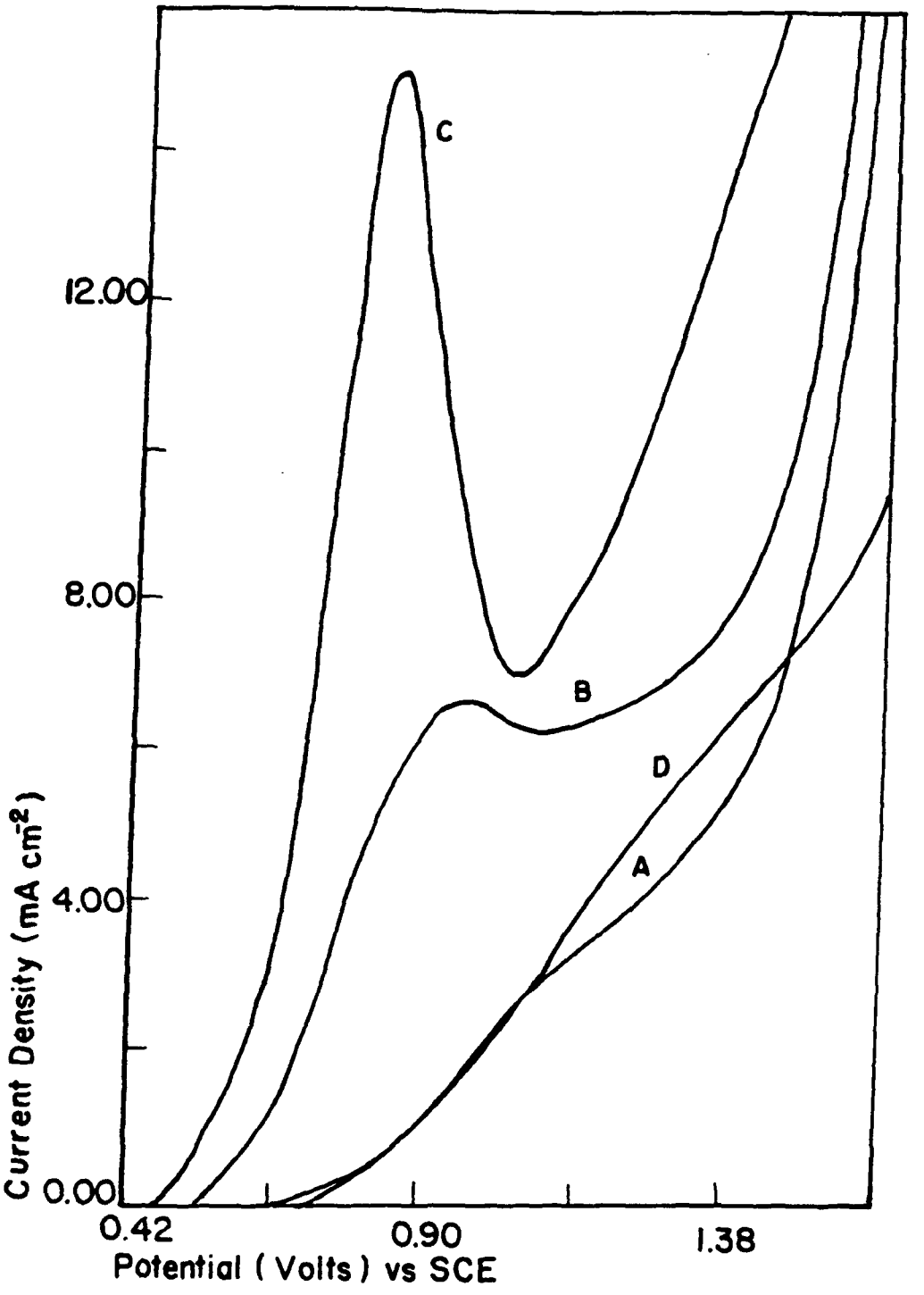
C
12.00
8.00
B
D
A
4.00
0.00
Current Density (mA cm⁻²)
0.42
0.90
1.38
Potential (Volts) vs SCE

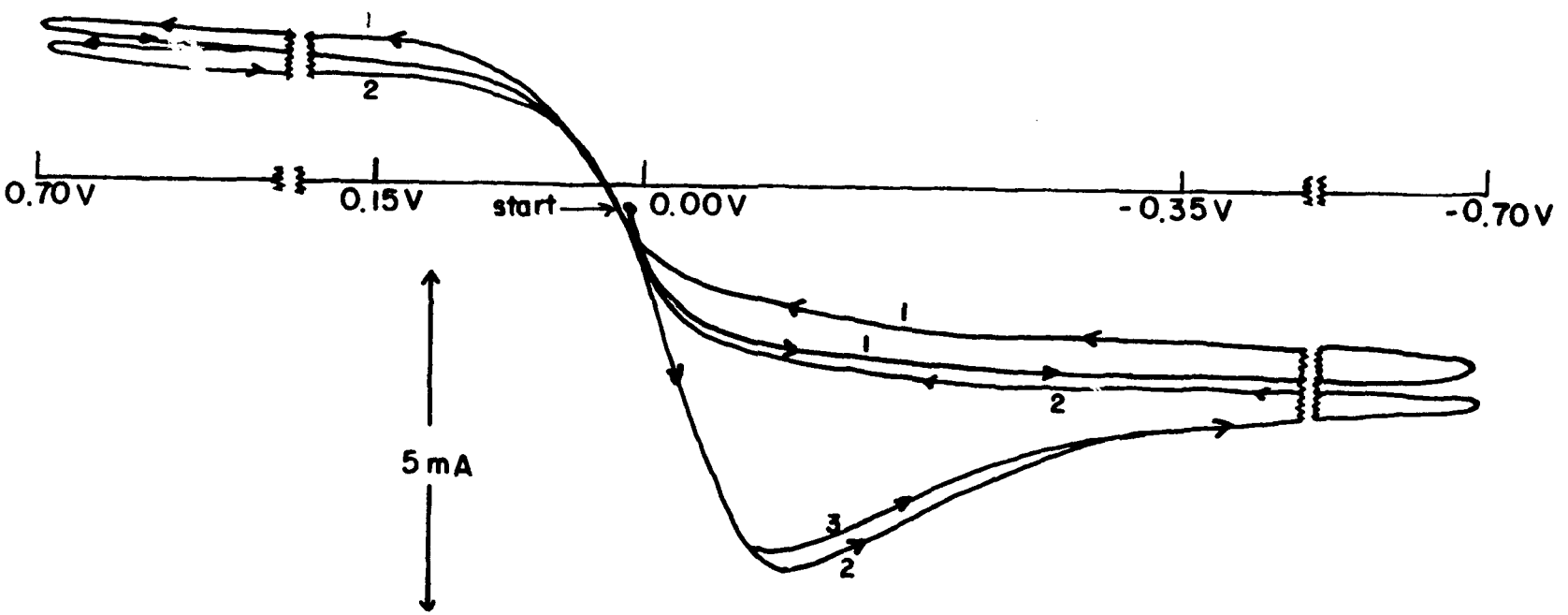
0.70V
0.15V
start
0.00V
-0.35V
-0.70V
5mA
1
2
1
1
2
3
2

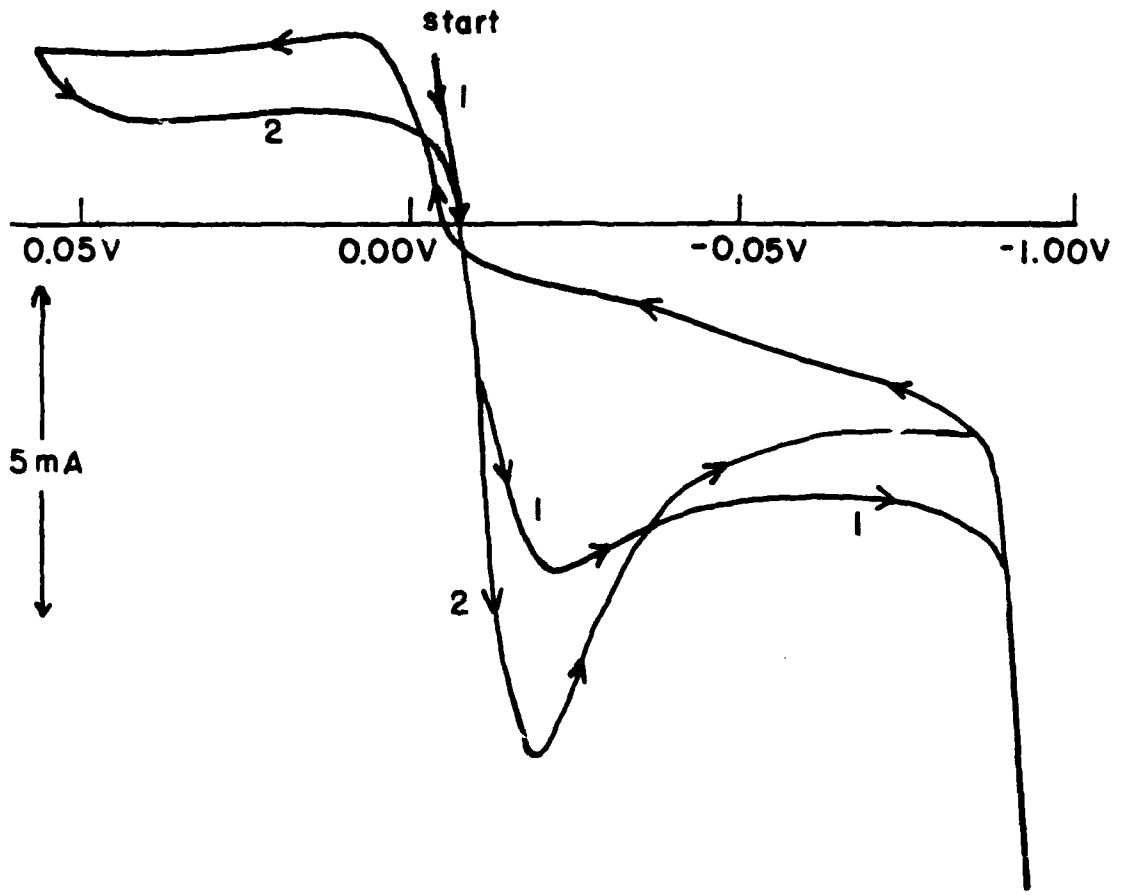

I-158

(8) # ELECTROCHEMISTRY OF INTRINSICALLY CONDUCTING POLYMER COLLOIDS

M. Aldissi, Champlain Cable Corp., 12 hercules Dr., Colchester, VT 05446

INTRODUCTION

The development of intrinsically conducting polymers in the form of copolymers and composites stemmed from applications driven needs for processable materials. Because of the rigid character of the conjugated backbone of these polymers, aggregation is predominant and true solutions are difficult to obtain. Once the polymer is doped to render it conducting, further aggregation takes place and insolubility results. Therefore, the synthesis of conducting polymers as copolymers or composites in the colloidal form is an attractive approach that would take advantage of the aggregated character. Thus, colloidal particles of conducting polymers in the form of dispersions in aqueous or organic media has become a viable route to producing processable conducting polymers.

Electrochemistry has played a major role in the synthesis and characterization of conducting polymers in general. Also, the application of electrochemistry to such materials lead to their use as electrode materials primarily in batteries. However, the use of electrochemistry for the synthesis and characterization of the colloidal forms of conducting polymers is in its infancy.

Received 5-3-91 PT

The object of this paper is to sum up the few efforts by various research groups and describe some electrochemical aspects of several conducting polymer colloids. The text is divided into two sections for reasons of clarity: electrochemistry of chemically synthesized colloids, and electrochemical synthesis of colloids.

I. ELECTROCHEMISTRY OF CHEMICALLY SYNTHESIZED COLLOIDS

1. Polyacetylene-Polyisoprene Block Copolymers

a) Background

Soluble block copolymers of acetylene and isoprene were produced (1) using anionic polymerization coupled with Ziegler-Natta catalyst. Copolymers of various comonomer ratios were obtained in toluene. Solubility/dispersability depends on these ratios, thus, a wide range of materials could be synthesized, and therefore "true" solutions as well as completely insoluble materials were obtained. Doping of the polymers with, for example, iodine resulted in an electrically active component (polyacetylene) and an inactive component (polyisoprene). The overall electrical properties resembled those of composites with a strong dependence of the electrical conductivity on the volume fraction of polyacetylene (2) with a percolation threshold at approximately 16 vol%. The colloidal character of the soluble/dispersable samples was evidenced by small angle neutron scattering studies (3). Samples whose polyacetylene volume fraction was 10% were studied as a "solution" in toluene. Based on a fractal model developed for similar materials (4), the aggre-

gates were spherical with an average particle diameter of 120 A. Further aggregation of these particles by i.e., partial solvent removal results in dispersions with a fractal dimensionality of 2.6. When polyacetylene volume fraction is increased to 20%, the particles become elliptical with an average diameter of 500 A that would aggregate further as spherical particles with a fractal dimensionality of 2.4. The stability of the dispersions can be maintained by shaking when kept in an inert atmosphere. Above 20 vol%, the copolymers are not dispersable and the larger aggregates dimensionality is decreased to 1.5 resulting in rods that are i.e., 1500 A at 30 vol%.

b) Electrochemical Studies (5)

Based on our knowledge of the possible use of polyacetylene as electrode material, films of the 10% solution and 20% dispersion were characterized in terms of electrochemical activity (film conductivity was in the range of 1-10 $(\Omega\ cm)^{-1}$). This study was done on films deposited on platinum electrodes in aqueous and organic media. In the latter case, a slight oxidation/doping was necessary to cause enough aggregation to prevent redispersion.

Similarly to the homopolymer polyacetylene (6,7), films of these dispersions were used as electrodes in a cell which contained a lithium counter electrode and $LiClO_4$ in THF or propylene carbonate. The choice of the solvent depended on whether the copolymer was being reduced (THF) or oxidized (propylene carbonate). Reduction took place in the poten-

tial range of 2.5-0.8 V versus lithium, and oxidation took place between 2.5 and 3.5 V (Fig. 1).

Doping of polyacetylene segments took place in few minutes with good coulombic recovery, thus, faster kinetics were obtained as compared to those of the homopolymer. This was attributed to greater swelling of the copolymer with the electrolyte which probably provided improved wetting and an enlarged effective surface area.

The potential ranges are narrower than for polyacetylene (0.5-4.0 V) due to more extensive self-discharge processes. These processes were found to be due in part to splitting of short-chain polyenes (5-10 double bonds as was shown by uv-vis-near ir) which became soluble when ionized causing a yellow or blue color in the electrolyte solution.

2. Polyaniline Colloids: Graft Copolymers

a) Background

The preparation of colloidal forms of conducting polymers using dispersion polymerization was applied successfully to polypyrrole and polyaniline. Polypyrrole colloids were obtained by dispersion polymerization in the presence of steric stabilizers which simultaneously physically adsorbed, via hydrogen bonding, onto polypyrrole chains/particles. The resulting spherical particles had a diameter in the range 50-450 nm depending mostly on the nature of the steric stabi-

lizer (8-12) with 10-15 wt% of the latter forming a homogeneous outer layer around polypyrrole.

Unlike polypyrrole, stable dispersions of polyaniline colloids could be obtained by chemical grafting of polyaniline onto the steric stabilizer chains. For this purpose, p-aminostyrene (equivalent to the aniline repeat unit) was grafted onto poly(vinyl pyridine) or PVP and Poly(vinyl alcohol-co-vinyl acetate) or PVA which were used in the dispersion polymerization as steric stabilizers. Potassium iodate was added to the aqueous solution as the oxidant for aniline to be polymerized on the graft sites resulting in colloidal dispersions as the graft copolymerization proceeds (13-15). The colloidal particles had a needle-like shape with a length in the range of 100-200 nm and a width in the range of 10-50 nm. Film conductivity was in the range of 0.5-2.0 $(\Omega\ cm)^{-1}$.

b) Electrochemistry: Cyclic Voltammetry (14,15)

Cyclic voltammetry was performed on films deposited on a platinum disc electrode. Thick films were obtained by placing a drop of the dispersion on the electrode surface and allowing the solvent to evaporate. Thin films were prepared by spin coating onto the electrode. In the case of P4VP-based dispersions, PVA was added as appropriate for better film-forming properties. The cyclic voltammograms were recorded in HCl solutions for scan rates limited to the range 10-100 mV/s to avoid overoxidation of the polymer, and the reference electrode was a dynamic hydrogen electrode.

The data is similar to that obtained for anodically grown bulk polyaniline films with no indication of significant effects of the steric stabilizer layer. The variation in reversibility with scan rate as seen for example in the case of PVA-based colloids (Fig. 2), indicate that a limited rate of electrochemical charging took place, probably due to (i) the limited concentration and/or conductivity of the electrolyte, and (ii) the high thickness of the film (>1 μm). Another factor in the electrochemical response could be the limited concentration of chloride ions as could be seen from electrolyte concentration effects on the apparent reversibility of charging shown in Fig. 3.

Both colloids behave similarly to the bulk polymer. This includes (i) quasi reversibility of the first voltammetric peak and the large capacitive current observed in the voltammograms recorded with limited end potentials, and (ii) the loss of charge capacity in the first peak region and the apparent lowered conductivity when cycling with higher anodic end potentials (Fig. 4).

II. ELECTROCHEMICAL SYNTHESIS OF CONDUCTING POLYMER COLLOIDS

1. Polymerization of Pyrrole in the Presence of Latex Particles (16)

This technique consisted of the use of latex particles in the dispersion form as dopants for polypyrrole as the polymerization proceeds. The latex particles must therefore have anionic groups such as sulfonates or sulfates to oxidize pyrrole and act as the polymeric counter anion.

Commercial latices such as acrylates, methacrylates, vinylidene chlorides and ethylene/vinyl acetate copolymers, were modified to incorporate the anionic species. Pyrrole monomer was polymerized in the presence of these active latex particles at 1 V versus an $Ag/AgNO_3$ reference electrode in acetonitrile. The "composite" is obtained as a conductive film on the platinum anode with a polypyrrole content in the range of 2-30 wt% having a conductivity in the range of 10^{-3}-5 $(\Omega\ cm)^{-1}$. The level of conductivity depends on various parameters including the nature of the latex particles and its relative content in the final composition.

The conducting particles consisted of latex cores with polypyrrole as the outer layer. These materials, as for all colloidal forms of conducting polymers, were synthesized for processing purposes. The material can be ground into small particles and highly swollen with shear to give dispersions that can yield films which retain their electrical conductivity.

2. Electrosynthesis of Polypyrrole on Metal Oxide Suspensions (17)

Suspensions of negatively charged metal oxides in water were prepared by adding NaOH amounts such that the pH of suspensions is greater than the isoelectric point of oxides. Polypyrrole-coated oxide particles could be deposited on a gold electrode in the form of films in non stirred suspensions. This technique was evaluated for various oxides.

Successful oxide incorporation was achieved in suspensions whose pH was less than 11 in the case of WO_3 and SiO_2 in the form of thick films. Thin films only could be obtained in the case of Ta_2O_5, SnO_2 and TiO_2. No incorporation took place in the case of CeO_2, MnO_2 and ZnO.

It was observed in general that suspensions with smaller isoelectric points resulted with thicker films. Conductivity of these films depends strongly on the isoelectric point of the oxide similarly to the strong dependence of conductivity of polypyrrole on the dissociation constant of the electrolyte anions in the case of regular polypyrrole. Oxides having large isoelectric points possess high affinities to positively charged protons, therefore, when incorporated, they interact strongly with the positive charges of polypyrrole chains resulting in resistive films which in turn inhibit further growth.

Although this is the first attempt at incorporating metal oxides in polypyrrole electrochemically, it is worth noting that hematite (α-Fe_2O_3) and cerium oxide (CeO_2) were coated chemically with polypyrrole in ethanol/water suspensions of the oxides (18). In all cases the isoelectric point was approximately 4.

CONCLUSION

Electrochemistry has played an important role in the synthesis and characterization of intrinsically conducting polymers since the early days of their development. In most cases, the techniques are applied in the solid state where the polymer is obtained and/or further characterized

as a film or a compressed pellet, including processable forms of these polymers. Because most of the processable forms are composites or copolymers often made of hydrophobic and hydrophilic components, there is a tendency for these compositions to aggregate in colloidal forms whose size and shape vary with the nature of both components and their ratio. Electrochemistry of these colloids or dispersions has proven that although the electrically inactive component is used as a processing aid, the materials behave similarly to their bulk counterparts. However, more detailed impedance measurements are required to determine whether any intrinsic charging barriers are caused by the presence of insulating layers. Electrosynthesis of colloidal dispersions of conducting polymers is still in its early development, but its feasibility has been proven, although not in a straight forward manner. Future work has to focus on the use of steric stabilizers that would act as the polymeric dopant/electrolyte. Upon formation of the colloidal particles, redispersion would take place instantaneously when the appropriate solvent is used. Advantages of such a process include (i) a good control of the polymerization process and therefore the particle size by control of the current density of the anode where the colloid is being formed, and (ii) a better homogeneity of the particles. Conditions for the above two parameters are often dictated by the oxidative strength of the oxidant/dopant in chemical synthesis techniques.

REFERENCES

1. Aldissi, M. J. Chem. Soc., Chem. Commun. 1984, 4, 1347-1348.
2. Aldissi, M.; Bishop, A. R. Polymer 1985, 26, 622-625.
3. Aldissi, M.; Henderson, S. J.; Hofflin, P.; White, J. W. Mol. Cryst. Liq. Cryst. 1990, 180A, 9-24.
4. Texeira, J. In On Growth and Form; Stanley, H. E.; Ostrowski, W., Ed.; Martinus Nijhoff, 1986.
5. Aldissi, M.; Bishop, A. R. Synth. Met. 1986, 14, 13-18.
6. Nigrey, P. J.; MacInnes Jr., D.; Nairns, D. P.; MacDiarmid,A. G.; Heeger, A. J. J. Electrochem. Soc. 1981, 128, 1651.
7. Kaner, R. B.; MacDiarmid, A. G.; Mammone, R. J. in Polymers in Electronics; Davidson, T. Ed.; ACS, 1984, 575.
8. Bjorklund, R. B.; Liedberg, B. J. Chem. Soc., Chem. Commun. 1986, 1293.
9. Armes, S. P.; Miller, J. F.; Vincent, B. J. Colloid Interface Sci. 1987, 118, 410.
10. Vincent, B.; Obey, T. M.; Cawdery, N. J. Chem. Soc., Chem. Commun. 1988, 1189.
11. Armes, S. P.; Aldissi, M.; Agnew, S. Synth. Met. 1989, 28, C837-C848.
12. Armes, S. P.; Aldissi, M. Polymer, 1990, 31, 569-574.
13. Armes, S. P.; Aldissi, M. J. Chem. Soc., Chem. Commun. 1989, 88-89.
14. Armes, S. P.; Aldissi, M.; Agnew, S.; Gottesfeld, S. Mol. Cryst. Liq. Cryst. 1990, 190, 63-74.

15. Armes, S. P.; Aldissi, M.; Agnew, S.; Gottesfeld, S. Langmuir, 1990, 6/12, 119-122.

16. Jasne, S. J.; Chiklis, C. K. Synth. Met. 1986, 15(2-3), 175-182.

17. Yoneyama, H.; Shoji, Y.; Kawai, K. Chem. Soc. Japn., Chem Lett., 1989, 88, 1067-1070.

18. Partch, R.;Gangolli, S. G.; Cwen, D.; Ljungquist, C.; Matijevic, E. ACS Proceedings, PMSE Div., 1991, 64, 351.

FIGURE CAPTIONS

Fig. 1 V_{oc} *versus* Li/Li^+ as a function of the percentage of oxidation or reduction in polyacetylene block copolymers/lithium cells.

Fig. 2 Cyclic voltammograms of a colloidal PVA/polyaniline film recorded in 2M HCl solutions at scan rates of 10 mV/s (solid curve) and 100 mV/s (dashed curve). The current bar corresponds to 4 and 40 mA/cm^2 respectively.

Fig. 3 Cyclic voltammograms of colloidal PVA/polyaniline films recorded in 0.2M HCl (dashed curve) and in 2M HCl (solid curve) at a scan rate of 10 mV/s. The current bar corresponds to 4 mA/cm^2 for both curves.

Fig. 4 Cyclic voltammograms of a colloidal PVA/polyaniline film recorded in 2M HCl solutions in a restricted potential domain (solid curve), in an extended potential domain (dashed curve) and returning to the restricted domain (dotted curve). Scan rate is 10 mV/s and the current bar corresponds to 4 mA/cm^2.

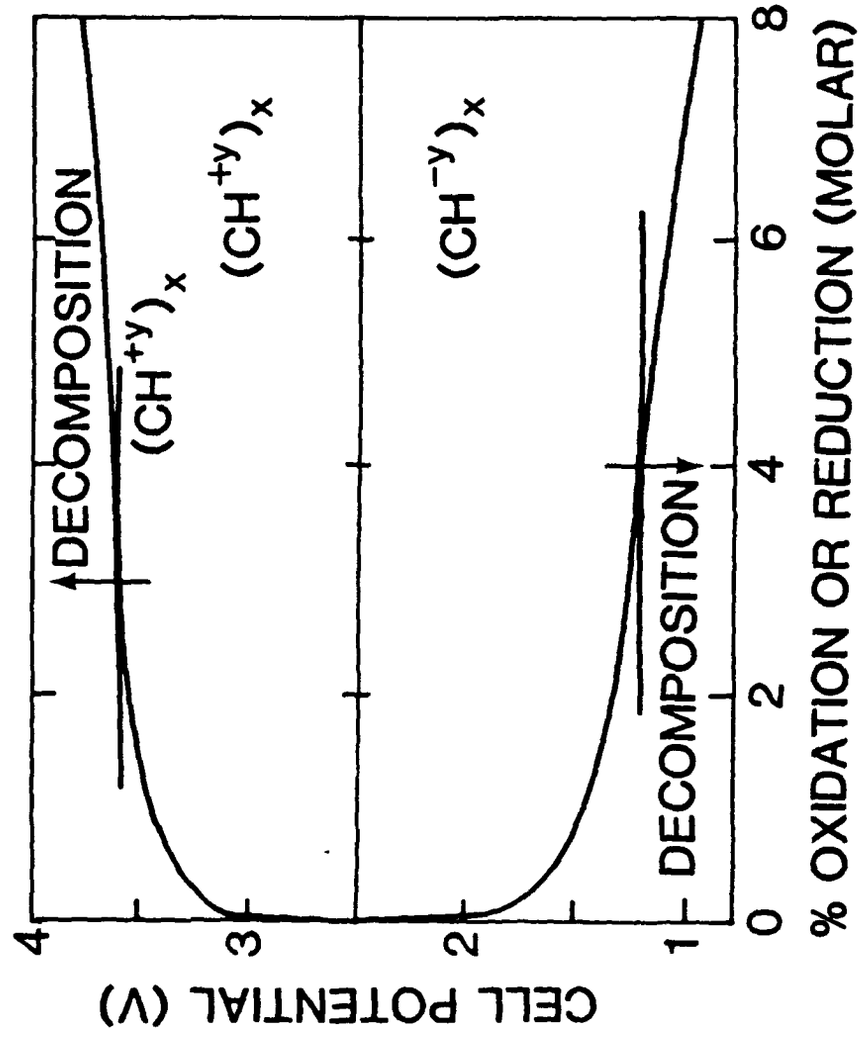
DECOMPOSITION
$(CH^{+y})_x$
$(CH^{+y})_x$
$(CH^{-y})_x$
DECOMPOSITION
CELL POTENTIAL (V)
% OXIDATION OR REDUCTION (MOLAR)
4
3
2
1
0
2
4
6
8

SG-257

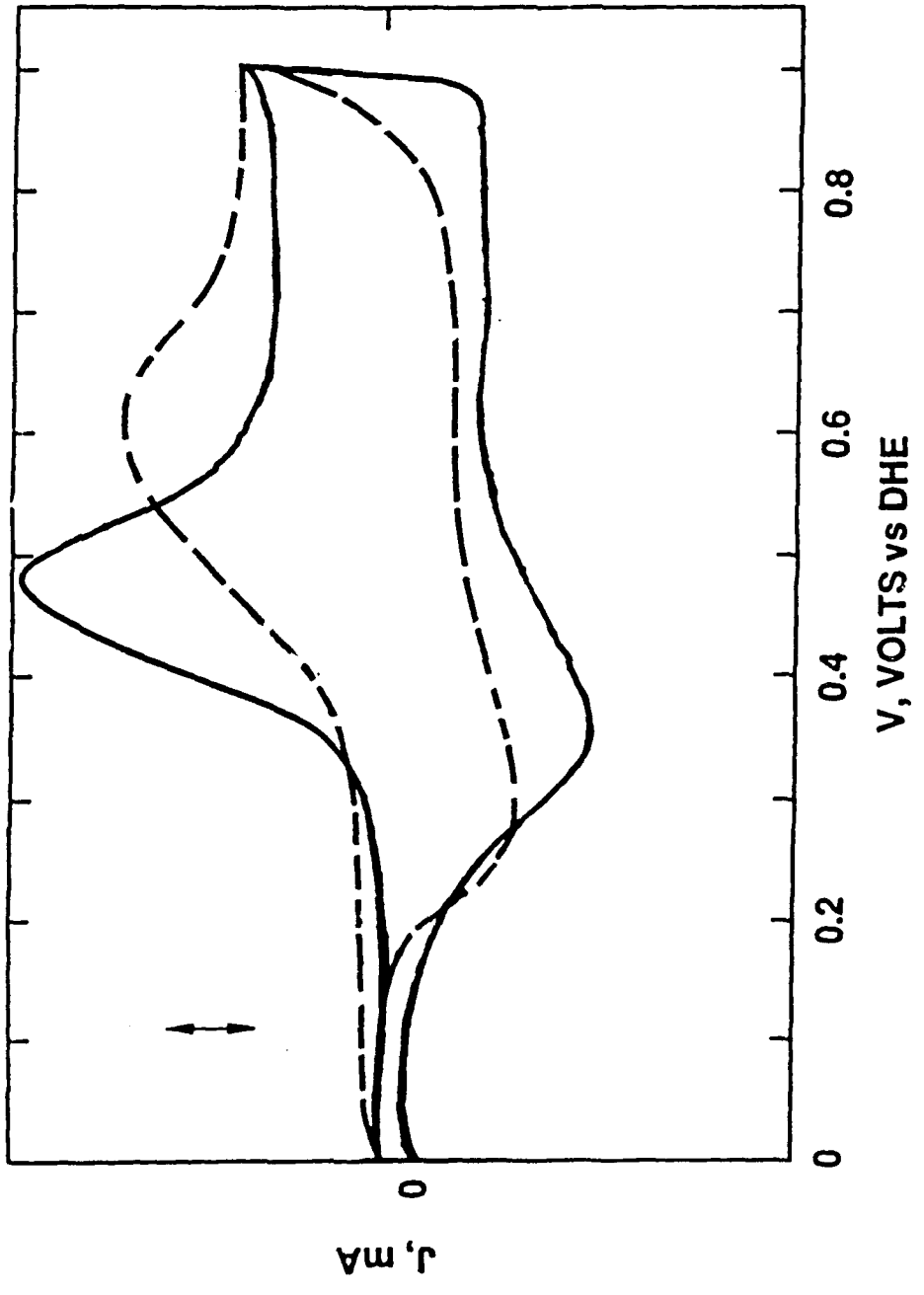

EC1-I

SG-256

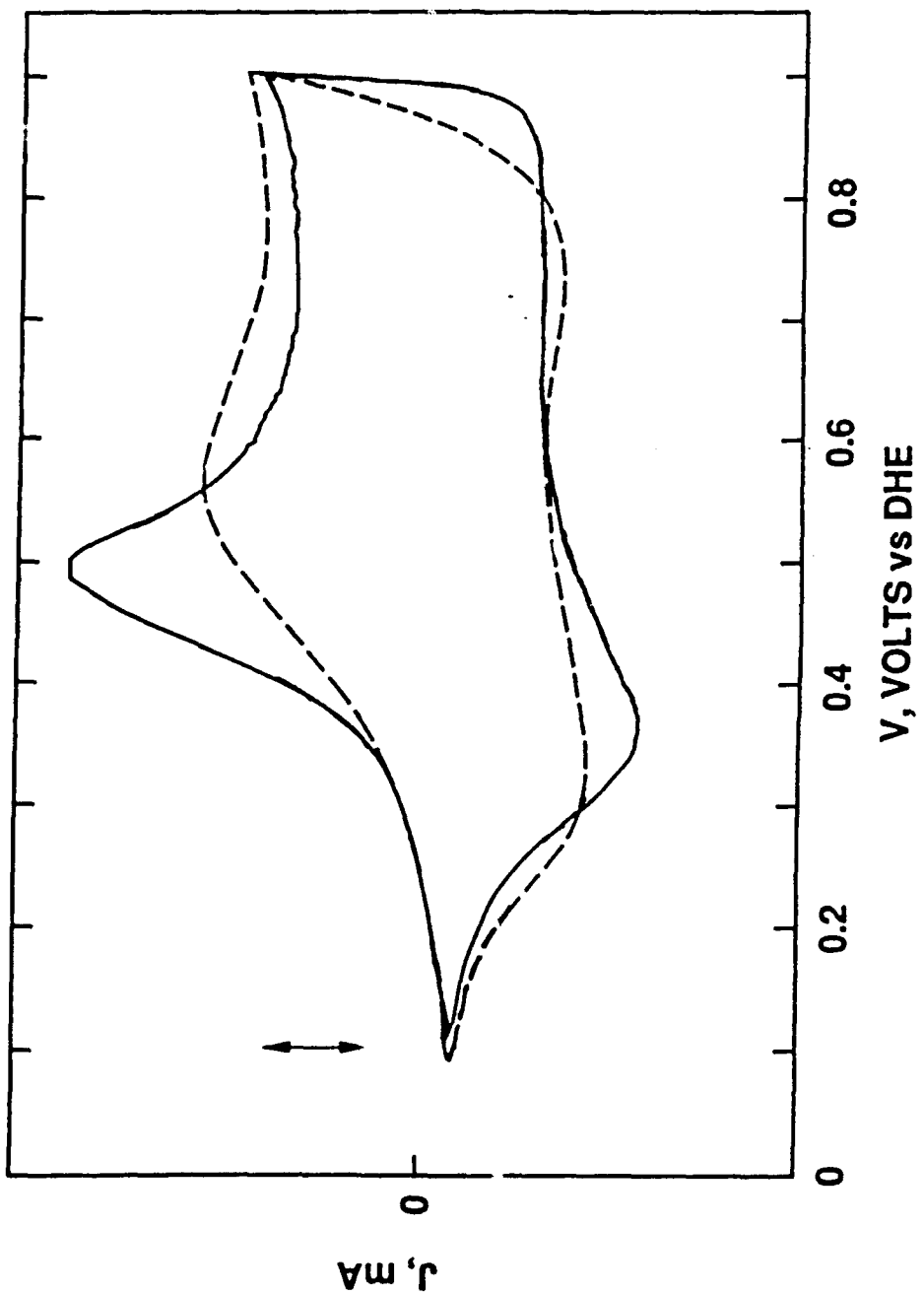

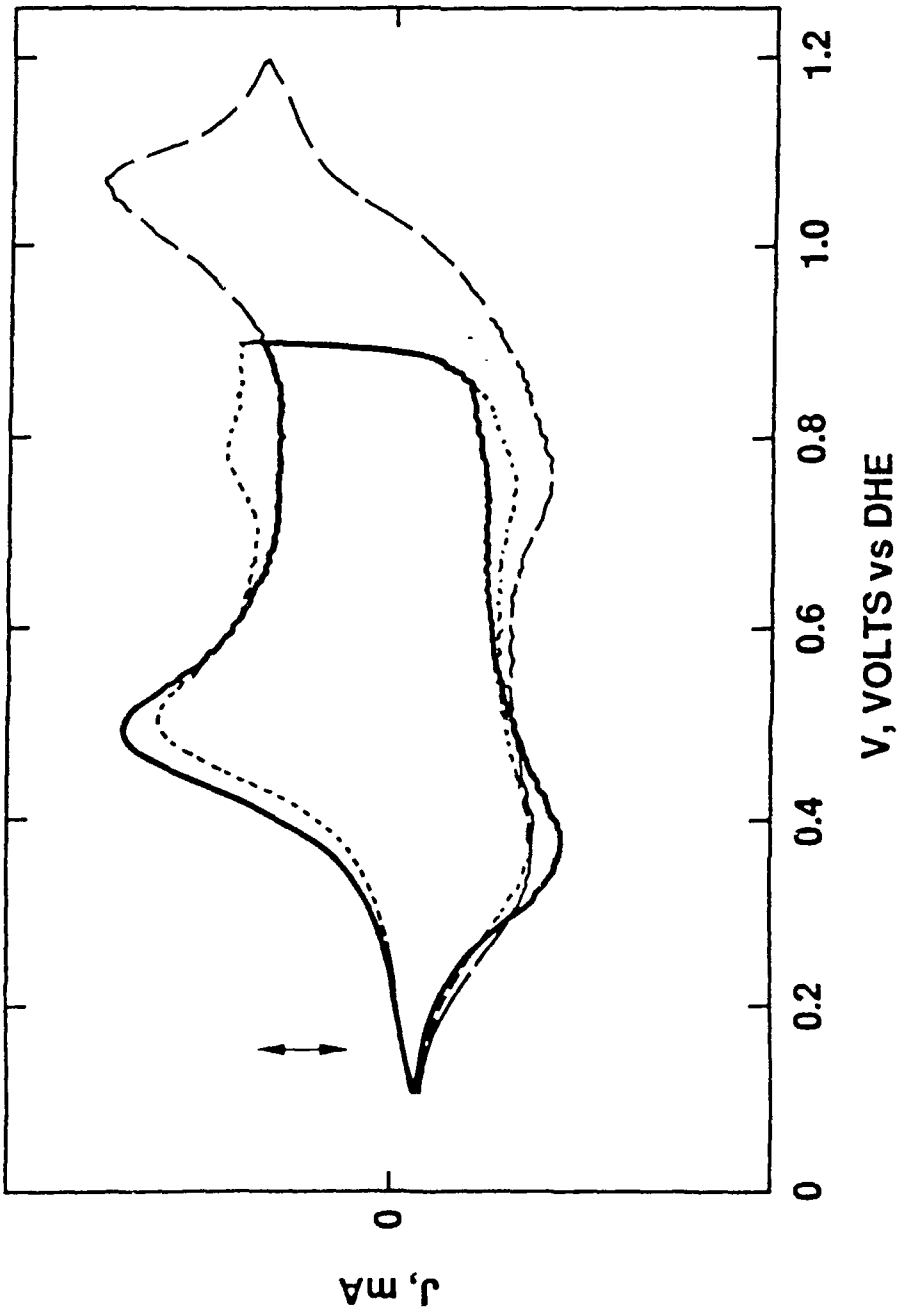
0
0.2
0.4
0.6
0.8
1.0
1.2
V, VOLTS vs DHE
0
j, mA

(9) Voltammetric Investigation of Proton Transport in Ordered Polymer Latices

S. E. Morris and J. G. Osteryoung

University at Buffalo, State University of New York

Acheson Hall, Buffalo, NY 14214

Abstract

Polymer particles of monodisperse size have been exploited as model colloids. Aqueous suspensions of charged polymer colloids with small electrolyte concentrations order spontaneously into liquid crystalline phases; the most noticeable features of a liquid crystal is a striking iridescence. We apply pulse voltammetry at microelectrodes to the ion-specific (H^+) measurement of properties affecting ion transport in ordered polymer colloids. Transport-limited reduction of proton at platinum microelectrode (disk radius 12.5 μm) in extremely dilute aqueous electrolyte is measured using square-wave voltammetry. Currents measured for reduction of proton in latex suspension are normalized to currents predicted in the absence of colloid, using a model for similar reductions in homogeneous solution, to account for variation in transport-limited currents of proton with changes in concentration of inert electrolyte. We have observed the transport of proton to increase substantially upon disordering of polymer colloid suspensions with electrolyte. Diffusion-limited current for oxidation of a neutral molecule (TEMPOL) is largely unaffected by a transition in the phase of colloid. Observations of transport of proton in latex suspension have not quantitatively related to factors effecting the order-disorder transition. However, normalized values of the current for reduction of proton in suspensions of charged polymer colloids exhibit sensitivity to the presence of the particles in a manner which is not predicted by simple excluded volume or ionic strength considerations.

Introduction

Colloidal systems, consisting of suspensions of particles with radial dimensions on the order of 10^{-7}-10^{-3} cm, are of interest in both naturally occurring media (soils and biological systems) and in industrial systems (1,2). Monodisperse latex consists of spherical particles, formed in emulsion polymerization of monomers such as styrene (3), having regular shape, submicron diameters and narrow size dispersion. Accordingly they have been exploited as model colloids. When suspended in a polar medium such as water, the surface charge on each sphere stabilizes the particle suspension through repulsive forces between particles; the properties of the suspension may be manipulated by effecting variations in the repulsive forces by changing the chemical composition of the suspending solution.

Under appropriate conditions of volume fraction, φ, and total electrolyte concentration in aqueous suspensions, the strong electrostatic interactions of these charged colloidal particles lead to ordering of particles in the suspending medium into a crystalline phase; these phases exhibit increased viscosity and diffraction of light in the visible range, thus displaying marked iridescence. A change in the colloid to a disordered, more fluid state is induced by increasing the electrolyte concentration. The resulting suspension has lower viscosity and is not iridescent. Such a phase transition is related to the solid-liquid melting transition in molecular materials. Identification of the order-disorder transition is not easily accomplished except by observation of iridescence.

Visible aspects of order-disorder transitions and crystal structure in ordered model colloidal suspensions have been characterized using visible appearance (4, 5), absorbance and reflectance spectrometry (6, 7) and small angle neutron scattering (8) as functions of particle volume fraction and electrolyte concentrations. Phase transitions in model charged colloids have been predicted using primarily models of effective hard sphere diameter and screened coulombic interactions (9, 10). Experimental phase diagrams have been constructed (1, 11) and compared with various predictive models. The important parameters in the predictions are the surface charge and potential, and electrolyte and particle concentrations. Conductivity and electrophoretic transport

(11,12) and titration of total surface charge (12-14) in suspensions are used to determine particle surface charge and potential.

Only conductivity probes directly the ion activity and transport within a concentrated state of a suspension. Conductivity provides an average measure of ionic strength and mobility, but provides no information which is ion-specific. Electrophoretic mobilities of colloidal particles are measured at extreme dilutions ($\varphi \sim 10^{-5}$), not in the more concentrated suspensions of interest. Potentiometry is ion-specific. However potentiometric measurements in colloids are confounded by interaction of the potential-sensitive measuring surface with particle double layers in concentrated suspensions (15). In addition, potentiometry is not sensitive to mobility of ions. Total surface charge does not distinguish the degree of dissociation of surface groups under various conditions, nor does it indicate ion mobility. In short, the visible appearance of iridescence in the region of the order-disorder transition is the main experimental evidence used to test the predictions of models. Factors affecting particle interaction potentials in suspension will also affect specific ion mobility, thus direct measurement using techniques sensitive to specific ion mobility or activity will be sensitive to exactly that coulombic screening of surface charge which determines the particle interaction potential.

To our knowledge, no voltammetric techniques have been applied to the measurement of transport and activity of ions or neutral molecules in monodisperse polymer colloids. Measurement of current for faradaic reactions in solutions of low conductance is made feasible by the use of a platinum disk microelectrode (radius 12.5 μm). Limited conversion of material at microelectrodes on short time scales (for square wave voltammetry at 1 Hz, the amount of material converted is <10 pmol) ensures that the technique probes, but does not change, the equilibrium phase of the suspension.

We have measured transport-limited pulse voltammetric currents for reduction of proton in monodisperse suspensions of negatively charged polystyrene microspherical particles in which proton is the only cation. Addition of inert electrolyte effects the transition from the ordered to the disordered state. Proton reduction in latex suspensions has been identified and calibrated by

comparing it with the reduction of proton in dilute aqueous solutions of hydrochloric acid at comparable proton concentrations (< 2 mM). For comparison, the diffusion-limited current for oxidation of a neutral molecule (TEMPOL) has been measured. Linewidths for TEMPOL, a stable nitroxyl radical, have been measured within the same latex suspensions by electron paramagnetic resonance spectroscopy. The preliminary results of an investigation of transport of proton in the order-disorder transition region of suspensions of 0.106 μm polystyrene latex are presented.

Experimental Method

Monodisperse polystyrene microparticles (Duke Scientific Corp., Palo Alto, CA) of diameter 0.106 μm, equilibrated for 48 hours over a mixed bed ion-exchange resin (Bio-Rad, Richmond, CA) were used for all measurements. All volume fractions used were prepared by dilution from volume fraction 0.101 stock (determined gravimetrically with drying at 70 °C; density of polystyrene 1.05 g cm^{-3}). Deionized latexes were visibly iridescent at all volume fractions from 0.025 to 0.101. Viscosity was measured in suspensions with various added concentrations of potassium chloride, in an Ostwald-type viscometer at 25 °C. Total surface charge was determined by titration of proton in ion-exchanged suspension to conductimetric endpoint with NaOH (10, 11); surface charge density measured for the 0.106 μm latex is 1.66 μC cm^{-2}. All voltammetry was performed using platinum wire counter and mercury sulfate (EG&G PARC, Princeton, NJ) reference electrodes isolated in 0.1 M KCl from the 0.75-mL working electrode chamber via a Vycor "thirsty glass" frit. All voltammetry was accomplished with software for square wave voltammetry implemented on a Digital Equipment Corporation pdp/8e microcomputer, which was used to control an EG&G PARC 273 potentiostat (16). The working electrode chamber was deaerated with argon. Temperature was controlled in the jacketed electrochemical cell to 25 °C with a circulating water bath. Hydrochloric acid and potassium chloride (Fluka) were used as received (puriss. grade). The compound 4-hydroxy-2,2',6,6'-tetramethylpiperidine-oxy, or TEMPOL (Aldrich reagent), was used as received. EPR lines were measured with an IBM/Bruker ER-200SRC X-band EPR spectrometer, at ambient temperature

(21 °C) in a Varian aqueous solution (flat) cell, for deaerated latex, $\varphi = 0.0505$, with 0.2 mM TEMPOL at various KCl concentrations.

Results and Discussion

Continuous iridescence was taken to indicate the crystalline phase of the latex. Complete disorder cannot be judged by appearance; ordered regions in coexistence with disordered regions may have the appearance of "crystallites" or may not show iridescence if ordered regions are too small. This is corroborated by measurements of viscosity of suspensions. The variation in the relative viscosity, η/η_0, where η_0 is the viscosity of pure water at 25 °C, with volume fraction at various electrolyte concentrations is shown in Figure 1. A condition of no electrostatic interactions corresponds to the straight (lowest) line in Figure 1, which illustrates the familiar Einstein relation for viscosity of a suspension of non-interacting (uncharged) hard spheres,

$$\eta/\eta_0 = 1 + 2.5\,\varphi. \qquad (1)$$

Because of interactions of charged particles, and in contrast with the viscosities of dilute solutions and suspensions of uncharged particles, viscosities of concentrated suspensions of charged particles depart from a linear dependence on φ (1, 17). Viscosity decreases smoothly with decrease in volume fraction as shown in Figure 1. As shown in Figure 2, it also decreases smoothly with increase in the concentration of added electrolyte.

For this latex, only suspensions with relative viscosity values of 1.5 or greater are visibly iridescent. The lowest added electrolyte concentration used (0.01 mM KCl) showed a "break" in the viscosity curve with a loss of iridescence, but no other obvious order-disorder transition is observed in any of the measured viscosity values. A large fraction of the combinations of volume fraction and electrolyte concentration fall below the iridescent ordered state and above the line for non-interacting spheres: there is likely to be a continuous variation in the sizes of ordered regions in coexistence with disordered regions as the transition is crossed. This is consistent with the representation of the same in Figure 2, which shows only smooth changes, without any sharp order-disorder transition.

At extremely small values of added electrolyte the major source of ions in latex is the ionogenic groups of the colloid surface. In deionized colloids, this counterion is proton, which is derived from dissociation of surface acid groups of the microparticles. The surface charges of these particles are provided by sulfate groups (manufacturer's literature). They are strong acids, completely dissociated even in concentrated suspension. Conductimetric titration data are consistent with the strong acid nature of the surface groups (13, 14). Figure 3 presents a conductimetric titration curve of 0.106 μm latex suspension with dilute NaOH.

Square wave voltammograms for reduction of proton are shown in Figure 4 for 0.43 mM HCl and for a suspension of 0.106 μm particles (0.31 mM H^+), both with 0.5 mM KCl. The usual hydrogen adsorption waves on Pt are normally observed at the foot of the hydrogen reduction wave at higher frequencies, but are not seen at this extremely low frequency. The identical position and shape of the waves (including the adsorption waves at higher frequency) in both dilute HCl and in latex suspension are used to verify that indeed the reduction investigated in suspensions is that of proton.

The nearly steady-state current at the plateau of wave 1 in Figure 4 is limited by diffusion and migration. (At steady-state the forward and reverse currents should be the same.) Because we desire to use this current as a probe of structure in the suspensions, and to manipulate the structure by changing electrolyte concentrations, we need to normalize the measured currents by those measured at the same concentration of electrolyte in the absence of the colloid. This is done in the following way.

Figure 5 shows the diffusion-limited current for reduction of proton in 0.5 M KCl. Theory predicts that for these conditions the maximal current is within 6% of the steady-state value, and the near coincidence of the limiting values (as in Figure 4) confirms that the steady state is nearly achieved. The steady-state (plateau) current limited by diffusion alone is given by (18)

$$i = 4 n F D C r, \qquad (2)$$

where n (stoichiometric number of electrons transferred) = 1, F is the value of the Faraday constant, D is the diffusion coefficient of H^+, C is the concentration of H^+ and r is the electrode

radius. The slope of line 2 of Figure 5 and equation 2 can be combined to give values for D_{H^+}/ $cm^2\ s^{-1} = 0.91 \times 10^{-4}$ (0.1 M KCl) and 0.84×10^{-4} (0.5 M KCl). These values assume that the measured currents are steady-state currents. Published values are 0.93×10^{-4} (from mobility at infinite dilution) (19, 20) and 0.75×10^{-4} (1 M KCl) (21).

Plateau currents for reduction of H^+ from HCl in the absence of added electrolyte are used to construct the calibration plot for steady-state proton reduction, line 1 in Figure 5. The currents at any point on the curve are greater than those predicted from diffusional transport, given by line 2. The contribution of migration to the transport of proton decreases with added electrolyte. For reduction of a singly charged cation, the ratio of the steady-state transport-limited current, i_γ, to the diffusion-limited current, i_d, decreases from 2 to 1 with the following dependence on γ, the ratio of electrolyte to proton concentration (22):

$$i_\gamma / i_d = 2 + 2\gamma - [\ (1 + 2\gamma)^2 - 1\ ]^{1/2}. \qquad (3)$$

Limiting currents for HCl measured at various values of γ are normalized by dividing by the appropriate value of i_l obtained from line 2 of Figure 5. Normalized values are plotted with the theoretical curve (equation 3) in Figure 6. As noted above, the value of D depends on ionic strength. Strictly speaking, the normalizing factor should be, not i_d (0.5 M KCl), but rather i_d (0.5 M KCl) D(x M KCl)/D (0.5 M KCl). The systematic positive deviation of measured values from the theoretical curve, and difference between different concentrations of HCl, arise from this simplification. For example the maximum concentration of KCl in Figure 6 is 0.10 M, and D (0.1 M)/ D (0.5 M) = 1.083. The data of Figures 5 and 6 describe the dependence of limiting current on the concentration of indifferent electrolyte in homogeneous solution, thus they serve to calibrate the results of similar experiments in latex suspensions.

We also have measured limiting currents for oxidation of TEMPOL, a neutral molecule. The compound TEMPOL is oxidized quasireversibly in aqueous solution, with loss of a single

electron to form the oxoammonium cation:

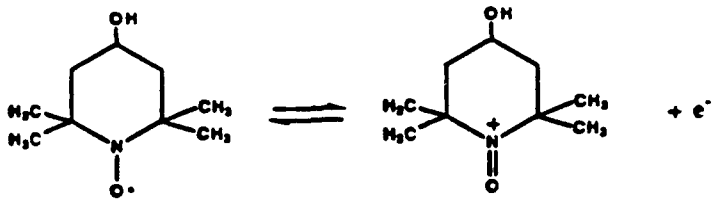

A square-wave voltammogram for oxidation of TEMPOL is shown in Figure 7. Unlike those for proton reduction, plateau current values for TEMPOL are diffusion-limited even in the absence of inert electrolyte, as one would expect for a neutral molecule. For 0<[KCl]/mM<10, i_{TEMPOL} /nA = 7.34 ± 0.15 at 2.25 mM TEMPOL. Thus TEMPOL provides a probe of local viscosity and transport-limited current, independent of interactions with latex spheres or variations in solution conductivity. The transport-limited current is not necessarily the same under these conditions as the diffusion-limited current observed in homogeneous solution, because the volume occupied by a particle is inaccessible to diffusion.

Currents for oxidation of TEMPOL measured for latex suspensions are compared with the values predicted in the absence of the colloid in Table 1. Predicted current values for TEMPOL are calculated directly from the added concentration and a diffusion coefficient value of D_{TEMPOL}/ cm^2 sec^{-1} = 0.63×10^{-5} (10 mM KCl), which was determined using the concentration plot of Figure 8. Current ratios for TEMPOL are less than unity in the latex, and they decrease by about 10% in the transition from ordered to disordered latex. Diffusion coefficients are expected to be less within latex suspensions (23) because of the excluded volume of the particles. For polystyrene latices, self-diffusion of water is observed by pulsed H-nmr to have $D/D_0 = 0.953$ for φ=0.096. The decrease in current ratio with disordering of the latex is consistent with partial blocking of the electrode as the particle positions are randomized in the disordered state, but the effect is certainly a small one. In general, the current ratios for TEMPOL indicate that diffusion coefficients measured for any species will be less in a latex suspension than in homogeneous solution, and that the neutral molecule is insensitive to changes in the ordering of the latex effected by added electrolyte. Linewidths for TEMPOL measured by EPR spectroscopy are also insensitive to variations in added electrolyte concentration. When an F-test is applied, variances of averaged linewidths are not

significantly different from variances of a linear fit of linewidths to a monotonic increase in added electrolyte concentration. The linewidth does not change significantly from ordered to disordered latex, thus the local viscosity, as expected, is not changed by particle ordering.

Table 2 presents the measured limiting currents and their normalized values for proton reduction in latex. For proton reduction in HCl, the predicted values are the product of i_d for titrated $[H^+]$ and the appropriate excess electrolyte ratio i_γ / i_d. The normalized value is the ratio of the value in latex to the predicted value in latex-free solution of the same composition. The effect of changes in electrolyte concentration on the transport of proton in the latex is dramatically different from the effect of the same changes on TEMPOL diffusion. The decreased ddiffusivity of TEMPOL in the latex suspensions is relatively insensitive to ordering of the latex. The normalization procedure employed here accounts for changes in transport due to changes in migration current, in the case of proton.

Two points are important to observe in Table 2. First is the increase in limiting current for proton reduction with added electrolyte. The second is that the normalized values are nearly the same at a given electrolyte concentration for all volume fractions. Averaged current ratios are plotted in Figure 9. A noticeable change in the transport of proton as represented by normalized current values is seen for these concentrations of KCl, which effect an order to disorder state in the suspensions over the concentration range shown.

Transport of proton has been measured voltammetrically in the region of an order-disorder transition in suspensions of colloidal polymer particles. Our preliminary work shows that diffusion of a neutral molecule is largely unaffected by changes in order of a colloidal suspension, while the transport of proton is dramatically increased over the same region. We effect an order-disorder transition by changes in the ionic stength of the suspension with added inert electrolyte, thus we have normalized the current measured for reduction of proton in latex suspension with currents predicted for the same proton concentration in the absence of the colloid. To predict the current in the latex-free solution, we have used a model for similar reductions in homogeneous solution which predicts the changes of transport-limited currents of ions with changes in

concentration of inert electrolyte. We have not quantitatively related our observations of transport of proton in latex suspension to factors effecting the order-disorder transition. However, normalized values of the current for reduction of proton in suspensions of charged polymer colloids exhibit sensitivity to the presence of the particles in a manner which is not predicted by simple excluded volume or ionic strength considerations.

Acknowledgments

Support for the work was provided through NSF Grant CHE9024846. The help of R. Allendoerfer with EPR experiments and their interpretation is gratefully acknowledged.

Literature Cited

1. Russel, W. B.; Saville, D. A.; Schowalter, W. R. Colloidal Dispersions; Cambridge University Press: Cambridge; 1989.
2. Clark, A. H.; Lips, A.; Hart, P. M. In Food Colloids; Bee, R. D.; Richmond, P.; Mingins, J., Eds., Royal Society of Chemistry: Cambridge; 1989; pp. 154-171.
3. Vanderhoff, J. W.; Vitkuske, J. F.; Bradford, E. B.; Alfrey, T. J. Polymer Sci. 1956, 20, 225-234.
4. Hachisu, S.; Kobayashi, Y.; Kose, A. J. Colloid Interface Sci. 1973, 42, 342-348.
5. Hachisu, S.; Kobayashi, Y. J. Colloid Interface Sci. 1974, 46, 470-476.
6. Hiltner, P. A.; Krieger, I. M. J. Phys. Chem. 1969, 73, 2386-2389.
7. Goodwin, J. W.; Ottewill, R. H.; Parentich, A. J. Phys. Chem. 1980, 84, 1580-1586.
8. Ashdown, S.; Markovic, I.; Ottewill, R. H.; Lindner, P.; Oberthur, R. C.; Rennie, A. R. Langmuir 1990, 6 , 303-307.
9. Voegtli, L. P.; Zukoski, C. F., IV. J. Colloid Interface Sci. 1991, 141, 79-91.
10. Shih, W. Y.; Aksay, I. A.; Kikuchi, R. J. Chem. Phys. 1987, 86, 5127-5132.
11. Monovoukas, Y.; Gast, A. P. J. Colloid Interface Sci. 1989, 128, 533-548.
12. Voegtli, L. P.; Zukoski, C. F., IV. J. Colloid Interface Sci. 1991, 141, 92-108.
13. van den Hul, H. J.; Vanderhoff, J. W. J. Colloid Interface Sci. 1968, 28, 336-337.
14. van den Hul, H. J.; Vanderhoff, J. W. J. Electroanal. Chem. 1972, 37, 161-182.
15. Oman, S.; Godec, A. Electrochim. Acta 1991, 36, 59-67.
16. Osteryoung, J.; O'Dea, J. J. In Electroanalytical Chemistry, Vol. 14; Bard, A. J., Ed.; Marcel Dekker: New York, 1986; pp. 209-308.
17. Stone-Masui, J.; Watillon, A. J. Colloid Interface Sci. 1968, 28, 187-202.

18. Carslaw, H. S.; Jaeger, J. C. Conduction of Heat in Solids, 2nd ed.; Oxford University Press: Cambridge, 195[illegible]; p. 215.

19. [illegible]ockris, J. O'M.; Re[illegible]dy, A. K. N. Modern Electrochemistry; Plenum Press: New York, 1970; p. 376.

20. McInnes, D. A. The Principles of Electrochemistry; Dover Press: New York, 1961; p. 342.

21. Adams, R. N. Electrochemistry at Solid Electrodes; Marcel Dekker, Inc.: New York, 1969; p. 221.

22. Amatore, C.; Fosset, B.; Bartelt, J.; Deakin, M. R.; Wightman, R. M. J. Electroanal. Chem. 1988, 256, 255-268.

23. Venema, P.; Struis, R. P.W.; Leyte, J. C.; Bedeaux, D. J. Colloid Interface Sci. 1991, 141, 360-373.

Table 1. Limiting currents for oxidation of TEMPOL in suspensions of latex and predicted values without latex.[b]

φ	[TEMPOL][a] /mM added	[KCl][a] /mM, added	i /nA with latex, measured	i^b /nA without latex, calculated	Ratio[c]
0.0505	1.91	0	4.2	5.8	0.72
		3.2	3.8		0.66
0.101	0.83	0	1.9	2.5	0.75
		3.2	1.7		0.67

[a] Corrected for volume fraction of water.

[b] Calculated with D_{TEMPOL}/ cm^2 sec^{-1} = 0.63×10^{-5} and r_{Pt} = 12.5 μm.

[c] Ratio of the current in the presence of latex to that without latex.

Table 2. Limiting currents for proton reduction in latex suspension and predicted values for comparable proton concentrations in the absence of colloid, over a range of added [KCl].

φ	Titratable [H+][a] / mM	Added [KCl][b] / mM	$i_{l,latex}$ /nA	$i_{l,HCl}$[c] /nA	Ratio[d]
0.03	0.31	0	0.2	24.6	0.01
		0.1	3.2	16.5	0.19
		0.2	4.9	15.1	0.32
		0.3	5.1	14.4	0.35
		0.4	6.2	14.0	0.44
		0.5	6.1	13.7	0.44
		10	9.1	12.4	0.73
0.0505	0.52	0	2.3	41.2	0.06
		0.1	6.5	29.4	0.22
		0.2	9.1	27.0	0.34
		0.3	11.0	26.2	0.43
		0.4	11.0	25.8	0.44
		0.5	11.7	24.3	0.48
		10	16.1	20.9	0.77
0.075	0.79	0	3.7	62.4	0.05
		0.1	9.7	46.7	0.21
		0.2	14.8	42.9	0.34
		0.3	17.3	40.9	0.42
		0.4	18.7	39.3	0.48
		0.5	18.0	38.2	0.47
0.101	1.09	0	9.0	86.2	0.10
		0.1	13.7	66.8	0.21
		0.2	19.0	62.1	0.31
		0.3	20.9	58.6	0.36
		0.4	24.3	56.9	0.43
		0.5	24.5	54.9	0.45
		10	33.6	44.2	0.76

[a] Obtained by conductimetric titration, corrected for volume fraction of water.

[b] Corrected for volume fraction of water.

[c] $i_{l,HCl}$ is calculated from the interpolated value from line 2 of Figure 5 multiplied by i_γ/i_d for the appropriate excess electrolyte ratio.

[d] $i_{l,latex}/i_{l,HCl}$

Figure Captions

Figure 1. Relative viscosity (η/η_0) of suspensions of 0.106 μm latex vs. volume fraction φ for deionized and electrolyte-added suspensions; T = 25.0 °C, η_0 = 0.8904 cp. Concentrations of added KCl: (o) 0, (Δ) 0.01, (v) 0.1, (◆) 0.25, (*) 0.5 mM, (—) ω (theory).

Figure 2.
Relative viscosity (η/η_0) of latex suspension vs. KCl concentration; T = 25 °C, η_0 = 0.8904 cp. Volume fractions φ: (◆) 0..03, (v) 0.0505, (Δ) 0.075, (o) 0.101.

Figure 3.

Conductimetric titration of ion-exchanged latex suspension with NaOH.

Figure 4.

Forward (Δ) and reverse (v) square wave currents for reduction of proton at Pt, disk radius 12.5 μm; (1) 0.43 mM HCl, 0.5 mM KCl; (2) latex suspension, φ = 0.03, 0.5 mM KCl; E_s = 10 mV, E_{sw} = 25 mV, f = 0.5 Hz.

Figure 5.

Square wave forward limiting currents for proton reduction at Pt, disk radius 12.5 μm; (1) HCl alone; (2) HCl with 0.5 M KCl; E_s = 10 mV, E_{sw} = 25 mV, f = 0.5 Hz.

Figure 6.
Theoretical (o) and measured ratios of i_γ/i_d for concentrations of HCl: (x) 0.86 mM, (*) 1.29 mM, (+) 1.77 mM, (◆) 2.14 mM. While no curve fitting is intended, a single line has been drawn through the measured values to guide the eye.

Figure 7.

Square wave forward (Δ) and reverse (v) currents for oxidation of 2.25 mM TEMPOL in 10 mM KCl at Pt, disk radius 12.5 μm; E_s = 10 mV, E_{sw} = 25 mV, f = 0.5 Hz.

Figure 8.

Limiting forward currents for oxidation of TEMPOL at Pt, disk radius 12.5 μm, vs. concentration of TEMPOL; E_s = 10 mV, E_{sw} = 25 mV, f = 0.5 Hz.

Figure 9.

Averaged current ratios $i_{l,\,latex}/i_{l,\,HCl}$ for proton reduction in latex suspension. $i_{l,HCl}$ is calculated from the interpolated value from line 2 of Figure 5 multiplied by i_f/i_d (equation 3) for the appropriate excess electrolyte ratio.

Figure 1.

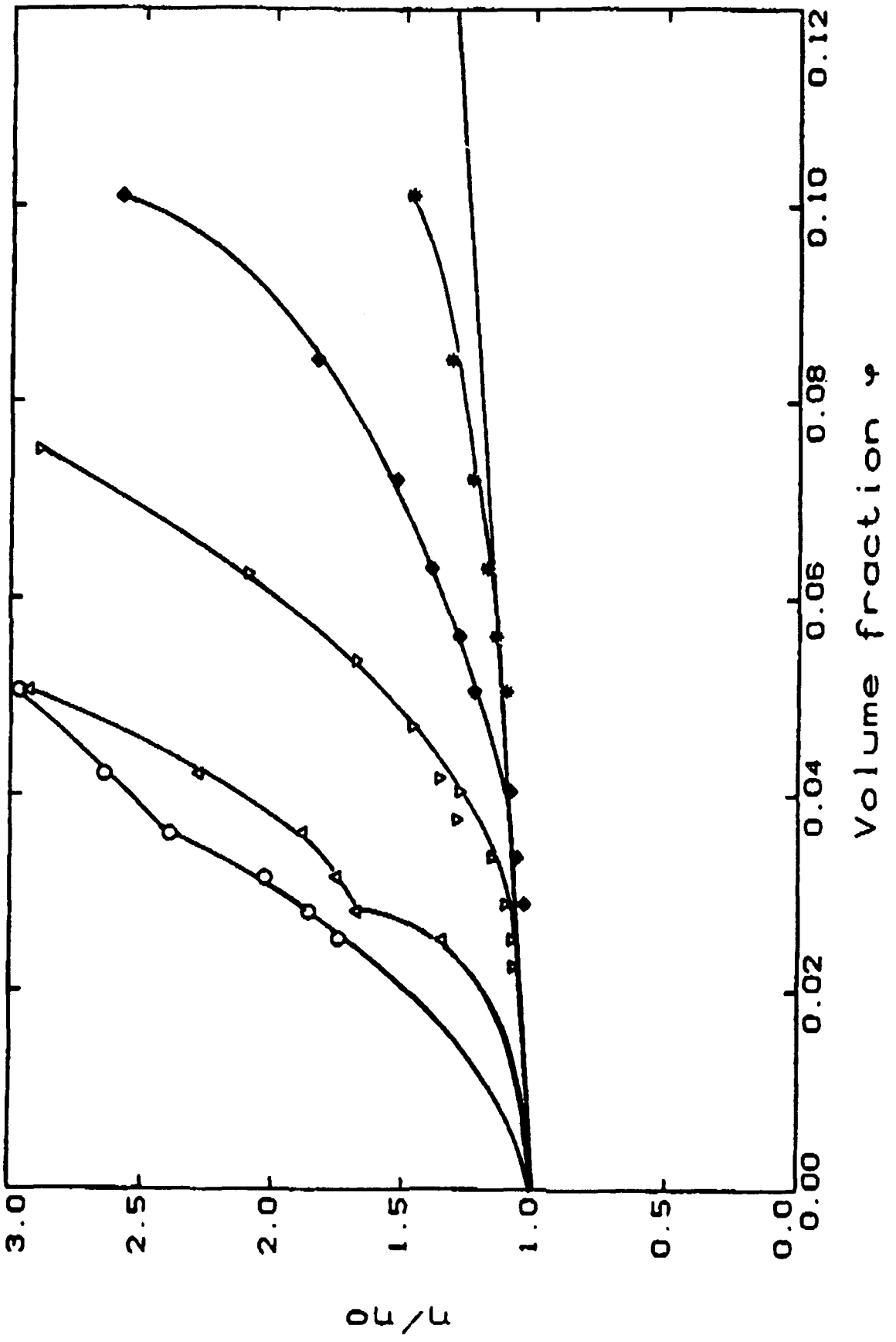

I-152

Figure 2.

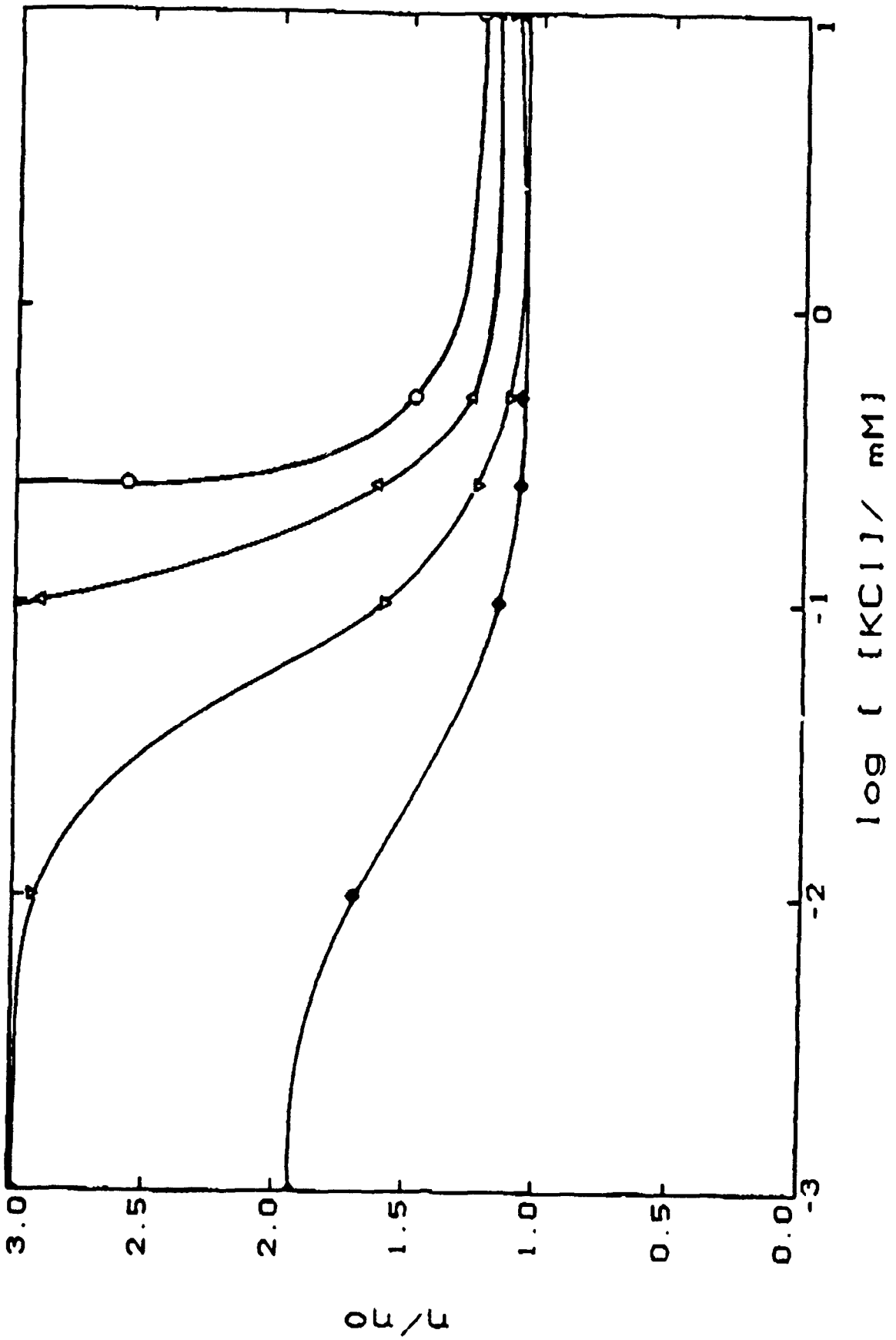

J-193

Figure 3.

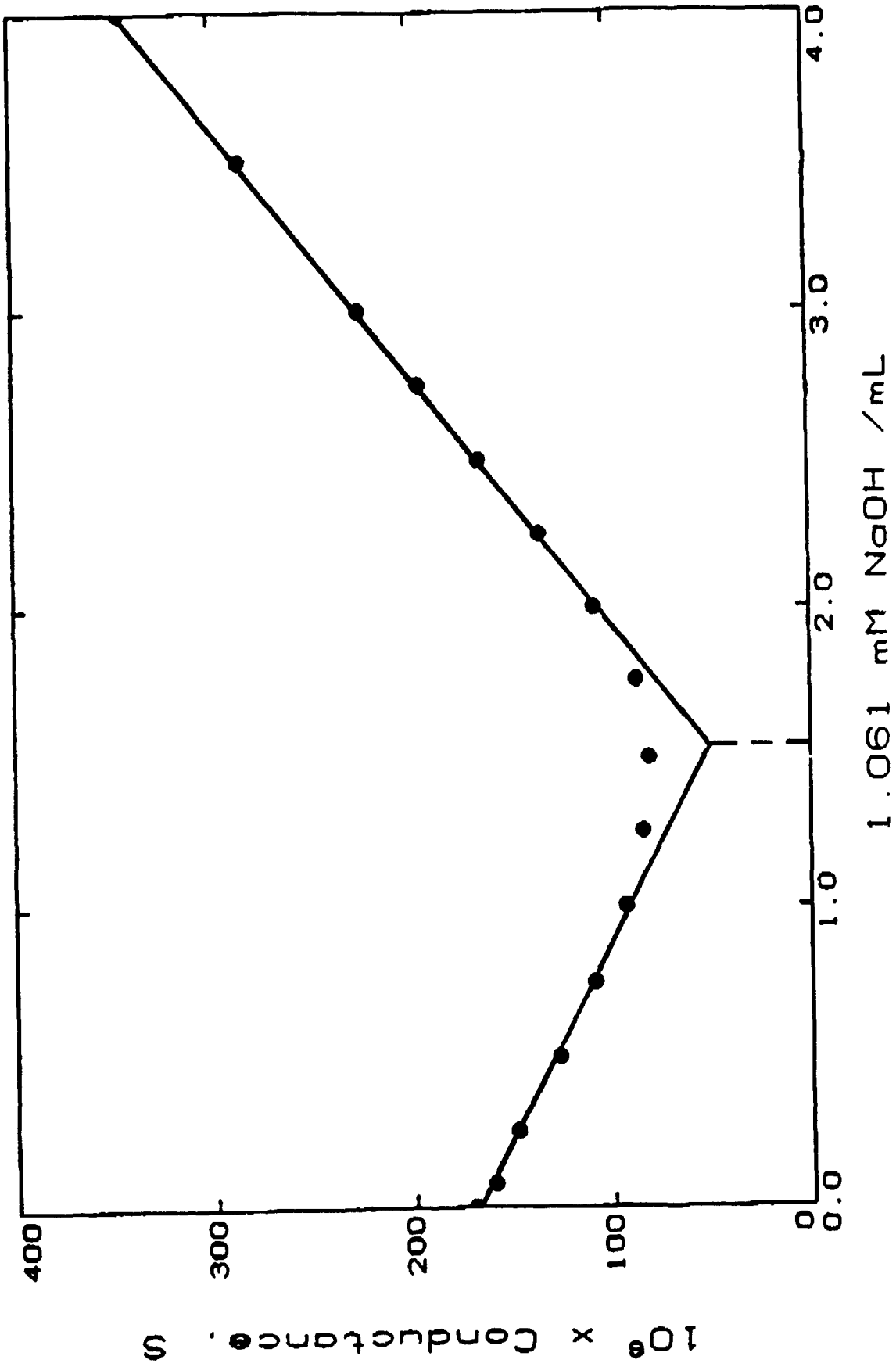
10⁸ x Conductance, S
400
300
200
100
0
0.0
1.0
2.0
3.0
4.0
1.061 mM NaOH /mL

Figure 4.

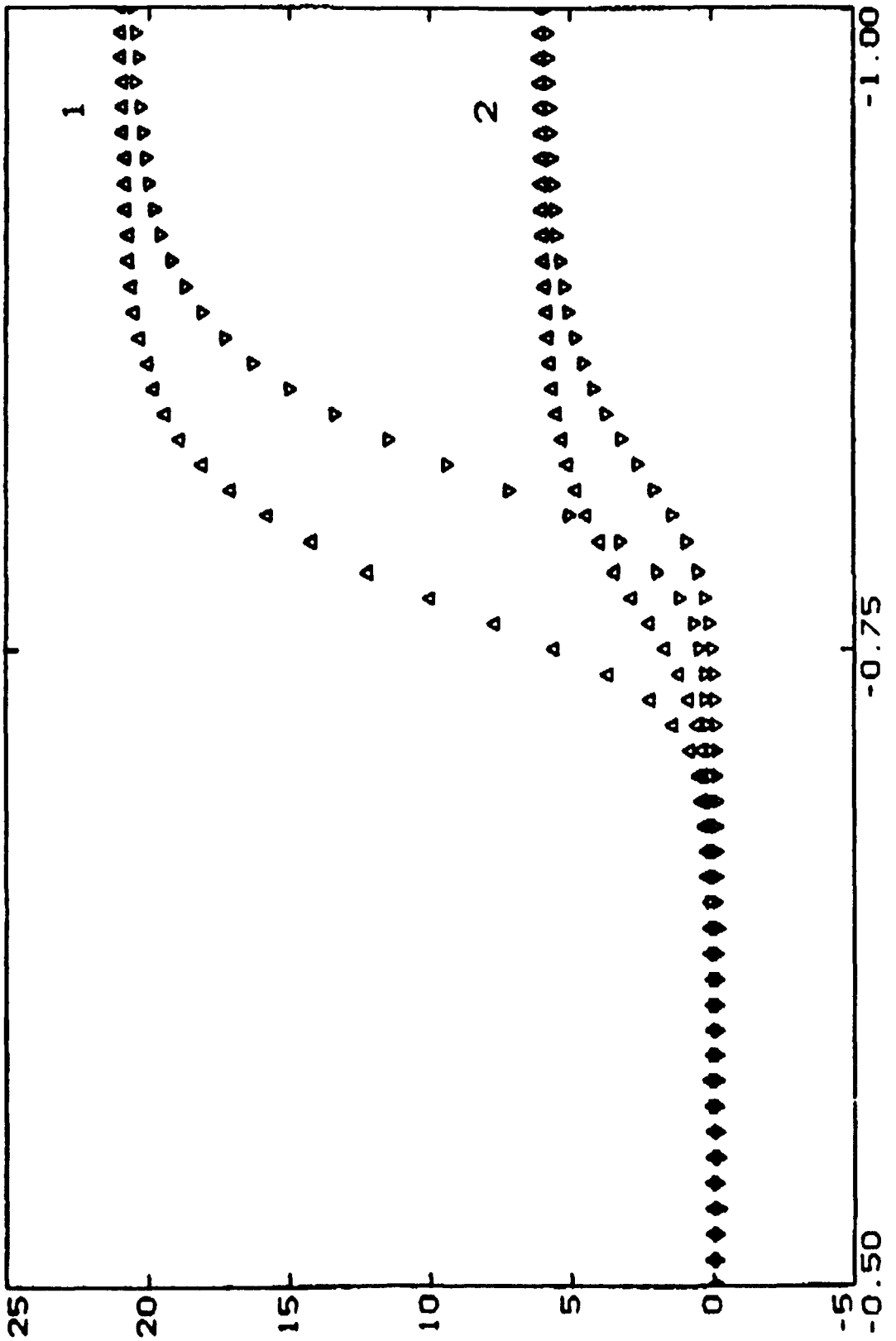

Figure 5.

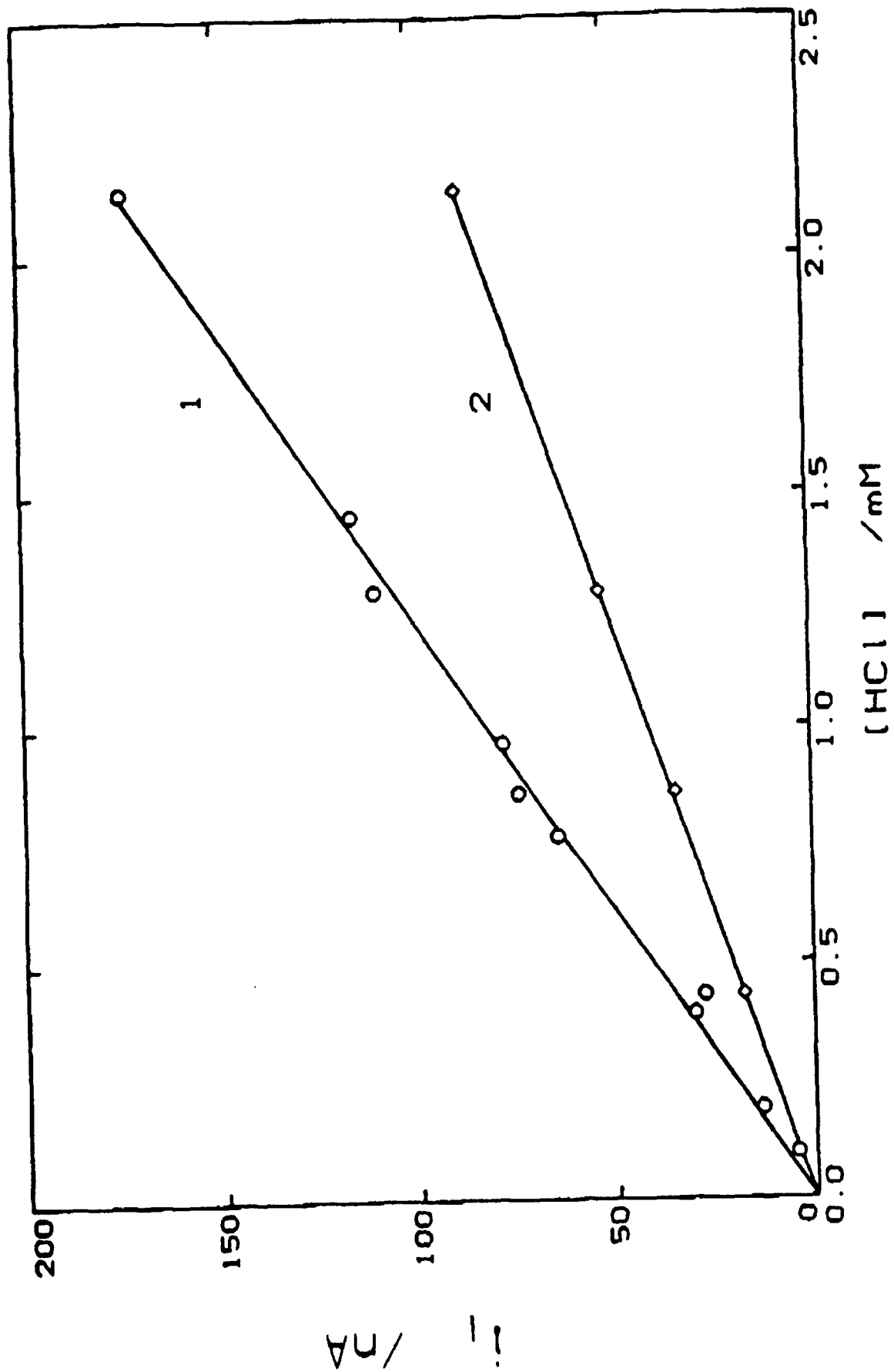

Figure 6.

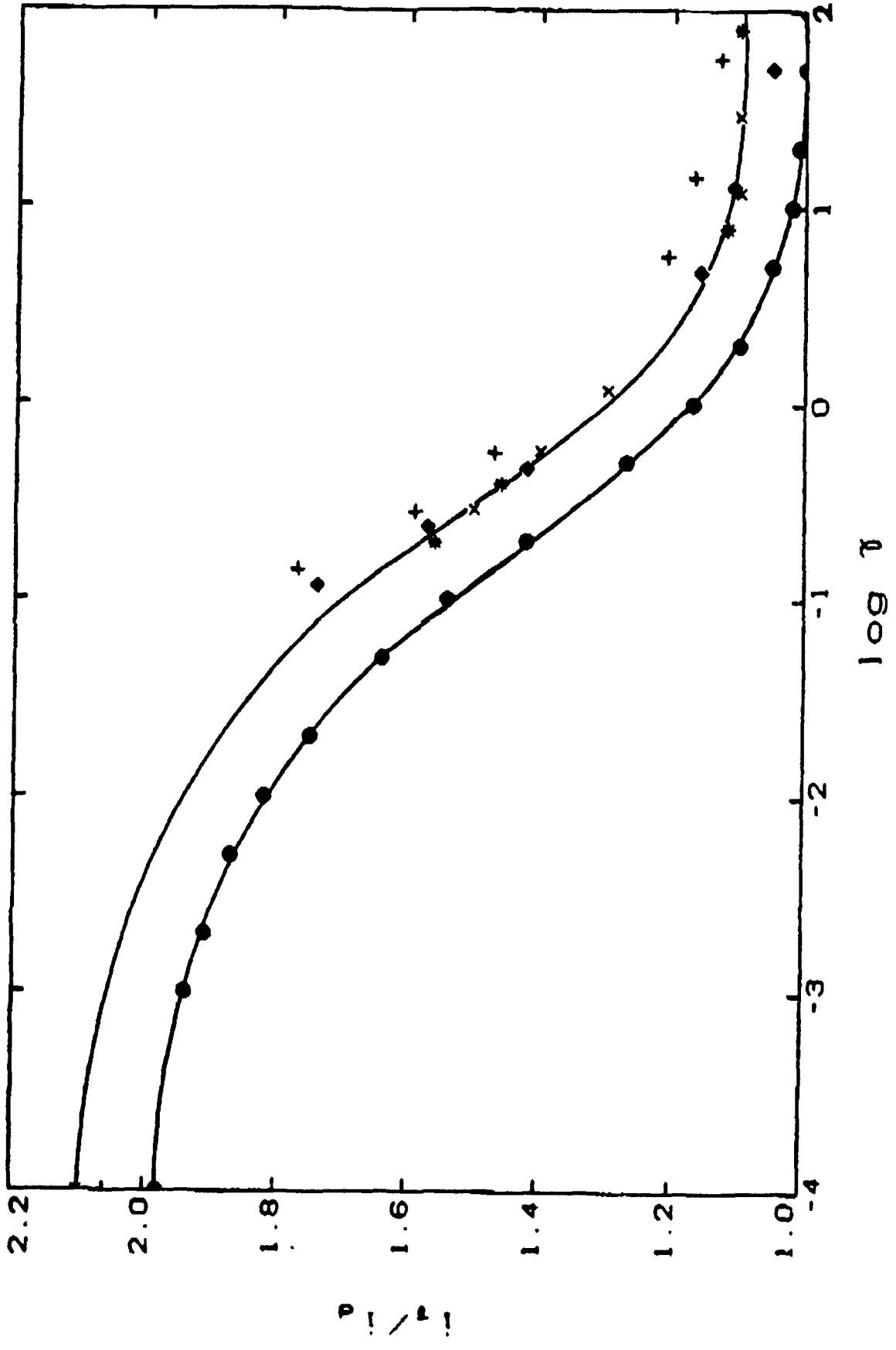

Figure 7.

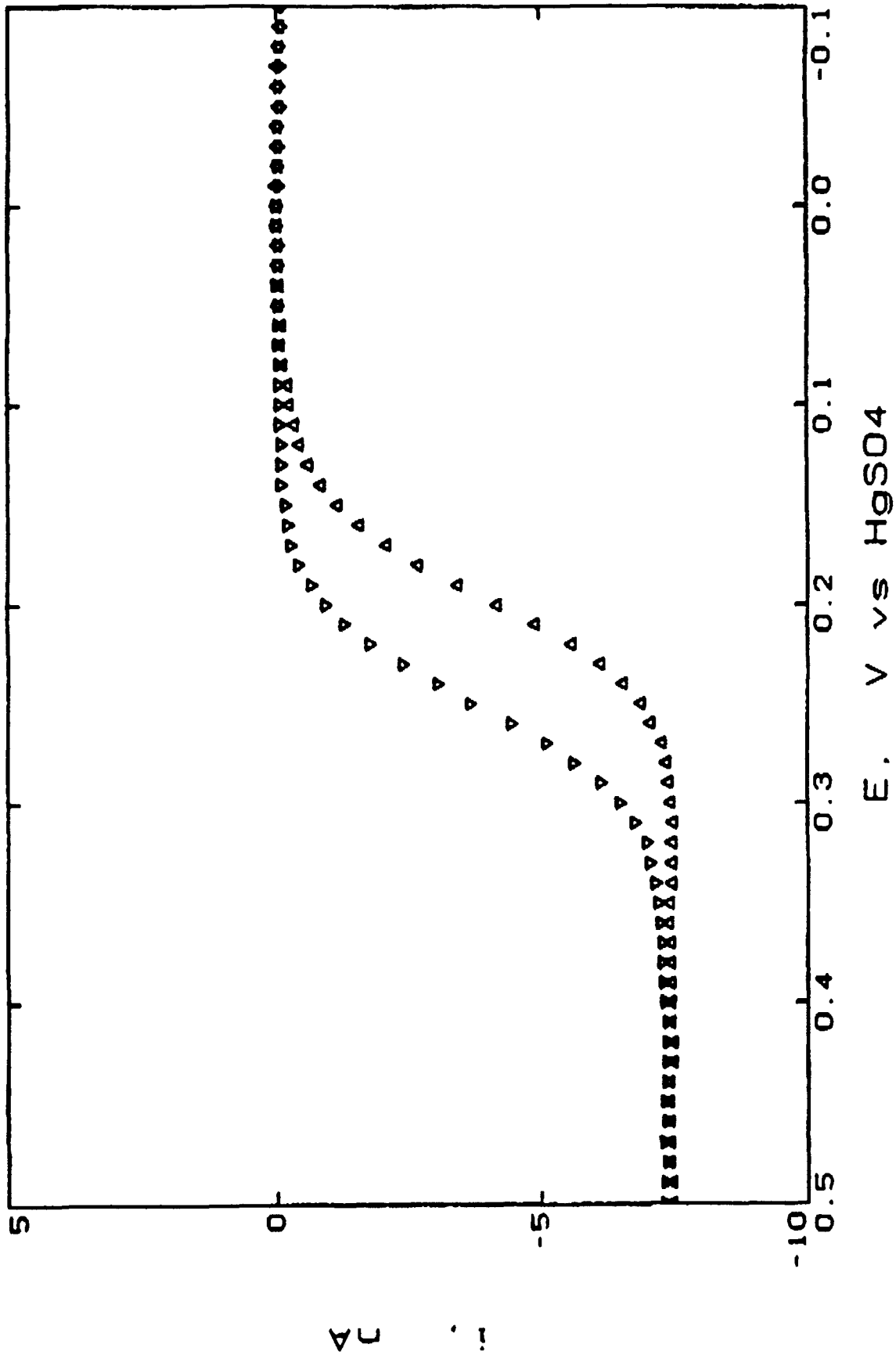

Figure 8.

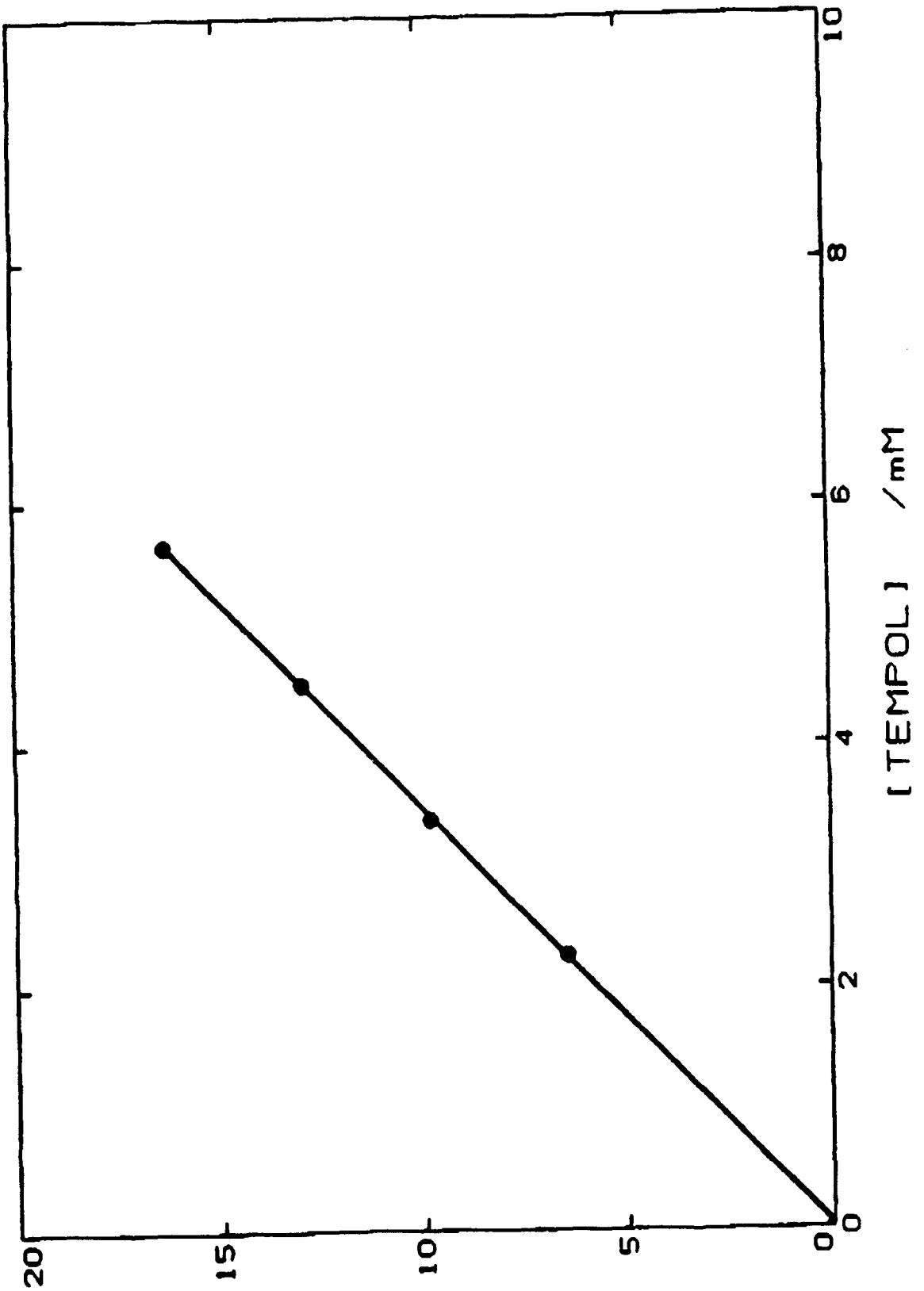

Figure 9.

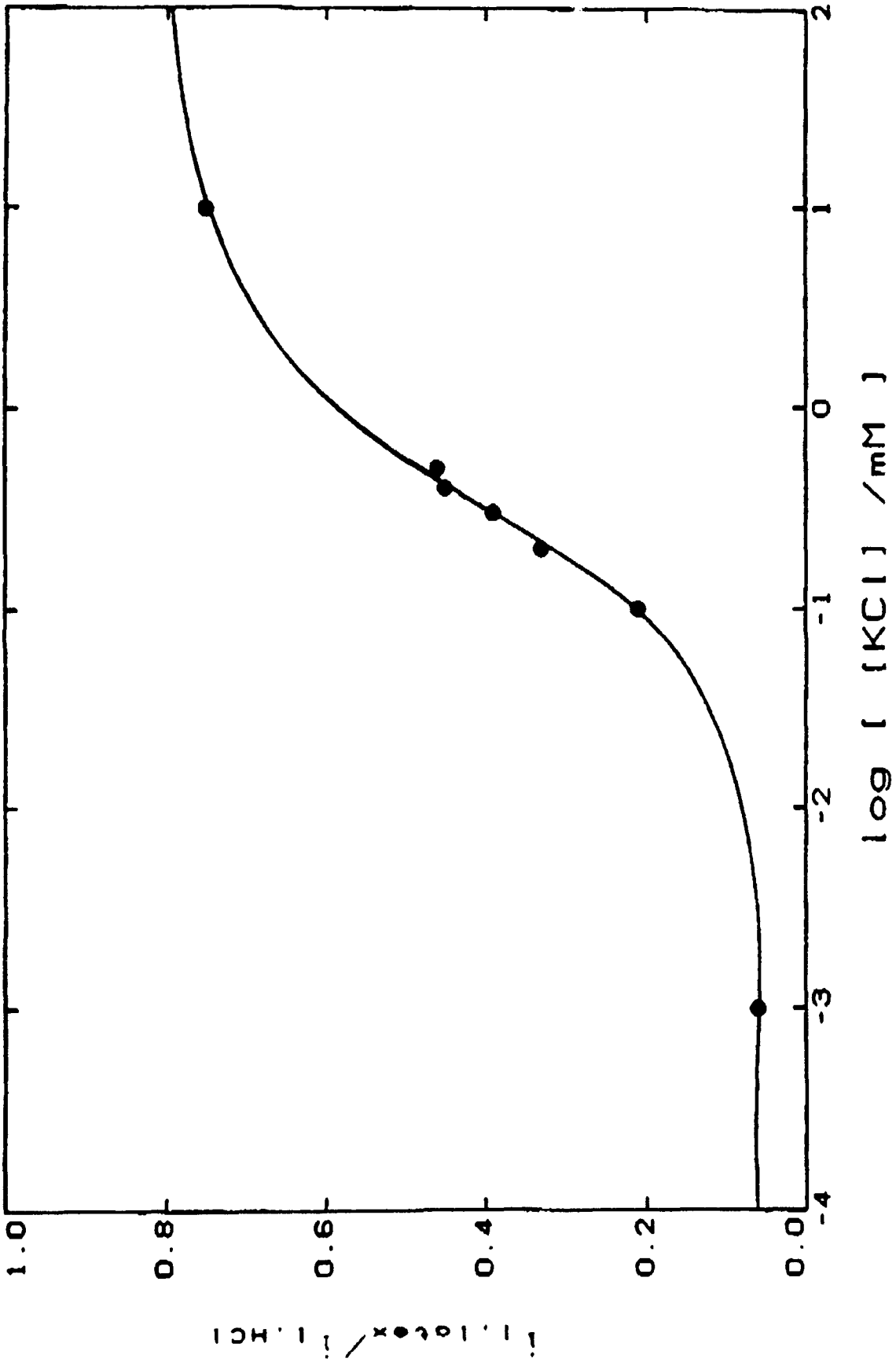

I-200

(10) COULOMETRIC INITIATION OF MICROEMULSION POLYMERIZATION

E. García§, J.Texter†, §Analytical Technology Division, Eastman Kodak Company, Rochester, N.Y. *14652-3706*, and †Photographic Research Laboratories, Eastman Kodak Company, Rochester, N.Y. *14650-2109*

Abstract:

The coulometric initiation of acrylamide polymerization in an Aerosol OT (AOT)-toluene inverse microemulsion (water in oil) have been studied using Pt / Nafion solid polymer electrodes (SPE). Electrolytic polymerization in the highly resistive toluene media is accomplished when an SPE is used to separate the non conductive inverse microemulsion phase from a $+N(CH_3)_4$-Cl (TMACl) aqueous electrolyte phase. The Pt coated side is of the SPE is placed in contact with the microemulsion phase and current flows through the polymer between the two inmisible phases. Polymerization is initiated by the constant potential electrolytic reduction of $K_2S_2O_8$ (radical initiator) in the microemulsion. Solution suspended latex particles (with turbidimetry of 165 NTU's), and solid polyacrylamide are obtained. The electrolyticaly produced polymers where characterized by light scattering, electrolytic charge and average molecular weight. Cyclic and square wave voltammetry at ultramicroelectrodes was used to probe the electrochemical characteristics of inverse microemulsion over a wide acrylamide concentration range. The oxidative signal of acrylamide monomer, in the water swollen inverse micelles, was found to be dependent on the charge carriers inside the micelles and not on added non ionic electron mediators solublized in the toluene phase. Voltammetry of $K_4Fe^{II}(CN)_6$ / $K_4Fe^{III}(CN)_6$ in the inverse microemulsion is similar to that observed in aqueous solutions. The oxidative peak currents obtained are approximately what is predicted for the Ferrocyanide concentration inside the inverse micelles.

— Introduction —

Since the introduction of ultramicroelectrodes (UME's, 1-4) electrochemical investigations in highly resistive media have possible. The attractive characteristics of UME's have made voltammetric studies possible in solvents such as acetonitrile (3,4), benzene (5), heptane (6), hexane (7), and toluene (8), in some cases without purposely added electrolyte. Since this electrodes draw small currents, generally nA for 10 μm diameter electrode, they are not subject to large uncompensated (iR) voltage drops . Typically, for a solution resistances of a few kΩ and a 1nA current flow the iR drop of a few mV's are obtained. These characteristics make UME's excellent probes for electrochemical studies in highly resistive media.

Recently, carbon UME's have been successfully used to probe non-conductive inverse microemulsions (water-in-oil, 9) Microemulsion are thermodynamically stable, oil / water systems which are stabilized by and interfacial surfactant layer (10). In contrast to emulsions, which are opaque, unstable and macrodisperse, microemulsions are transparent and stable with particle sizes ranging between 50-100 Å. Microemulsions are of interest primarily for their capability for dissolving both hydrophobic and hydrophilic solutes. Given the microscopic organization and the stability of microemulsions, they are of particular interest to analytical chemistry.

Although UME's can be used to probe such resistive media as inverse microemulsions, bulk electrolytic investigations in these highly resistive media have not been possible. Thus, the scope of usefulness of microemulsions has been limited to the study of the phisico-chemical aspects of these mixed media. To our knowledge, no reports on the use of inverse microemulsions for the electrosynthesis of stabilized redox active materials have been reported to date. In contrast to the oil in water microemulsions, which display a fairly high electrical conductivity and to which electrolytes can be added, the inverse microemulsions are poor electrical conductors.

Thus conventional bulk-electrolytic methods are ineffective in these highly resistive media. Addition of ionic species to the hydrophobic phase of the emulsion is not possible without disturbing, or destroying the equilibrium of the system.

We report here the use of solid polymer electrodes (SPE's) in the bulk electrolysis of hydrophilic electroactive redox species in an inverse microemulsion. Bard and co-workers (11,12) have demonstrated the usefulness of Pt-SPE for voltammetric investigations in acetonitrile without purposely added electrolyte, tertahydrofuran, and toluene. Ogumi et. al. (13) reported the use of SPE's for the electro-hydrogenation of olefins in hexane at constant current. Other uses of SPE's have been proposed for electrosynthesis (14-16). We have studied the redox initiated electropolymerization of acrylamide via persulfate reduction ($K_2S_2O_8$) in Aerosol-OT (AOT) / toluene inverse microemulsions. This system has been extensively studied by Candau et. al (17, and references therein). Candau and co-works have studied the thermal and UV polymerization of acrylamide monomers in inverse microemulsions with a azobisisobutyronitrile (AIBM) hydrophobic initiator. They have characterized both the inverse micelles and the polymerized acrylamide latex particles in the microemulsion via ultracentrifugation, light-scattering, viscosity and molecular weight distribution. These studies will serve as a point of reference our investigations, in which we will compare the differences of using hydrophobic (AIBM) and hydrophilic ($K_2S_2O_8$) initiators.

We also report here the use of UME's as probes for the redox chemistry of these systems. Potassium Ferrocyanide ($K_4Fe^{II}(CN)_6$) has been used to characterize the ability of charge transfer to and from the UME to hydrophilic redox active species in the inverse microemulsion.

— Experimental —

Electrochemical measurements were made with a BAS 100a Electrochemical Analyzer with a faraday cage and PA1 preamplifier (Bioanalytical Systems, Inc.; West Lafayette, Indiana). 2μm Pt and 10 μm Pt and carbon ultramicroelectrodes (UME's) where used for all fast cyclic and square wave voltammetric (REF) investigations (Bioanalytical Systems, Inc.; West Lafayette, Indiana). All solutions were extensively deaerated with toluene saturated N_2 before electrochemical investigation. All UME working electrodes were successively polished with 6, 3, 1, and 0.25 μm diamond paste. A large surface area reticular vitreous carbon (RVC) was employed as a counter electrode and all potentials were referenced to an aqueous saturated calomel electrode (SCE).

Microemulsion solutions were prepared by previously published procedures (17) by adding the aqueous solutions mixtures (Table 1) to a solution of AOt in toluene in the appropriated proportions. Toluene (Kodak xxx), Aerosol-OT (German xxx), Acrylamide (Kodak xxx), $K_4Fe^{II}(CN)_6$ (xxx) and $K_2S_2O_8$ (xxx) where used as received.

Solid polymer electrodes where prepared by the establish procedure (11,18). E.I. du Pont Nafion -115 (Aldrich Chemical Co., Milwaukee, Wisconsin) polymer was boiled in 50% nitric acid for 3 hrs. and then Milli-Q water (Continental Water Systems, El Paso Texas) for 5 hrs. The polymer was then clamped between to half cells (exposed polymer diameter approximately 25 mm) with on compartment containing 0.2 M Hydrazine (Kodak xxx) in a pH=13 NaOH solution, and the other containing K_2PtCl_6 in a pH=2 HCl solution as should in Figure 1a. The cell was allowed to stand for 24 hrs. while constantly stirred in both half cells. The membrane was converted to the Na+ form by allowing it to stand in the cell with pH =2 HCl for two hrs. Afterwards, the HCl solution is discarded and the cell is rinsed with milli-Q water and filled with 1M NaOH and allowed to react over night.

During electrolysis the SPE is clamped between to half cells of a smaller exposed electrode area (exposed SPE diameter approximately 20 mm diameter). The

solution facing the SPE is filled with 25 mL of working solution (mixture of acrylamide / water / $K_2S_2O_8$, and AOT / toluene) and deaerated with N_2. The un-platinized side of the electrode faced the auxiliary electrode compartment. The auxiliary electrode half cell was filed with a 1.0 M aqueous tetramethyl ammonium chloride (TMACl, Southwestern Analytical, Austin Texas xxx).and is where the aqueous reference electrode (SCE) is placed, as shown in Figure 1b. Contact was made to the working electrode by clamping and alligator clip onto the exposed platinized polymer. When the SPE potential is sweeped to where the substrate in the working solution is reduced or oxidized, an ionic migration through the membrane occurs in order to maintain electroneutrality (Figure 1b). Concurrently, the opposite reaction occurs at the auxiliary electrode in the aqueous electrolyte. Thus, electrolysis is carried out in the microemulsion without the need of purposely added electrolyte.

During UME voltammetric investigations a single compartment cell is used. In this set-up a Pt wire is used as an auxiliary electrode the SCE reference is placed directly in the inverse microemulsions solutions. Although leakage from the aqueous reference electrode could effect the inverse microemulsion equilibrium, no change in the voltammetric response was observed during these studies. The amount of KCL-water leaked into the inverse microemulsion is thought to be neglegable in the voltammetric time scale.

— Results —

— Voltammetry—

Estimates of possible background redox chemistry can be obtained from voltammetric investigation of a toluene -AOT mixture(solution A, Table 1). Cyclic and square wave voltammograms for the amphiphilic AOT in toluene solution mixtures are shown in Figure 2. The cyclic voltammogram (CV) appears to be totally non-faradaic.

The positively and negatively going scans are separated by double-layer charging currents. Similarly, the oxidative and reductive square wave voltammograms (SWV) show no faradaic processes, Figure 2b and 2c respectively. The lack of faradaic process within the scanned potential window is not expected. The oxidation of AOT might be possible within the given scanned potential, as well as the oxidation of toluene (oxidation $E_{1/2}$ ~ +2.xxx V vs. SCE, 19 and references therein). The absence of faradaic processes within the 6.4 volts potential scan is most probably due to the lack of charge carriers in the solution. Although and estimated xx.x mM concentration of AOT is present, it does not ionized in the absence of water.

An better estimate of the background current, that given by the oxidation of H_2O, AOT, or toluene, was obtained from an inverse microemulsion containing only water - toluene and AOT (solution B Table 1). An oxidative SWV for solution B is shown in Figure 3a. No peaks were observed. within 0 and +2.2 Volts vs. SCE. An sloping anodic current was observed between +0.8 and +2.2 volts with about 0.64 nA current at +2.2 volts. When the same scan (obtained with the same electrodes) is is performed on an inverse microemulsion containing 4.4% acrylamide (AM, solution C) a broad oxidation peak is observed at +1.71 volts vs. SCE. The peak current at 1.71 volts is 23 nA, or 36 times that of the background. Thus this peak is directly related to the addition of AM.

— Electrolysis—

Solution C, Table 1, was electrolysis with a Pt-SPE until the current for the reduction of $K_2S_2O_8$ was either 10 or 50 % of the original current [$i_{initial}$ / (10 or 2) = i_{final}]. For the 10% electrolysis, the resulting electrolyzed microemulsion solution was opaque with a slightly bluish tint, similar to that reported by Candau and co-workers (17). The turbidimetry, measured with an XXX turbidimetry and referenced to the microemulsion before electrolysis, of the 10% electrolysis solution was 35 NTU's (National Turbidimetry

Units). If the electrolysis is extended to 50 %, solid polyacrylamide precipitates on the cell walls and on the electrode surface. The turbidimetry of the decanted (suspended) portion of the electrolyzed microemulsion was obtained at 165 NTU's.

Table 1 Grams of materials used to prepare microemulsion solutions.

Microemulsion	Toluene	AOT	AM	H_2O	$K_2S_2O_8$	$K_4Fe^{II}(CN)_6$	K_2SO_4
A	70.39	17.7					
B	70.39	17.7		8.00			
C	70.39	17.7	3.3	8.90			
D	70.39	17.7	4.4	7.85	0.044		
E	70.39	17.7	5.0	7.23			
F	70.39	17.7	4.4	7.85			
G	70.39	17.7	2.2	10.0			
H	70.39	17.7	1.1	11.1			
I[§]	70.39	17.7	0.5	11.7			
J[§]	70.39	17.7	0.1	12.1			
K	70.39	17.7	5.0	7.23			1.2
L	70.39	17.7		11.2		1.0	1.2

[§] These solutions are not inverse microemulsions, but inverse emulsions. They appeared opaque and upon standing for 10 mins. a phase separation was observed.

Table 2 Approximate aqueous molar concentrations for prepare microemulsion solutions.

Microemulsion	H_2O (g)	[AM]	$[K_2S_2O_8]$	$K_4Fe^{II}(CN)_6]$	$[K_2SO_4]$
B	8.00				
C	8.90	8.01			
D	7.85	9.83	0.0276		
E	7.23	12.1			
G	10.0	3.86			
H	11.1	1.74			
I	11.7	0.75			
J	12.1	0.14			
K	7.23	12.1			0.6713
L	10.2			0.2427	0.6713

— References—

1. Howell, J. O.; Wightman, R. M.; Analitical Chemistry 1984, 56, 524-
2. Wightman, R. M.; Analitical Chemistry 1981, 53, 524-
3. Bond, A. M.; Feischman, M.; Robinson, J.; J. Electroanal. Chem. 1984, 168, 299-
4. Bond, A. M.; Lay, J.; J. Electroanal. Chem. 1986, 199, 285-
5.
6.
7.
8.
9. Chen, S. W.; Georges, J; . J. Electroanal. Chem. 1986, 210, 205- 211.
10. Kaler, E. W.; Davis, H. T.; Scriven, L. E.; J. Chem. Phys. 1983, 79, 5685-
11. DeWulf, D. W.; Bard, A. J.; J. Electrochem. Soc. 1988, 135, 1977-1985
12. DeWulf, D. W.; Bard, A. J.; J. Macromol. Sci.-Chem. 1989, A26, 1205-1209
13. Ogumi, Z.; Nishio, K.; Takehara, Z.; Yoshizawa, S.; Electrochim. Acta. 1981, 26, 1779-.
14. a) Ogumi, Z.; Yashita, H; Nishio, K.; Takehara, Z.; Yoshizawa, S.; Electrochim. Acta. 1983, 28, 1687- ; b) Ogumi, Z.; Osashi, S.; Takehara, Z.; Electrochim. Acta. 1985, 30, 121- .
15. a) Raoult, E.; Sarrazin, J.; Tallec, A.; J. Appl. Electrochem. 1984, 14, 639-; b) Raoult, E.; Sarrazin, J.; Tallec, A.; J. Appl. Electrochem. 1985, 15, 85- ; c) Raoult, E.; Sarrazin, J.; Tallec, A.; J. Membr. Sci. 1987, 30, 23- .
16. a) Katayama-Aramata, A.; Ohnishi, R.J. Amer. Chem. Soc. 1983, 105, 658-; b) Aramata, A.; Ohnishi, R.J. Electroanal. Chem. 1984, 162, 153-; c) Katayama-Aramata, A.; Nakajima, H.; Fujikawa, K; Kita, H. Electrochim. Acta.

1983, 28, 777- .

17 Candau, F.; Leong, Y. S.; Poouyet, G.; Candau, S.; J. Colloid and Inter. Sci. 1984, 1, 167-183.

18. Takenaka, H.; Torikai, H.; KoKai Tokkyo Koho (Japan Patent); 1980, 55, 38934.

19. Strietwiser xxx

— Figure Captions —

Figure 1)

A) Electrochemical cell configuration B) Schematic diagram for electrochemistry with SPE's in highly resistive media.

Figure 2)

Voltammetry of Solution A (AOT in Toluene, see Table 1) at a 10 μm Pt UME. A) Cyclic voltammogram at 500 mV/ sec,. Square wave voltammograms at 131 Hz, 40 mV AC amplitude, and 4 mV step height; B) i) oxidative scan, ii) reductive scan.

Figure 3)

Oxidative square wave voltammetric scan at a 10μm Pt UME, at 131 Hz, 40 mV AC amplitude, and 4 mV step height for: A) solution B (i) net current, S=200 pA (ii) Forward and Reverse currents, S= 0.625 nA. B) Solution C, 4.4 % Acrylamide in inverse microemulsion (i) Net current, S= 5nA. (ii) Forward and reverse currents, S= 2.5 nA.

Figure 4) Cyclic voltammogram of solution D at a 10μm Pt UME and 1 V/s. A) single scan, S = 10 nA. B) five consequitive scans, S = 5 nA

Figure 5) Oxidative SWV scan at 131 Hz with step height = 4 mV and AC amplitude = 40 mV, for solution L containing AM and $Fe(CN)_6^{4-}$. i) net current, S = 10 nA ii) Foward and reverse currents, S = 5.5 nA

Figure 6) Cyclic voltammogram of 1 mM $FeCp_2$ in acetonitrile without added supporting electrolyte at a 15 mm diameter Pt-SPE Electrode; Scan rate = 10 mV/sec.

Figure 7) A)(i) CV of 10 mM K_4FeCN_6 in 0.1 M $CsNO_3$ at 50 mV/sec, S = 5 mA. (ii) CV of 10 mM K_4FeCN_6 in 0.1 M $CsNO_3$ at 5 mV/sec; S = 2 mA. B) Cyclic voltammogram at a conventional size Pt-disk electrode in 10 mM K_4FeCN_6 in 0.1 $CsNO_3$ at 50 mV/sec.

I-2/2

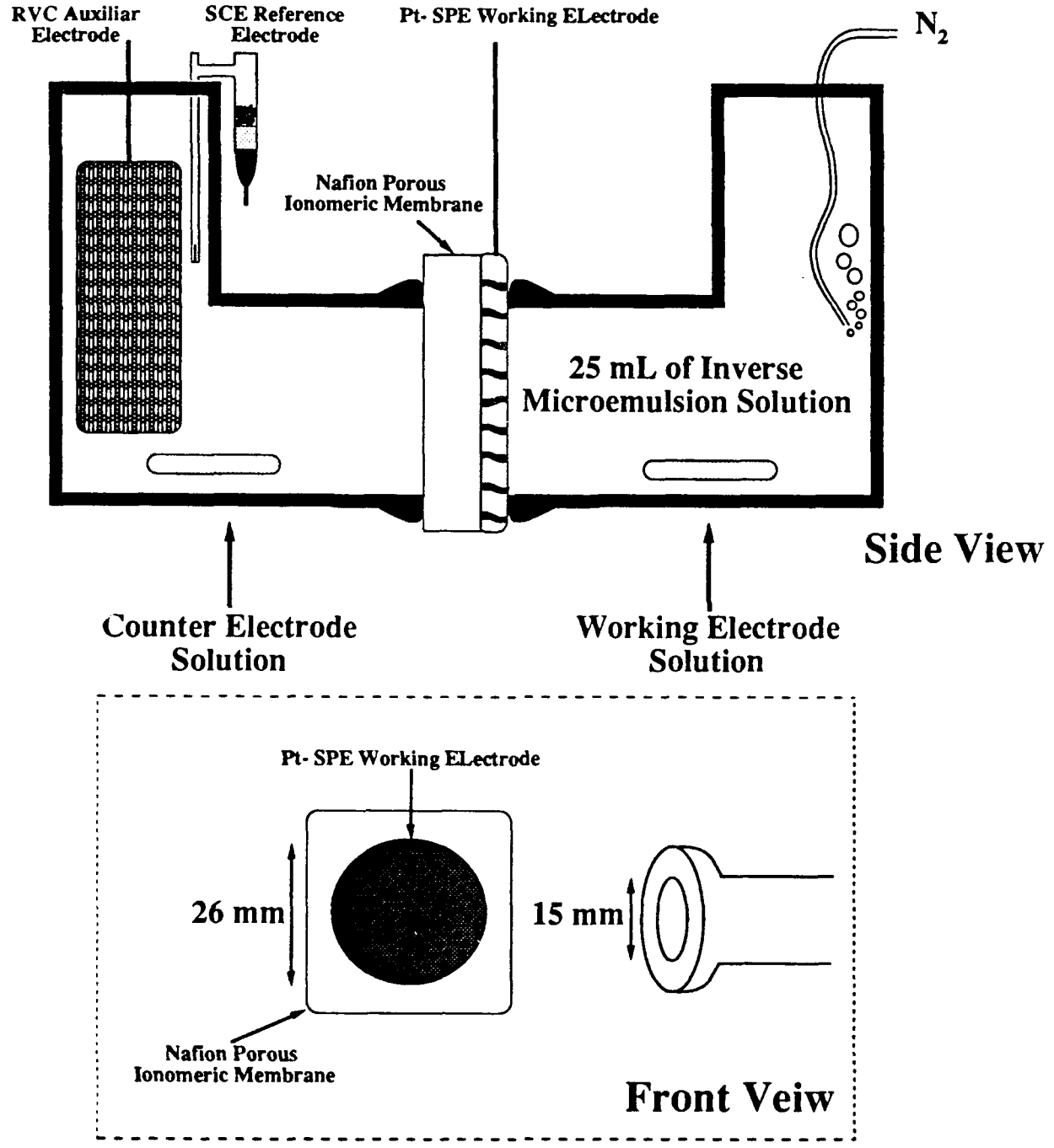
RVC Auxiliar Electrode
SCE Reference Electrode
Pt- SPE Working ELectrode
N_2
Nafion Porous Ionomeric Membrane
25 mL of Inverse Microemulsion Solution
Side View
Counter Electrode Solution
Working Electrode Solution
Pt- SPE Working ELectrode
26 mm
15 mm
Nafion Porous Ionomeric Membrane
Front Veiw

Figure 1A

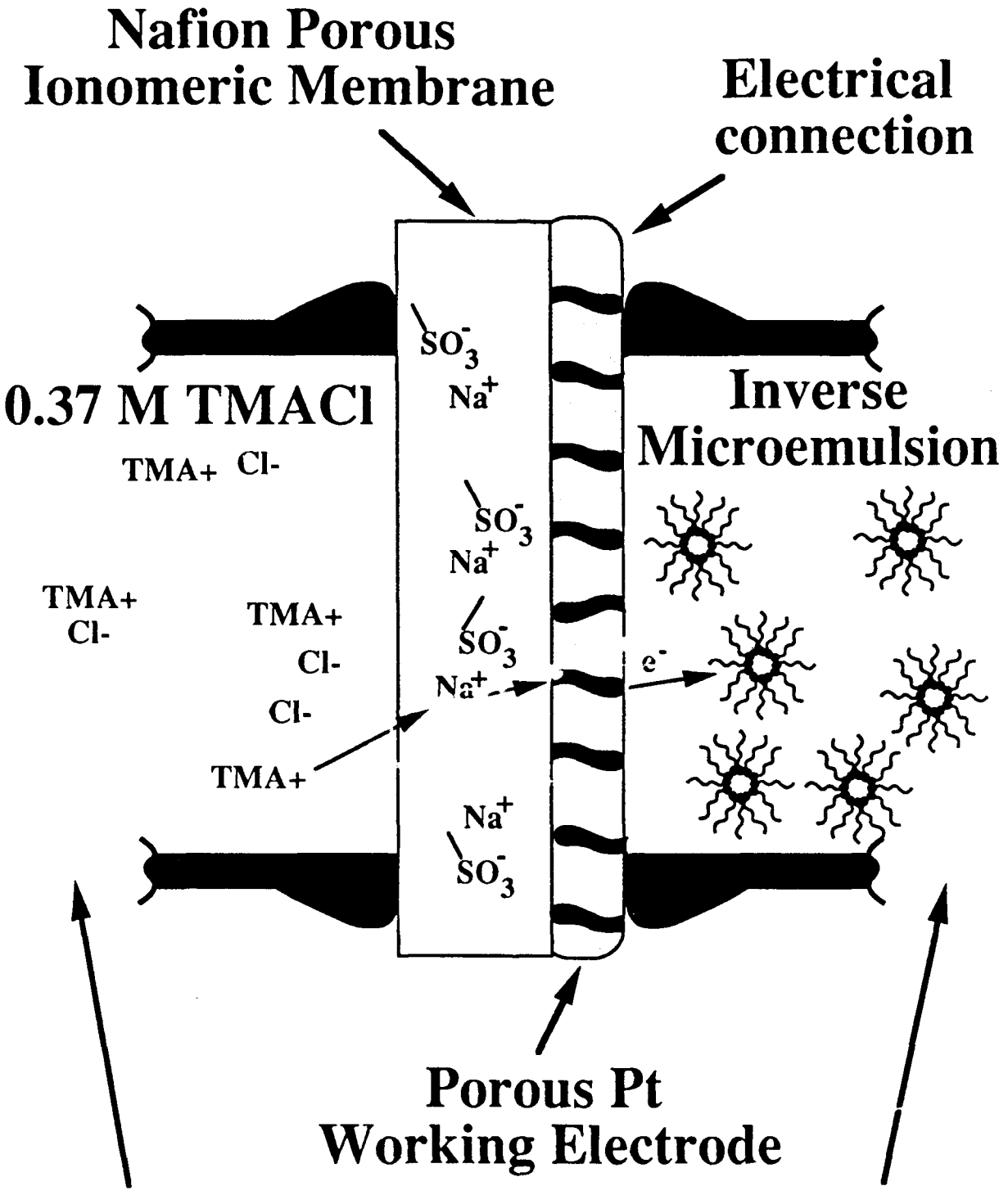
Nafion Porous
Ionomeric Membrane
Electrical
connection
0.37 M TMACl
TMA+ Cl-
Inverse
Microemulsion
SO3-
Na+
TMA+
Cl-
e-
Porous Pt
Working Electrode
Counter Electrode
Solution
Working Electrode
Solution

Figure 1B

Figure 2A

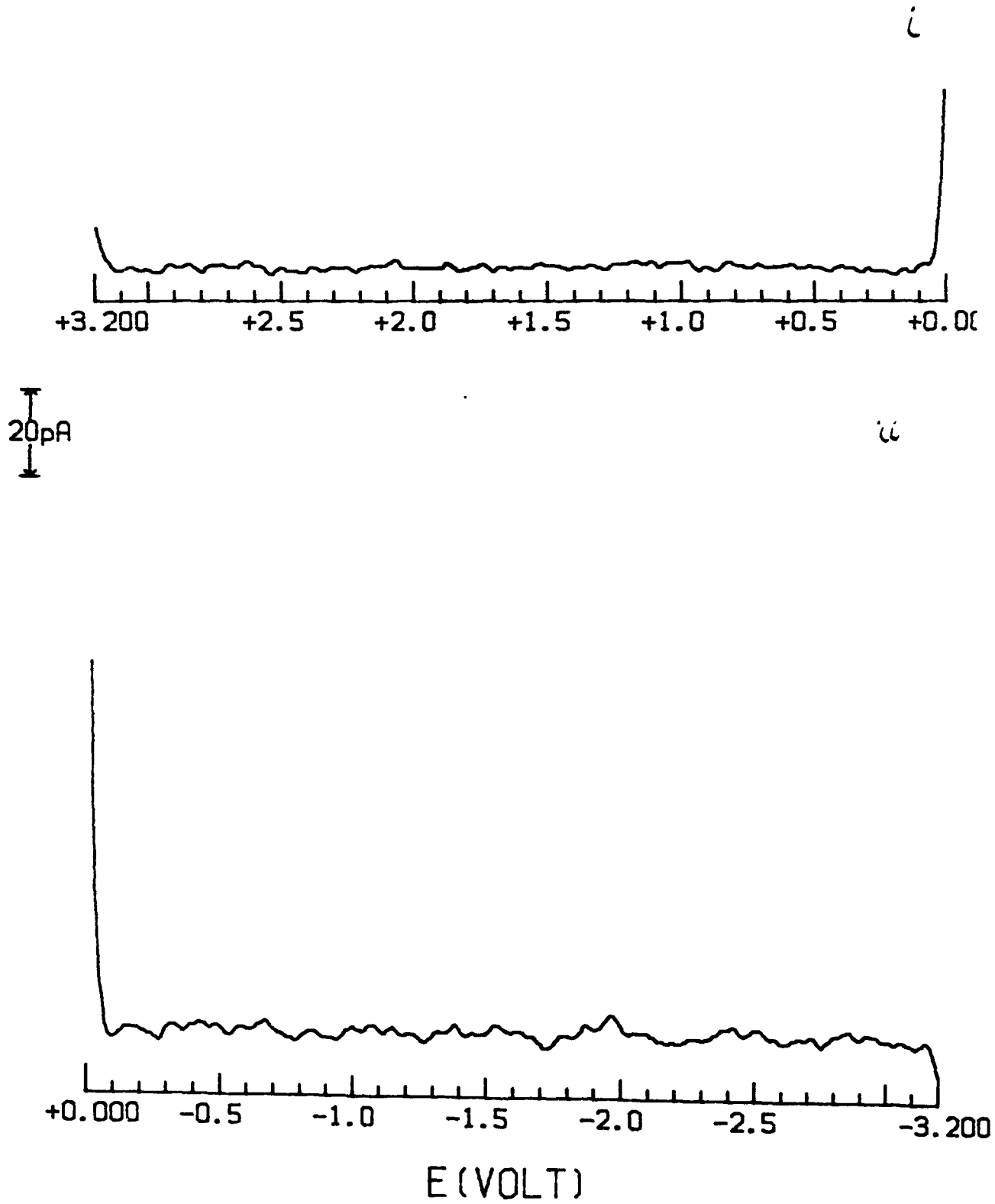

Figure 2B

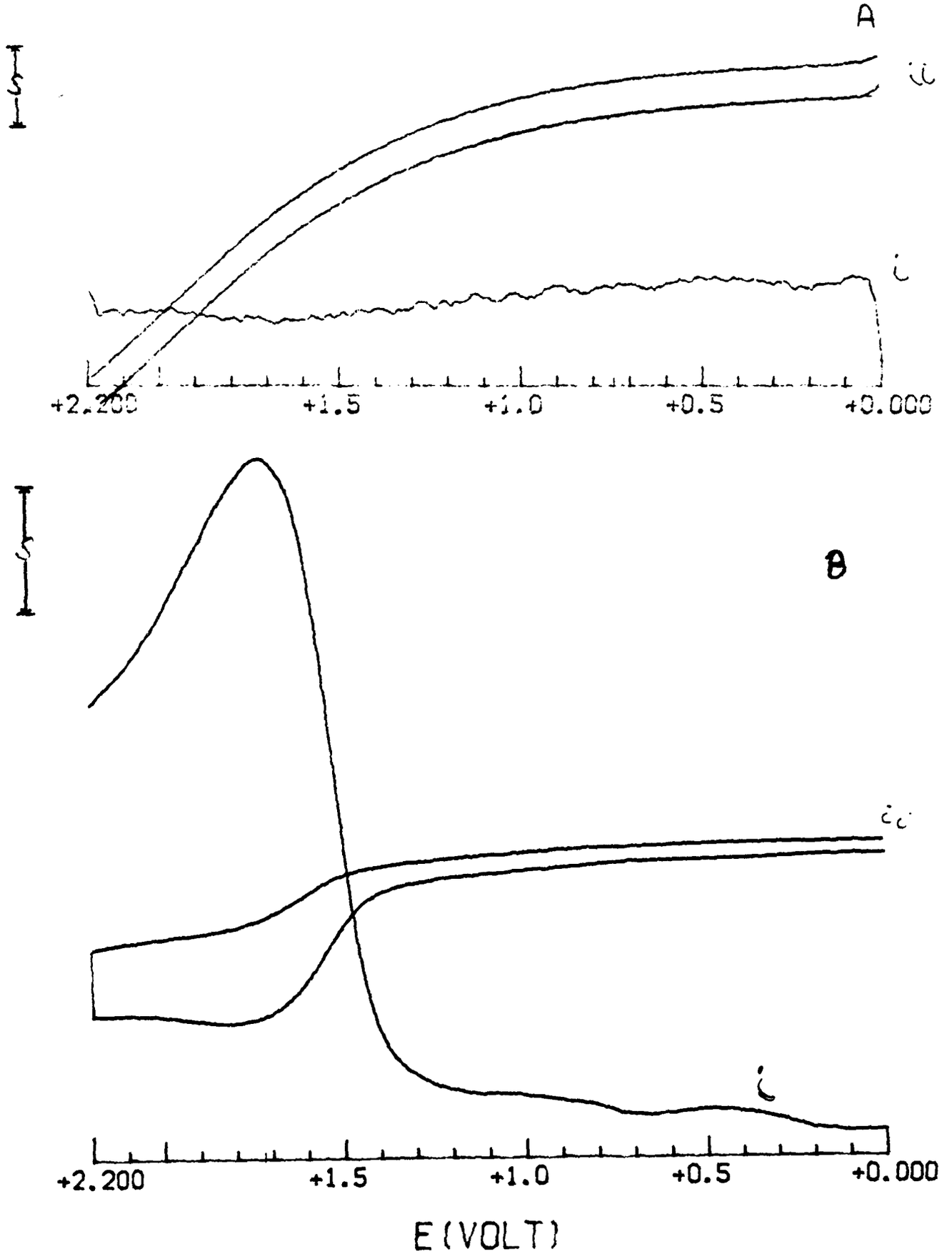

Figure 3

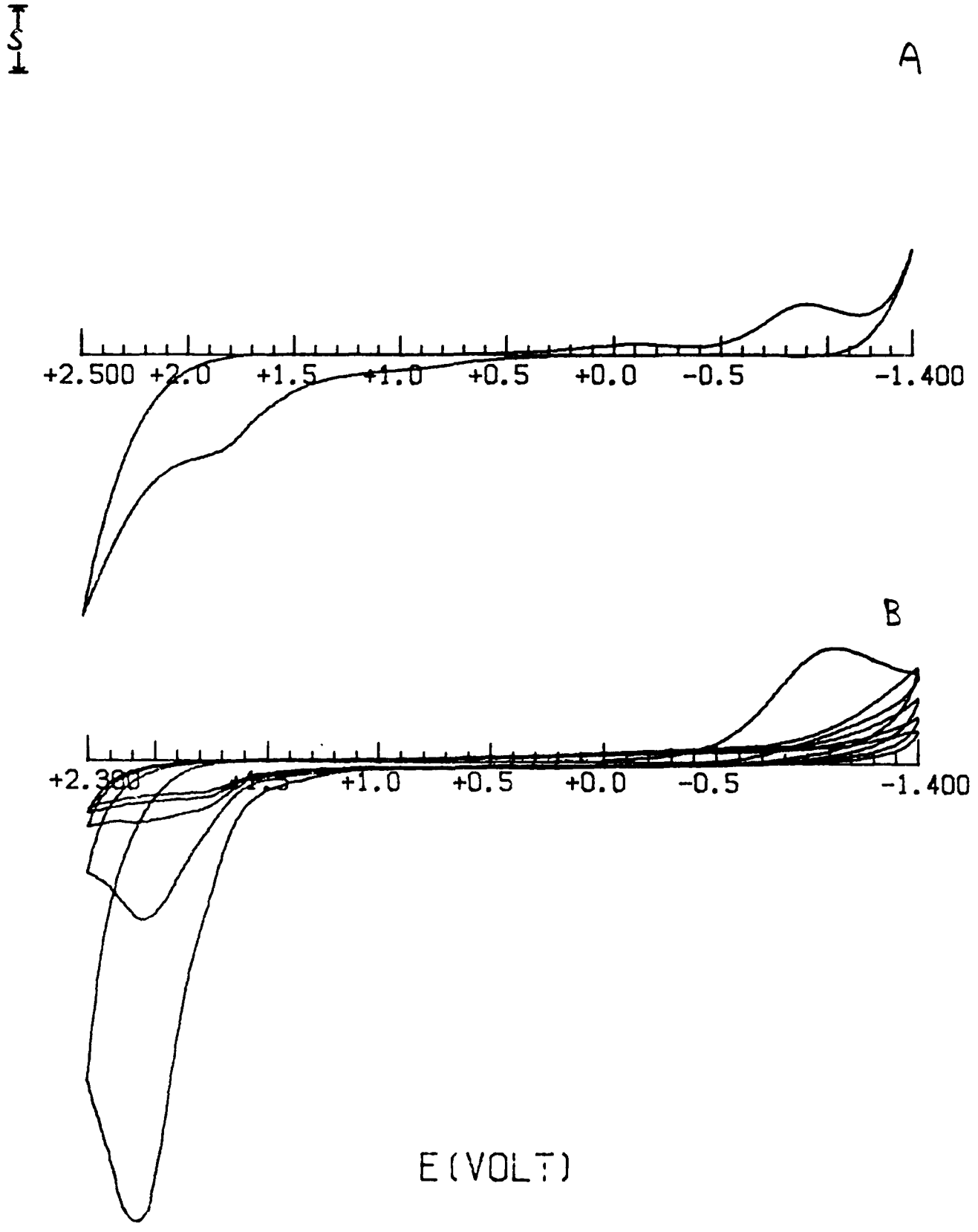

Figure 4

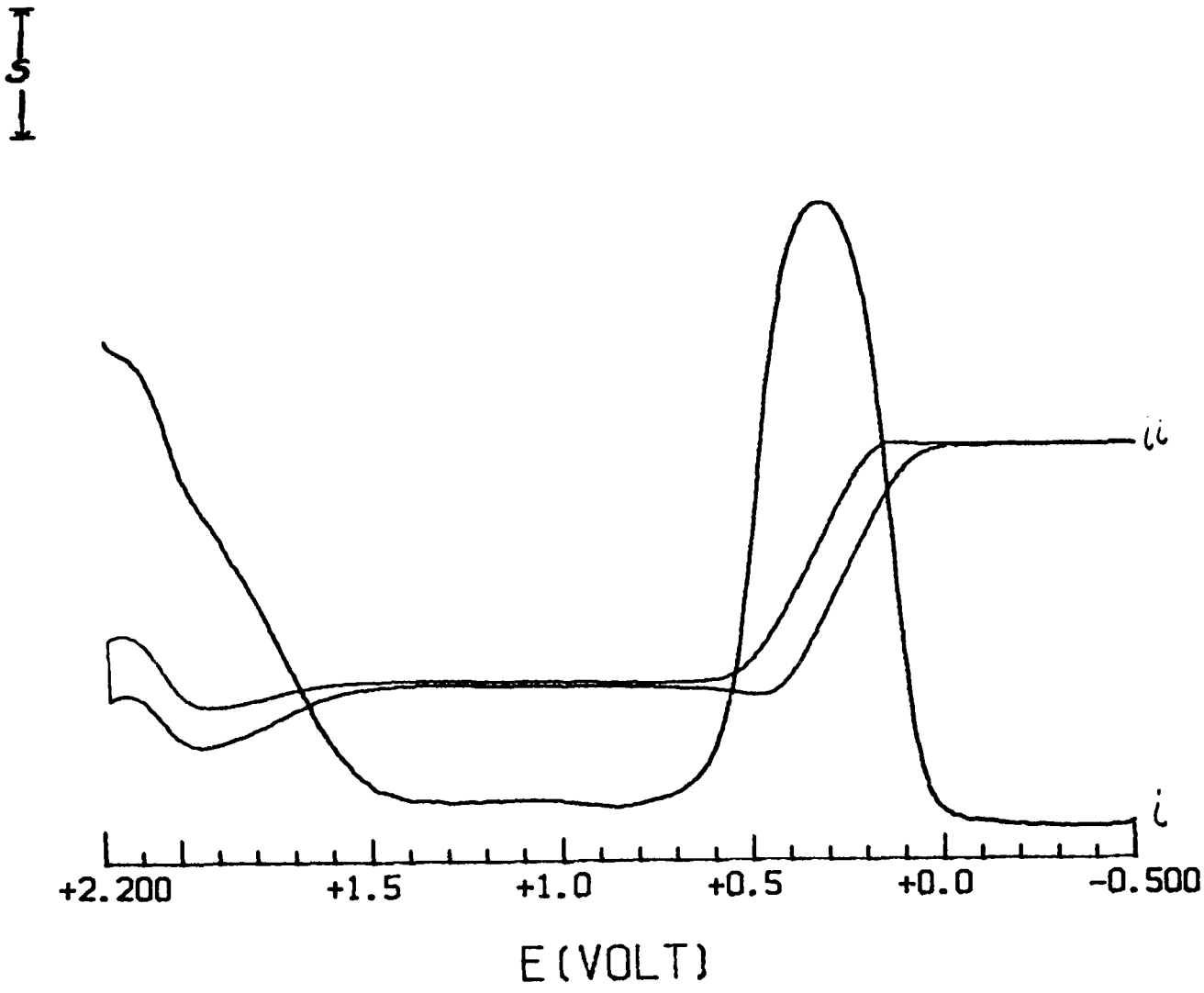

Figure 5

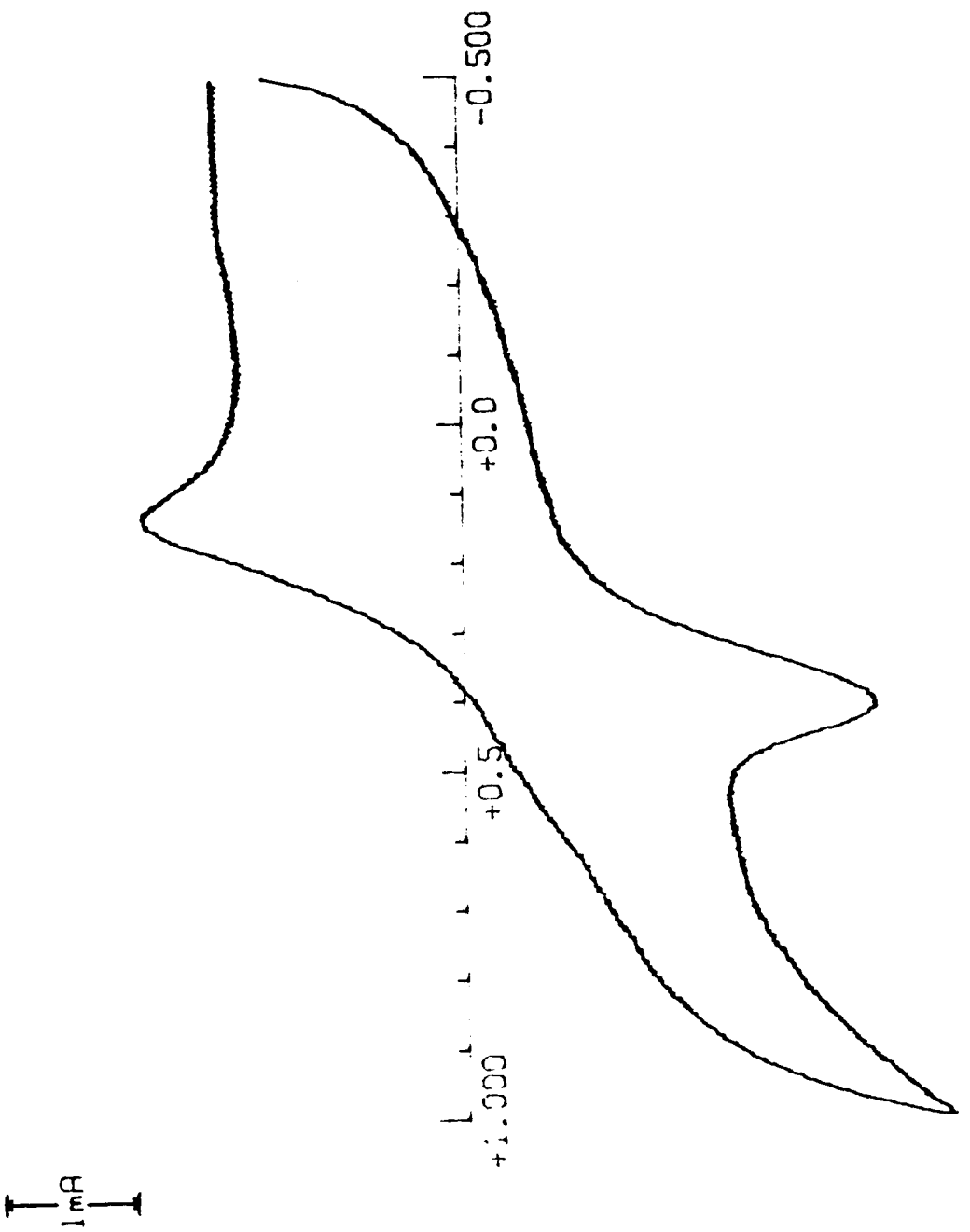

Figure 6

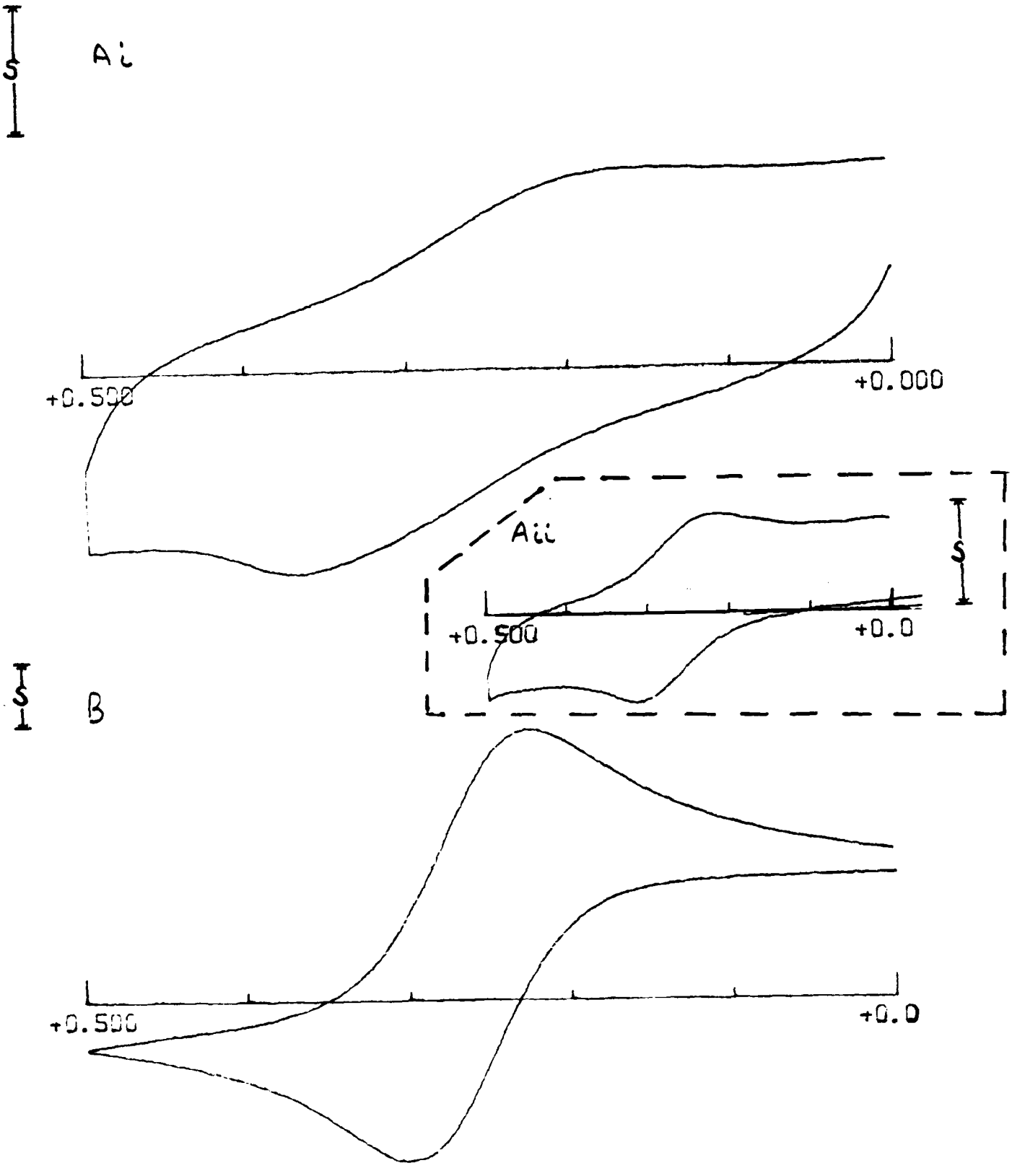

Figure 7